Acquisition and activity of bacterial symbionts in marine invertebrates

Dissertation
zur Erlangung des Grades eines
Doktors der Naturwissenschaften
- Dr. rer. nat. -

dem Fachbereich Biologie/Chemie der
Universität Bremen
vorgelegt von

Cécilia Wentrup

Bremen
September 2012

Front cover image: Cross section through the posterior most part of a gill of *Bathymodiolus puteoserpentis* (by A. Wendeberg)

Back cover image: *Olavius algarvensis* under the dissecting scope (by C. Wentrup)

Die Untersuchungen zur vorliegenden Arbeit wurden in der Symbiose-Gruppe am Max-Planck-Institut für Marine Mikrobiologie in Bremen durchgeführt.

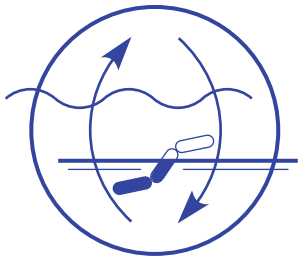

1. Gutachter: Prof. Dr. Nicole Dubilier
2. Gutachter: Prof. Dr. Monika Bright

Tag des Promotionskolloquiums: 26.10.2012

Table of content

Summary

Chemosynthetic symbioses evolved multiple times in a wide diversity of host species and from many different bacterial lineages. The symbionts provide nutrition to the hosts by fixing CO_2 into biomass using reduced inorganic compounds as energy sources. This gives the hosts a physiological advantage to colonize and thrive in nutrient poor habitats. Two key questions that have emerged in symbiosis research are 1) how do the hosts acquire their symbionts and 2) what reduced compounds can be used by the symbionts as energy source to fix CO_2 into biomass. This PhD thesis consists of two parts that will each deal with one of these two fundamental questions.

In the first part of this thesis, two manuscripts describe the symbiont colonization of host tissues in the deep-sea mussel *Bathymodiolus* from hydrothermal vents. *Bathymodiolus* harbors its chemosynthetic symbionts intracellularly in gill tissues and, as in all bivalves, the gills grow throughout the mussel's life. This raises the question how the newly developed gill tissues are colonized by symbionts. Symbiont colonization of newly formed gill tissues was investigated using fluorescence in situ hybridization with symbiont-specific probes on semi-thin sections of whole juveniles. In addition, posterior ends of adult gills were also analyzed, as new gill filament formation occurs here. In the smallest juveniles, symbionts had colonized a wide range of epithelial tissues, revealing a widespread distribution of symbionts in many different juvenile organs. In contrast, juveniles larger than 9 mm had symbionts only in their gills. These observations indicate an ontogenetic shift in symbiont colonization from an indiscriminate infection of almost all epithelia in early life stages to spatially restricted colonization of gills in later developmental stages of *Bathymodiolus*. Analyses of the posterior end of both juvenile and adult gill tissues further showed that all gill filaments except the first most recently formed 7 to 9 filaments harbored symbionts. Newly formed gill tissues of *Bathymodiolus* are thus initially symbiont free and only later become infected with symbionts as they extend and differentiate, suggesting a life long *de novo* colonization by the endosymbionts of aposymbiotic host cells.

In the second part of this thesis I investigated the physiological capabilities of the symbionts of *Olavius algarvensis.* This marine worm lacks both a digestive and excretory system. Instead it relies on a symbiotic community of two gammaproteobacterial sulfur oxidizers, two deltaproteobacterial sulfate reducers, and a spirochete for nutrition and waste recycling. External energy sources for the symbiotic association have remained enigmatic because of extremely low concentrations of reduced sulfur compounds and organic substrates in the worms' habitat. Using a metaproteomic approach and incubation experiments I showed that hydrogen (H_2) and carbon monoxide (CO) are additional energy sources for the symbiosis of *O. algarvensis*. The finding of elevated CO and H_2 concentrations in the worm's habitat further confirmed the ecological importance of both substrates for the worm symbiosis. One of the sulfur-oxidizing symbionts incorporated high amounts of CO_2 into its biomass in the presence of CO, which was determined using ^{13}C-labeled bicarbonate in the incubation medium and subsequent nanoSIMS analyses. The metaproteomic study further revealed a high expression of proteins involved in highly efficient pathways and high-affinity uptake transporters for the recycling and conservation of energy, nitrogen, and carbon sources. This indicates that the nutrient-poor nature of the worm's habitat exerted a strong selective pressure in shaping this association.

Zusammenfassung

Chemosynthetische Symbiosen sind mehrfach in verschiedenen Wirten und mit verschiedenen bakteriellen Symbionten entstanden. Die Symbionten versorgen dabei ihren Wirt mit Nahrung, indem sie chemische Energie aus reduzierten inorganischen Verbindungen nutzen, um CO_2 in Biomasse umzuwandeln. Auf diese Weise ist es den Wirten möglich, nahrungsarme Lebensräume zu besiedeln. Zwei wichtige Fragen in der Symbioseforschung sind 1) wie die Wirte ihre lebensnotwendigen Symbionten aufnehmen und 2) welche reduzierten Verbindungen die Symbionten als Energiequellen nutzen können. Diese Arbeit besteht aus zwei Teilen, die sich jeweils mit einer der beiden Fragen beschäftigen.

Der erste Teil umfasst zwei Manuskripte, die die Symbiontenbesiedelung im Gewebe der Tiefseemuschel *Bathymodiolus* beschreiben. Diese Muschel mit intrazellulären chemosynthetischen Symbionten im Kiemengewebe kommt an Hydrothermalquellen vor. Ihre Kiemen wachsen, wie in allen anderen Bivalven, ein Leben lang. In dieser Arbeit wurde mittels Fluoreszenz *in situ* Hybridisierung mit Symbionten-spezifischen Sonden auf Semi-Dünnschnitten von ganzen juvenilen Muscheln untersucht, wie neu gebildetes Kiemengewebe von den Symbionten besiedelt wird. In den kleinsten juvenilen Muscheln besiedelten die Symbionten das Epithelgewebe zahlreicher Organe. Im Gegensatz dazu waren die Symbionten in Juvenilen, die größer als 9 mm waren, nur in den Kiemen zu finden. Dies deutet auf eine ontogenetische Veränderung der Symbiontenbesiedelung des Wirtsgewebes hin. Die Infektion verschiebt sich dabei von einer breiten, fast alle Organe umfassenden in frühen Stadien zu einer auf das Kiemengewebe beschränkten in späteren Entwicklungsstadien. Zusätzliche Untersuchungen der hinteren Kiemenenden von juvenilen und adulten Muscheln zeigten außerdem, dass alle Kiemenfilamente, bis auf die jüngsten 7 bis 9 Filamente, Symbionten enthielten. Dies deutet auf eine lebenslange Neubesiedelung von Kiemenzellen durch die Symbionten hin, bei der neu gebildetes Kiemengewebe anfänglich keine Symbionten enthält und erst zu einem späteren Zeitpunkt von den Symbionten besiedelt wird.

In dem zweiten Teil dieser Arbeit habe ich die physiologischen Fähigkeiten der Symbionten des Wurms *Olavius algarvensis* untersucht. Dieser Wurm ohne Verdauungs- und Exkretionssystem beherbergt zwei schwefeloxidierende Gammaproteobakterien und zwei sulfatreduzierende Deltaproteobakterien, die ihn ernähren und seine Abfallprodukte wiederverwerten. Die Energiequellen dieser symbiotischen Gemeinschaft waren bisher unbekannt, da die Konzentrationen an reduzierten Schwefelverbindungen und organischen Substraten im Lebensraum des Wurms sehr niedrig sind. Eine metaproteomische Analyse der Symbionten sowie Inkubationsexperimente mit ganzen Würmern und ihren Symbionten haben gezeigt, dass Wasserstoff (H_2) und Kohlenmonoxid (CO) zusätzliche Energiequellen für diese Symbiose sein können. Die ökologische Relevanz dieser Substrate für die Symbiose wurde durch erhöhter H_2 und CO Konzentrationen im Wurmhabitat bestätigt. Mittels ^{13}C-makiertem CO_2 im Inkubationsmedium und einer anschließenden nanoSIMS-Analyse wurde außerdem gezeigt, dass einer der schwefeloxidierenden Symbioten mit CO vermehrt CO_2 in seine Biomasse fixierte. Das Metaproteom zeigte weiterhin stark exprimierte Proteine, die in höchst effizienten Stoffwechselwegen und hoch-affinen Aufnahmetransportern für das Wiederverwerten und Konservieren von Energie-, Stickstoff- und Kohlenstoffquellen eine wichtige Rollen spielen. Dies deutet darauf hin, dass das nährstoffarme Habitat des Wurms als eine stark selektierende Kraft auf diese Symbiose wirkt.

List of abbreviations

ASW	artificial seawater
ATP	adenosine triphosphate
CARD	catalyzed reporter deposition
CO	carbon monoxide
CODH	carbon monoxide dehydrogenase
COI	cytochrome oxidase subunit I
DAPI	4',6-diamidino-2-phenylindol
DNA	deoxyribonucleic acid
et al.	and others
FISH	fluorescence in situ hybridization
H_2	hydrogen
MAR	Mid-Atlantic Ridge
PBS	phosphate-buffered saline
PCR	polymerase chain reaction
PHA	polyhydroxyalkanoate
reductive acetyl CoA	reductive acetyl coenzyme A
RNA	ribonucleic acid
mRNA	messenger RNA
rRNA	ribosomal RNA
SEM	scanning electron microscopy
TEM	transmission electron microscopy

Chapter 1: State of the Art

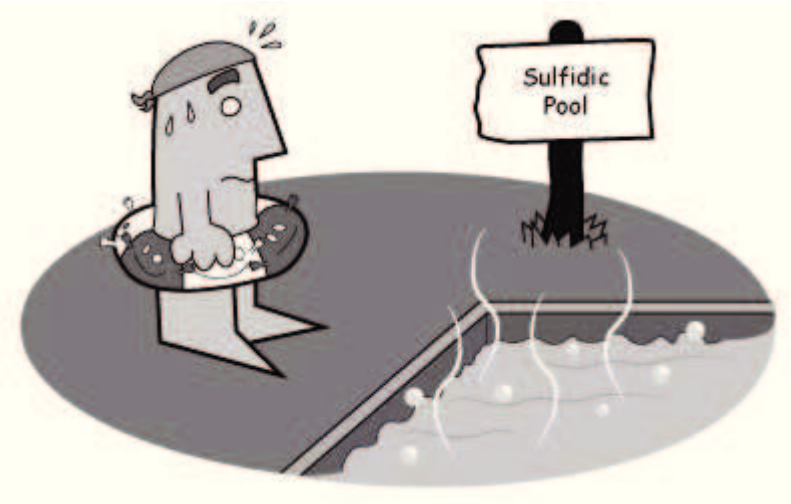

“What can go wrong with a symbiont buoy?”

1.1 Symbiosis

The term symbiosis comes from the ancient Greek syn "with" and biosis "living". It describes a close, long-term or persistent relationship of two or more different species that live together, regardless of the effect their interactions may have on one another's fitness (de Bary, 1879; Frank, 1877; McFall-Ngai, 2002). However, the following modifiers can be used to specify different types of symbiotic associations: 1) beneficial or mutualistic for symbioses in which all symbiotic partners benefit from the association and increase their fitness, 2) neutral or commensalistic for symbioses in which one partner benefits and the other is neither harmed nor benefited and 3) harmful or parasitic for symbioses in which one of the organisms exploits the other and thereby significantly decreases its partner's fitness. The nature of an association is not always fixed. For example, a mutualistic symbiosis can change to an exploitative parasitism with changing environmental conditions (Sapp, 1994). In this thesis I will use the term symbiosis as "a long-term association between two or more organisms of different species that is integrated at the behavioral, metabolic or genetic level" (Moya *et al.*, 2008).

To distinguish between the different partners of a symbiotic association, I will use the term "host" for the larger partner and "symbiont(s)" for the smaller partner(s) as suggested by Starr (1975). Furthermore, depending on where the hosts harbor their symbionts, I will refer to symbionts as ecto- or endosymbionts (Starr, 1975). Ectosymbionts live attached to the outside of their hosts' surfaces, while endosymbionts live inside their hosts either intra- or extracellularly. Intracellular endosymbionts live inside host cells and extracellular endosymbionts live outside host cells in the extracellular space.

1.2 Symbiosis – a driving force in evolution

Symbioses exist among and between species of all three domains of life and they are thought to have a major impact on the evolution, development and physiology of the species involved (Boetius *et al.*, 2000; Kouris *et al.*, 2007; Margulis & Fester, 1991; McFall-Ngai, 2001, 2002; Moya *et al.*, 2008; Paracer & Ahmadjian, 2000; Stewart *et al.*, 2005). The symbiotic origin of eukaryotes is one of the most well known examples for the evolutionary success of symbiosis. Mitochondria and plastids, e.g. chloroplasts, originated from free-living bacteria that were taken up inside another cell. Both cells engaged in an intimate relationship that led to such a strong dependence on one another over time that their genomes became incorporated into one multicellular organism (Margulis, 1970; Margulis, 1993; Szathmary & Smith, 1995).

It has been proposed that the establishment of interdependent relationships between two cells might have been triggered by metabolic cross-feeding (syntrophy) of two dissimilar cells (i.e. one cell type feeding on the metabolic products of another cell type) (Schink & Stams, 2006; Stahl *et al.*, 2006). Besides syntrophy, intimate relationships between different cell types might also have evolved from direct physical contact between two cells, or through the transfer of a chemical signal from one cell to another (Kaiser, 2006). In all three scenarios, mutation, gene transfer and natural selection on both partners would have played their role in shaping and improving the interactions between these cells resulting in successful symbioses. Deep-sea mussels and shallow water oligochaete symbioses are examples for such successful symbioses and they will be presented in detail in the sections 1.5 and 1.6 of this introduction.

1.3 Maintenance of a symbiosis – transmission of symbionts

To maintain symbioses, symbionts have to be transmitted to each new host generation (Bright & Bulgheresi, 2010; Cavanaugh *et al.*, 2006; Dubilier *et al.*, 2008; Vrijenhoek, 2010). This can be achieved in two ways. Firstly, hosts can acquire their symbionts from co-occurring hosts or from a free-living symbiont population in the environment (Gros *et al.*, 2003; Harmer *et al.*, 2008; Nussbaumer *et al.*, 2006; Won *et al.*, 2003). This is termed horizontal transmission. Secondly, the host can pass on its symbionts directly to its offspring, for example through its germ lines (Cary, 1994; Cary & Giovannoni, 1993; Endow & Ohta, 1990; Gustafson & Reid, 1988; Krueger *et al.*, 1996; Peek *et al.*, 1998). This is termed vertical transmission. Vertical transmission ensures that offspring are equipped with the appropriate symbiont from the beginning, but it bears the cost that the dispersing offspring might not carry the optimal bacterial strain required in the particular environment the host settles in. Horizontal transmission, on the other hand, can benefit the host by enabling it to acquire symbiont strains that are optimally adapted to the environment, assuming that the respective symbionts occur as free-living stages in the environment the aposymbiotic host colonizes.

In some hosts, mixed transmission modes occur in which symbionts can be acquired through both horizontal and vertical transmission. Vesicomyid symbionts for example are predominantly passed on directly from one clam generation to the next (Peek *et al.*, 1998), but in one vesicoymid species, a second less abundant symbiont strain was apparently acquired horizontally during an earlier period of this host species evolution (Stewart & Cavanaugh, 2009; Stewart *et al.*, 2008). In hosts that regularly harbor multiple symbiont strains such as the gutless oligochaetes (see section 1.6.2 for more information), mixed transmission might occur very often or possibly every generation, with some of the symbionts acquired directly from the parent and others from the environment (Dubilier *et al.*, 2006).

The effects of vertical and horizontal transmission on symbiont diversity, genome evolution and symbiont-host specificity differ greatly (Dale *et al.*, 2003; McCutcheon & Moran, 2007; Moran, 2007; Moran *et al.*, 2008; Moran *et al.*, 2009; Sachs & Wilcox, 2006; Stewart *et al.*, 2008). Strictly vertically transmitted symbionts for example spend their entire life 'trapped' inside a host, disconnected from free-living bacterial populations that could allow genetic recombination. In addition, because only a few symbiont cells are actually transmitted to the next host generation, the symbiont population experiences an increasing genetic drift due to the population bottleneck during transmission. The consequences are the accumulation of slightly deleterious mutations in non-essential genes and the loss of genes that have become superfluous for the obligate symbiotic life style of the symbionts (examples include genes required for mobility, cell division and cell envelope) (Kuwahara *et al.*, 2008; Kuwahara *et al.*, 2007; Moran, 2003; Newton *et al.*, 2007). In addition proliferation of pseudogenes, genome rearrangements, and ultimately genome reduction due to the loss of genes or entire gene fragments have been proposed to be mediated by mobile elements, which have been reported to increase in frequency after a bacterium adapts to an intracellular or pathogenic lifestyle (Bordenstein & Reznikoff, 2005; Dobrindt *et al.*, 2004; Moran & Plague, 2004; Parkhill *et al.*, 2003; Siguier *et al.*, 2006; Wernegreen, 2005).

Strictly vertically transmitted symbionts therefore have typically reduced genomes with a higher mutation rate at non-coding sites than their free-living relatives. These symbionts are no longer able to survive on their own in the environment. In contrast, horizontally transmitted symbionts do not experience genome reduction, because they live in a large environmental population that gives them access to a large gene pool through genetic recombination and because they can not 'afford' to have reduced genomes during their free-living stage (e.g. Dubilier *et al.*, 2008).

1.4 Chemosynthetic symbioses

1.4.1 Chemosynthesis

Microorganisms can use two different kinds of energy sources to fix one-carbon molecules such as carbon dioxide into organic matter. They can either use light (photosynthesis) or chemical energy (chemosynthesis). Unlike photosynthesis that can be carried out by bacteria, archaea and eukaryotes, chemosynthesis is a process that can only be carried out by bacteria and archaea. The bacteria and archaea gain the chemical energy through redox reactions in which electrons are transferred from a reduced compound (the electron donor) to an oxidized compound (the electron acceptor) with the help of enzymes. The energy yield per reaction depends on the difference in the redox potential between electron donor and electron acceptor and on their availability (concentration). Energetically favorable reactions that can lead to the fixation of carbon are for example sulfide and methane oxidation (Table 1). Chemosynthetic organisms can be either chemolithoautotrophs that use inorganic chemicals as electron donors and carbon dioxide as carbon source or chemoorganoheterotrophs that use methane as both electron donor and carbon source.

Table 1: Some energetically favorable redox reactions for free-living microorganisms and chemosynthetic symbionts listed according to their free energy change

Metabolism	e^--donor	e^--acceptor	Redox reaction	ΔG_0'[kJ/rnx][a]	Symbiotic bacteria[b]
Aerobic					
Methane oxidation	CH_4	O_2	$CH_4 + 2O_2 \rightarrow HCO_3^- + H^+ + H_20$	-813	yes
Sulfide oxidation	H_2S	O_2	$H_2S + 2O_2 \rightarrow SO_4^{2-} + 2H^+$	-796	yes
Carbon monoxide oxidation	CO	O_2	$CO + 0.5O_2 \rightarrow CO_2$	-257	
Nitrification	NH_3	O_2	$NH_3 + 1.5O_2 \rightarrow NO_2^- + H_2O$	-248	
Hydrogen oxidation	H_2	O_2	$H_2 + 0.5O_2 \rightarrow H_2O$	-237	yes
Manganese oxidation	Mn^{2+}	O_2	$Mn^{2+} + 0.5O_2 + H_2O \rightarrow MnO_2 + 2H^+$	-71	
Iron oxidation	Fe^{2+}	O_2	$Fe^{2+} + 0.5O_2 + H^+ \rightarrow Fe^{3+} + 0.5H_2O$	-81	
Anaerobic					
Sulfide oxidation/ Nitrate reduction	HS^-	NO_3^-	$5HS^- + 8NO_3^- + 3H^+ \rightarrow 5SO_4^{2-} + 4N_2 + 4H_2O$	-3722	yes
CO oxidation/ Sulfate reduction	CO	SO_4^{2-}	$4CO + SO_4^{2-} + H^+ \rightarrow H_2S + 4\ CO_2$	-272	
CO oxidation/ Nitrate reduction	CO	NO_3^-	$CO + NO_3^- \rightarrow CO_2 + NO_2^-$	-183	
Hydrogen oxidation/ Nitrate reduction	H_2	NO_3^-	$H_2 + NO_3^- \rightarrow NO_2^- + H_2O$	-163	
H_2 oxidation/ Sulfate reduction	H_2	SO_4^{2-}	$4H_2 + SO_4^{2-} + H^+ \rightarrow HS^- + 4H_2O$	-152	yes
Methanogenesis	H_2	CO_2	$4H_2 + CO_2 \rightarrow CH_4 + 2H_2O$	-131	
Fumarate respiration	H_2	Fumarate	H_2 + Fumarate → Succinate	-86	

[a] energy available (ΔG_0') in kJ per reaction
[b] 'yes' indicates that this metabolism has been identified in symbiotic bacteria

1.4.2 Chemosynthetic symbionts

So far chemosynthetic symbionts have been shown to use sulfide, methane and hydrogen as electron donors and oxygen, nitrate and sulfate as electron acceptors. Other energy sources such as carbon monoxide, iron, manganese, and ammonia have been considered, but they have not yet been conclusively shown to be used by chemosynthetic symbionts (Cavanaugh *et al.*, 2006; Kleiner *et al.*, 2012, Chapter 4-5). Electron donors and acceptors for chemosynthetic symbionts have been inferred from incubations with the respective substrate (Cary *et al.*, 1988; Cavanaugh *et al.*, 2006; Childress *et al.*, 1986; Childress *et al.*, 1991;

Dubilier *et al.*, 2001; Fisher & Childress, 1992; Fisher *et al.*, 1988; Fisher *et al.*, 1987; Petersen *et al.*, 2011; Watsuji *et al.*, 2010) as well as the detection and expression of marker genes involved in chemosynthetic pathways (Cavanaugh *et al.*, 2006; Elsaied *et al.*, 2006; Fiala-Médioni *et al.*, 2002; Markert *et al.*, 2007; Petersen *et al.*, 2011; Stewart *et al.*, 2011; Stewart *et al.*, 2005; Wendeberg *et al.*, 2012). Examples for proteins encoded by marker genes that are involved in chemosynthetic pathways include the ribulose-1,5-bisphosphate carboxylase/ oxygenase of the Calvin-Benson-Bassham-cycle for autotrophy, the methane monooxygenase for methanotrophy, the dissimilatory adenosine-5′-phosphosulfate reductase for thiotrophy and the NiFe-hydrogenase for hydrogen oxidation.

1.4.3 Chemosynthetic symbioses and their habitats

In 1977 the first deep-sea hydrothermal vent with large communities of invertebrate animals was discovered (Figure 1). This finding was astonishing, because until then life in the deep-sea was assumed to be a dark, hostile, and nutrient limited environment unable to support large animal communities. This view changed when researchers analyzed the geochemistry of the hydrothermal vent fluids and found high concentrations of reduced compounds that were able to sustain free-living chemosynthetic microorganisms (Jannasch & Wirsen, 1979; Ruby *et al.*, 1981). Later anatomical and ultrastructural analyses of the deep-sea hydrothermal vent fauna (Cavanaugh *et al.*, 1981; Felbeck, 1981; Rau, 1981) revealed that a wide variety of marine invertebrates lived in symbiosis with such chemosynthetic bacteria (van Dover, 2000).

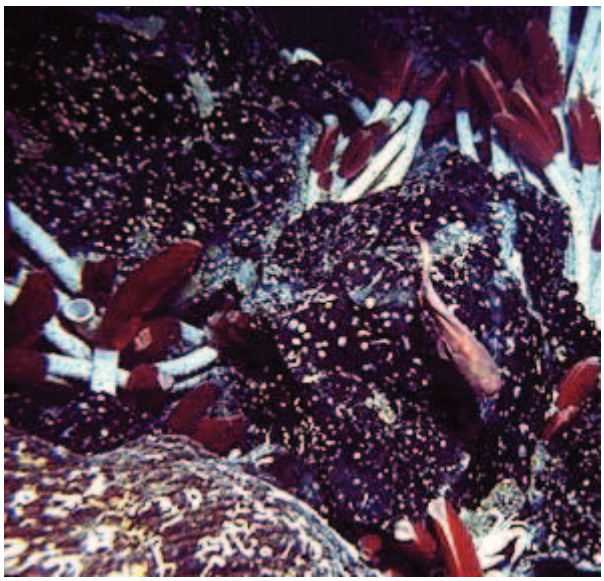

Figure 1: Tubeworms (*Riftia pachyptila*), a white Galatheid crab, and a pink fish gather at a Galápagos Rift vent site. (http://www.divediscover.whoi.edu/ventcd/vent_discovery)

Inspired by the discovery of chemosynthetic symbioses at hydrothermal vents, scientists looked for similar symbioses in other marine habitats. Chemosynthetic symbioses have now been found in many different environments including reducing sediments on continental margins, cold seeps, mud volcanoes, whale and wood falls, coral reef sediments, tidal mud flats and mangrove swamps as well as shallow-water coastal sediments (Figure 2) (Dubilier *et al.*, 2008). All these habitats provide reduced compounds to their chemosynthetic inhabitants such as sulfide (in this thesis, the term sulfide refers to total dissolved sulfide: H_2S, HS^- and S^{2-}), methane, and hydrogen. These compounds are produced either through abiotic processes such as water-rock reactions at high temperatures and pressures (German & Lin, 2004; Stein & Stein, 1994) or biotic processes such as the anaerobic degradation of organic matter (Schink & Stams, 2006). Instead of being anaerobically decomposed organic matter can also be buried, compressed over time, and exposed to high temperature to form reduced compounds such as for example thermogenic methane (Schoell, 1988). The electron acceptors required by the symbionts for the oxidation of these reduced compounds, such as oxygen and nitrate are usually available in the surrounding or overlying seawater.

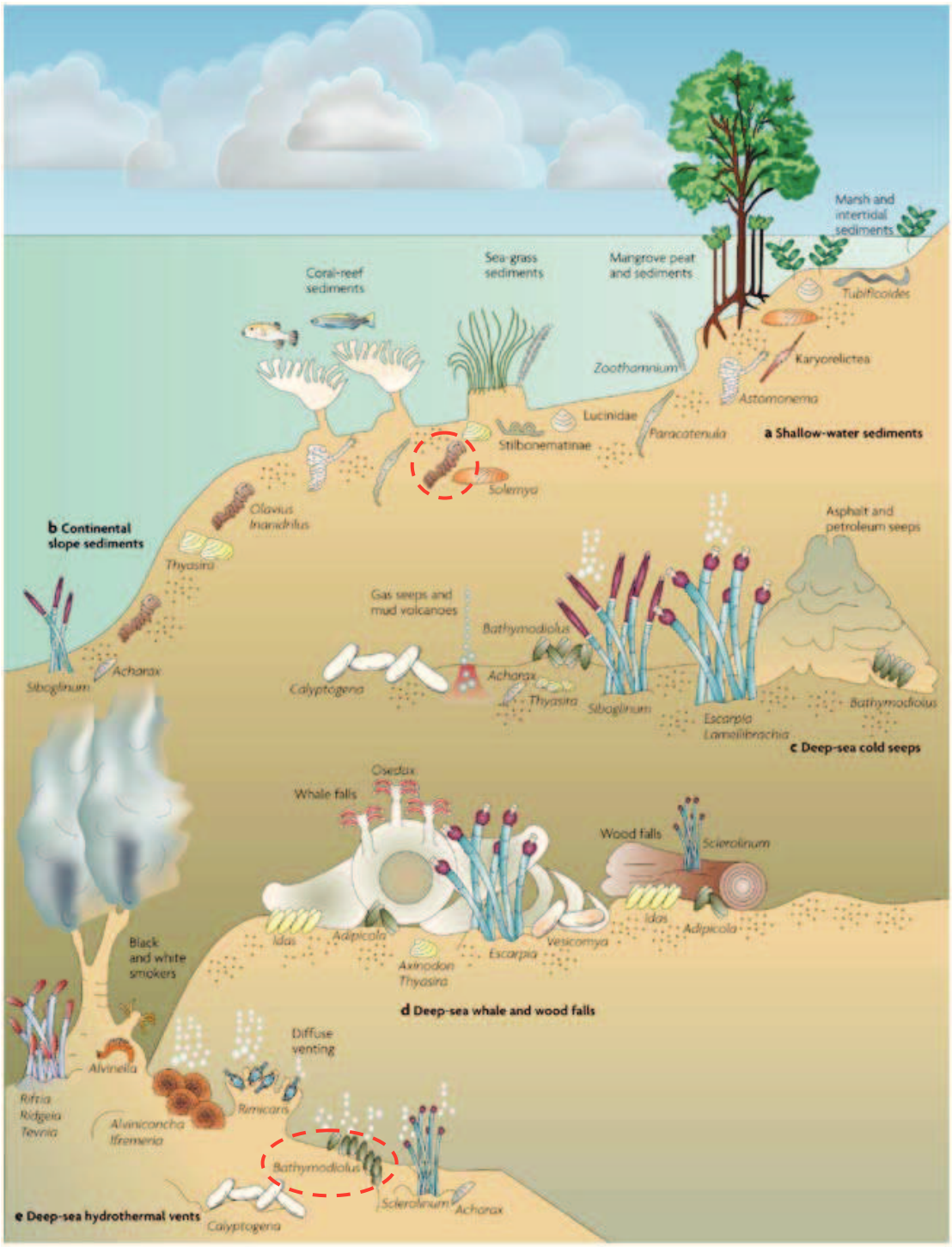

Figure 2: Habitats of chemosynthetic symbioses. Chemosynthetic symbioses occur in a wide range of marine habitats, including shallow-water sediments (a), continental slope sediments (b), cold seeps (c), whale and wood falls (d), and hydrothermal vents (e). Some host groups are found in only one habitat (such as *Osedax* on whale bones), whereas others occur in several different environments (such as thyasirid clams, which are found in shallow-water sea-grass sediments and in the deep-sea at cold seeps, whale falls and hydrothermal vents). The animals are not drawn to scale; for example, *Idas* and *Adipicola* mussels are much smaller than *Bathymodiolus* mussels. Organisms investigated during this PhD study, the gutless oligochaete *Olavius algarvensis* and the deep-sea hydrothermal vent mussels *Bathymodiolus puteoserpentis* and *B. azoricus* are circled in red. (Modified from Dubilier *et al.*, 2008)

1.4.4 Chemosynthetic symbioses – diversity of hosts and symbionts

Symbioses between marine invertebrates and their chemosynthetic symbionts are mutualistic and evidently very successful, since at least seven different host phyla (Ciliophora, Annelida, Platyhelminthes, Arthropoda, Mollusca, Nematoda and Porifera) are associated with chemosynthetic symbionts (Dubilier *et al.*, 2008; Gruber-Vodicka *et al.*, 2011; Petersen *et al.*, 2010; Ruehland & Dubilier, 2010; Verna *et al.*, 2010). In these associations benefits for the partners can include protection and defense against predators and toxic compounds, mobility, a stable environment, recycling of waste products, and nutritional and energy supply (Cavanaugh *et al.*, 2006; Dubilier *et al.*, 2006; Moran, 2007; Moya *et al.*, 2008; Stahl *et al.*, 2006). In addition most hosts have also developed behavioral, morphological or metabolic adaptations for harboring their symbionts and providing them with electron donors and acceptors (reviewed in Cavanaugh *et al.*, 2006 and ; Dubilier *et al.*, 2008), which are often temporarily or spatially separated, due to consumption or in the case of sulfide rapid precipitation by iron and other metals and spontaneous oxidation in the presence of oxygen (Fisher, 1996; Schmidt *et al.*, 2008; Zhang & Millero, 1993). The host receives its nutrition from the symbiont via transfer of organic compounds or lysis of symbiont cells. This allows the host to thrive in environments that many non-symbiotic animals cannot easily colonize such as habitats in which organic matter is limiting.

Most chemosynthetic symbionts belong to the Gammaproteobacteria (Figure 5a) and the two main functional groups are: the sulfur-oxidizing (or thiotrophic) symbionts and the methane-oxidizing (methanotrophic) symbionts (Cavanaugh *et al.*, 2006; Distel & Cavanaugh, 1994; Dubilier *et al.*, 2008). However, sulfur-oxidizing symbionts belonging to the Epsilon- and Alphaproteobacteria have also been described (Dubilier *et al.*, 2008; Gruber-Vodicka *et al.*, 2011; Ruehland & Dubilier, 2010). Some host species are associated with additional symbionts that do not necessarily have the capability to live chemosynthetically or whose

metabolisms are still not known. These additional symbionts belong to the Alpha-, Gamma-, or Deltaproteobacteria, the Bacteroidetes, and the Spirochaetes. Harboring a variety of bacterial symbionts might be advantageous over harboring a single symbiont by providing access to a broader range of resources (Blazejak *et al.*, 2005; Blazejak *et al.*, 2006; Dubilier *et al.*, 2006; Duperron *et al.*, 2008; Duperron *et al.*, 2007; Ruehland *et al.*, 2008).

In the following sections I will focus on the chemosynthetic symbioses that have been the subject of my PhD thesis. I will first describe bivalves that live in symbiosis with chemosynthetic bacteria and in particular the deep-sea hydrothermal vent mussel *Bathymodiolus* with its sulfur-oxidizing and methane-oxidizing endosymbionts. I will then introduce the gutless worm *Olavius algarvensis*, which lives with five different bacterial endosymbionts in Mediterranean coastal sediments off the island Elba in Italy.

1.5 Bivalves with chemosynthetic symbionts

1.5.1 Occurrence of bivalves with chemosynthetic symbionts

Bathymodiolus mussels and *Calyptogena* clams from hydrothermal vents in the deep-sea were one of the first bivalves in which chemosynthetic symbionts were described (Boss & Turner, 1980; Cavanaugh, 1983; Fiala-Médioni & Metivier, 1986; Fiala-Médioni *et al.*, 1986; Kenk & B.R., 1985). Until now these symbionts have been shown to use sulfide, methane, and hydrogen as energy sources to sustain their hosts in the deep-sea (Cavanaugh *et al.*, 2006; Petersen *et al.*, 2011). After the discovery of chemosynthetic symbionts in bivalves at hydrothermal vents, hundreds of other bivalves with chemosynthetic symbionts were described from all over the world inhabiting numerous reducing environments such as sands and muds, mangrove sediments, sea grass beds, areas of sunken vegetation including wood

and bones, offshore sewage sites as well as cold seeps (Figure 2) (Cavanaugh, 1983; Cavanaugh *et al.*, 2006; Dubilier *et al.*, 2008; Taylor *et al.*, 2010).

1.5.2 Phylogeny of bivalves with chemosynthetic symbionts

Bivalves with chemosynthetic symbionts are known from six distinct families: Solemyidae, Nucinellidae, Mytilidae, Lucinidae, Thyasiridae, and Vesicomyidae (Figure 3). Of these, symbiosis has been identified so far in all species of Solemyidae (Stewart & Cavanaugh, 2006), Lucinidae (Glover & Taylor, 2007; Glover *et al.*, 2008; Taylor & Glover, 2006) and Vesicomyidae (Krylova *et al.*, 2010; Taylor *et al.*, 2010). In the Thyasiridae many species established a symbiosis, while others did not (Dufour, 2005), and in the family of Mytilidae only members of the subfamily Bathymodiolinae have symbionts (Duperron, 2010). A symbiotic association has additionally been inferred from morphological analysis of two species of the Nucinellidae, but very little is known about these symbioses (Reid, 1980). Phylogenetic analyses of the bivalve hosts indicated that the acquisition of chemosynthetic bacteria evolved independently at least five times (Figure 3) (Taylor *et al.*, 2010).

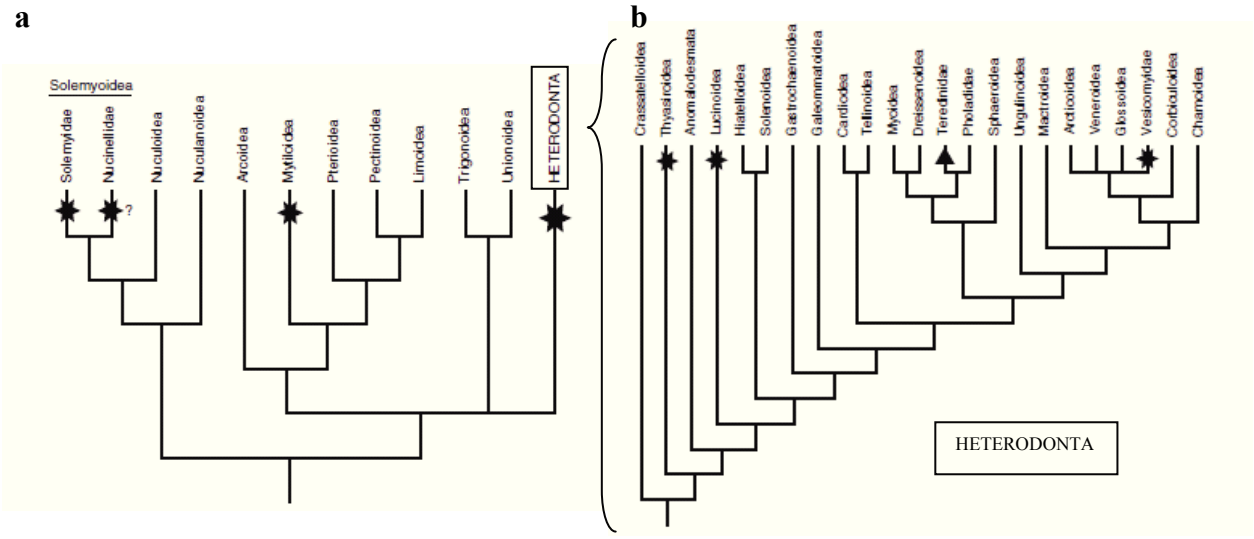

Figure 3: Phylogeny of chemosynthetic bivalves. (a) Phylogenetic tree of bivalve superfamilies. Families with chemosymbionts with star. (b) Phylogenetic tree of Heterodonta families. Families with chemosymbionts with star, cellulolytic symbionts with triangle. (Modified from Taylor *et al.*, 2010)

1.5.3 Morphological adaptations of bivalves to the symbiosis

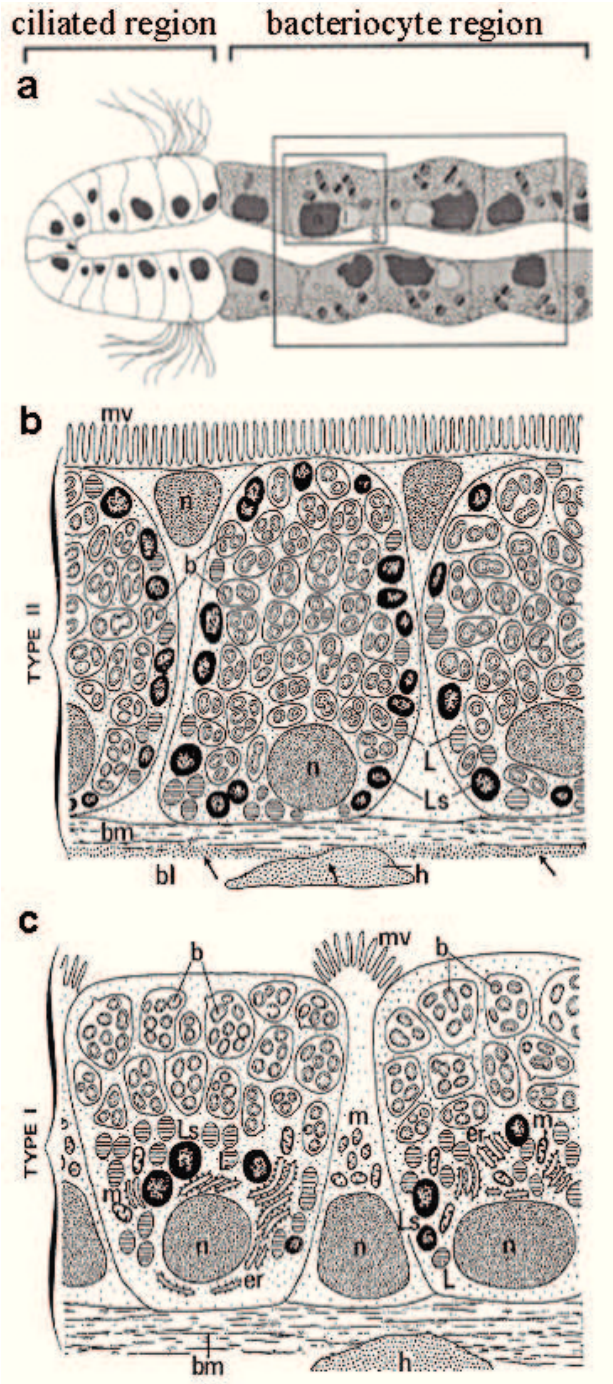

Figure 4: Simplified cell arrangement in gills of chemosynthetic bivalves. (a) Typical gill filament of chemosynthetic bivalves. (b, c) Bacteriocyte region of a Vesicomyidae species, representative for all other chemosynthetic bivalves (b) and *Bathymodiolus* (c). The bacteriocytes in (b) and (c) are separated by intercalary cells. Note that the bacteriocytes harbor only sulfur-oxidizing bacteria. Abbreviations: b, bacteria; bm, basal membrane; er, endoplamatic reticulum; L, lipids; Ls, lysosomes; m, mitochondria; mv, microvilli; n, nucleus; h, hemocyte; s, blood sinus. (From Distel *et al.*, 1995; Fiala-Médioni & Le Pennec, 1987)

Bivalves that harbor chemosynthetic symbionts show morphological differences in comparison to close relatives that do not harbor symbionts. The most apparent changes occurred in the digestive system and the gills, the respiratory organs of bivalves. The digestive system is usually simplified or even completely reduced in bivalves living with chemosynthetic symbionts in comparison to non-symbiotic bivalves reflecting the nutritional reliance of these animals on their symbionts (reviewed in Cavanaugh *et al.*, 2006). With the reduction of the digestive system also goes along the inability to filter-feed as effectively as related bivalves that do not have symbionts (Page *et al.*, 1990; von Cosel, 2002). The gills, which are the symbiont bearing organs, are usually enlarged in comparison to non-symbiotic bivalves (Cavanaugh *et al.*, 2006; Distel, 1998; Taylor *et al.*, 2010). All bivalves with chemosynthetic symbionts have modified their gills in a similar manner to harbor their

symbionts. This is remarkable given that the acquisition of the symbionts evolved independently at least five times in very different bivalve species (Figure 3). The ciliated region (Figure 4a) at the frontal side of the gill filaments is similar to non-symbiotic bivalves. However, unlike non-symbiotic bivalves the entire gill filaments, but their ciliated frontal parts contain bacteriocytes on either side of a central blood or hemolymph space. Bacteriocytes are specialized gill cells that house the symbionts (Figure 4b-c). Most symbiotic bivalves harbor their chemosynthetic bacteria inside these bacteriocytes as intracellular endosymbionts (Figure 4) and only some species of symbiotic Thyasiridae and the bathymodiolin species *Idas* and *Adipicola* harbor ectosymbionts outside their gill cells attached to microvilli (Dufour, 2005; Duperron, 2010; Fujiwara *et al.*, 2010; Southward, 2008; Taylor *et al.*, 2010).

Bacteriocytes containing endosymbionts form the majority of the epithelial cells and they are regularly interspersed by much less abundant intercalary cells that do not contain symbionts (Figure 4b-c). Bacteriocytes and intercalary cells usually posses microvilli to increase the respiratory surface of the gills (Figure 4b) (Taylor *et al.*, 2010). Exceptions are bacteriocytes of *Bathymodiolus* mussels, which do not have microvilli (Figure 4c) (Fiala-Médioni & Le Pennec, 1987, Chapter 3).

1.5.4 Diversity and phylogeny of chemosynthetic symbionts in marine bivalves

Most symbiotic bivalves are associated with a single chemosynthetic symbiont phylotype based on 16S ribosomal RNA (rRNA) sequence analysis, which belongs to the Gammaproteobacteria (Figure 5a) (Dubilier *et al.*, 2008). These bivalve symbionts form nine clades within the Gammaproteobacteria. Some of those clades contain symbionts from a closely related group of hosts, while others like the symbionts of *Solemya* clams are spread throughout the phylogenic tree of the Gammaproteobacteria (Figure 5a). All clades of bivalve

symbionts within the Gammaproteobacteria contain sulfur-oxidizing symbionts, but one, which only comprises methane-oxidizing symbionts of bathymodiolin mussels (for exceptions, see below). The methane-oxidizing symbionts form up to six distinct clades that are interspersed with free-living bacteria (Petersen *et al.*, 2012, Appendix-A) and their closest cultivated relatives are free-living aerobic methanotrophs of the genera *Methylobacter*, *Methylosarcina*, *Methylomicrobium* (reviewed by all three Cavanaugh *et al.*, 2006; Dubilier *et al.*, 2008; Petersen & Dubilier, 2009). The sulfur-oxidizing symbionts of bathymodiolin mussels, on the other side, form at least four separate, distinct clades that are interspersed with free-living SUP05 bacteria. Their closest symbiotic relatives are the symbionts of vesicoymid clams (Figure 5b, Appendix-A) (Cavanaugh *et al.*, 2006; Distel & Cavanaugh, 1994; Dubilier *et al.*, 2008; Petersen *et al.*, 2012). Most sulfide-oxidizing symbionts of shallow water bivalves (Solemyidae, Lucinidae, and Thyasiridae) also cluster together within the Gammaproteobacteria, but their clades are distinct from the symbiont clades associated with the deep-sea bivalves (Dubilier *et al.*, 2008).

It is noteworthy that not only the symbionts of *Bathymodiolus* mussels, but of almost all bivalves form clusters that are interspersed with free-living bacteria and separated from another by clusters of free-living bacteria (Figure 5). This indicates that different bacterial species were capable of forming symbioses with bivalves independently several times (Dubilier *et al.*, 2008; Petersen *et al.*, 2012, Appendix-A).

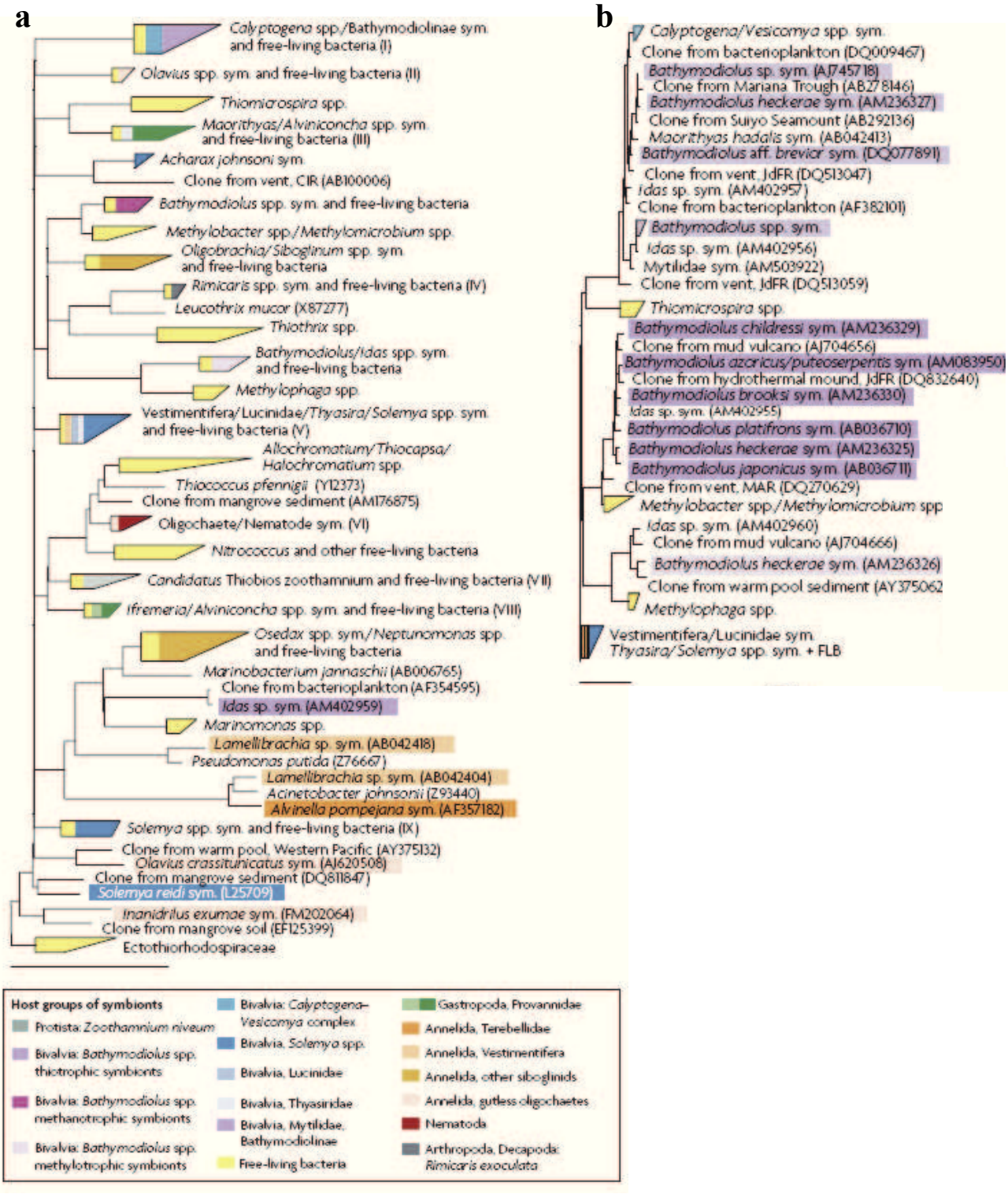

Figure 5: (a) Phylogenetic diversity of gammaproteobacterial, chemosynthetic symbionts based on their 16S ribosomal RNA gene sequences. (b) *Calyptogena* spp./Bathymodiolinae sym. from boxed sequence cluster in (a). Symbionts from the same host group are shown in the same color, and free-living bacteria are shown in yellow. Symbiont phylogeny is based on maximum likelihood analyses of 16S ribosomal RNA (rRNA) gene sequences. Sequences of almost full length were chosen from the ARB or SILVA database (release 94; March 2008), aligned and analyzed with the ARB software package. The scale bar indicates 10% estimated sequence divergence. Numbers in brackets are the accession numbers of the 16S rRNA sequences. CIR, Central Indian Ridge; I–IX, clades with chemoautotrophic symbionts. Sym., symbionts. (From Dubilier *et al.*, 2008)

1.5.5 Symbiont diversity of *Bathymodiolus* mussels

Bathymodiolus mussels occur worldwide at deep-sea hydrothermal vents and cold seeps, where they dominate the biomass due to their symbiotic associations with chemosynthetic bacteria. Depending on the species, mussels harbor either sulfur-oxidizing or methane-oxidizing symbionts or both in vacuoles inside their bacteriocytes (Distel *et al.*, 1995; Dubilier *et al.*, 2008; Duperron, 2010; Duperron *et al.*, 2006; Fiala-Médioni *et al.*, 2002; Fisher *et al.*, 1993). The sulfur-oxidizing symbionts are coccoid cells usually ~ 0.3 – 0.5 µm in diameter, while the methane-oxidizing symbionts are generally bigger coccoid cells (~ 1.5 – 2.0 µm in diameter) with intracytoplasmic membranes that are typical for type I methanotrophs (DeChaine & Cavanaugh, 2006; Duperron, 2010; Duperron *et al.*, 2008; Fisher *et al.*, 1987).

Besides the usual thiotrophic and methanotrophic symbionts, the cold-seep mussel *B. heckerae* was reported to harbor two additional endosymbiont types, a second thiotroph and a methylotrophic symbiont (Figure 5b) (Duperron *et al.*, 2007). *B. heckerae* was recently also shown to harbor a hydrocarbon degrading bacterium of the genus *Cycloclasticus* in its gills, which might use hydrocarbons as an energy and carbon source (Raggi, 2010). This diversity of symbionts may reflect the ability of deep-sea mussels to acquire symbionts that are well adapted to the environment and enable them to access a wide range of energy sources. In addition to hosting symbionts with different metabolic capacities, single individuals of *Bathymodiolus* mussels from the same population have been reported to harbor different strains of thiotrophic symbionts based on sequence differences of the rapidly evolving 16S-23S rRNA internal transcribed spacer. The different thiotrophic symbionts strains might also have slightly different metabolic capacities (DeChaine *et al.*, 2006; Won *et al.*, 2003).

1.5.6 Transmission of symbionts in chemosynthetic bivalves

Chemosynthetic bivalves have developed different transmission mechanisms to ensure that symbionts are acquired by their offspring. Transmission strategies have mainly been inferred from phylogenetic evidence (presence or absence of co-speciation between host and symbiont) or the presence of bacterial DNA in the gonads of the host. Based on these findings, the symbionts of Solemyidae and Vesicomyidae are thought to be passed on directly from one generation to the next (Cary & Giovannoni, 1993; Endow & Ohta, 1990; Hurtado *et al.*, 2003; Krueger *et al.*, 1996). However, a recent study suggested that the symbionts of vesicomyid clams are not always strictly vertically transmitted (Stewart & Cavanaugh, 2009).

Symbionts of lucinid clams and *Bathymodiolus* mussels on the other hand are thought to be acquired from the environment by each new host generation (Gros *et al.*, 1998a; Gros *et al.*, 1998b; Salerno *et al.*, 2005; Won *et al.*, 2003). This assumption is not only based on molecular evidence (DeChaine *et al.*, 2006; Gros *et al.*, 1996; Won *et al.*, 2008), but also on experimental tests. Both lucinid clams and *Bathymodiolus* mussels were able to re-establish their symbiont pool in their gills after an induced loss of symbionts in the laboratory in the presence of a symbiont population (environmental acquisition) or healthy specimens of the same bivalve species containing symbionts (intraspecific acquisition) (Elisabeth *et al.*, 2012; Gros *et al.*, 2012; Gros *et al.*, 1998b; Gros *et al.*, 2003; Kadar *et al.*, 2005). It has been hypothesized that the symbionts are taken up by the bacteriocytes via endocytosis in both bivalve species and that they later grow inside the bacteriocytes until they are digested. The mechanisms of how the bivalve host recognizes, integrates and maintains its symbiont population remain to be shown.

1.6 Gutless oligochaetes

Gutless oligochaetes are small segmented marine worms that form a monophyletic group (i.e. have descended from a single common ancestor) within the Annelida (Clitellata, Naididae, Phallodrilinae) (Erseus, 1984, 1992; Erseus *et al.*, 2002; Nylander *et al.*, 1999; Sjolin *et al.*, 2005). They lack a mouth, gut, and anus as well as nephridia (kidney-like excretory organs). While the lack of a digestive system is also known from other symbiotic animals, the reduction of an excretory system is not known from any other free-living marine animal (Dubilier *et al.*, 2006; Erséus, 1979; Giere, 1979). The reduction of the digestive and excretory systems in these small worms of 0.2 mm diameter and 10-20 mm length has evolved through their obligate association with endosymbiotic bacteria that live in an extracellular space just below the cuticle (Figure 6) (Giere, 1981; Giere *et al.*, 1991; Giere & Langheld, 1987). This symbiotic relationship has been found in more than 80 gutless oligochaete species around the world belonging to the genus *Olavius* or *Inanidrilus*. The genus *Inanidrilus* is monophyletic, while the genus *Olavius* is likely to be paraphyletic (Nylander *et al.*, 1999).

1.6.1 Occurrence of gutless oligochaetes

Most gutless oligochaetes occur in tropical and subtropical marine sediments including calcareous coral reef sediments as well as coastal sand sediments, but they have also been found in soft sediments covered by mats of sulfide-oxidizing bacteria in 300 m depth off the Peruvian coast (Figure 2) (Bright & Giere, 2005; Dubilier *et al.*, 2006; Erseus, 1984; Erseus & Bergfeldt, 2007; Erseus *et al.*, 2004; Giere & Krieger, 2001; Giere *et al.*, 1995). Most marine sediments colonized by gutless oligochaetes have a reduced zone at some depth below an oxic surface layer between which the worms are thought to migrate to supply their chemosynthetic symbionts with both reduced sulfur compounds and oxygen (Bright & Giere,

2005). However, gutless oligochaetes have also been found in the oligotrophic sediments off the coast of Elba (Italy) where only traces of hydrogen sulfide occur (Dubilier *et al.*, 2001; Kleiner *et al.*, 2012, Chapter 4). The key to their great success in colonizing such diverse habitats lies in the acquisition of remarkably diverse symbiont communities that can compensate for different microenvironments in their habitat.

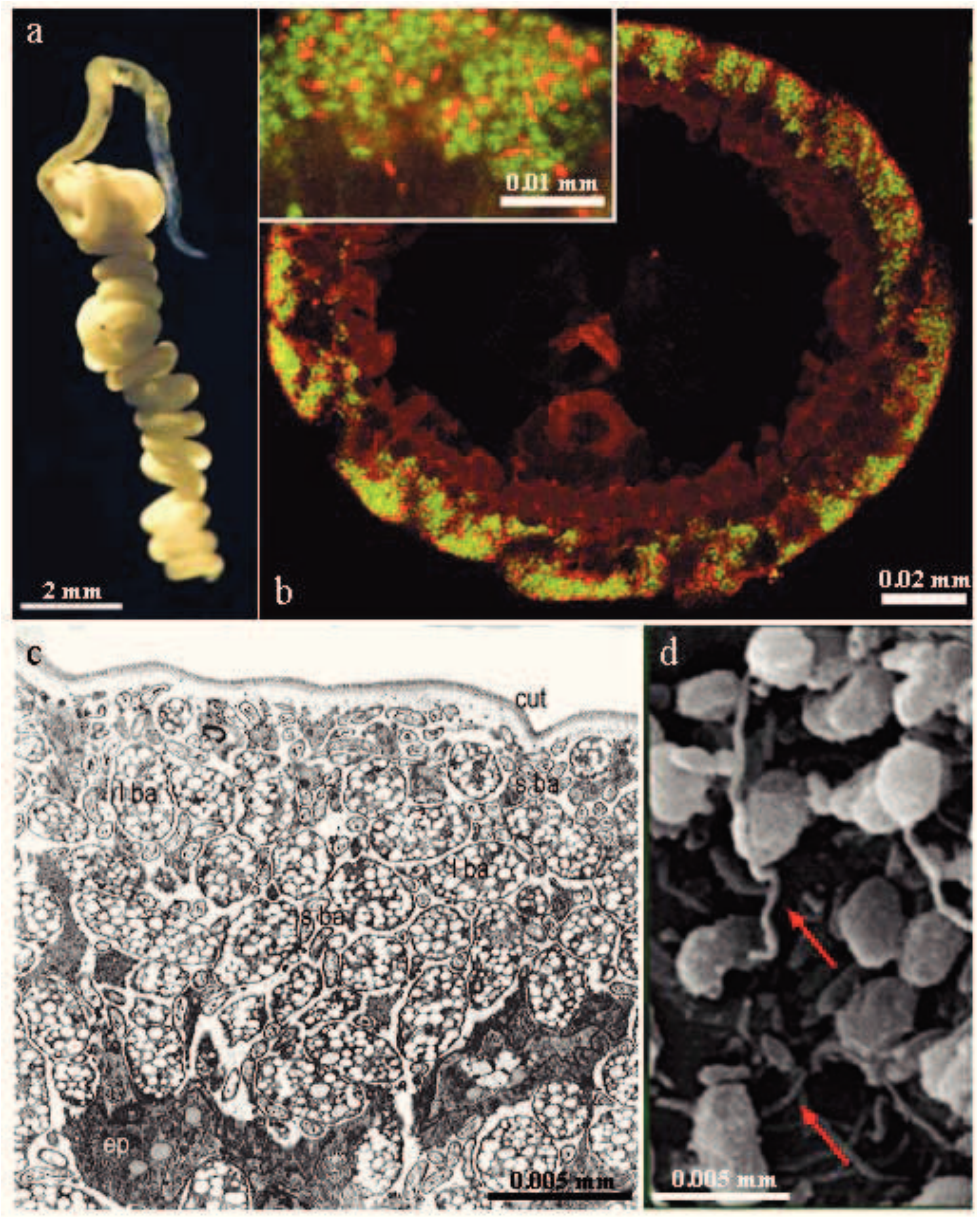

Figure 6: *O. algarvensis* and its symbionts (a) Image of a worm under the dissecting scope. The worm is white because of the sulfur and PHA granules in the symbionts just below its cuticle. (b) FISH image of a cross section through the worm showing the symbionts (sulfur-oxidizing symbionts in green, sulfate-reducing symbionts in red). (c) TEM micrograph of cross section showing symbionts with at least two different morphotypes. Granules are visible as white areas in the larger symbionts (cut, cuticle; ep, epidermal cell; lba, large bacteria; sba, small bacteria). (d) SEM micrograph of the symbionts. The large cells are the γ1-symbionts, the smaller cells are either γ3-, δ1-, or δ4- symbionts, and the long cells are the spirochetes. (From Dubilier *et al.*, 2001; Giere, 2006; Kleiner *et al.*, 2011)

1.6.2 Diversity and phylogeny of symbionts of gutless oligochaetes

The symbionts are consistently located between the cuticle and the epidermis cells of all gutless oligochaetes described so far (Dubilier *et al.*, 2008; Dubilier *et al.*, 2006). This symbiotic region is densely packed with symbionts of different morphotypes. Large oval-shaped cells with an average size of 3 x 1.5 µm are common to all gutless worms (Giere, 1985; Giere & Erseus, 2002; Giere *et al.*, 1995). They regularly have inclusion bodies that are either membrane bound storage vacuoles with polyhydroxyalkanoate (PHA) or non-membrane bound sulfur globules (Figure 6c) (Giere & Krieger, 2001; Giere & Langheld, 1987; Krieger *et al.*, 2000). Besides these large morphotypes at least two additional morphotypes have been described (Figure 6). One consists of small rod-shaped or coccoid cells with a size range of 1.1 – 1.8 x 0.32 – 0.6 µm and the other one of thin elongated cells with a size of 0.3 x 9 µm. The small morphotypes co-occur with the large cells in all host species studied so far, while the elongated filiform morphotypes have only been described in a few host species (Dubilier *et al.*, 1999; Giere & Krieger, 2001; Ruehland *et al.*, 2008). The symbiont-containing region of a gutless worm can make up to 25% of the total volume of a worm, with one million to one billion symbiont cells per worm (Giere & Langheld, 1987, personal communication with Manuel Kleiner).

The oligochaete symbiont morphotypes have been identified with molecular methods and belong to the Proteobacteria and Spirochetes (Figure 7) (Dubilier *et al.*, 2008; Dubilier *et al.*, 2006). The large morphotype was consistently identified as the primary endosymbiont belonging to the monophyletic clade of γ1-symbionts within the Gammaproteobacteria, which is closely affiliated to free-living sulfur oxidizers such as *Allochromatium vinosum* (Chromatiaceae) (Dubilier *et al.*, 2006; Dubilier *et al.*, 1995). The only exception is the primary endosymbiont of *I. exumae* from Bahamas that belongs to the gammaproteobacterial group γ4 (Bergin, 2009). The γ1-symbiont clade also contains ectosymbionts of marine

stilbonematinid nematodes, endosymbionts of *Astomonema* nematodes, and clone sequences from pelagic environments (Dubilier *et al.*, 2008; Heindl *et al.*, 2011).

Molecular analyses of the smaller, rod-shaped or coccoid cells revealed that these symbionts belong to the Alpha-, Gamma-, or Deltaproteobacteria, while the filiform symbionts belong to the Spirochaetes (Dubilier *et al.* 2006). Phylogenetic analyses showed that most of these symbionts formed clades including free-living bacteria within the Proteobacteria and one clade within the Spirochaetes (Figure 7). Despite this diversity, these symbiotic associations have been shown to be highly specific and stable within all individuals of a host species (Blazejak *et al.*, 2005; Blazejak *et al.*, 2006; Dubilier *et al.*, 1999; Dubilier *et al.*, 2006; Dubilier *et al.*, 2001; Ruehland *et al.*, 2008).

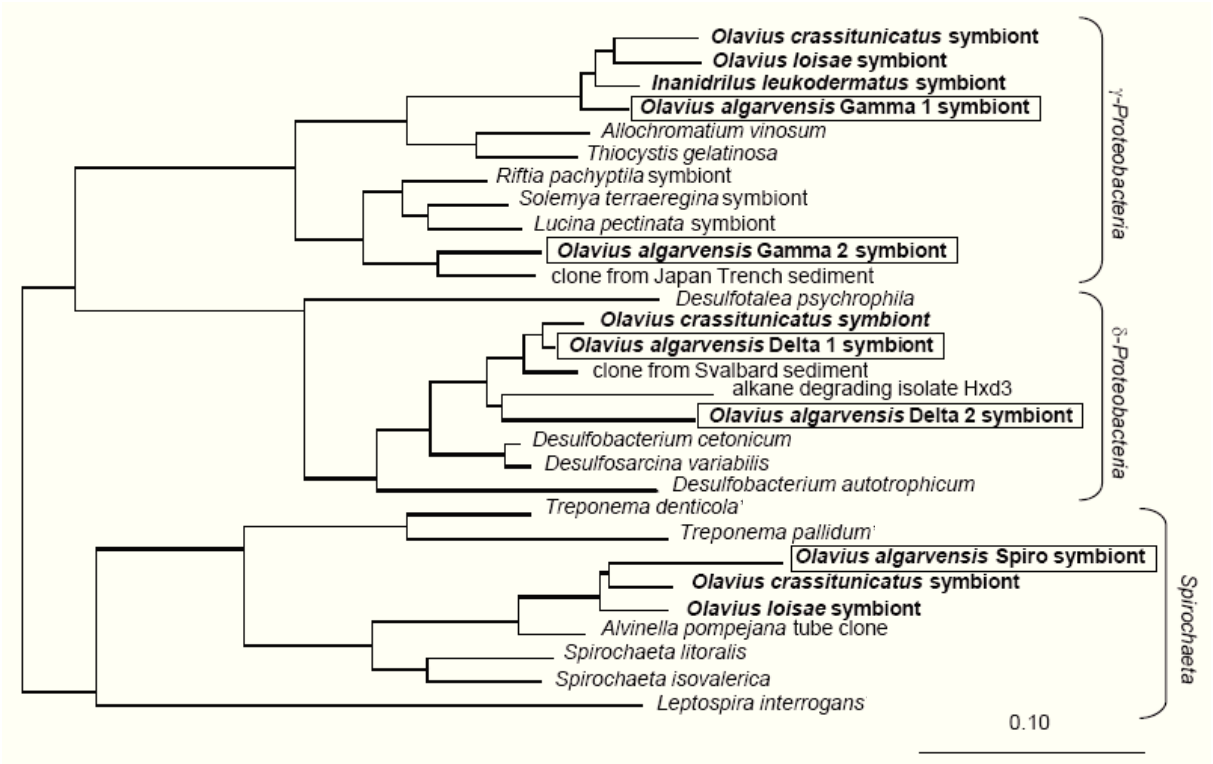

Figure 7: Phylogenetic tree of gutless oligochaete symbionts based on parsimony analyses of 16S rRNA sequences. Symbionts of gutless oligochaetes are bold with *O. algarvensis* symbionts boxed. Scale bar indicates 0.10 expected substitutions per site. (Provided by Nicole Dubilier)

Earlier physiological and morphological studies indicated that the gutless oligochaete symbiosis is driven by chemosynthesis. The symbionts were thought to provide their hosts

with nutrition by using reduced inorganic sulfur compounds as an energy source for the autotrophic fixation of CO_2 into organic compounds (Felbeck, 1983; Giere, 1981). Later these findings were confirmed by molecular, immunocytochemical and spectroscopic analyses as well as incubation experiments showing that the primary endosymbionts were chemoautotrophic sulfur oxidizers (Bergin, 2009; Dubilier *et al.*, 2001; Giere & Krieger, 2001; Giere *et al.*, 1988; Krieger *et al.*, 2000; Ruehland *et al.*, 2008).

The deltaproteobacterial symbionts were found to be sulfate reducers based on molecular analyses as well as incubation experiments with radioactively labeled sulfate (Dubilier *et al.*, 2001; Ruehland *et al.*, 2008; Woyke *et al.*, 2006). In the symbiosis of *O. algarvensis* and *O. ilvae*, which inhabit the sulfide-poor sediments off the coast of Elba, the deltaproteobacterial symbionts therefore have been proposed to be involved in a syntrophic sulfur cycle with the sulfur-oxidizing symbionts.

The metabolisms of the alphaproteobacterial and the spirochete symbionts are still unknown. However, it has been hypothesized that the alphaproteobacterial symbionts might be involved in the recycling of host waste products, since the gutless oligochaetes lack nephridia (Blazejak *et al.*, 2006; Dubilier *et al.*, 2006). In addition the alphaproteobacterial symbionts might also be capable of storing carbon similar to the primary gammaproteobacterial symbionts, as inferred from the presence of small granules in the alphaproteobacterial symbionts of *I. leukodermatus* (Giere & Langheld, 1987). The spirochete symbionts have been proposed to either ferment carbohydrates to actetate, ethanal, CO_2, and H_2 or produce acetate chemoautotrophically using CO_2 and H_2. In addition, they could also be involved in the fixation of nitrogen. These hypotheses are based on known metabolisms of free-living marine spirochetes and spirochete symbionts of termites and remain to be shown (Dubilier *et al.*, 2006).

Because most knowledge about the symbiosis of gutless oligochaetes derives from the symbiosis of *O. algarvensis* and because *O. algarvensis* was extensively studied during this PhD thesis I will focus on this gutless worm and its symbionts in the following.

1.6.3 The symbiosis of *Olavius algarvensis*

The habitat of *O. algarvensis*

Olavius algarvensis was first discovered in subtidal sediments off the coast of southern Portugal (Giere *et al.*, 1998). A few years later *O. algarvensis* was also found in silicate sediments around sea grass beds in the bay of Sant' Andrea off the coast of Elba (Italy) (Dubilier *et al.*, 2001; Giere & Erseus, 2002) and in calcareous sediments around sea grass beds off the coast of Pianosa (Italy) (personal observation), in 6 – 8 m water depth at both sites. At these sites at least two additional gutless oligochaete species co-occur with *O. algarvensis*, but in lower abundances: *O. ilvae* (Giere & Erseus, 2002; Ruehland *et al.*, 2008) and "*O. filicauda"* (C. Wentrup and O. Giere, in prep.). An unnamed fourth species was recently discovered at the Sant' Andrea site (C. Lott, unpublished data).

At Sant' Andrea, *O. algarvensis* can make up to 25.000 individuals per m^2 with highest abundances in a sediment depth of 12 cm (C. Lott, unpublished data). At this site sulfide concentrations are very low (in the nM range) and not likely to be sufficient to sustain the chemosynthetic symbiosis of *O. algarvensis*. In addition, oxygen does not penetrate into the deeper sediment layers in which *O. algarvensis* is usually found. However, oxygen might be obtained from the oxygenated sediment surface when the worms migrate into the upper layers to fulfill their own requirements (Woyke *et al.*, 2006). Nitrate (up to 6 µM) has so far only been measured for up to 3 days in a row in the pore waters of the Sant' Andrea sediments after a storm (C. Lott, unpublished data). It is assumed that oxygen was flushed into deeper sediment layers through heavy wave actions, and that ammonia was then converted to nitrite

and ultimately to nitrate in the presence of oxygen during nitrification. Since nitrate is a good electron acceptor for many free-living bacteria in the sediment it was presumably consumed 3 days after the storm. Overall, the concentrations of the common electron acceptors and donors necessary to fuel chemosynthesis are rather low in the shallow water Sant' Andrea sediments. The sediments of Pianosa are not as well known as the sediments of Sant' Andrea and therefore not further described in this thesis.

Physiological functions of the *O. algarvensis* symbionts

O. algarvensis lives in an intimate relationship with five symbionts: two gammaproteobacterial symbionts (referred to as γ1- and γ3-symbionts), two sulfate-reducing symbionts (referred to as δ1- and δ4-symbionts) and a spirochete. A metagenomic study investigated the metabolic capacities of the gamma- and deltaproteobacterial symbionts in *O. algarvensis* and provided a model of how these might interact with each other and their host (Figure 8) (Woyke *et al.*, 2006). These analyses confirmed that the two gammaproteobacterial symbionts were sulfur-oxidizing chemoautotrophs and the two deltaproteobacterial symbionts sulfate-reducing bacteria and supported the hypothesis of the internal synthrophic sulfur cycle between the symbionts (see above section 1.6.2) and (Dubilier *et al.*, 2001; Ruehland *et al.*, 2008; Woyke *et al.*, 2006).

Besides sulfur cycling other intermediates were also predicted to be exchanged between the different symbiotic partners. Under anaerobic conditions the worm is expected to accumulate metabolites of its anaerobic metabolism such as acetate, succinate, propionate, and malate as known from other invertebrates during environmental anaerobiosis (Grieshaber *et al.*, 1994; van Hellemond *et al.*, 2003). Succinate could therefore be used as an electron donor by the sulfate-reducing symbionts and the corresponding product, fumarate, could serve as an electron acceptor for the sulfur-oxidizing symbionts under anoxic conditions (Woyke *et al.*, 2006).

Another intermediate that could be exchanged between the different symbionts is hydrogen. Hydrogen could be released by the γ3-symbiont during pyruvate oxidation and used by the deltaproteobacterial symbionts as energy source to fix carbon dioxide autotrophically. Both deltaproteobacterial symbionts were shown to have the genetic potential for heterotrophy as well as autotrophy (Woyke *et al.*, 2006). The ability of all four investigated symbionts to fix CO_2 autotrophically provides the host with a variety of carbon and energy sources, which might be the key to the success of this symbiosis in the otherwise rather nutrient poor habitat.

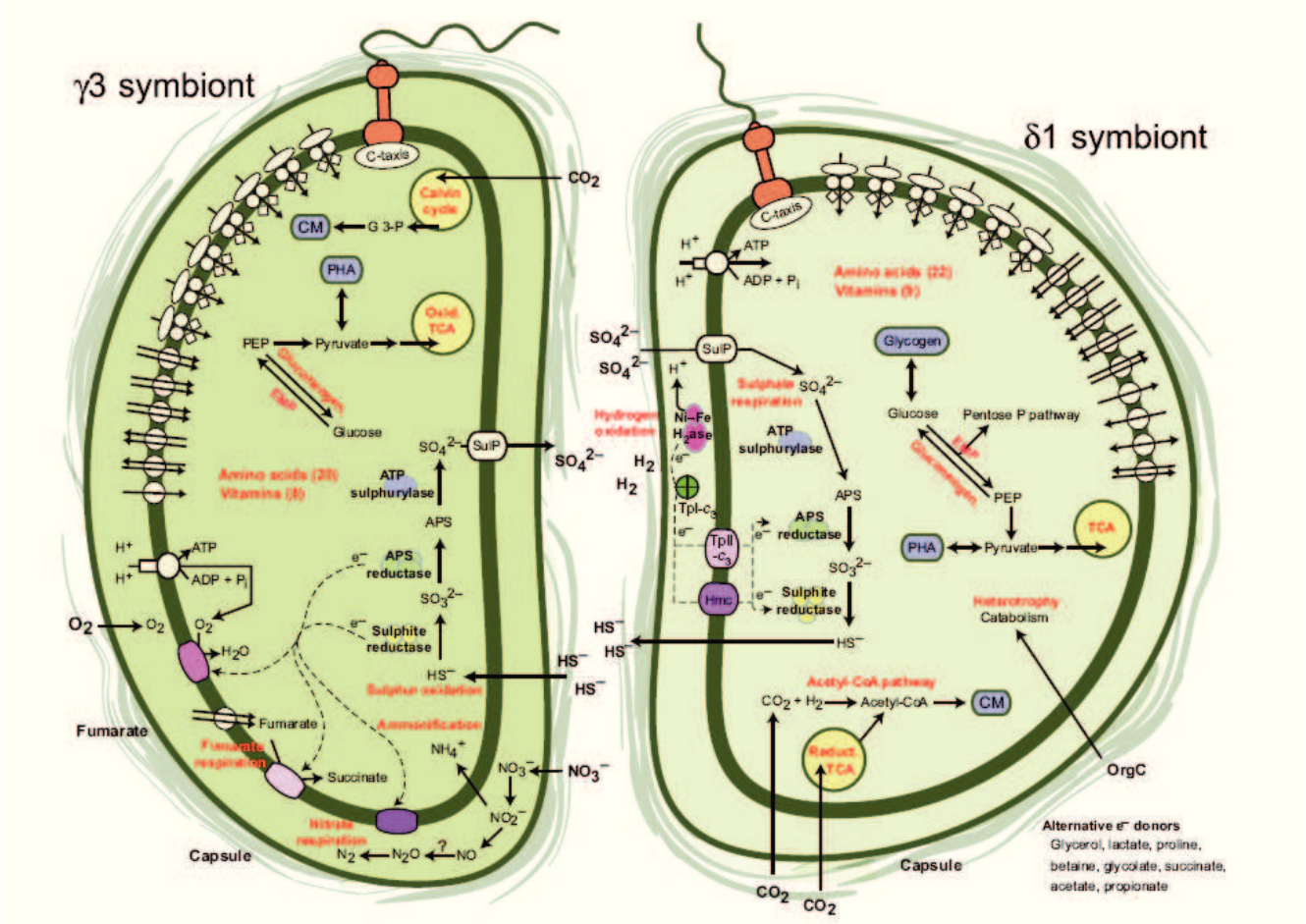

Figure 8: Reconstruction of the symbionts' physiology. APS, adenosine 59-phosphosulphate; CM, cell material; CoA, coenzyme A; C-taxis, chemotaxis; EMP, Embden–Meyerhof pathway; G 3-P, glyceraldehyde 3-phosphate;H2ase, hydrogenase; Hmc, high-molecular-weight cytochrome c; OrgC, organic compounds; PEP, phosphoenolpyruvate; PHA, polyhydroxyalkanoates; TCA, tricyclic acid; TpI/II-c3, type I/II tetrahaem cytochrome c3; SulP, sulphate permease. A question mark (?) indicates the lack of nitric oxide reductase in the γ3 genome bin. (From Woyke *et al.*, 2006)

The metagenomic study also gave first insights into how the symbionts might have enabled gutless oligochaetes to reduce their nephridia, which are essential for the excretion of nitrogenous waste products and osmoregulation in other oligochaetes. The symbiont genomes revealed a number of genes involved in the uptake and breakdown of waste products from the host metabolism including ammonium and urea. The functional replacement of the nephridia by the symbionts might have an additional advantage for the entire symbiosis, as it allows the recycling and conservation of valuable nitrogen and other compounds (Woyke *et al.*, 2006).

Until now only little is known about how the host acquires nutrients from its symbionts. The heterotrophically or autotrophically synthesized organic compounds could either be released by the symbionts and taken up by the host or entire symbiont cells could be digested by the host. The latter could also play a role in controlling the symbiont number (Dubilier *et al.*, 2006). Morphological analyses suggested that symbionts are lysed and digested by their host (Giere & Erseus, 2002; Giere & Langheld, 1987). Furthermore, the symbiont's metagenomes did not reveal noticeable genes coding for amino acid or sugar exporters supporting the hypothesis that the symbionts are digested rather than "milked" (Woyke *et al.*, 2006). Incubation experiments with ^{13}C-labeled bicarbonate as the sole carbon source showed highly ^{13}C-enriched γ1-symbionts after 25 hours under oxic conditions and only a slight transfer of ^{13}C-labeled compounds to the host tissue (C. Bergin and C. Lott, in prep.). A model based on this incubation and accounting for all carbon fluxes within the symbiosis of *O. algarvensis*, however, could still not resolve the question of carbon transfer from the symbionts to the host completely. It remains uncertain if the transfer happens via lysis of the symbionts, excretion of the storage compound PHA and excretion of freshly fixed carbon or if only a subset of these transfer modes is used.

1.6.4 Transmission of symbionts in gutless oligochaetes

When gutless oligochaetes become fully mature they develop so-called genital pads (Figure 9a-b). These genital pads are a pair of sack-like pockets on the ventral side of the worms close to the oviporus, which is the opening through which eggs are deposited. These genital pads are packed with symbionts and separated from the environment by a very thin cuticle layer of the worm. All genital organs and the maturing eggs inside the worms appeared to be free of bacteria as determined morphologically by transmission electron microscopy (Giere & Langheld, 1987; Krieger, 2000) and by fluorescence in situ hybridization analyses with the general eubacterial probe (B. Noriega and C. Wentrup, unpublished data) (Figure 9). At a later developmental stage, bacteria were observed in freshly laid eggs between the inner egg membrane and the outer egg integument (Giere & Langheld, 1987; Krieger, 2000). It was proposed that disruption of the symbiont filled genital pads during oviposition infected the eggs. Several hours after egg deposition, bacteria were observed to concentrate at one pole of the egg and to penetrate the

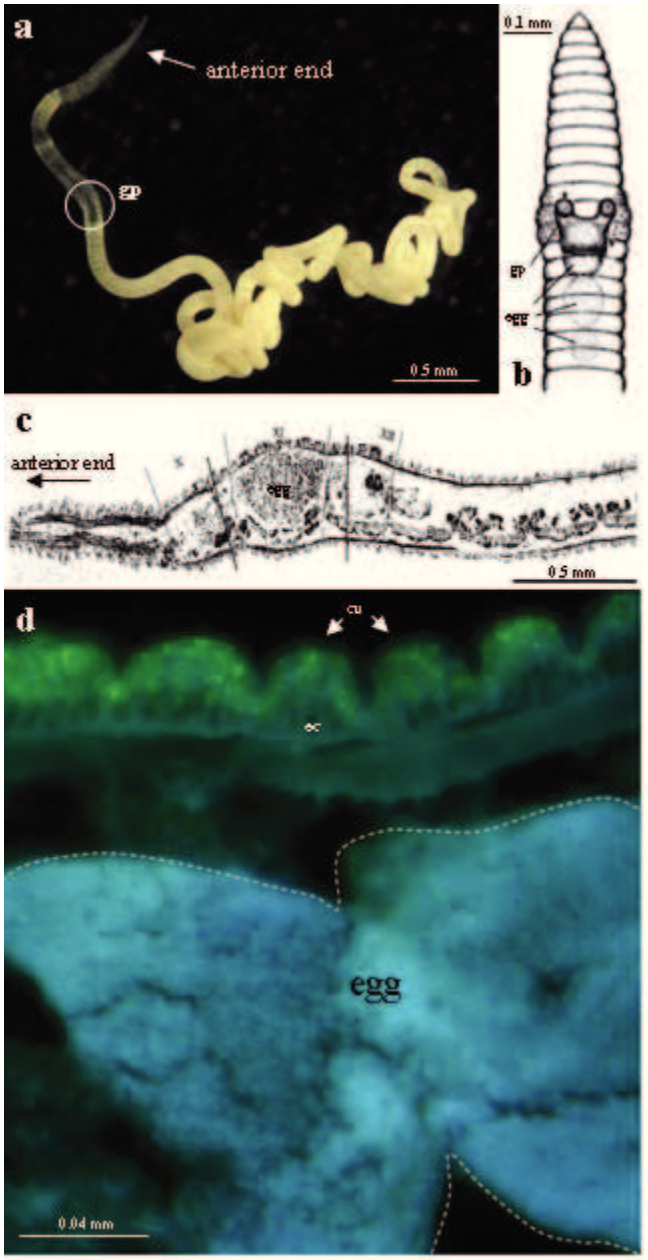

Figure 9: Mature gutless oligochaete with eggs. (a) Live worm with genital pads (gp). (b) Sketch of anterior part of gutless oligochaete with genital pads and eggs. (c) Light microscopic picture of longitudinal section through anterior part of gutless oligochaete. (d) Cross section through egg region with symbionts in green (targeted with a general eubacterial probe) located between the cuticle (cu) and epidermis cells (ec) of the worm. Egg is encircled with white dots. (From Giere, 2006; Krieger, 2000; Noriega, 2011)

egg membrane (Krieger, 2000). These results suggest that at least some symbionts are transmitted vertically. Additional information on symbiont transmission in gutless oligochaetes comes from the metagenomic study of *O. algarvensis* (Woyke *et al.*, 2006). The symbionts metagenome did not show genome reduction or the loss of essential metabolic pathways as found in strictly vertical transmitted symbionts (section 1.3). However, genome regions of the γ1-, γ3- and δ1-symbiont showed high numbers of genes coding for mobile elements and proteome analyses even revealed a high expression of the associated transposases in those mobile elements in the γ1- and δ1-symbiont (M. Kleiner, unpublished data). These latter findings suggest a recent switch to an obligate symbiotic lifestyle as increasing frequencies of mobile elements have been proposed to be markers for such a transition (section 1.3). If the hypothesis is correct that symbionts of *O. algarvensis* have switched to an obligate symbiotic lifestyle, it is likely that they do not have a free-living stage anymore and that they have to be transmitted directly from one host generation to the next to survive.

Alternatively, the symbionts or at least some of them could be acquired by the gutless oligochaetes from the environment anew every generation as discussed in previous studies (Blazejak *et al.*, 2005; Bright & Giere, 2005; Dubilier *et al.*, 2006). This hypothesis is supported by the observation that gutless oligochaetes deposit their eggs singly into the environment, in contrast to all other oligochaetes. The egg, which is covered with sticky mucous, adheres to the surrounding sediment right after deposition and might offer free-living bacteria an opportunity to invade the egg (Dubilier *et al.*, 2006). It has been discussed that this latter transmission mode might have been the original transmission mode for all symbionts of gutless worms (Blazejak *et al.*, 2005; Bright & Giere, 2005; Dubilier *et al.*, 2006). Furthermore, the acquisition of environmental symbionts could explain the high diversity of co-occurring symbionts in these hosts, as new symbionts could easily be taken up from the surrounding sediments (Dubilier *et al.*, 2006).

1.7 Why study symbioses and how?

1.7.1 The importance of symbioses

Symbioses enable the different partners to gain energy, nutrients or other metabolic benefits that they would not be able to access or produce on their own. The importance of symbioses that are based on energy and nutritional exchange has long been recognized and extensively studied in some model systems (Cavanaugh *et al.*, 2006; Dubilier *et al.*, 2008; Moran *et al.*, 2008; Oliver *et al.*, 2010). The symbionts of these symbioses have been shown to possess highly efficient pathways for gaining energy and fixing carbon, producing antibiotics and other pharmaceuticals, and converting plant matter into biofuels (Cavanaugh *et al.*, 2006; Haeder *et al.*, 2009; Kaltenpoth *et al.*, 2005; Stewart *et al.*, 2005; Suen *et al.*, 2010). Chemosynthetic symbioses in which all partners rely on one another for nutritional reasons in usually hostile and nutrient limited environments (Section 1.4) present ideal study subjects for understanding and discovering new energy efficient and carbon fixing pathways.

In addition the value of microbial communities over pure cultures to produce and degrade biofuel, bioplastics, pharmaceuticals and other organic compounds has been recognized, as pure cultures are often not able to carry out all required metabolic steps (Hu *et al.*, 2010; Purnick & Weiss, 2009). The highly stable, species-specific and low diversity consortia of marine invertebrates and their chemosynthetic symbionts can be seen as a small ecosystem and qualifies them for in depth analyses of interactions within microbial communities to consistently and efficiently produce and convert organic compounds.

Furthermore, microorganisms have been recognized to influence the evolution, development, and health of animals (Fraune & Bosch, 2010; McFall-Ngai, 2002; Moya *et al.*, 2008; Walker & Crossman, 2007). Studying chemosynthetic bacteria and their hosts will thus provide more insights into microbe-host interactions and might even provide new insights for infection biology research, since mutualistic symbionts and pathogens are known to share molecular

mechanisms essential for the association with their hosts (Dale & Moran, 2006; Dobrindt *et al.*, 2004; ffrench-Constant *et al.*, 2006; Hentschel *et al.*, 2000; Kimbell & McFall-Ngai, 2004; Ochman & Moran, 2001; Paulsen *et al.*, 2002).

1.7.2 Methods used in this study to investigate the mussel and oligochaete symbioses

Studying marine chemosynthetic symbioses is challenging, because most symbionts and hosts cannot be cultured apart from each other. In most cases, it is even challenging to keep the intact symbiosis alive in the laboratory. Exceptions on the host side are the lucinids, which can grow aposymbiotically (Gros *et al.*, 1999), the ciliate *Zoothamium* (Rinke *et al.*, 2007) and the flat worm *Paracatenula* (Dirks *et al.*, 2012). No chemosynthetic symbiont has been grown in culture so far, which is why culture-independent methods (such as microscopic, molecular, immunohistochemical, biochemical, and physiological) are invaluable to investigate and understand the partners' identity, distribution, abundance, interactions and metabolic capabilities (reviewed in Cavanaugh *et al.*, 2006; Dubilier *et al.*, 2008; Dubilier *et al.*, 2006).

In the following paragraphs I will describe some of these methods that have also been used in this study to investigate the symbiotic communities of the deep-sea mussel *Bathymodiolus* and the shallow water worm *O. algarvensis*.

Identifying symbionts - the 16S rRNA full cycle approach

In the last 15 years symbionts have generally been investigated by the cultivation independent full cycle rRNA approach (Amann *et al.*, 1995), which reveals the identity, phylogenetic relationships, and distribution within host tissue of the symbionts (e.g. Distel *et al.*, 1988; Dubilier *et al.*, 2001; Duperron *et al.*, 2007; Nussbaumer *et al.*, 2006; Petersen *et al.*, 2010;

Ruehland & Dubilier, 2010; Verna *et al.*, 2010). In this approach, the small subunit of the rRNA, the 16S rRNA, serves as an identifier and phylogenetic marker for both culturable and 'unculturable' microbes. The 16S rRNA gene sequences are obtained by PCR amplification from genomic DNA using universal primers. Depending on whether the genomic DNA derived from a mixed microbial population or a single microbe the retrieved PCR product has to be cloned to individualize 16S rRNA PCR products prior to sequencing. Fluorescently labeled oligonucleotide probes are then designed and applied to specifically match the 16S rRNA sequence of the target organism in the environment or host tissue. The hybridization process of the fluorescently labeled probe to its target molecule is often referred to as FISH for fluorescence in situ hybridization. In the end the target organism is microscopically visualized and identified (Amann *et al.*, 1995). The full cycle rRNA approach has proven itself to be extremely valuable, because it ensures that the obtained 16S rRNA sequences originated from the symbionts and not from bacterial contaminants.

To identify microbes and symbionts that have less ribosomal RNA molecules inside their cells more sensitive detection techniques such as the catalyzed reporter deposition (CARD)-FISH protocol have been developed (Pernthaler *et al.*, 2002) and successfully applied (Blazejak *et al.*, 2005; Ruehland *et al.*, 2008).

Identifying functions and pathways of symbionts

To link the identity of particular symbionts to their functions within chemosynthetic symbioses techniques such as metagenomics (Grzymski *et al.*, 2008; Kuwahara *et al.*, 2007; Newton *et al.*, 2007; Robidart *et al.*, 2008; Woyke *et al.*, 2006), metatranscriptomics (Bettencourt *et al.*, 2010; Stewart *et al.*, 2011) and metaproteomics (Gardebrecht *et al.*, 2011; Kleiner *et al.*, 2012; Markert *et al.*, 2007; Robidart *et al.*, 2011, Chapter 4) have been used. Metagenomics involves the sequencing of genomic DNA extracted from microbial populations and provides information about potential functions and metabolic pathways. In

contrast metatranscriptomics, which refers to sequencing analyses of mRNA isolated from a microbial population, and metaproteomics, which refers to the identification of the proteins expressed in a microbial community, reveal information about functions and pathways that are actually used in a microbial community under given conditions.

All meta-'omics'-studies are hampered by the presence of DNA, mRNA or proteins of the host and co-occurring symbionts in symbioses with multiple symbionts. It can therefore be difficult to link a particular function or metabolic pathway to a specific symbiont despite excellent bioinformatic algorithms and analyses. This limitation can be circumvented by enriching different fractions of a symbiotic community as proposed for microbial communities (Steward & Rappe, 2007; Warnecke & Hugenholtz, 2007). Fractioning the symbiotic community reduces the amount of host contamination and gives additional information about the origin of the analyzed biomolecules if the enriched population is simultaneously identified through 16S rRNA analysis and FISH. Furthermore low abundant species that would usually been overlooked could also be analyzed if they were sufficiently enriched. Cells for subsequent genome and proteome analyses have been separated using filtration (Baker *et al.*, 2006), centrifugation (Kleiner *et al.*, 2012; Markert *et al.*, 2007; Newton *et al.*, 2007; Woyke *et al.*, 2006, Chapter 4), and fluorescence-activated cell sorting (FACS) (Siegl *et al.*, 2010).

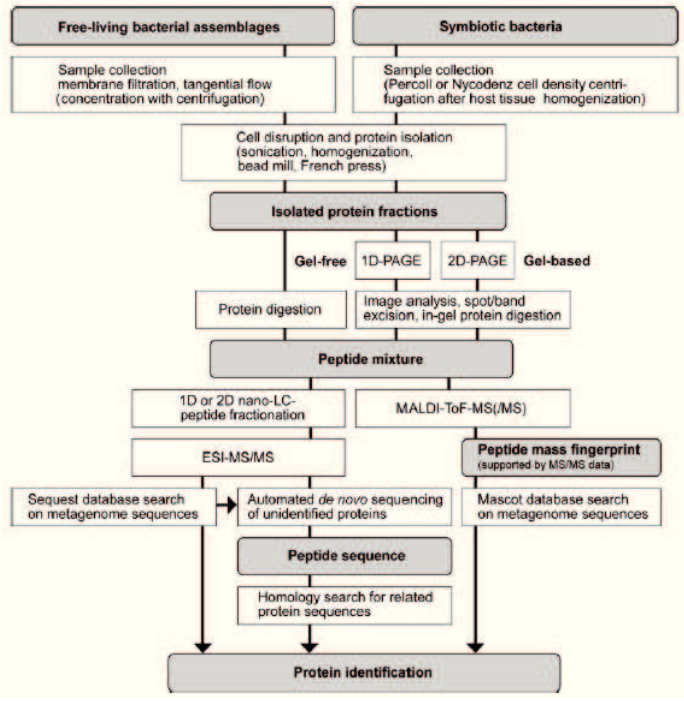

Figure 10: Schematic view of metaproteome analysis techniques for investigation of free-living microbial consortia and symbiotic bacteria. (From Schweder *et al.* 2008)

Because a proteomic study was conduced in this PhD study, I will briefly describe the work flow of a metaproteomic analysis (Figure 10) beginning with the different fractions enriched with one particular symbiont type. From these pre-sorted symbiont fractions the proteins have to first be extracted from the symbiont cells. This results in a protein mixture from which the individual proteins have to be separated by gel-based (one dimensional and two dimensional) or gel-free chromatography before they are digested and finally identified. Identification of the peptides of single proteins is done using mass spectrometry combined with bioinformatic programs which compare the masses of the measured peptides of the mass spectrometer with masses of peptides that were generated in silico based on available genome sequences (reviewed in (Schweder *et al.*, 2008) and (Hettich *et al.*, 2012)). Based on the symbiont fraction from which the sample came from, the identified proteins can be assigned to a given symbiont and conclusions about expressed proteins and pathways of the symbionts under different conditions can be drawn (see also Kleiner *et al.*, 2012 in Chapter 4).

Verifying functions and pathways of symbionts with incubation experiments

Incubations with labeled and unlabeled substrates has increased the understanding of physiological activities of chemosynthetic symbioses for decades (Anderson *et al.*, 1987; Bright *et al.*, 2000; Felbeck, 1983; Fisher & Childress, 1986; Kochevar *et al.*, 1992; Nelson & Fisher, 1995). However, linking metabolic processes to particular symbionts at the single-cell level has only become possible recently with technical developments and a combination of different methods. An example of such a new technology, which was also used during my PhD study, is nanoSIMS, in which the analysis of incorporated labeled substrates can be combined with the identification of active cells via in situ hybridization (see above) (Behrens *et al.*, 2008; Foster *et al.*, 2011; Lechene *et al.*, 2007; Li *et al.*, 2008; Musat *et al.*, 2008; Pernice *et al.*, 2012; Polerecky *et al.*, 2012). NanoSIMS analyzes the masses of secondary ions emitted from the sample after bombardment with a primary ion beam under high vacuum

(Figure 11) (Kuypers, 2007; Kuypers & Jorgensen, 2007; Lechene *et al.*, 2006). Ejected ionized atoms and molecules are then collected, separated according to their mass and detected by one of the up to seven ion detectors. Up to seven masses from the same sample field can thus be detected simultaneously. A system of electrostatic collectors furthermore allows imaging of the mass distribution and abundance of the ejected particles of the sample by retaining the topological information about the ions' origin from the sample to the detectors. The recorded data give information about the elemental or isotopic composition of the sample and uptake of a labeled substrate is for example detectable as an increased isotope ratio of the sample in comparison to the natural or background isotope ratio. In addition, nanoSIMS analysis can also quantify specific metabolic processes at the single-cell level (Lechene *et al.*, 2006).

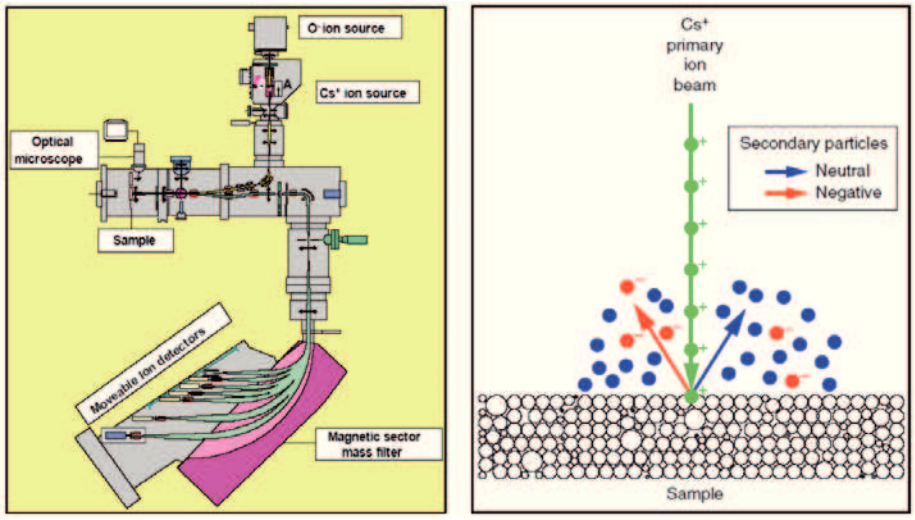

Figure 11: The principle of nanoSIMS: The sample is bombarded with a primary ion beam. The ions of the beam collide with the sample surface resulting in the ionization of surface particles. Secondary ions are collected into detectors according to their masses. (From CAMECA and Fiala-Médioni & Le Pennec, 1987; Lechene *et al.*, 2006)

In combination with in situ hybridization (see above), nanoSIMS can be applied to mixed communities and identify the active population (reviewed in Musat *et al.*, 2012). In situ hybridization can be performed using probes labeled with halogens or other elements that are easily ionized and otherwise rare in biological samples to avoid interference with the sample and provide a good in situ signal (Behrens *et al.*, 2008; Li *et al.*, 2008; Musat *et al.*, 2008). Alternatively, the in situ hybridization can be performed using fluorescently labeled probes.

This latter approach requires an additional step in which images of the cells of interest are recorded with an epifluorescence microscope prior to nanoSIMS analysis (Foster *et al.*, 2011; Polerecky *et al.*, 2012).

1.8 Aims of this thesis

1.8.1 Symbiont colonization in the deep-sea mussel *Bathymodiolus*

The deep-sea mussel *Bathymodiolus* acquires its symbionts horizontally from the environment (section 1.5.6). However, only little is known about the colonization process of the symbionts in *Bathymodiolus*, especially in the mussel's gill tissues that are known to grow throughout the animal's life time. The goals of this project were therefore to investigate 1) the overall colonization processes of the symbionts in early-stage *Bathymodiolus* juveniles and 2) the colonization process of the symbionts in newly formed gill tissues using fluorescence in situ hybridization with symbiont-specific probes on sections of whole juveniles as well as the posterior ends of adult gills where new gill filaments are constantly formed.

1.8.2 Physiological functions of symbionts in the gutless oligochaete *O. algarvensis*

The metagenomic study of the symbionts of *O. algarvensis* suggested several models for the metabolism of the symbionts (section 1.6.3). However, it remained to be shown which of the proposed metabolic pathways actually play a role in the environment under natural conditions. Therefore, the goals of this project were to 3) identify expressed metabolic pathways of the symbionts under environmental conditions using a proteomic approach and to 4) confirm some of these pathways in incubation experiments with labeled substrates and subsequent nanoSIMS analyses.

The findings of each goal will be described successively in the following chapters. Every chapter is composed as a manuscript and will provide a brief introduction, a material and methods part as well as a comprehensive result and discussion part.

Chapter 2: Shift from widespread symbiont infection of host tissues to specific colonization of gills in juvenile deep-sea mussels

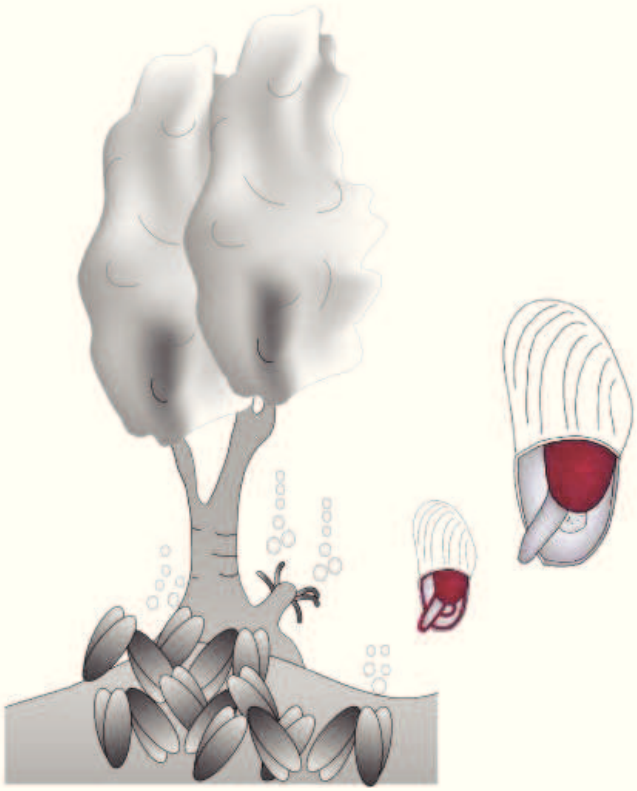

(modified after Dubilier *et al.* 2008)

Title: Shift from widespread symbiont infection of host tissues to specific colonization of gills in juvenile deep-sea mussels

Cecilia Wentrup[1*], Annelie Wendeberg[2*], Julie Y. Huang[3], Christian Borowski[1] and Nicole Dubilier[1*]

[1]Max Planck Institute for Marine Microbiology, Symbiosis Group

Celsiusstr. 1, 28359 Bremen, Germany

[2] UFZ, Helmholtz Centre for Environmental Research, Department of Environmental Microbiology, Permoserstraße 15, 04318 Leipzig, Germany

[3] Stanford University, Department of Microbiology and Immunology

299 Campus Drive Stanford, CA 94305 USA

*Corresponding Authors

Email: ndubilie@mpi-bremen.de, annelie.wendeberg@ufz.de, cwentrup@mpi-bremen.de

Intended as a short communication in: ISME journal

Running title: Symbiont colonization in juvenile *Bathymodiolus*

Abstract

The deep-sea mussel *Bathymodiolus* harbors chemosynthetic bacteria in its gills that provide it with nutrition. Symbiont colonization is assumed to occur in early life stages by uptake from the environment, but little is known about this process. In this study, we used fluorescence in situ hybridization to examine symbiont distribution and the specificity of the infection process in juvenile *B. azoricus* and *B. puteoserpentis* (4-21 mm). In the smallest juveniles, we observed symbionts, but no other bacteria, in a wide range of epithelial tissues. This suggests that despite the widespread distribution of symbionts in many different juvenile organs, the infection process is highly specific and limited to the symbiotic bacteria. Juveniles ≥ 9 mm only had symbionts in their gills, indicating an ontogenetic shift in symbiont colonization from indiscriminate infection of almost all epithelia in early life stages to spatially restricted colonization of gills in later developmental stages.

Key words: *Bathymodiolus*, Mid-Atlantic-Ridge, symbiont transmission, hydrothermal vents

Introduction

Associations with chemosynthetic bacteria have evolved independently in at least four lineages of marine bivalves (Dubilier et al., 2008). In all these associations, the symbionts are generally restricted to the gills in adult bivalves (Taylor and Glover, 2010), except hosts that transfer their symbionts directly to their offspring and harbor symbionts in their gonads (Cary and Giovannoni, 1993; Endow and Ohta, 1990). In adult *Bathymodiolus* mussels, symbionts have only been observed in the gills (Distel et al., 1994; Duperron, 2010). These mussels occur worldwide at hydrothermal vents and cold seeps and harbor their intracellular sulfur- and methane-oxidizing symbionts in gill cells called bacteriocytes. *Bathymodiolus* is assumed to acquire its symbionts from the environment, but the developmental stage at which this occurs is not known (Duperron et al., 2007; Won et al., 2003). Post-larval *Bathymodiolus azoricus* and *B. heckerae* as small as 0.12 mm appear to already harbor symbionts in their gills based on transmission electron microscopy (TEM) observations of bacteria morphologically similar to the sulfur- and methane-oxidizing symbionts (Salerno et al., 2005). These bacterial morphotypes were also found in mantle epithelia of post-larval and juvenile *B. azoricus* and *B. heckerae* (0.12 – 8.4 mm). Similarly, in *B. childressi* juveniles (4-8 mm) TEM revealed bacteria that looked like the methane-oxidizing symbionts in gills as well as mantle and foot epithelia, and labeling experiments showed that these bacteria fixed carbon from methane (Streams et al., 1997). These studies suggest that *Bathymodiolus* is colonized by its symbionts at a very early stage and that other organs besides the gills also contain symbionts.

In this study, we focused on the following questions: 1) Do the symbionts indiscriminately infect all host tissues of juvenile *Bathymodiolus*? 2) Are the symbionts the only bacteria that colonize juvenile mussels? 3) Given that adult mussels are assumed to only have symbionts in their gills, is there a developmental stage at which the broad colonization of host tissues ends? To answer these questions we analyzed eight *B. puteoserpentis* and five *B. azoricus* juveniles

(4 to 21 mm) from two vent sites on the Mid-Atlantic-Ridge by fluorescence in situ hybridization (FISH). Semi-thin sections of whole juveniles were examined with symbiont-specific probes as well as a general eubacterial and a negative probe as previously described (Duperron et al., 2006; Wendeberg et al., 2012).

Results

Symbionts broadly colonize tissues of smallest juvenile mussels

We observed symbiont-specific FISH signals indicating the presence of both the sulfur- and the methane-oxidizing symbionts in gill bacteriocytes of all 13 *Bathymodiolus* juveniles (Figure 1). In the smallest individuals (4-7 mm), we also found symbiont-specific FISH signals in the epithelial cells of the mantle, foot, and retractor muscles (Table 1, Figure 1), but not in other tissues or organs. The distribution and abundance of both symbionts was comparable in all organs except for the much denser colonized gills, based on microscopic observations.

The symbionts are the only bacteria that colonize juvenile host tissues

Extensive FISH analyses of all 13 juveniles showed overlap between the symbiont-specific and general eubacterial probes (as well as with DAPI staining) in all colonized host tissues (Figure 1). This indicates that the sulfur- and methane-oxidizing symbionts are the only bacteria that colonize juvenile mussels.

Larger *Bathymodiolus* mussels only have symbionts in their gill tissues

In contrast to *B. azoricus* and *B. puteoserpentis* juveniles ≤ 7 mm, larger juveniles of both species (9 – 21 mm) had symbiont-specific FISH signals only in their gills. To examine if this spatial restriction of colonization to the gills is also maintained in adult *Bathymodiolus*, we

examined mantle tissues attached to gills dissected from *B. azoricus* (n = 6, 55 – 100 mm). We only observed the symbionts in the gills but never in the mantle.

Discussion and Conclusions

Our study provides FISH-based evidence that the symbionts of early-stage *B. azoricus* and *B. puteoserpentis* ≤ 7 mm colonize a wide range of epithelial tissues. Together with earlier studies on juvenile *B. azoricus*, *B. heckerae and B. childressi* (Salerno et al., 2005; Streams et al., 1997), these results indicate a consistent pattern of indiscriminate symbiont colonization of a wide range of epithelial tissues in *Bathymodiolus* ≤ 8.4 mm (Table 1). This is remarkable given that in most symbioses, infection sites are spatially limited to specific tissues or areas, even in early life stages of the host (Bright and Bulgheresi, 2010). Despite the pervasive infection of *Bathymodiolus* juvenile epithelia, our study shows that colonization is only achieved by the symbionts (although we did not check for the intranuclear bacterial parasite that can also infect these hosts (Zielinski et al., 2009)). Clearly, the infection process must be highly regulated and specific to ensure that only the symbionts colonize host cells.

The most obvious explanation for the widespread colonization of host epithelia in juvenile *Bathymodilus* is that it provides the host with additional nutrition. However, the much smaller surface areas of mantle, foot and retractor muscle epithelia would provide only a minimal nutritional benefit in comparison to the much larger surface volume of the gills. Also, filter-feeding is assumed to be common in *Bathymodiolus* and could provide juveniles with enough additional nutrition (Pile and Young, 1999; Riou et al., 2010).

In both *Bathymodiolus* species investigated in this study from two vent sites separated by almost 3000 km, we observed that juveniles ≥ 9 mm only had symbionts in their gills. This indicates an ontogenetic shift in symbiont colonization from indiscriminate infection of

different epithelia to a highly restricted spatial limitation to gill bacteriocytes at a developmental stage between 8.4 – 9 mm. *Bathymodiolus* gills with their greatly enlarged surface areas and cilial ventilation are by far the most efficient tissues for providing the symbionts with the oxygen and reduced compounds they need to gain energy. However, the thin outer layer of non-gill epithelia apparently has sufficient access to oxidants and reductants to harbor symbionts in juveniles ≤ 9 mm, and it is not clear how this would change when mussels become larger. Alternative explanations for the observed colonization shift are that the costs of harboring symbionts in many different tissues outweigh the nutritional benefits in larger mussels, or that the immune system of early stage *Bathymodiolus* is not sufficiently developed to prevent indiscriminate infection (Huan et al., 2012; Luna-Gonzalez et al., 2004). Teasing apart the processes that lead to this ontogenetic shift will provide a better understanding of how bacterial colonization patterns are established, maintained, and regulated in animal symbioses.

Acknowledgements

We thank Silke Wetzel and Agnes Zimmer for excellent technical assistance, and the chief scientists, captains and crew of the Hydromar I M60/3 and MenezMAR M82/3 cruises as well as the ROV MARUM-Quest team for their support. The funding for this study was provided by the Max Planck Society, the DFG Cluster of Excellence "The Ocean in the Earth System" at MARUM, Bremen, and the DFG Program SPP 1144 “From Mantle to the Ocean: Energy-Material- and Life-Cycles at Spreading Axes”. CW was supported by a scholarship of the “Studienstiftung des deutschen Volkes” and JYH by a Fulbright Fellowship.

Figure 1

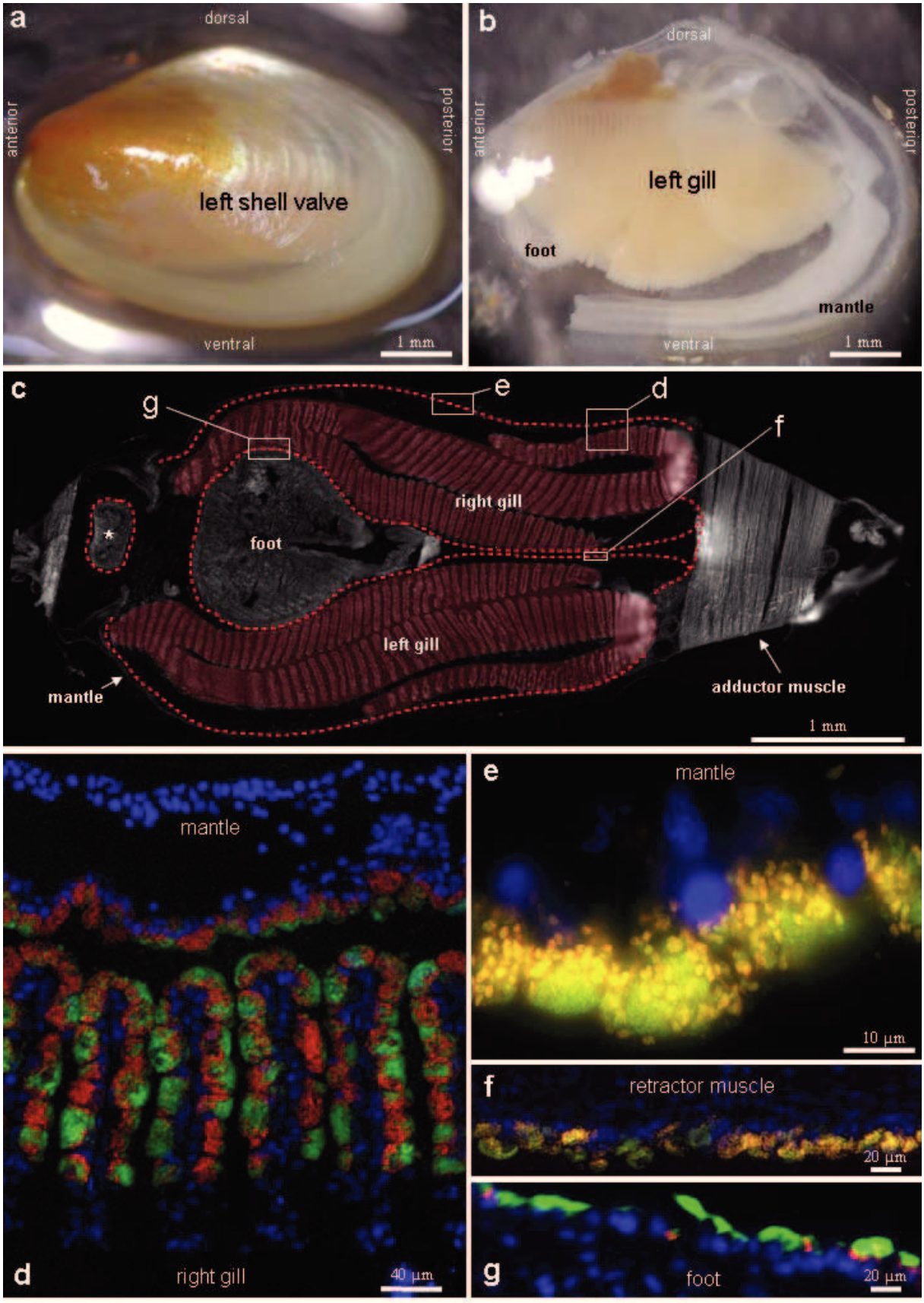
a
dorsal
anterior
posterior
left shell valve
ventral
1 mm
b
dorsal
anterior
posterior
left gill
foot
mantle
ventral
1 mm
c
g
e
d
f
right gill
foot
left gill
mantle
adductor muscle
1 mm
mantle
d
right gill
40 µm
e
mantle
10 µm
f
retractor muscle
20 µm
g
foot
20 µm

Legend to Figure 1:

Symbionts colonize many different epithelial tissues in juvenile *B. puteoserpentis* and *B. azoricus*. The mussels are shown in the same orientation in all images with the anterior end on the left and the posterior end on the right. a), b) and g) are *B. azoricus*; c) - f) are *B. puteoserpentis*. a, b) Lateral view of small juvenile with a) and without b) shell valves. c) Epifluorescence micrograph of a cross section (ventral view) through entire juvenile mussel. The asterisk marks the foot tip that was curled dorsally. Mussel tissue that is colonized throughout the mussel life cycle is colored in light red, while mussel tissues that are only infected in juveniles < 9 mm are marked with a red dashed line. d-g) Symbiont specific FISH signals of the sulfur-oxidizing symbionts (green) and the methane-oxidizing symbionts (red) in epithelial cells of d) gills and mantle, e) mantle, f) retractor muscle, and g) foot. In e) and f) signal overlap in a triple hybridization with the two symbiont-specific probes (red and green) and the eubacterial probe (EUB338 in yellow) makes the methane-oxidizing symbionts appear orange and the sulfur-oxidizing symbionts yellow-green. Due to differences in signal intensity of the specific probes versus the eubacterial probe some symbionts appear more yellow than others. The triple hybridization indicates that only the symbionts and no other bacteria are present. Nuclei of the host cells are stained with DAPI (blue).

Table 1: Relationship between shell length and symbiont colonization patterns in *Bathymodiolus* mussels

	B. puteo-serpentis (this study)		*B. azoricus* (this study)		*B. childressi* (Streams et al., 1997)	*B. heckerae* (Salerno et al., 2005)		*B. azoricus* (Salerno et al., 2005)	
Number of specimens	2	6	3	2	24 (in total)	18	4	15	4
Shell length (mm)	6 – 7	9 – 21	4 – 5	27 - 29	4 – 8	0.12 - 8.4	adult (size nd)	0.12 - 8.4	adult (size nd)
Symbionts in gills	yes	yes	yes	yes	yes	yes	yes	yes	yes
Symbionts in epithelia besides gills	mantle, foot and retractor muscles	no	mantle, foot and retractor muscles	no	mantle and foot	mantle	nd	mantle	nd

nd: not determined

References

Bright M, Bulgheresi S (2010) A complex journey: transmission of microbial symbionts. *Nat Rev Microbiol* **8:** 218-230.

Cary SC, Giovannoni SJ (1993) Transovarial inheritance of endosymbiotic bacteria in clams inhabiting deep-sea hydrothermal vents and cold seeps. *Proc Natl Acad Sci U S A* **90:** 5695-5699.

Distel D, Felbeck H, Cavanaugh C (1994) Evidence for phylogenetic congruence among sulfur-oxidizing chemoautotrophic bacterial endosymbionts and their bivalve hosts. *J Mol Evol* **38:** 533-542.

Dubilier N, Bergin C, Lott C (2008) Symbiotic diversity in marine animals: the art of harnessing chemosynthesis. *Nat Rev Microbiol* **6:** 725-740.

Duperron S, Bergin C, Zielinski F, Blazejak A, Pernthaler A, McKiness ZP *et al.* (2006) A dual symbiosis shared by two mussel species, *Bathymodiolus azoricus* and *Bathymodiolus puteoserpentis* (Bivalvia: Mytilidae), from hydrothermal vents along the northern Mid-Atlantic Ridge. *Environ Microbiol* **8:** 1441-1447.

Duperron S, Sibuet M, MacGregor BJ, Kuypers MMM, Fisher CR, Dubilier N (2007) Diversity, relative abundance and metabolic potential of bacterial endosymbionts in three *Bathymodiolus* mussel species from cold seeps in the Gulf of Mexico. *Environ Microbiol* **9:** 1423-1438.

Duperron S (2010). The Diversity of Deep-Sea Mussels and Their Bacterial Symbioses. In: Kiel S (ed). *Vent and Seep Biota: Aspects from Microbes to Ecosystems*. Springer Netherlands. pp 137-167.

Endow K, Ohta S (1990) Occurence of bacteria in the primary oocytes of vesicomyid clam *Calyptogena soyae*. *Mar Ecol Prog Ser* **64:** 309-311.

Huan P, Wang HX, Liu BZ (2012) Transcriptomic Analysis of the Clam *Meretrix meretrix* on Different Larval Stages. *Mar Biotechnol* **14:** 69-78.

Luna-Gonzalez A, Maeda-Martinez AN, Ascencio-Valle F, Robles-Mungaray M (2004) Ontogenetic variations of hydrolytic enzymes in the Pacific oyster *Crassostrea gigas*. *Fish Shellfish Immunol* **16:** 287-294.

Pile AJ, Young CM (1999) Plankton availability and retention efficiencies of cold-seep symbiotic mussels. *Limnol Oceanogr* **44:** 1833-1839.

Riou V, Colaco A, Bouillon S, Khripounoff A, Dando P, Mangion P *et al.* (2010) Mixotrophy in the deep sea: a dual endosymbiotic hydrothermal mytilid assimilates dissolved and particulate organic matter. *Marine Ecology-Progress Series* **405:** 187-201.

Salerno JL, Macko SA, Hallam SJ, Bright M, Won YJ, McKiness Z *et al.* (2005) Characterization of symbiont populations in life-history stages of mussels from chemosynthetic environments. *Biol Bull* **208:** 145-155.

Streams ME, Fisher CR, FialaMedioni A (1997) Methanotrophic symbiont location and fate of carbon incorporated from methane in a hydrocarbon seep mussel. *Mar Biol* **129:** 465-476.

Taylor JD, Glover EA (2010). Chemosymbiotic Bivalves. *Vent and Seep Biota: Aspects from Microbes to Ecosystems*. pp 107-135.

Wendeberg A, Zielinski FU, Borowski C, Dubilier N (2012) Expression patterns of mRNAs for methanotrophy and thiotrophy in symbionts of the hydrothermal vent mussel *Bathymodiolus puteoserpentis*. *Isme Journal* **6:** 104-112.

Won YJ, Hallam SJ, O'Mullan GD, Pan IL, Buck KR, Vrijenhoek RC (2003) Environmental acquisition of thiotrophic endosymbionts by deep-sea mussels of the genus *Bathymodiolus*. *Appl Environ Microbiol* **69:** 6785-6792.

Zielinski FU, Pernthaler A, Duperron S, Raggi L, Giere O, Borowski C *et al.* (2009) Widespread occurrence of an intranuclear bacterial parasite in vent and seep bathymodiolin mussels. *Environ Microbiol* **11:** 1150-1167.

Chapter 3: Symbiont colonization in chemosynthetic deep-sea bivalves occurs continuously throughout the lifetime of the bivalves

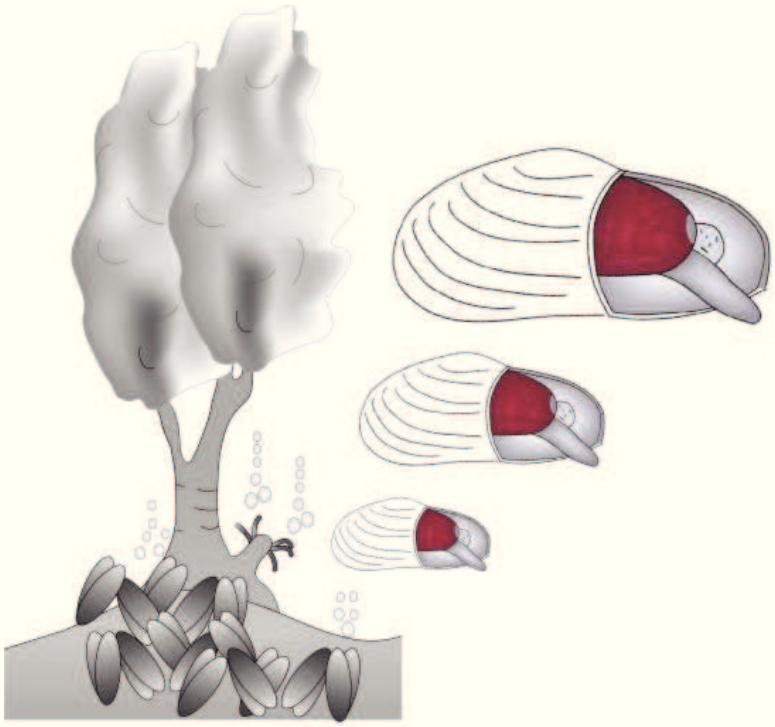

(modified after Dubilier *et al.* 2008)

Title: Symbiont colonization in chemosynthetic deep-sea bivalves occurs continuously throughout the lifetime of the bivalves

Cecilia Wentrup[1*], Christian Borowski[1*], Annelie Wendeberg[2], Mario Schimak[1], and Nicole Dubilier[1*]

[1]Max Planck Institute for Marine Microbiology, Department of Molecular Ecology

Celsiusstr. 1, 28359 Bremen, Germany

[2] UFZ, Helmholtz Centre for Environmental Research, Department of Environmental Microbiology, Permoserstraße 15, 04318 Leipzig, Germany

*Corresponding Author

Email: cwentrup@mpi-bremen.de, cborowsk@mpi-bremen.de, ndubilie@mpi-bremen.de

Intended as an article in: ISME J

Abstract

The deep-sea bivalves *Bathymodiolus* and "*Calyptogena*" *ponderosa* from hydrothermal vents and cold seeps harbor chemosynthetic bacteria in their gills that provide them with nutrition. These intracellular symbionts are housed in gill cells called bacteriocytes. As in all bivalves, the gills grow throughout the bivalves' lifetime raising the question how newly developed gill tissue is colonized by symbionts. Symbionts could either be present in the undifferentiated cells of the gill growth zones and be passed on to developing gill tissue, or symbionts could colonize newly developed filaments *de novo*. In this study, we used fluorescence in situ hybridization with symbiont-specific probes and transmission electron microcopy to analyze sections of the posterior ends of juvenile and adult gills where new gill filaments are constantly formed by undifferentiated cells in the so-called budding zone. We show that the budding zones of the gills, the youngest gill filaments as well as the ventral growth zones of the gill filaments of *Bathymodiolus* and "*C*." *ponderosa* contained no symbionts. These observations indicate that the undifferentiated cells of the gill growth zones are typically free of symbionts in deep-sea bivalves. It further implies that symbionts colonize newly formed gill tissues continuously *de novo* and that this colonization process happens throughout the entire life of the bivalves.

Keywords: *Bathymodiolus*/*Calyptogena*/Symbiont colonization/Budding zone

Introduction

Symbiotic associations between marine bivalves and chemosynthetic bacteria are widespread in the world's oceans. The habitats of these symbioses usually provide reduced inorganic compounds (hydrogen, hydrogen sulfide and methane) that the chemosynthetic bacteria can use as energy sources (e.g. reviewed in Cavanaugh *et al.*, 2006; Dubilier *et al.*, 2008). The energy released during oxidation of these reduced compounds is used by the symbionts to fix carbon into biomass to provide their animal hosts with a source of nutrition (Cavanaugh *et al.*, 1981; Childress *et al.*, 1986; DeChaine and Cavanaugh, 2006; Petersen *et al.*, 2011; Stewart *et al.*, 2005). The establishment of such symbioses has given the hosts a physiological advantage to colonize and thrive in habitats such as deep-sea hydrothermal vents and cold seeps where the input of organic matter from photosynthesis is extremely low (van Dover, 2000).

Most hosts of these chemosynthetic symbioses cannot survive and grow without their symbionts, and therefore have to acquire their symbionts at an early developmental stage (Bright and Bulgheresi, 2010). The offspring either inherit their symbionts from their parents (vertical transmission) or they acquire the symbionts from the environment (horizontal transmission) or these two modes are mixed. In deep-sea bivalves all transmission modes have been described in different species (reviewed in Dubilier *et al.*, 2008; Stewart and Cavanaugh, 2009). While the transmission of symbionts between generations is well documented for several symbioses (Bright and Bulgheresi, 2010), how newly formed host cells of symbiont-containing organs are colonized as they grow remains elusive. This is particularly interesting in bivalve hosts that harbor their chemosynthetic symbionts in specialized epithelia cells of their gills, because these animals grow throughout their entire ontogenetic life span. Their gills are continuously extended by budding of new filaments from undifferentiated cells at the posterior tips of the gills and every gill filament is also expanded dorso-ventrally at the edges of each gill filament (Neumann and Kappes, 2003a), raising the question how newly developed gill tissues are colonized by symbionts. To our knowledge this

colonization process has never been described and two options are possible: (1) the symbionts are present in the undifferentiated cells of the gill growth zones and these develop into mature gill filaments or (2) the symbionts colonize filaments *de novo* after they are formed. To clarify this, we investigated two mytilid species *Bathymodiolus puteoserpentis* and *B. azoricus* from the Mid-Atlantic Ridge (MAR). These two species live in dual symbiosis with sulfur-oxidizing and methane-oxidizing bacteria (Duperron *et al.*, 2006), and they are both assumed to acquire their symbionts from the environment (Won *et al.*, 2003). We analyzed the distribution of symbionts in the posterior ends of the gill sections including the budding zone and newly formed gill filaments using fluorescence in situ hybridization (FISH) and transmission electron microcopy (TEM). To compare our results with the symbiont distribution in host species with vertical symbiont transmission, we also investigated gill sections of the clam "*Calyptogena*" *ponderosa* from the Gulf of Mexico that is associated with sulfur-oxidizing symbionts (Cary and Giovannoni, 1993; Endow and Ohta, 1990; Stewart *et al.*, 2008). For both the studied mussels and clams our results provide evidence that gill budding zones are free of symbionts and that symbionts continuously colonized young gill filaments.

Material and Methods

Sample collection and preparation

Symbiotic bivalves were collected at deep-sea hydrothermal vents and hydrocarbon seeps (Table 1) using the ROV Marum Quest 4000m (Marum, Germany) and DSV Alvin (Woods Hole Oceanographic Institution, USA). *B. puteoserpentis* was collected in February 2004 during research cruise M 60/3 with RV Meteor to the Logatchev hydrothermal vent field on the MAR at 14°45.2'N, 44°58.7'W, *B. azoricus* was collected in September 2010 during RV Meteor cruise M 82/3 at the Menez Gwen hydrothermal vent field on the MAR at 37°50.7'N, 31°31.2'W and "*Calyptogena*" *ponderosa* was collected in May 2006 with DSV Alvin in the

Golf of Mexico at 28°07.64'N, 89°08.47'W, during the Deep Chemosynthetic Community Characterization Cruise, leg AT 15-3 with RV Atlantis. Symbiont containing gill tissues of adult mussels and clams were dissected and fixed on board. Additionally, entire juvenile specimens (5-29 mm shell length) of the two *Bathymodiolus* species were also fixed. Dissections and entire specimens provided for fluorescence in situ hybridization (FISH) analyses (Table 1) were preserved as described previously (Wendeberg *et al.*, 2012) and stored at -20°C or on dry ice for transport to the home laboratories. Dissected tissues for transmission electron microscopy (TEM) analyses (Table 1) were fixed in Trump's Fixative (McDowell and Trump, 1976) and stored at 4°C until further processing.

Probe design and testing for the symbiont of "*C.*" *ponderosa*

Identity of "*C.*" *ponderosa* specimens and their symbiotic bacteria (Stewart *et al.*, 2008) were verified by sequences analyses of the cytochrome c oxidase subunit I (COI) gene of the host and the 16S rRNA gene of the symbionts as previously described (van der Heijden *et al.*, 2012). The amplified sequences were identical to published COI sequences of "*C.*" *ponderosa* (AF008278, EU403473) and the 16S rRNA gene sequence of the symbiont of "*C.*" *ponderosa* (EU403436), respectively. Specific oligonucleotide probes (Cpon_826, Cpon_831, Cpon_1014) targeting the gammaproteobacterial 16S rRNA sequence of the "*C.*" *ponderosa* symbiont (EU403436) (Stewart *et al.*, 2008) were designed using the ARB software package (Ludwig *et al.*, 2004) and the SILVA database (Pruesse *et al.*, 2007) (Table 2). Probes were fluorescently labeled with cy3 or cy5 dyes (Biomers, Ulm, Germany). Hybridizations with probe Cpon_1014 additionally used unlabeled helper oligonucleotides (Table 2) that bind adjacent to the probe target site (Fuchs *et al.*, 2000). The specificities of the "*C.*" *ponderosa* symbiont probes were tested against the gammaproteobacterial sulfur-oxidizing symbiont of *B. azoricus*, which had one mismatch to the probe Cpon_1014 and 5 mismatches to the probes Cpon_826 and Cpon_831.

Fluorescence in situ hybridization (FISH) of rRNA

Juvenile specimens of *B. puteoserpentis* and *B. azoricus* and dissected gill tissues of *B. azoricus* and "*C.*" *ponderosa* adults were embedded in Steedman's wax (Steedman, 1957) (Table 1) and sectioned (Wendeberg *et al.*, 2012). Hybridizations on tissue sections were performed as described previously (Wendeberg *et al.*, 2012). The two investigated *Bathymodiolus* species harbor identical sulfur-oxidizing and methane-oxidizing symbionts based on 16S rRNA sequences (Duperron *et al.*, 2006). We therefore used probe BNMAR_193_thio targeting the sulfur oxidizer and probe BNMAR_845_meth targeting the methane oxidizer for both *Bathymodiolus* species (Duperron *et al.*, 2006). Gill sections of "*C.*" *ponderosa* specimens were double hybridized using mixes of two differently labeled probes (Cpon_826 + Cpon_1014 + helpers or Cpon_831 + Cpon_1014 + helpers).

Immunohistochemistry (IHC)

For the detection of proliferating host cells in *Bathymodiolus* gill sections we used a mouse monoclonal PCNA-antibody (PCNA, proliferating cell nuclear antigen, Dako Cytomation, Hamburg, Germany) and followed the protocol by Wendeberg *et al*. (2012). One section per slide was incubated without the PCNA-antibody as a negative control. After incubation with the secondary goat-anti-mouse antibody labeled with $Alexa_{488}$ (Molecular Probes, Leiden, The Netherlands) (diluted 1:100 in 1 x PBS, 1% [w/v] Blocking Reagent, 1% Bovine Serum Albumin for 1 h at RT) unbound secondary antibodies were washed off (2 x in 1 x PBS for 10 min and 2 x in MilliQ water for 1 min). Sections were dehydrated (1 x 50% ethanol, 1 min; 1 x 100% ethanol, 1 min) and air dried.

Microscopic evaluation

Tissue sections of posterior gill ends of mussels and clams (Table 1) were analyzed using an Axioskop II epifluorescence microscope (Zeiss) and a confocal laser scanning microscope

DM6000B with LAS AF-TCS SP5 software (Leica). Additional overview images were obtained using a fluorescent dissecting scope M205 FA (Leica).

Sample preparation for transmission electron microscopy (TEM)

TEM fixed gill budding zones (Table 1) were post-fixed, washed, dehydrated, and finally embedded in Spurr's resin following the protocol described in Katz *et al*. (2010). *B. azoricus* specimens (Table 1) were ultrathin sectioned (70 nm) in the dorsal to ventral direction using a diamond knife (Reichert Ultracut S microtome). Sections were stained with uranyl acetate (25 min) and lead citrate (7 min). Gill sections were examined with a Zeiss Libra 120 and Zeiss EM 902 transmission electron microscope.

Results

FISH on gill growth zones of *Bathymodiolus*

Bathymodiolus gills showed a typical filibranch gill structure. Each gill filament consisted of a descending and ascending lamella and neighboring gill filaments were clearly separated and not interconnected by tissue junctions (for further explanations of *Bathymodiolus* gill composition see Figure 1a-c).

Strong FISH signals of the symbiont-specific oligonucleotide probes indicated that sulfur-oxidizing and methane-oxidizing symbionts were abundant in all analyzed individuals (Figure 1d, f, h-i). Their distribution pattern generally corresponded to the typical distribution of symbiont-containing bacteriocytes in the lateral regions of *Bathymodiolus* gill filaments but not in the ciliated filament edges. However, FISH signals were never observed in the budding zones at the posterior gill tips and in the youngest gill filament buds (Figure 1d). Symbiont distribution in young filaments showed a consistent pattern in all adult and juvenile specimens. Symbiont colonization began in the 7^{th} – 9^{th} filament and co-occurrence of signals from the two symbiont-specific probes indicated that the sulfur- and methane-oxidizing

symbionts were both involved in the initial colonization (Figure 1d). Earliest colonization was always observed in the descending lamella. Slightly older filaments generally showed higher signal intensities in the descending lamella than in the ascending lamella (Figure 1d, h). Newly colonized gill filaments always showed stronger FISH signals because of more symbiont cells per bacteriocyte on their anterior than on their posterior sides indicating that bacterial colonization on anterior sides had progressed further (Figure 1d). We also observed that symbionts were absent from the ventral edges of the gills (Figure 1f).

All growth areas including the symbiont-containing regions of the budding zone, uninfected freshly-formed filaments and the ventral edges of the gills showed strong signals of the PCNA-antibody indicating that these areas were characterized by highly active cell division (Figure 1d, f). In contrast, no signals from the PCNA-antibody were observed in symbiont-containing bacteriocytes.

TEM analyses of *Bathymodiolus* gill budding zones and filament buds

TEM analyses confirmed the colonization patterns observed with FISH. Micrographs of the posterior gill tips showed that the budding zone and youngest filament buds did not contain symbionts (Figure 2a). The typical epithelia cells in this region had a rectangular and slender shape and their outer surfaces were densely covered by microvilli (Figure 2b). Symbiotic colonization was first observed in filaments 7-9 from the budding zone (Figure 2a). Host cells in this region which were colonized by endosymbionts differed morphologically from uninfected cells. They were flatter and wider and had significantly less microvilli on their surface. These first bacteriocytes harbored only a few methanotrophic and thiotrophic symbionts which were individually enclosed in vacuoles (Figure 2c). They were always located at the apical pole of the host cell and these vacuoles were often open to the environment at the outermost surface of the host cell. We also observed many vacuoles that appeared as if they had recently been closed as indicated by the close proximity of

invaginations of the bacteriocyte surface membrane to these vacuoles (Figure 2c-d). In bacteriocytes of slightly older gill filaments, symbionts of both morphotypes were successively more abundant (Figure 2e). The outer surfaces of these bacteriocytes were smooth and microvilli were only rarely observed.

In the youngest filaments that were colonized by symbionts, the formation of bacteriocytes always started in contiguous and centrally confined areas of the anterior filament surfaces (filament 8 in Figure 2a). In proceeding older filaments, formation of bacteriocytes overlapped to the posterior filament sides and the bacteriocyte areas widened progressively (filament 12 in Figure 2a).

FISH on gills of "*C.*" *ponderosa*

Sections of "*C.*" *ponderosa* gills reflected a eulamellibranchial gill structure that is characterized by fused filaments (i.e. not divided into ascending and descending lamellae) and tissue junctions connecting neighboring filaments (Figure 3a). FISH with symbiont specific probes indicated that the sulfur-oxidizing symbionts were abundant in all three investigated specimens. Bacteriocytes densely filled with symbionts occurred regularly on the surfaces of the filaments, in the interfilamental junctions (Figure 3a) and in tissues connecting the bases of the filaments (Figure 3b). Symbionts were not observed in the ciliated filament edges and in the ventral edges (Figure 3a). The developmental stage of young filaments was difficult to determine because the posterior gill tips were strongly twisted in all three investigated specimens. Symbiont distribution in the youngest gill filaments was therefore difficult to assess, but symbionts were clearly absent in the budding zones at the posterior gill tips (Figure 3b).

Discussion

Symbiont colonization of gill tissue in *Bathymodiolus*

Gill filament formation in filibranch mytilids begins with the splitting of undifferentiated tissue folds from the budding zone which subsequently differentiate into complex gill filament structures consisting of an ascending and a descending lamella (Neumann and Kappes, 2003b) (Figure 1). The FISH and TEM analyses presented here provide to our knowledge the first observations on symbiont distribution in this growth area of *Bathymodiolus* gills. Our results of juvenile and adult individuals showed that symbionts were always absent in the budding zones and also in the youngest yet undivided filaments. However, they were always present shortly before or after the splitting into descending and ascending lamellae. This indicates that initial symbiont colonization co-occurs with the filament differentiation into separate lamellae. Similar distribution patterns in juveniles and adults of shell lengths ranging from 6 to 100 mm indicate that the colonization process is similar in different ontogenetic stages of the host. This strongly suggests that colonization of developing filaments is a continuous process that occurs consistently during the entire growth of the gill and thus throughout the entire life span of the host.

The lack of symbionts in the ventral edges of the filaments is consistent with earlier observations. Similar to other bivalves, the outer filament edges in *Bathymodiolus* consist of specialized cells which maintain the respiratory water flow around the gill and transport food particles to the mouth. Cross sections of gill filaments have regularly shown that these highly differentiated cells do not contain symbionts (e.g. Distel *et al.*, 1995; Le Pennec and Hily, 1984). In addition, Leibson and Movchan (1975) showed for mytilids and other bivalves that the junction point of descending and ascending lamellae in gill filaments also contains accumulations of low-differentiated cells which are actively dividing. These differ fundamentally from the majority of the gill cells. The observed overlap of areas with proliferating cells, as indicated by bound PCNA-antibody, and symbiont-free areas in our

Bathymodiolus material (Figure 1d, f) suggests that zones of active cell division as a rule do not contain bacteria.

There is indirect molecular and morphological evidence that *Bathymodiolus* take up their symbionts from the environment and do not transfer them via the germ line between generations (Eckelbarger and Young, 1999; Le Pennec and Beninger, 1997; Won *et al.*, 2003), but it remains unknown how exactly the symbionts colonize the mussel gills. Environmental bacteria enter the mantle cavity with the incoming water flow and are guided through the gills. Many observations suggest that they enter the gill tissue by invasion. Symbiont-containing vacuoles that resemble invaginations of the bacteriocyte surface membrane and have contact to the external environment have been observed in several *Bathymodiolus* species (Dubilier *et al.*, 1998; Le Pennec *et al.*, 1988; Salerno *et al.*, 2005; Won *et al.*, 2003) and they have been considered as an indication for environmental endocytosis (Le Pennec *et al.*, 1988; Won *et al.*, 2003). Endocytosis has never been directly observed in *Bathymodiolus*, but several of our observations are consistent with observations made in symbiotic lucinid *Codaki orbicularis* clams that had lost their symbionts during experimental starvation and had reacquired them after being returned to their natural habitat (Gros *et al.*, 2012). Small numbers of envacuolated symbionts were soon present in bacteriocytes of confined regions of the gills that were exposed to circulating seawater. These first bacteria were always located in apical regions of the bacteriocytes suggesting that endocytosis had occurred. In the *Bathymodiolus* investigated in this study, the few methanotrophic and thiotrophic symbionts located in close proximity to the outer host cell membrane in the apical region of the newly formed bacteriocytes as well as the invaginations of symbiont-containing vacuoles (Figure 2d-e) strongly suggest that these colonizers invaded from the environment. While symbiont abundances rapidly increased in bacteriocytes of slightly older filaments, we did not observe conspicuous numbers of dividing cells, and it is unclear if the abundances had increased by cell division or continuous invasion.

A second interpretation for the function of open vacuoles is possible: Open ducts to the external medium might also serve as exits for the release of symbionts from the bacteriocytes. We hypothesize that such a symbiont release exists and that it is a regularly occurring process which ensures that symbionts are present in the gaps between filaments and can instantly colonize newly formed gill filaments. We consistently observed with FISH and TEM that first bacterial colonizers in new filaments were found opposite and in close proximity to earlier colonized filament surfaces (Figure 1d-e, 2a). This suggests that the colonizers originated from opposite bacteriocytes, and that symbionts can "jump" between filaments. If this is the case, symbionts released into the mantle cavity might maintain a free-floating symbiont population which could serve as a permanent colonization resource. Exhalent water might even transport symbionts from the mantle cavity into the environment where they could invade other host individuals. There is no direct evidence yet for such an export and release of symbionts from bacteriocytes. However, an indication for an exchange of symbionts between host individuals might come from *B. azoricus* individuals that had lost most of their thiotrophic symbionts during a starvation period of experimental sulfide depletion in aquaria, and in which symbiont populations recovered after they had been brought together with other untreated mussels (Kadar *et al.*, 2005).

Symbiont distribution in gill growth zones of *"C." ponderosa*

Genetic and morphological data show that chemosynthetic vesicomyid clams transmit their symbionts vertically (e.g. Cary and Giovannoni, 1993; Endow and Ohta, 1990; Hurtado *et al.*, 2003; Kuwahara *et al.*, 2008; Peek *et al.*, 1998). Endosymbiotic cells have been localized in vitellogenic oocytes and follicle cells of parental individuals (Cary and Giovannoni, 1993; Endow and Ohta, 1990), but it is unclear how symbionts reach the gills in the offspring. The absence of FISH signals in the gill budding zones of "*C.*" *ponderosa* suggests that filaments buds do not contain symbionts from the beginning, but our material did not make clear at

which stage the initial colonization occurs. Cross sections of the ventral edges revealed a similar symbiont colonization pattern as in ventral edges of *Bathymodiolus* gills suggesting that areas of undifferentiated cells in the growth zones of "*C*." *ponderosa* are not colonized. In the chemosynthetic *Solemya velum* clam which transmits its symbionts also vertically, bacteria were observed at the basis of gill buds (Krueger *et al.*, 1996) indicating that symbionts colonize newly formed gill filaments from their basis. Symbiont colonization of protobranch gills in *Solemya* may differ from colonization of the much more complex eulammellibranch gills of vesicomyids. However, symbionts in the tissue interconnecting the bases of young gill filaments in "*C*." *ponderosa* (Figure 3b) might indicate that symbionts in this species also initially invade the gill from its basis. In addition bacteriocytes in the junctions between the filaments of "*C*." *ponderosa* (Figure 3a) suggest that symbionts spread among filaments via these tissue bridges. Further investigations are needed to clarify the exact colonization process.

Bacteriocyte formation in *Bathymodiolus*

Our results indicate that colonization by symbionts co-occurs with a modification of the host cell. Invariably all cells in filament buds containing bacteria showed typical bacteriocyte characteristics which were lacking in un-colonized cells (i.e. the wide and somewhat inflated shape and the lack of microvilli) (Figure 2b-e). We do not yet know how these modifications occur, but we hypothesize that they are initiated by the invasion of bacteria across the outer host cell membrane. Enteroinvasive pathogens such as *Salmonella*, *Shigella, Listeria* and *Yersinia* use common strategies for cell entry including e.g., the binding to eukaryotic surface receptors, rearrangement of the actin cytoskeleton of the host cell, membrane extension which causes the effacement of microvilli, and in many cases the induction of a vacuole that engulfs the bacterium (reviewed in Cossart and Sansonetti, 2004). It is striking that (*i*) bacteriocytes in all *Bathymodiolus* symbioses investigated are smooth while neighboring intercalary cells

which do not contain symbionts are densely covered by microvilli (e.g. Duperron, 2010; Fiala-Médioni and Le Pennec, 1987; Fisher *et al.*, 1987) and that (*ii*) the bacteriocytes in symbioses without external symbiont invasion also carry microvilli such as in other mytilids closely related to *Bathymodiolus* that are associated with extracellular symbionts and also in the vertically transmitting vesicomyids (e.g. Duperron, 2010; Fiala-Médioni and Le Pennec, 1987; Fujiwara *et al.*, 2010). It is possible that chemosynthetic *Bathymodiolus* symbionts exhibit similar entry mechanisms as invasive pathogens. Future research will reveal if this is true and how these mechanisms function.

Conclusion

We observed a consistent colonization pattern of the symbionts in all investigated *Bathymodiolus* mussels, despite the different ontogenetic ages as inferred from their different shell sizes. Our analyses showed for the first time that the major growth zones of gills in juvenile and adult *Bathymodiolus* do not contain symbionts and that symbiont colonization of newly formed gill tissue in the terminal end and the ventral edge co-occurs with the differentiation of this tissue. *"C." ponderosa* gills also indicated the absence of symbionts in the gill budding zone and the ventral edge suggesting that newly formed clam gill tissue is also initially free of symbionts. These concurrent observations strongly suggest that chemosynthetic symbionts in bivalves as a rule colonize gill filaments after their formation and that this colonization is a continuous process throughout the life span of the host.

Our results further strongly support uptake of symbionts in *Bathymodiolus* by invasion through the external cell membrane. It is very likely that many diverse strains of free-living symbiotic 16S rRNA phylotypes co-exist in hydrothermal vent habitats, and the availability of symbiont strains in the environment may vary locally and temporarily. Mid-Atlantic Ridge mussels have revealed within single individuals a considerable diversity of symbiont strains on the phylogenetic level of ITS genotypes (DeChaine *et al.*, 2006). If environmental

symbiont uptake in *Bathymodiolus* is continuous, they may take up different strains at different times. It is thus possible that the composition of strains in the gills varies over time and possibly also in different parts of the gill. Nothing is known on spatial and temporal patterns of strain diversity in *Bathymodiolus* gills and future studies will reveal if such patterns exist.

Acknowledgement

We thank the chief scientists, captains and crews of the RV Meteor and RV Atlantis during cruises Hydromar I M60/3, MenezMAR M82/3 and leg AT 15-3 as well as the teams of ROV Marum Quest 4000 m and DSV Alvin. We are very grateful to Silke Wetzel, Ute Kuhlicke and Agnes Zimmer for excellent technical assistance. We are also very grateful to Thomas Neu who helped with microscopic evaluation. Monica Bright and her group at the University of Vienna are also specially acknowledged for their support during TEM analyses and for valuable discussions. The funding for this study was provided by German Research Foundation within the framework of the Program SPP 1144 “From Mantle to the Ocean: Energy- Material- and Life-Cycles at Spreading Axes”, the DFG Cluster of Excellence "The Ocean in the Earth System" at MARUM, Bremen, and the Max Planck Society. CW was supported by a scholarship of the “Studienstiftung des deutschen Volkes”, MS was funded by the European Commission through Marie Curie Initial Training Network “Symbiomics”.

References

Bright M, Bulgheresi S (2010) A complex journey: transmission of microbial symbionts. *Nat Rev Microbiol* **8:** 218-230.

Cary SC, Giovannoni SJ (1993) Transovarial inheritance of endosymbiotic bacteria in clams inhabiting deep-sea hydrothermal vents and cold seeps. *P Natl Acad Sci USA* **90:** 5695-5699.

Cavanaugh CM, Gardiner SL, Jones ML, Jannasch HW, Waterbury JB (1981) Prokaryotic cells in the hydrothermal vent tube worm *Riftia pachyptila* Jones - possible chemoautotrophic symbionts. *Science* **213:** 340-342.

Cavanaugh CM, McKiness ZP, Newton ILG, Stewart FJ (2006). Marine chemosynthetic symbioses. In: Dworkin M, Falkow SI, Rosenberg E, Schleifer K-H, Stackebrandt E (eds). *The Prokaryotes*. Springer: New York. pp 475-507.

Childress JJ, Fisher CR, Brooks JM, Kennicutt MC, 2nd, Bidigare R, Anderson AE (1986) A methanotrophic marine molluscan (bivalvia, mytilidae) symbiosis: mussels fueled by gas. *Science* **233:** 1306-1308.

Cossart P, Sansonetti PJ (2004) Bacterial invasion: The paradigms of enteroinvasive pathogens. *Science (New York, NY* **304:** 242-248.

DeChaine EG, Bates AE, Shank TM, Cavanaugh CM (2006) Off-axis symbiosis found: characterization and biogeography of bacterial symbionts of *Bathymodiolus* mussels from Lost City hydrothermal vents. *Environ Microbiol* **8:** 1902-1912.

DeChaine EG, Cavanaugh CM (2006) Symbioses of methanotrophs and deep-sea mussels (Mytilidae: Bathymodiolinae). *Prog Mol Subcell Biol* **41:** 227-249.

Distel DL, Lee HK-W, Cavanaugh CM (1995) Intracellular coexistence of methano- and thioautotrophic bacteria in a hydrothermal vent mussel. *P Natl Acad Sci USA* **92:** 9598-9602.

Dubilier N, Windoffer R, Giere O (1998) Ultrastructure and stable carbon isotope composition of the hydrothermal vent mussels *Bathymodiolus brevior* and *B*. sp. *affinis brevior* from the North Fiji Basin, western Pacific. *Mar Ecol Prog Ser* **165:** 187-193.

Dubilier N, Bergin C, Lott C (2008) Symbiotic diversity in marine animals: the art of harnessing chemosynthesis. *Nat Rev Microbiol* **6:** 725-740.

Duperron S, Bergin C, Zielinski F, Blazejak A, Pernthaler A, McKiness ZP *et al.* (2006) A dual symbiosis shared by two mussel species, *Bathymodiolus azoricus* and *Bathymodiolus puteoserpentis* (Bivalvia: Mytilidae), from hydrothermal vents along the northern Mid-Atlantic Ridge. *Environ Microbiol* **8:** 1441-1447.

Duperron S (2010). The diversity of deep-sea mussels and their bacterial symbioses. In: Kiel S (ed). *Vent and Seep Biota: Aspects from Microbes to Ecosystems*. Springer: Dordrecht. pp 137-167.

Eckelbarger KJ, Young CM (1999) Ultrastructure of gametogenesis in a chemosynthetic mytilid bivalve (*Bathymodiolus childressi*) from a bathyal, methane seep envirnment (northern Gulf of Mexico). *Mar Biol* **135:** 635-646.

Endow K, Ohta S (1990) Occurence of bacteria in the primary oocytes of vesicomyid clam *Calyptogena soyae*. *Mar Ecol Prog Ser* **64:** 309-311.

Fiala-Médioni A, Le Pennec M (1987) Trophic structural adaptations in relation to the bacterial association of bivalve mollusks from hydrothermal vents and subduction zones. *Symbiosis* **4:** 63-74.

Fisher CR, Childress JJ, Oremland RS, Bidigare RR (1987) The importance of methane and thiosulfate in the metabolism of the bacterial symbionts of two deep-sea mussels. *Mar Biol* **96:** 59-71.

Fuchs BM, Glockner FO, Wulf J, Amann R (2000) Unlabeled helper oligonucleotides increase the in situ accessibility to 16S rRNA of fluorescently labeled oligonucleotide probes. *Appl Environ Micrbiol* **66:** 3603-3607.

Fujiwara Y, Kawato M, Noda C, Kinoshita G, Yamanaka T, Fujita Y *et al.* (2010) Extracellular and mixotrophic symbiosis in the whale-fall mussel *Adipicola pacifica*: A trend in evolution from extra- to intracellular symbiosis. *PloS ONE* **5**.

Gros O, Elisabeth NH, Gustave SD, Caro A, Dubilier N (2012) Plasticity of symbiont acquisition throughout the life cycle of the shallow-water tropical lucinid *Codakia orbiculata* (Mollusca: Bivalvia). *Environ Microbiol* **14:** 1584-1595.

Hurtado LA, Mateos M, Lutz RA, Vrijenhoek RC (2003) Coupling of bacterial endosymbiont and host mitochondrial genomes in the hydrothermal vent clam *Calyptogena magnifica*. *Appl Environ Microbiol* **69:** 2058-2064.

Kadar E, Bettencourt R, Costa V, Santos RS, Lobo-Da-Cunha A, Dando P (2005) Experimentally induced endosymbiont loss and re-acquirement in the hydrothermal vent bivalve *Bathymodiolus azoricus*. *J Exp Mar Biol Ecol* **318:** 99-110.

Katz S, Klepal W, Bright M (2010) The skin of *Osedax* (Siboglinidae, Annelida): An ultrastructural investigation of its epidermis. *J Morphol* **271:** 1272-1280.

Krueger DM, Gustafson RG, Cavanaugh CM (1996) Vertical transmission of chemoautotrophic symbionts in the bivalve *Solemya velum* (Bivalvia: Protobranchia). *Biol Bull* **190:** 195-202.

Kuwahara H, Takaki Y, Yoshida T, Shimamura S, Takishita K, Reimer JD *et al.* (2008) Reductive genome evolution in chemoautotrophic intracellular symbionts of deep-sea *Calyptogena* clams. *Extremophiles* **12:** 365-374.

Le Pennec M, Hily A (1984) Anatomie, structure et ultrastructure de la branchie d'un Mytilidae des sites hydrothermeaux du Pacifique oriental. *Oceanol Acta* **7:** 517-523.

Le Pennec M, Diouris M, Herry A (1988) Endocytosis and lysis of bacteria in gill epithelium of *Bathymodiolus thermophilus, Thyasira flexuosa* and *Lucinella divaricata* bivalve molluscs. *J Shellfish Res* **7:** 483-490.

Le Pennec M, Beninger PG (1997) Ultrastructural characteristcs of spermatogenesis in three species of deep-sea hydrothermal vent mytilids. *Can J Zool* **75:** 308-316.

Leibson NL, Movchan OT (1975) Cambial zones in gills of Bivalvia. *Mar Biol* **31:** 175-180.

Ludwig W, Strunk O, Westram R, Richter L, Meier H, Yadhukumar *et al.* (2004) ARB: a software environment for sequence data. *Nucleic Acids Res* **32:** 1363-1371.

McDowell EM, Trump BF (1976) Histologic fixatives suitable for diagnostic light and electron-microscopy. *Arch Pathol Lal Med* **100:** 405-414.

Neumann D, Kappes H (2003b) On the growth of bivalve gills initiated from a lobule-producing budding zone. *Biol Bull* **205:** 73-82.

Peek AS, Feldman RA, Lutz RA, Vrijenhoek RC (1998) Cospeciation of chemoautotrophic bacteria and deep sea clams. *P Natl Acad Sci USA* **95:** 9962-9966.

Petersen JM, Zielinski FU, Pape T, Seifert R, Moraru C, Amann R *et al.* (2011) Hydrogen is an energy source for hydrothermal vent symbioses. *Nature* **476:** 176-180.

Pruesse E, Quast C, Knittel K, Fuchs BM, Ludwig W, Peplies J *et al.* (2007) SILVA: a comprehensive online resource for quality checked and aligned ribosomal RNA sequence data compatible with ARB. *Nucleic Acids Res* **35:** 7188-7196.

Salerno JL, Macko SA, Hallam SJ, Bright M, Won YJ, McKiness Z *et al.* (2005) Characterization of symbiont populations in life-history stages of mussels from chemosynthetic environments. *Biol Bull* **208:** 145-155.

Steedman HF (1957) Polyester wax; a new ribboning embedding medium for histology. *Nature* **179:** 1345.

Stewart FJ, Newton IL, Cavanaugh CM (2005) Chemosynthetic endosymbioses: adaptations to oxic-anoxic interfaces. *Trends Microbiol* **13:** 439-448.

Stewart FJ, Young CR, Cavanaugh CM (2008) Lateral symbiont acquisition in a maternally transmitted chemosynthetic clam endosymbiosis. *Mol Biol Evol* **25:** 673-687.

Stewart FJ, Cavanaugh CM (2009) Pyrosequencing analysis of endosymbiont population structure: co-occurrence of divergent symbiont lineages in a single vesicomyid host clam. *Environ Microbiol* **11:** 2136-2147.

van der Heijden K, Petersen JM, Dubilier N, Borowski C (2012) Genetic connectivity between North and South Mid-Atlantic Ridge chemosynthetic bivalves and their symbionts. *Plos One* **7**.

van Dover CL (2000). *The ecology of deep-sea hydrothermal vents*. Princeton University Press: Princeton, New Jersey.

Wendeberg A, Zielinski FU, Borowski C, Dubilier N (2012) Expression patterns of mRNAs for methanotrophy and thiotrophy in symbionts of the hydrothermal vent mussel *Bathymodiolus puteoserpentis*. *ISME J* **6:** 104-112.

Won YJ, Hallam SJ, O'Mullan GD, Pan IL, Buck KR, Vrijenhoek RC (2003) Environmental acquisition of thiotrophic endosymbionts by deep-sea mussels of the genus *Bathymodiolus*. *Appl Environ Microbiol* **69:** 6785-6792.

Figure 1

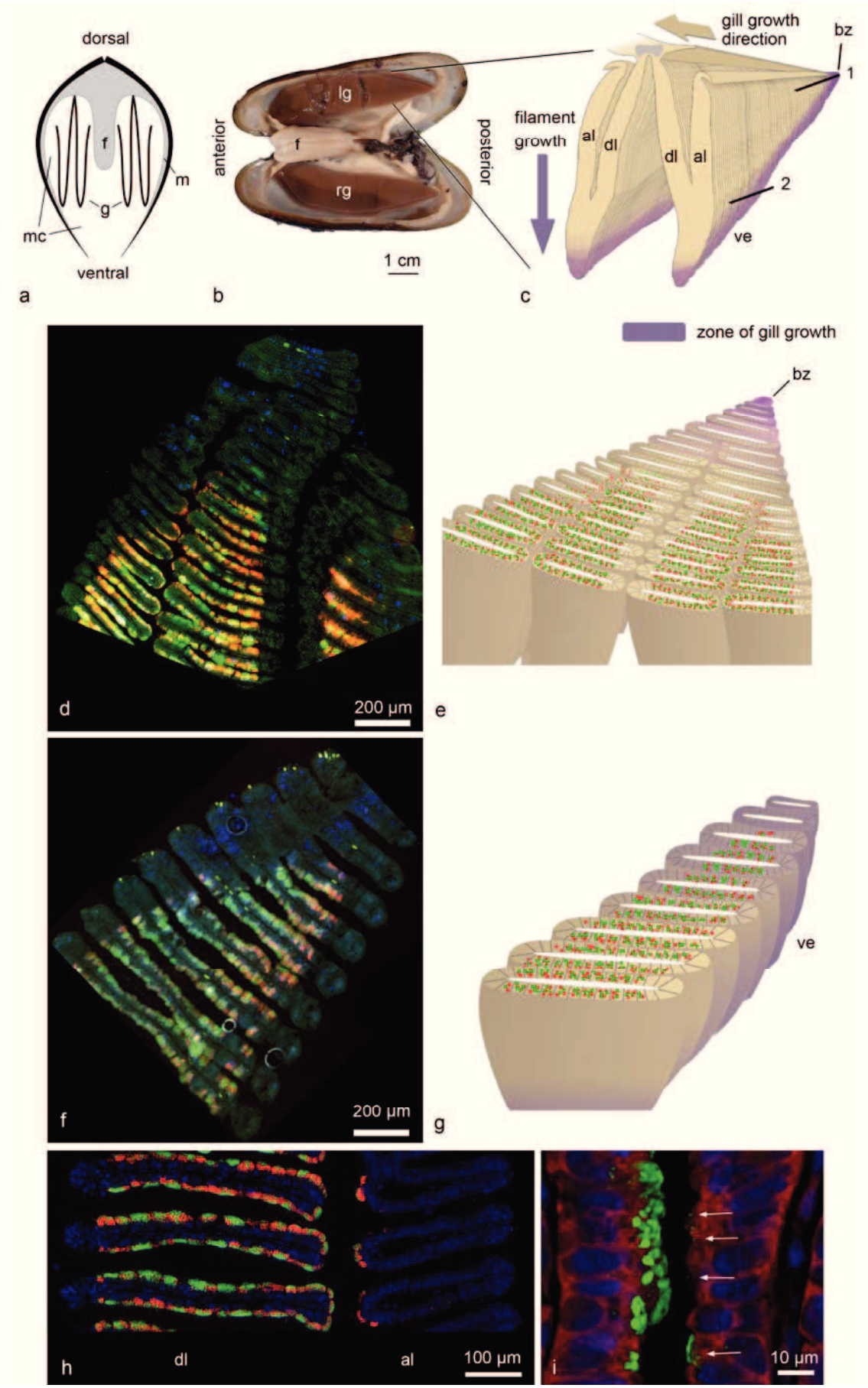
dorsal
f
m
g
mc
ventral
a
lg
f
rg
anterior
posterior
1 cm
b
gill growth direction
bz
1
filament growth
al
dl
dl
al
2
ve
c
zone of gill growth
bz
d
200 µm
e
f
200 µm
g
ve
h
dl
al
100 µm
i
10 µm

Legend of Figure 1: FISH and PCNA immuno-hystochemistry on cross sections of *B. puteoserpentis* gills and schematic interpretations of symbiont distribution. **a-c)** Overview of *Bathymodiolus* gill morphology. **a)** Schematic cross section through a mussel in anterior view showing the localization of the two W-shaped filibranch gills in the mantel cavity on either side of the body. **b)** Opened mussel giving view into the mantel cavity with the two large gills lying flat on the mantel. **c)** Schematic drawing of the posterior end of the left gill. Each gill consists of thousands of gill filaments that are arranged like the lamella in a lamella curtain. Each gill filament consists of a descending and an ascending lamella. Gill filaments are interconnected at the distal ends of their ascending lamella, but otherwise without tissue junctions. Gill growth includes two major processes occurring throughout the lifetime of the animal: 1) Longitudinal gill growth is by continuous proliferation of new gill filaments from a budding zone at the posterior end of each gill. 2) Youngest gill filament buds extend ventrally and form a descending lamella before they bend upwards and develop the ascending lamella. At subsequent developmental stages the filaments primarily extend at the ventral edges resulting in ventral growth of the gill. al, ascending lamella; bz, budding zone; dl, descending lamella; f, foot; g, gill; id, inner demibranch; lg, left gill; m, mantel; mc, mantle cavity; od, outer demibranch; rg, right gill; ve, ventral edge. Solid black lines in c indicate the two cross section planes of d & f. c modified after Le Pennec and Hily (1984). **d)** Cross section of posterior end of the gill (section plane 1 in Figure 1c) with FISH of thiotrophic (green) and methanotrophic (red) symbionts (overlay in yellow) and bound PCNA-antibodies (blue). Symbionts are only present in filaments that have developed ascending and descending lamellae (lower image area). Youngest gill filaments (upper area) indicate strong host cell proliferation activity and do not contain symbionts (budding zone is out of the section plane in this image). **e)** Schematic interpretation of symbiont distribution in d: The budding zone at the posterior tip of each gill produces gill buds that divide into two separate gill filaments which later divide into descending and ascending lamellae. Red and green dots illustrate the

distribution of symbionts. **f)** FISH of thiotrophic (red) and methanotrophic (green) symbionts (overlay in yellow) on cross section of ventral gill filament edge (section plane 2 in Figure 1c). Symbionts occur in filament regions with less or no proliferation activity (blue). Host cell proliferation is most active in ventral margin of the ventral gill edge. **g)** Schematic interpretation of cross section plane in f: Red and green dots illustrate the distribution of symbionts. **h)** FISH of thiotrophic (red) and methanotrophic (green) symbionts on cross sections of young gill filaments. In descending lamellae symbionts densely colonize the entire lateral faces with exception of the ciliated edges on the left, while colonization of the developing ascending lamellae has just started. **i)** FISH of *Bathymodiolus* endosymbionts with a eubacterial probe (green) on a cross section of two successive young gill filaments. Symbiont colonization of the older filament on the left has already progressed while only a few cells (arrows) are visible in the opposing younger filament on the right. At that stage, all endosymbionts concentrate next to the outer cell wall of the bacteriocytes. Host nuclei in blue (DAPI). al, ascending lamella; bz, budding zone; dl, descending lamella; ve, ventral egde of the gill.

Figure 2

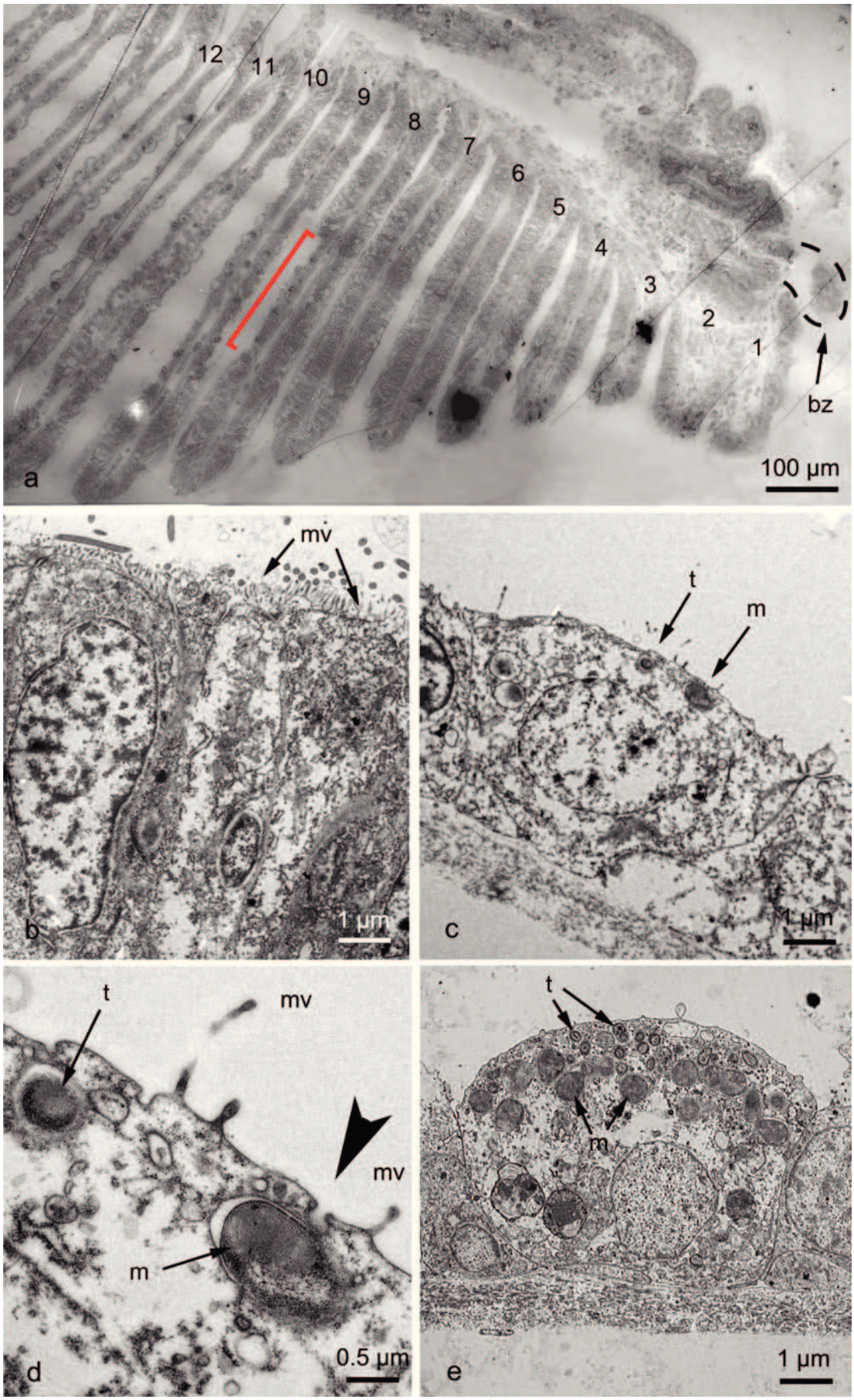
12
11
10
9
8
7
6
5
4
3
2
1
bz
a
100 µm
mv
b
1 µm
t
m
c
1 µm
t
mv
mv
m
d
0.5 µm
t
m
e
1 µm

Figure 2: Transmission electron micrographs of posterior gill tips of *B. azoricus*. **a)** Composed image of a longitudinal section through the postrior gill tip showing the budding zone and the fifteen youngest gill filaments. The budding zone was only in part sectioned and its outline is marked with a dashed line. Budding zone and filaments 1-7 did not contain symbionts and bacteriocytes occurred first on the anterior side of filament 8 (bacteriocyte region marked by red bracket). Filament 9 and all subsequent ones showed bacteriocytes on both filament sides and the bacteriocyte region gradually widened. **b)** Epithelial cells of a young uncolonized gill filament (number 6 in a). These cells were typically slender and their outer cell walls were densely covered by microvilli. **c)** Bacteriocyte at an early colonization stage (corresponding to filament 8 in a) with very few symbionts and a few microvilli on the outer cell wall. **d)** Zoom into c. Arrowhead points to opening of vacuole. **e)** Bacteriocyte of a slightly older filament containing numerous symbionts. These bacteriocytes always lacked microvilli. **e)** m, methanotropic symbionts; mv, microvilli; t, thiotrophic symbionts.

Figure 3

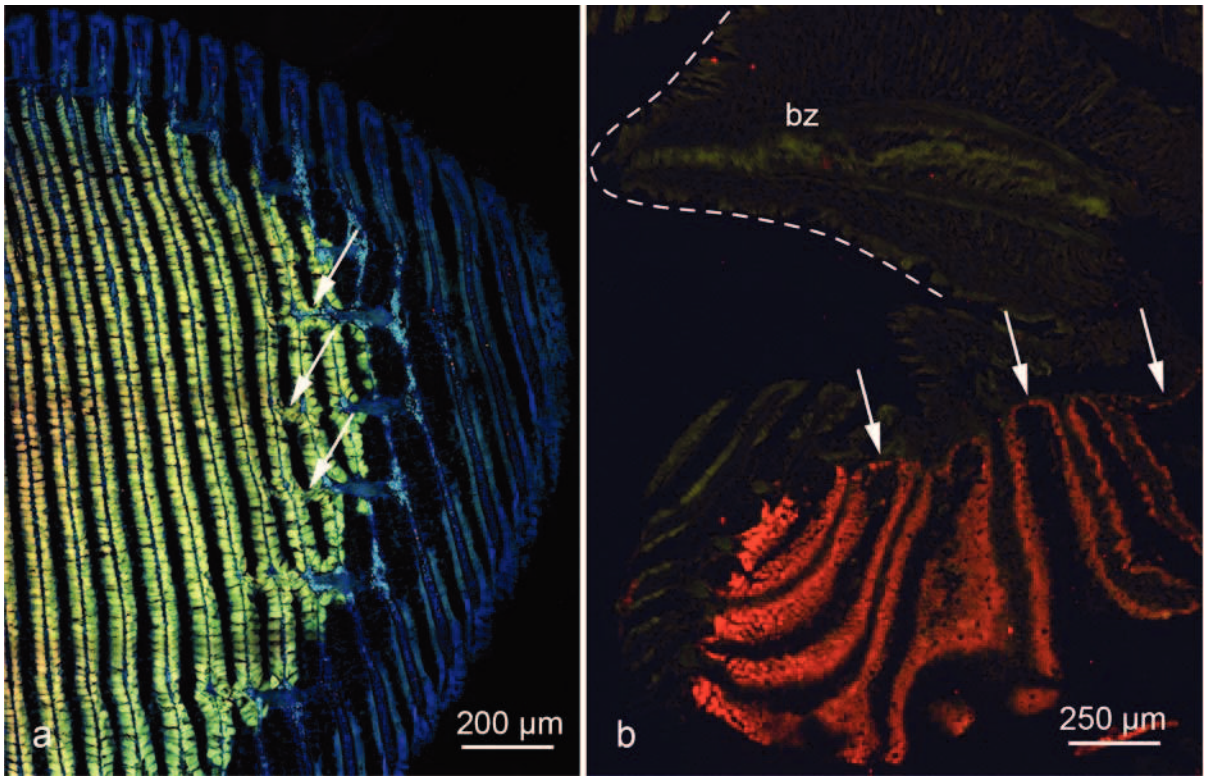

Figure 3: FISH on cross sections of "*C. ponderosa* gills. a) Double hybridization of thiotrophic symbionts in ventral gill filament edge with two differently labeled probes resulting in yellow/green overlay signal. Arrows indicate interfilamental junctions containing bacteriocytes. **b)** Cross section of the posterior gill tip (single hybridization with probe 1014 and Cy3 label). The outline of the budding zone is indicated by a dashed line. Arrows indicate symbionts in tissue interconnecting gill filaments at their bases. bz, budding zone.

Table 1: Number of specimens investigated in this study and their collection sites at the Mid-Atlantic Ridge (MAR) and the Golf of Mexico (GoM)

Host species	**Number of individuals**	**Shell length (mm)**	**Material**	**Specific analysis**	**Location (coordinates)**	**Habitat**	**Water depth (m)**	**Vessel, cruise & date**
B. puteoserpentis	7	6 – 21	Entire animal	FISH	Logatchev, MAR (14°45.20'N, 44°58.78'W)	Vent	3035	RV Meteor, M60/3, February 2004
B. azoricus	5	5 – 29	Entire animal	FISH	Menez Gwen, MAR (37°84.45'N, 31°51.85'W)	Vent	840	RV Meteor, M82/3, September 2010
	6	55-100	Dissections of posterior gill filaments including budding zone	FISH				
	2	55-100	Dissections of posterior gill filaments including budding zone	TEM				
"*C.*" *ponderosa*	3	≥ 60	Dissections of posterior gill filaments including budding zone	FISH	Mississippi Canyon 853, GoM (28°07.64'N, 89°08.47'W)	Seep	1070	RV Atlantis, Deep Chemosynthetic Community Characterization Cruise, leg AT 15-3, May 2006

Table 2: FISH probes used in this study

Probe name	Target organism (without mismatch)	Probe sequence (5´-3´)	*E. coli* position	FA[a] [%]	Reference
Cpon_826	"*C.*" *ponderosa* symbiont, *Vesicomya cordata* symbiont, *Vesicomya stearnsii* symbiont, *Calyptogena nautilei* symbiont	AAC CCC CCT CAA CGA CTA	826[b]	30-35	This study
Cpon_831	"*C.*" *ponderosa* symbiont, *Vesicomya cordata* symbiont, *Vesicomya stearnsii* symbiont, *Calyptogena nautilei* symbiont	AGG GTA ACC CCC CTC AAC	831 [b]	30-35	This study
Cpon_1014	"*C.*" *ponderosa* symbiont, *Vesicomya cordata* symbiont, 4 uncultured bacteria	CGA AGG CAC TTT TCC ATC	1014 [b]	30-35	This study
Cpon_1014_Helper1		TCTGGAAAGTTTGCGATATG			
Cpon_1014_Helper2		AGCACCTGTATTCGCATTCC			
BNMAR_193_thio	Thiotrophic symbiont of *B. azoricus* and *B. puteoserpentis*	CGA AGG TCC TCC ACT TTA	193 [b]	35	(Duperron *et al.*, 2006)
BNMAR_845_meth	Methanotrophic symbiont of *B. azoricus* and *B. puteoserpentis*	GCT CCG CCA CTA AGC CTA	845 [b]	35	(Duperron *et al.*, 2006)

a. Formamide concentration in the FISH hybridization buffer in % (v/v).
b. Position in the 16S rRNA of *E. coli.*
c. Position in the 23S rRNA of *E. coli.*

Chapter 4: Metaproteomics of a gutless marine worm and its symbiotic microbial community reveal unusual pathways for carbon and energy use

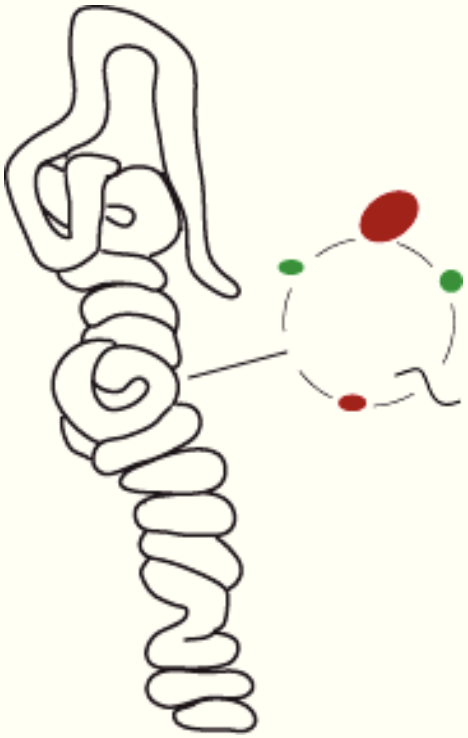

(modified after Dubilier *et al.* 2008)

Metaproteomics of a gutless marine worm and its symbiotic microbial community reveal unusual pathways for carbon and energy use

Manuel Kleiner[a,b,1], Cecilia Wentrup[a], Christian Lott[a,c], Hanno Teeling[a], Silke Wetzel[a], Jacque Young[d,e], Yun-Juan Chang[d], Manesh Shah[d], Nathan C. VerBerkmoes[d], Jan Zarzycki[f], Georg Fuchs[f], Stephanie Markert[g], Kristina Hempel[b], Birgit Voigt[b], Dörte Becher[b], Manuel Liebeke[h,i], Michael Lalk[h], Dirk Albrecht[b], Michael Hecker[b,g], Thomas Schweder[g,h,1], and Nicole Dubilier[a,1]

[a]*Symbiosis Group, Max Planck Institute for Marine Microbiology, 28359 Bremen, Germany;* [b]*Institute for Microbiology and* [h]*Institute of Pharmacy, University of Greifswald, 17487 Greifswald, Germany;* [c]*Elba Field Station, HYDRA Institute for Marine Sciences, Località Fetovaia, 57034 Campo nell'Elba, Italy;* [d]*Oak Ridge National Laboratory, Chemical Science Division, Oak Ridge, TN 37831;* [e]*Graduate School for Genome Science and Technology, University of Tennessee, Knoxville, TN 37996;* [f]*Department of Microbiology, Faculty of Biology, University of Freiburg, 79104 Freiburg, Germany;* [g]*Institute of Marine Biotechnology, 17489 Greifswald, Germany; and* [i]*Biomolecular Medicine, Department of Surgery and Cancer, Faculty of Medicine, Imperial College London, London, United Kingdom SW7 2AZ*

AUTHOR SUMMARY

Low nutrient availability is one of the major constraints for life on Earth, and organisms have evolved numerous strategies for overcoming this challenge. Symbiotic associations have been remarkably successful in enabling organisms to live in nutrient-poor environments. Particularly striking are the associations between chemosynthetic bacteria and marine animals, because the symbionts allow their hosts to thrive on inorganic energy and carbon sources such as sulfide and CO_2, thus enabling them to flourish in habitats where they otherwise could not live, such as the deep sea or nutrient-limited shallow-water sediments (1). In this study, we reveal the intricate network of metabolic interactions in the gutless marine worm *Olavius algarvensis* and its chemosynthetic microbial community that could explain how this symbiosis thrives in its oligotrophic habitat. We propose previously undescribed pathways for coping with energy and nutrient limitations and show that some of these pathways may be widespread in both free-living and symbiotic bacteria (Fig. P1).

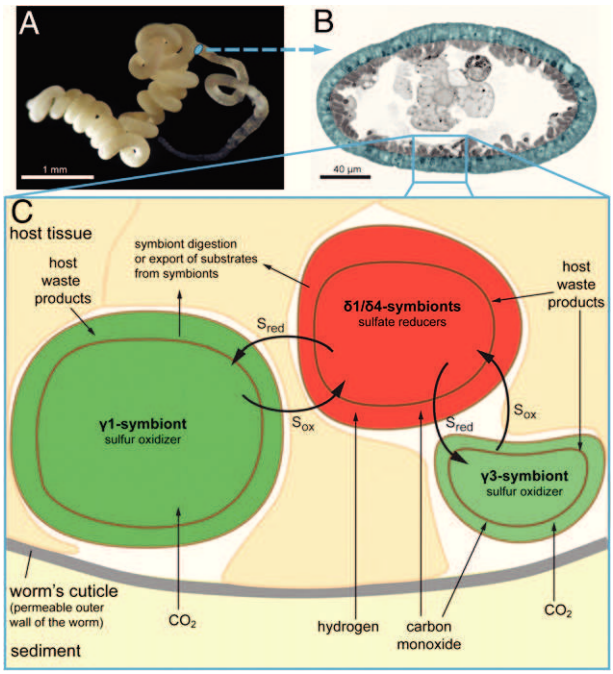

Fig. P1. Overview of symbiotic metabolism based on metaproteomic and metabolomic analyses. (*A*) Live *O. algarvensis* specimen. (*B*) Light micrograph of a cross section through *O. algarvensis*. The region containing the symbionts is highlighted in blue. (*C*) Schematic diagram of possible energy and carbon sources for the symbiosis. External sources of energy and carbon could include carbon monoxide, hydrogen, and carbon dioxide; internal sources could include reduced sulfur compounds and host waste products, such as acetate and glycine betaine. S_{ox}, oxidized sulfur compounds; S_{red}, reduced sulfur compounds.

The microbiome of the worm *O. algarvensis* is highly specific and consists of five bacterial symbionts. Two of these symbionts are gammaproteobacterial sulfur oxidizers, two are deltaproteobacterial sulfate reducers, and the fifth is a spirochete (2). Previous studies, including metagenomic analyses of the bacterial symbionts, revealed how the worms can thrive in sulfide-poor coastal sediments of the Mediterranean (3, 4). The sulfate-reducing δ-symbionts provide the sulfur-oxidizing γ-symbionts with reduced sulfur compounds as an internal energy source for the autotrophic fixation of CO_2. However, the external sources of energy for the symbiosis that enable net growth and reproduction have remained unclear.

In this study, we used various analytical methods to gain an in-depth understanding of the intricate interactions between *O. algarvensis* and its microbial symbiont community and between these organisms and their environment. Specifically, we used metaproteomics and metabolomics. We also used enzyme assays and in situ analyses of potential energy sources. Like the great majority of symbiotic microbes, the *O. algarvensis* symbionts have defied cultivation attempts, making cultivation-independent techniques like those used here essential for their analysis. While metagenomic analyses provide evidence for the metabolic potential of a microbial community, metaproteomic and metabolomic analyses can reveal the metabolic and physiological processes that actually are used by the community members.

Author contributions: M.K., G.F., B.V., D.B., M. Liebeke, M. Lalk, M.H., and T.S. designed research; M.K., C.W., C.L., H.T., S.W., J.Y., Y.-J.C., N.C.V., J.Z., K.H., M. Liebeke, and D.A. performed research; N.C.V., G.F., M. Lalk, M.H., T.S., and N.D. contributed new reagents/analytic tools; M.K., C.W., J.Y., M.S., N.C.V., J.Z., S.M., B.V., D.B., M. Liebeke, and N.D. analyzed data; and M.K. and N.D. wrote the paper.

The authors declare no conflict of interest.

This article is a PNAS Direct Submission.

Freely available online through the PNAS open access option.

[1]To whom correspondence may be addressed. E-mail: mkleiner@mpi-bremen.de, schweder@uni-greifswald.de, or ndubilie@mpi-bremen.de.

See full research article on page E1173 of www.pnas.org.

Cite this Author Summary as: PNAS 10.1073/pnas.1121198109.

We developed a method called "proteomics-based binning" to decipher metabolic pathways and identify the symbiont from which they originated. Our goal was to understand the functional roles of the different symbiotic partners and their interactions within the symbiosis. Further, we aimed to identify the metabolic pathways that could explain how *O. algarvensis* is able to thrive in its oligotrophic habitat.

We identified and quantified 2,819 proteins and 97 metabolites in the *O. algarvensis* symbiosis. The identified proteins included 530 proteins from the host, thus providing insight into the metabolism of a marine oligochaete, a group of segmented annelid worms for which no genomic data are available. Our analyses revealed (*i*) multiple symbiont pathways for the recycling of host waste products, including a pathway for the assimilation of acetate, propionate, succinate, and malate; (*ii*) the potential use of carbon monoxide as an energy source, a substrate previously not known to play a role in marine invertebrate symbioses; (*iii*) the potential use of hydrogen as an energy source; (*iv*) the extremely abundant expression of high-affinity uptake transporters that allow the uptake of a wide range of substrates at very low concentrations; and (*v*) as yet undescribed energy-efficient steps in CO_2 fixation and sulfate reduction involving pyrophosphate-dependent enzymes.

Our results show that a large proportion of the proteins expressed in the *O. algarvensis* symbiosis are involved in nutrient and energy uptake and conservation. This finding suggests that the organisms' impoverished environment exerts a strong selective pressure for metabolic pathways that maximize these processes. Some of the metabolic strategies used by the *O. algarvensis* symbionts also appear to play an important role in free-living bacteria such as planktonic SAR11 bacteria from low-nutrient ocean waters that express high-affinity uptake transporters at high abundances similar to those of the *O. algarvensis* δ-symbionts (5). Furthermore, our comparative analyses of the genes used by the *O. algarvensis* symbionts for energy-efficient pathways revealed that these genes appear to be widespread in free-living chemoautotrophic and sulfate-reducing bacteria. Thus, our study shows that the *O. algarvensis* symbiosis is an excellent model system for understanding how life has evolved to survive environments with low nutrient and energy availability.

1. Dubilier N, Bergin C, Lott C (2008) Symbiotic diversity in marine animals: The art of harnessing chemosynthesis. *Nat Rev Microbiol* 6:725–740.
2. Ruehland C, et al. (2008) Multiple bacterial symbionts in two species of co-occurring gutless oligochaete worms from Mediterranean sea grass sediments. *Environ Microbiol* 10:3404–3416.
3. Dubilier N, et al. (2001) Endosymbiotic sulphate-reducing and sulphide-oxidizing bacteria in an oligochaete worm. *Nature* 411:298–302.
4. Woyke T, et al. (2006) Symbiosis insights through metagenomic analysis of a microbial consortium. *Nature* 443:950–955.
5. Sowell SM, et al. (2009) Transport functions dominate the SAR11 metaproteome at low-nutrient extremes in the Sargasso Sea. *ISME J* 3:93–105.

Metaproteomics of a gutless marine worm and its symbiotic microbial community reveal unusual pathways for carbon and energy use

Manuel Kleiner[a,b,1], Cecilia Wentrup[a], Christian Lott[a,c], Hanno Teeling[a], Silke Wetzel[a], Jacque Young[d,e], Yun-Juan Chang[d], Manesh Shah[d], Nathan C. VerBerkmoes[d], Jan Zarzycki[f], Georg Fuchs[f], Stephanie Markert[g], Kristina Hempel[b], Birgit Voigt[b], Dörte Becher[b], Manuel Liebeke[h,i], Michael Lalk[h], Dirk Albrecht[b], Michael Hecker[b,g], Thomas Schweder[g,h,1], and Nicole Dubilier[a,1]

[a]Symbiosis Group, Max Planck Institute for Marine Microbiology, 28359 Bremen, Germany; [b]Institute for Microbiology and [h]Institute of Pharmacy, University of Greifswald, 17487 Greifswald, Germany; [c]Elba Field Station, HYDRA Institute for Marine Sciences, Località Fetovaia, 57034 Campo nell'Elba, Italy; [d]Oak Ridge National Laboratory, Chemical Science Division, Oak Ridge, TN 37831; [e]Graduate School for Genome Science and Technology, University of Tennessee, Knoxville, TN 37996; [f]Department of Microbiology, Faculty of Biology, University of Freiburg, 79104 Freiburg, Germany; [g]Institute of Marine Biotechnology, 17489 Greifswald, Germany; and [i]Biomolecular Medicine, Department of Surgery and Cancer, Faculty of Medicine, Imperial College London, London, United Kingdom SW7 2AZ

Edited by Charles R. Fisher, Pennsylvania State University, University Park, PA, and accepted by the Editorial Board February 29, 2012 (received for review December 22, 2011)

Low nutrient and energy availability has led to the evolution of numerous strategies for overcoming these limitations, of which symbiotic associations represent a key mechanism. Particularly striking are the associations between chemosynthetic bacteria and marine animals that thrive in nutrient-poor environments such as the deep sea because the symbionts allow their hosts to grow on inorganic energy and carbon sources such as sulfide and CO_2. Remarkably little is known about the physiological strategies that enable chemosynthetic symbioses to colonize oligotrophic environments. In this study, we used metaproteomics and metabolomics to investigate the intricate network of metabolic interactions in the chemosynthetic association between *Olavius algarvensis*, a gutless marine worm, and its bacterial symbionts. We propose previously undescribed pathways for coping with energy and nutrient limitation, some of which may be widespread in both free-living and symbiotic bacteria. These pathways include (*i*) a pathway for symbiont assimilation of the host waste products acetate, propionate, succinate and malate; (*ii*) the potential use of carbon monoxide as an energy source, a substrate previously not known to play a role in marine invertebrate symbioses; (*iii*) the potential use of hydrogen as an energy source; (*iv*) the strong expression of high-affinity uptake transporters; and (*v*) as yet undescribed energy-efficient steps in CO_2 fixation and sulfate reduction. The high expression of proteins involved in pathways for energy and carbon uptake and conservation in the *O. algarvensis* symbiosis indicates that the oligotrophic nature of its environment exerted a strong selective pressure in shaping these associations.

3-hydroxypropionate bi-cycle | Calvin cycle | proton-translocating pyrophosphatase | pyrophosphate dependent phosphofructokinase | metagenomics

Growth in nutrient-limited environments presents numerous challenges to organisms. Symbiotic and syntrophic relationships have evolved as particularly successful strategies for coping with these challenges. Such nutritional symbioses are widespread in nature and, for example, have enabled plants to colonize nitrogen-poor soils and animals to thrive on food sources that lack essential amino acids and vitamins (1). Chemosynthetic symbioses, discovered only 35 years ago at hydrothermal vents in the deep sea, revolutionized our understanding of nutritional associations, because these symbioses enable animals to live on inorganic energy and carbon sources such as sulfide and CO_2 (2, 3). The chemosynthetic symbionts use the energy obtained from oxidizing reduced inorganic compounds such as sulfide to fix CO_2, ultimately providing their hosts with organic carbon compounds. Chemosynthetic symbioses thus are able to thrive in habitats where organic carbon sources are rare, such as the deep sea, and the symbionts often are so efficient at providing nutrition that many hosts have reduced their digestive systems (4).

The marine oligochaete *Olavius algarvensis* is a particularly extreme example of a nutritional symbiosis: These worms are dependent on their chemosynthetic symbionts for both their nutrition and their excretion, because they have reduced their mouth, gut, and nephridial excretory organs completely (5). *O. algarvensis* lives in coarse-grained coastal sediments off the island of Elba, Italy, and migrates between the upper oxidized and the lower reduced sediment layers (6). It hosts a stable and specific microbial consortium consisting of five bacterial endosymbionts in its body wall: two aerobic or denitrifying gammaproteobacterial sulfur oxidizers (γ1- and γ3-symbionts), two anaerobic deltaproteobacterial sulfate reducers (δ1- and δ4-symbionts), and a spirochete with an unknown metabolism (7, 8). The sulfate-reducing δ-symbionts provide the sulfur-oxidizing γ-symbionts with reduced sulfur compounds as an internal energy source for autotrophic CO_2 fixation via the Calvin–Benson cycle, thus explaining how *O. algarvensis* can thrive in its sulfide-poor environment (6, 9). As in all living organisms, the symbiosis is dependent on external energy sources, but to date the identity of these sources has remained unclear.

Like the vast majority of symbiotic microbes, the *O. algarvensis* symbionts have defied cultivation attempts, making cultivation-independent techniques essential for their analysis. A metagenomic analysis of the *O. algarvensis* symbionts yielded initial insights into their potential metabolism (9), but the incomplete genome sequences hindered the reconstruction of complete metabolic pathways, leaving many questions unanswered (10). Fur-

Author contributions: M.K., G.F., B.V., D.B., M. Liebeke, M. Lalk, M.H., and T.S. designed research; M.K., C.W., C.L., H.T., S.W., J.Y., Y.-J.C., N.C.V., J.Z., K.H., M. Liebeke, and D.A. performed research; N.C.V., G.F., M. Lalk, M.H., T.S., and N.D. contributed new reagents/analytic tools; M.K., C.W., J.Y., M.S., N.C.V., J.Z., S.M., B.V., D.B., M. Liebeke, and N.D. analyzed data; and M.K. and N.D. wrote the paper.

The authors declare no conflict of interest.

This article is a PNAS Direct Submission. C.R.F. is a guest editor invited by the Editorial Board.

Freely available online through the PNAS open access option.

[1]To whom correspondence may be addressed. E-mail: mkleiner@mpi-bremen.de, schweder@uni-greifswald.de, or ndubilie@mpi-bremen.de.

See Author Summary on page 7148 (volume 109, number 19).

This article contains supporting information online at www.pnas.org/lookup/suppl/doi:10.1073/pnas.1121198109/-/DCSupplemental.

thermore, as in all genomic analyses, detailed insights into the physiology and metabolism of an organism are limited, because these analyses can predict only the metabolic potential of an organism, not its actual metabolism and physiology (11). This limitation is most apparent in a multimember community in which the interactions between the different members and between these members and their environment lead to a level of metabolic complexity that can greatly exceed the predictive ability of genomic reconstructions from single species.

Although metagenomic analyses reveal the metabolic potential of a microbial community, metaproteomic and metabolomic analyses provide evidence for the metabolic and physiological processes that actually are used by the community. In this study, we used metaproteomics and metabolomics as well as enzyme assays and in situ analyses of potential energy sources to gain an in-depth understanding of the intricate interactions between *O. algarvensis* and its microbial symbiont community and between the members of this community and their environment. Our goal was to identify the compounds that provide energy for the symbiosis, the functional roles of the different partners, and their interactions within the symbiosis.

Results and Discussion

High Coverage of the Symbiosis Metaproteome and Metabolome. We identified and quantified a total of 2,819 proteins and 97 metabolites in *O. algarvensis* and its symbiotic community (*SI Appendix*, Tables S1 and S2 and Datasets S1 and S2) using different methods for both the metaproteomic and the metabolomic analyses to overcome the intrinsic biases inherent in a single detection method (*SI Appendix*, *SI Text*). For host proteins, sequences from related annelids enabled the cross-species identification of 530 *O. algarvensis* proteins, thus providing insight into the metabolism of a marine oligochaete, a group of annelid worms for which no genomic data are available. For symbiont proteins, the published *O. algarvensis* symbiont metagenome, which contains only sequences assigned to specific symbionts through binning analyses (9), led to the identification of 1,586 proteins. The addition of unassigned sequences from the unbinned *O. algarvensis* symbiont metagenome allowed us to identify a total of 2,265 symbiont proteins, a 43% increase compared with the published metagenome alone. Because of the lack of metagenomic information for the spirochete, no proteins were found that could be assigned unambiguously to the spirochete symbiont of *O. algarvensis* (9).

To improve coverage of the metaproteome further, we developed a method using density-gradient centrifugation for physical separation of the *O. algarvensis* symbionts from each other and from host tissues (*SI Appendix*, *SI Text* and Fig. S1). This method greatly enhanced the number of identified symbiont proteins, particularly for those present in lower abundances (Fig. 1 and *SI Appendix*, Table S1). An additional advantage of symbiont enrichments was that we were able to assign proteins from the unbinned metagenomic sequences to a specific symbiont if they were detected in high abundances in enrichment fractions of the given symbiont (*SI Appendix*, *SI Text*). This proteomics-based binning allowed us to assign 544 previously unassigned proteins to a specific symbiont, thus significantly extending our understanding of the symbionts' metabolism (*SI Appendix*, Table S3 and Dataset S3).

Energy Sources for the *O. algarvensis* Symbiosis. One of the major unresolved questions in the *O. algarvensis* symbiosis is the identity of the sources of energy from the environment that fuel the association. Earlier studies found that reduced sulfur compounds are supplied internally as an energy source to the aerobic sulfur-oxidizing γ-symbionts by the anaerobic sulfate-reducing δ-symbionts. In return, the δ-symbionts are supplied with oxidized sulfur compounds as electron acceptors (6, 9). Our metaproteomic analyses are consistent with this model of syntrophic sulfur cycling, with abundantly expressed sulfur oxidation proteins detected in the γ-symbionts and sulfate reduction proteins detected in the δ-symbionts (Fig. 2 and *SI Appendix*, *SI Text* and Figs. S2 and S3*A*). However, for net growth and compensation of thermodynamic losses, external energy sources are required. Most chemosynthetic symbioses are fueled by an external supply of reduced sulfur compounds. However, concentrations of reduced sulfur compounds are extremely low in the habitat of *O. algarvensis* (6), indicating that other energy sources play an important role in the symbiosis.

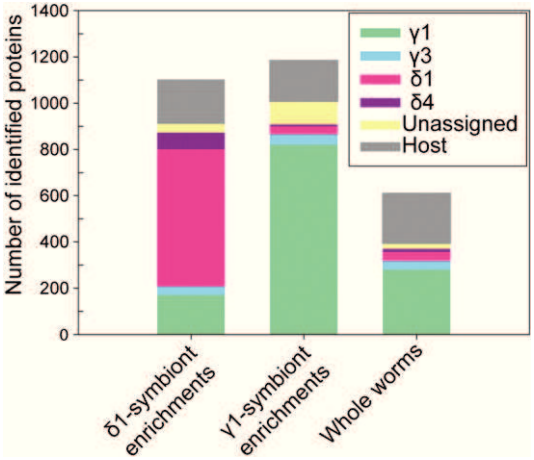

Fig. 1. Positive effect of symbiont enrichment using density-gradient centrifugation. Enrichment considerably increased the number of identified proteins from a given symbiont compared with analyses of whole worms. Average protein numbers were calculated for 2D LC-MS/MS experiments (*SI Appendix*, Table S1). n = 2 for γ1-symbiont enrichments; n = 2 for δ1-symbiont enrichments; and n = 4 for whole-worm samples. Both metagenomic and proteomic binning information was used for assignment of proteins to a symbiont.

Carbon monoxide may be used by three symbionts. Our metaproteomic analyses suggest that three of the *O. algarvensis* symbionts use carbon monoxide (CO) as an energy source. CO is not known to be used as an electron donor by chemosynthetic symbionts, and its toxicity to aerobic life suggested that this reductant would not play an important role in animal symbioses. We detected both aerobic and anaerobic CO dehydrogenases in the *O. algarvensis* consortium, the aerobic type in the γ3-symbiont and the anaerobic type in the δ-proteobacterial symbionts [for reviews of aerobic and anaerobic CO oxidation see King and Weber (12) and Oelgeschläger and Rother (13)]. The δ-proteobacterial symbionts express two versions of the anaerobic CO dehydrogenase, one that oxidizes free CO generating a proton gradient across the membrane, and one that likely is involved in the Wood–Ljungdahl pathway and oxidizes enzyme-bound CO (*SI Appendix*, *SI Text*).

To support the metaproteomic prediction that CO could be an energy source for the symbiosis, we measured CO concentrations in the *O. algarvensis* habitat. CO concentrations in the sediment pore waters ranged from 17–46 nM (*SI Appendix*, Fig. S4). These concentrations are sufficient to support free-living marine CO oxidizers, which can use concentrations of 2–10 nM in surface sea water (14, 15) and about 100 nM at hydrothermal vents (12). Pore water CO concentrations were well above the concentrations in the seawater overlying the sediment (8–16 nM) (*SI Appendix*, Fig. S4), indicating the presence of a CO source in the sediment. CO can be produced through abiotic and biotic processes from plant roots (16) and from decaying seagrass-derived organic matter (17), which are abundant at the collection site of the worms.

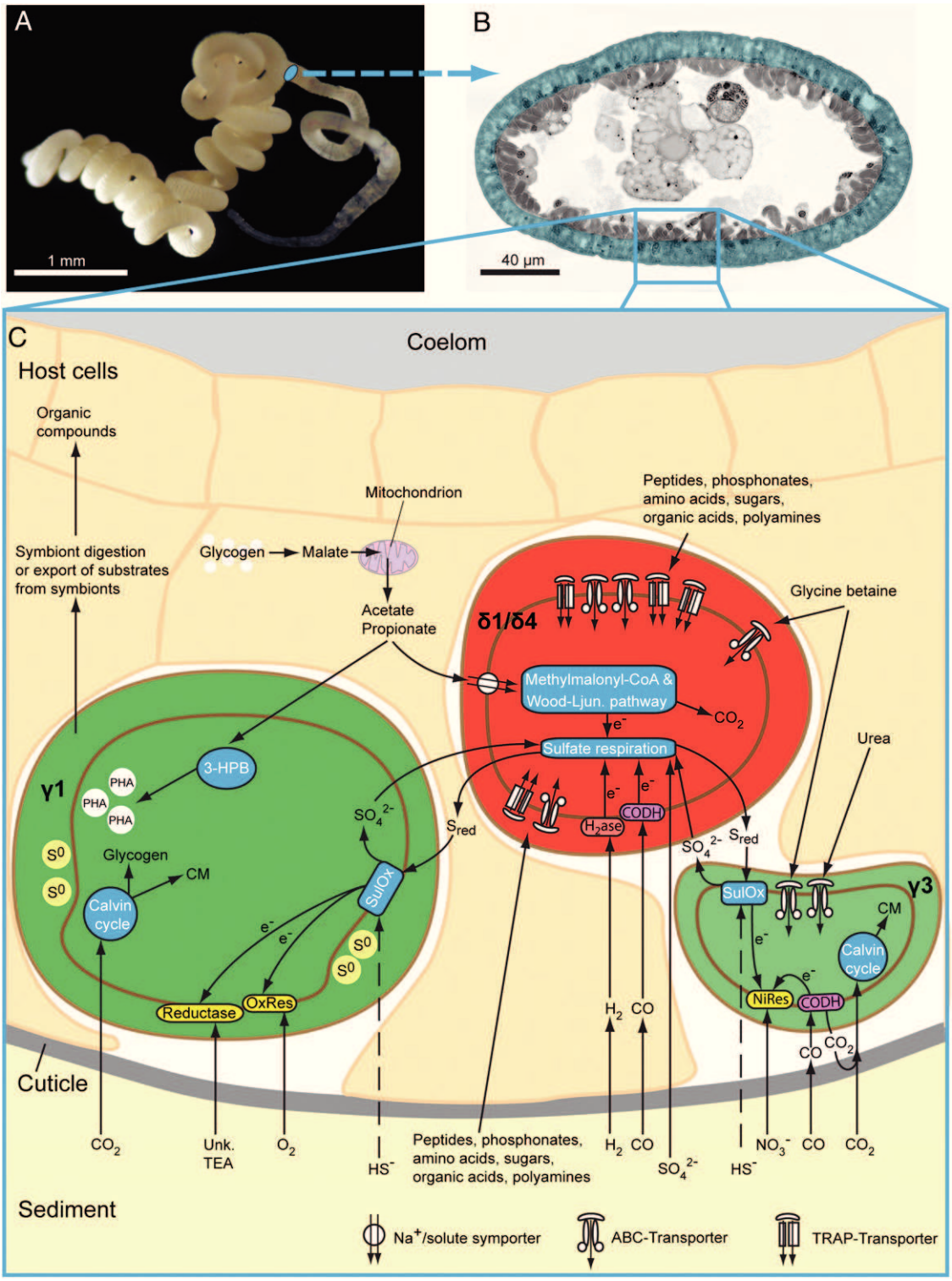

Fig. 2. Overview of symbiotic metabolism based on metaproteomic and metabolomic analyses. (*A*) Live *O. algarvensis* specimen. (*B*) Light micrograph of a cross section through *O. algarvensis*. The region containing the symbionts is highlighted in blue. (*C*) Metabolic reconstruction of symbiont and host pathways. The δ1- and δ4-symbionts are shown as a single cell, because most metabolic pathways were identified in the δ1-symbiont and only a small fraction of the same pathways were identified in the δ4-symbiont because of the low coverage of its metaproteome. 3-HPB, partial 3-hydroxypropionate bicycle; CM, cell material; CODH, carbon monoxide dehydrogenase (aerobic or anaerobic type); NiRes, nitrate respiration; OxRes, oxygen respiration; PHA, polyhydroxyalkanoate granule; S^0, elemental sulfur; S_{red}, reduced sulfur compounds; SulOx, sulfur oxidation; Unk. TEA, unknown terminal electron acceptor.

The CO_2/CO couple has a very negative redox potential, −520 mV (18), making CO an excellent electron donor whose electrons can be transferred to a variety of terminal electron acceptors such as oxygen, nitrate, elemental sulfur, and sulfate (12, 13, 19). Therefore CO could be used as an energy source by the *O. algarvensis* symbionts under all redox conditions as the worm

shuttles between sediment layers. In the reduced sediment layers, the δ-symbionts could use sulfate for the anaerobic oxidation of CO, thereby producing reduced sulfur compounds for the γ-symbionts; in the oxic and suboxic sediment layers, the γ3-symbiont could oxidize CO with nitrate as a terminal electron acceptor (*SI Appendix, SI Text, SI Results and Discussion*).

Hydrogen may be used by the sulfate-reducing symbionts. Our metaproteomic analyses revealed that hydrogen also may play an important role as an energy source in the *O. algarvensis* symbiosis, based on the abundant expression of periplasmic uptake [NiFeSe] hydrogenases in both δ-symbionts (δ1: SP088; δ4: SP089). These [NiFeSe] hydrogenases have high affinities for hydrogen (20), consistent with the low hydrogen concentrations reported for oligotrophic sediments (<10 nM) (21) and marine sediments in general (<60 nM) (22). Therefore we were surprised to measure unusually high concentrations of hydrogen, 438–2,147 nM, in the sediment pore waters at the *O. algarvensis* collection site (*SI Appendix*, Fig. S5). These high concentrations could be a result of biological H_2 production by anaerobic CO oxidizers and are consistent with the elevated CO concentrations at the collection site. The hydrogen concentrations in the worms' habitat are much higher than those needed by common hydrogen-oxidizing microorganisms for growth (23), indicating that the δ-symbionts could easily use the hydrogen present in the Elba sediment as an energy source.

The use of hydrogen as an energy source by chemoautotrophic sulfur-oxidizing symbionts was shown recently for deep-sea *Bathymodiolus* mussels from hydrothermal vents (24). Our study indicates that hydrogen also might play a role as an energy source in shallow-water chemosynthetic symbioses. As with CO, the use of externally supplied hydrogen might be another adaptation of the *O. algarvensis* symbiosis to life in the sulfide-depleted sediments of Elba.

Highly abundant uptake transporters for organic substrates in the δ-symbionts. The sulfate-reducing δ-symbionts expressed extremely high numbers and quantities of high-affinity uptake transport-related proteins, which enable them to take up organic substrates at very low concentrations (Datasets S2 and S4). In the δ1-symbiont, 89–116 transport proteins were detected per sample, corresponding to an average of 29% of all identified δ1-symbiont proteins. In terms of abundance, the δ1-symbiont transport proteins amounted to more than 38% of the total δ1-symbiont protein (*SI Appendix*, Table S4). To our knowledge, higher abundances of these types of transporters have been found only in the metaproteome of the α-proteobacterium *Pelagibacter ubique* (SAR11) from the Sargasso Sea during extreme low-nutrient conditions (*SI Appendix*, Table S4) (25).

Most of the identified transport proteins in the δ1-symbionts were periplasmic-binding proteins of high-affinity ATP-binding cassette (ABC)- or tripartite ATP-independent periplasmic (TRAP)-type transporters, which actively transport substrates against a large concentration gradient while using energy in the form of ATP or an ion gradient (26, 27). The great majority of the detected δ1-symbiont transport proteins are used for the uptake of a variety of substrates such as amino acids, peptides, di- and tricarboxylates, sugars, polyamines, and phosphonates, with amino acid and peptide transporters being the most dominant ones (Dataset S4). The abundance of transport-related proteins in the δ-symbionts suggests that these symbionts use organic substrates not only as an energy source but also as a source for preformed building blocks, thus saving resources by not having to synthesize these metabolic precursors de novo.

The organic substrates used by the δ-symbionts could be supplied internally from within the worms or externally from the environment. Our metabolomic analyses of whole worms revealed considerable amounts of dicarboxylates and some amino acids (in the low millimolar range), making an internal source of the organic substrates possible (*SI Appendix*, Fig. S7 and Table S2). However, the relatively high concentrations of these substrates are not consistent with the expression of energy-consuming high-affinity transporters by the δ-symbionts. In cultured bacteria (28–30) as well as in environmental communities (25, 31), ABC/TRAP transporters are induced at low substrate concentrations, and less energy-consuming transporters are used under nutrient-rich conditions. Most likely the metabolites that we measured in homogenized worms are not easily accessible to the δ-symbionts in situ, because the metabolites are enclosed in host or symbiont cells.

To examine if organic substrates are supplied externally from the *O. algarvensis* environment, we analyzed sediment pore waters from the worm's collection site with GC-MS for the presence of a large range of di- and tricarboxylates, amino acids, and sugars. None of these metabolites was measurable with detection limits at about 10 nM (*SI Appendix*, Fig. S8). Such oligotrophic conditions are consistent with the high expression of ABC/TRAP transporters that have extremely high affinities for substrates at concentrations far below the detection limits of our method (32, 33). The worm's cuticle is permeable for small, negatively charged compounds as well as substrates up to 70 kDa (5); thus the δ-symbionts would have access to both small organic compounds such as di- and tricarboxylates and larger organic substrates such as sugars and polyamines from the environment. The expression of transporters for a very broad range of substrates would allow the δ-symbionts to respond quickly to and take up many different substrates that could be consistently present at low concentrations in their environment or that could fluctuate over time and space as the worm migrates through the sediment.

Regardless of whether the organic substrates come from the environment or internally from within the symbiosis, the high abundances of high-affinity uptake transporters in the δ-symbionts indicate that the symbionts experience nutrient limitation, forcing them to dedicate a major part of their resources to the acquisition of substrates. Despite their endosymbiotic location, the lifestyle of these bacteria thus appears to resemble most closely that of planktonic SAR11 bacteria from low-nutrient extremes in the Sargasso Sea (25).

Recycling and Waste Management. Given the extremely low concentrations of nutrients in the *O. algarvensis* habitat, the conservation of substrates and energy should be highly advantageous for the symbiosis. Our metaproteomic and metabolomic analyses revealed several pathways that could enable the symbionts to recycle waste products of their hosts and conserve energy.

Proposed pathways for the recycling of host fermentative waste in multiple symbionts. Cross-species identification of host proteins enabled us to gain insight into the metabolism of *O. algarvensis*. Our analyses revealed that, when living in deeper anoxic sediment layers, *O. algarvensis* expressed proteins for an anaerobic metabolism that produces large amounts of acetate, propionate, malate, and succinate as fermentative waste products (*SI Appendix, SI Text* and Fig. S6 and Dataset S2) (34, 35). Correspondingly, we detected considerable amounts (1–8 mM) of malate, succinate, and acetate in the worm metabolome (*SI Appendix*, Fig. S7 and Table S2). Aquatic invertebrates without symbionts must excrete these fermentative waste products to keep their internal pH stable, thereby losing large amounts of energy-rich organic compounds. In *O. algarvensis*, the ability of the sulfate-reducing δ-symbionts to use their host's fermentative waste as substrates recycles and preserves considerable amounts of energy and organic carbon within the symbiotic system (*SI Appendix, SI Text*).

The dominant γ1-symbiont, previously assumed to fix only carbon autotrophically, also may function heterotrophically by assimilating acetate, propionate, succinate, and malate, thus also contributing to host waste recycling. We detected abundantly

expressed enzymes for an almost complete 3-hydroxypropionate bi-cycle (3-HPB) in the γ1-symbiont (Fig. 3 and *SI Appendix*, Fig. S3*B* and Dataset S2). The 3-HPB is used for autotrophic CO_2 fixation in *Chloroflexus aurantiacus,* a filamentous anoxygenic phototroph (36), but parts of the 3-HPB pathway also can be used for the heterotrophic assimilation of acetate, propionate, succinate, and malate (37).

In retrospect, it is clear why the 3-HPB pathway was not discovered in the metagenomic analyses of the *O. algarvensis* symbionts: Many of its genes occurred on sequence fragments that could not be assigned to a specific symbiont and therefore were not included in the annotation analyses (9). Here, we used our proteomics-based binning method described above to assign abundantly expressed 3-HPB enzymes encoded on unassigned metagenomic fragments to the γ1-symbiont (*SI Appendix*, *SI Text*, *Materials and Methods* and Dataset S3). This method enabled us to identify nearly all enzymes required for the complete 3-HPB, with the exception of two diagnostic enzymes of the 3-HPB, malonyl-CoA reductase and propionyl-CoA synthase, that were missing in both the metagenome and the metaproteome (Fig. 3).

To understand better how the 3-HPB might function in the symbionts, we performed enzyme assays with extracts from whole worms and enriched γ1-symbionts. Activities of all 3-HPB enzymes were detected, except for the two diagnostic enzymes that also were absent from the metaproteome (*SI Appendix*, Table S5). We therefore propose a modified incomplete 3-HPB as shown in Fig. 3, which the γ1-symbiont could use to assimilate the host's fermentative waste products acetate, propionate, succinate, and malate. The abundant expression of the modified 3-HPB suggests that it plays an important role in the central carbon metabolism of the γ1-symbionts. The net fixation of CO_2 is unlikely because of the absence of the two diagnostic enzymes and the low activities of the carboxylases involved in the 3-HPB (*SI Appendix*, Table S5). The pathway could also be linked to the synthesis and/or mobilization of the storage compound polyhydroxyalkanoate (PHA). A putative PHA synthase (2004222379) and a phasin protein (PHA granule protein, 6frame_RASTannot_14528) are highly expressed in the γ1-symbiont metaproteome, showing the importance of PHA synthesis for this symbiont. Under anaerobic conditions, PHA synthesis not only would produce a valu-

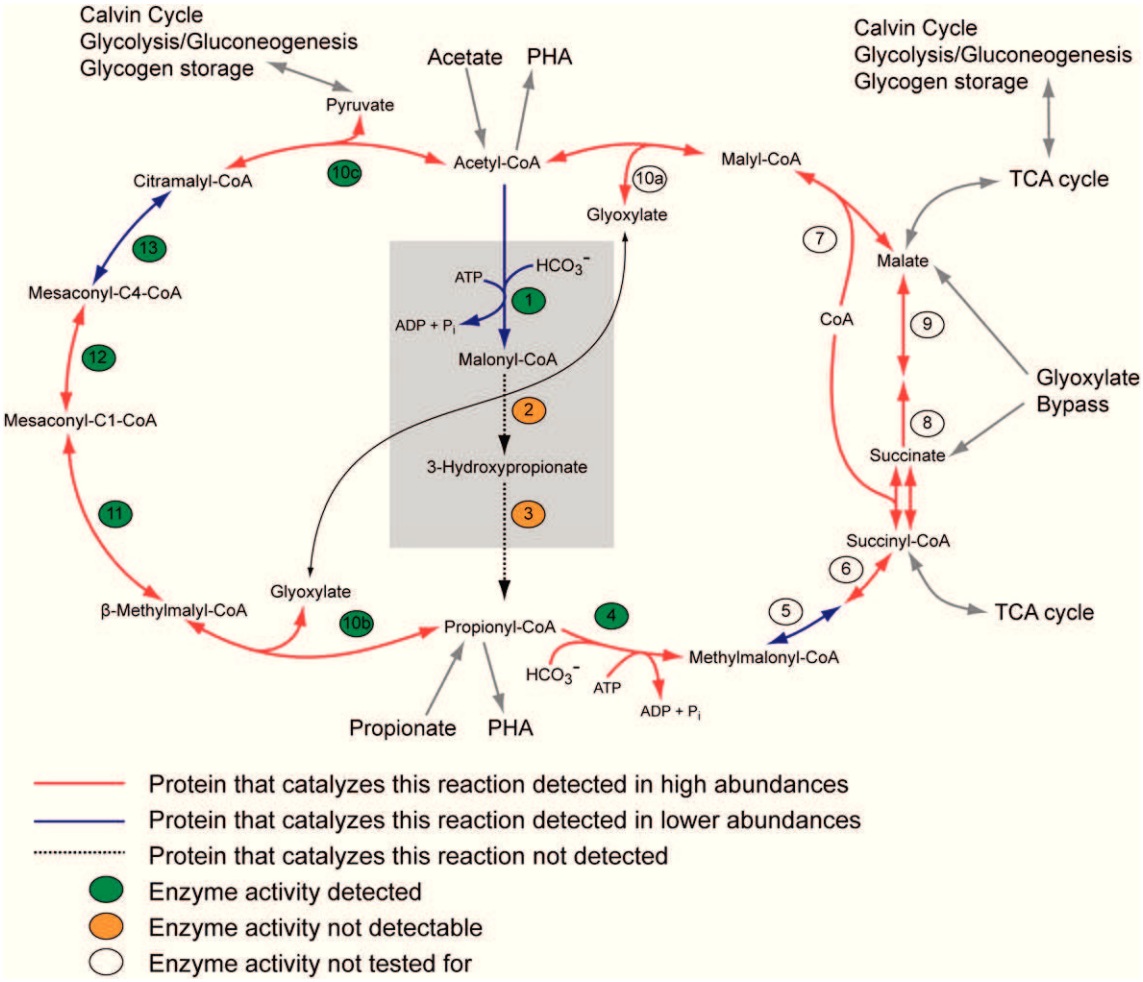

Fig. 3. Modified version of the 3-HPB in the γ1-symbiont. Reactions not needed for the assimilation of propionate and acetate are shown in the gray box; reaction 1 also can play a role in fatty acid metabolism. (1) Acetyl-CoA carboxylase (2004223475); (2) malonyl-CoA reductase; (3) propionyl-CoA synthase; (4) propionyl-CoA carboxylase (2004223080); (5) methylmalonyl-CoA epimerase (RASTannot_91923); (6) methylmalonyl-CoA mutase (RASTannot_20798); (7) succinyl-CoA:(*S*)-malate-CoA transferase (RASTannot_529, RASTannot_48547); (8) succinate dehydrogenase (2004223104, 2004223105); (9) fumarate hydratase (2004223692); (10 a,b,c) (*S*)-malyl-CoA/β-methylmalyl-CoA/(*S*)-citramalyl-CoA (MMC) lyase (RASTannot_91504); (11) mesaconyl-C1-CoA hydratase (β-methylmalyl-CoA dehydratase) (2004222675); (12) mesaconyl-CoA C1-C4 CoA transferase (RASTannot_38616); (13) mesaconyl-C4-CoA hydratase [(*S*)-citramalyl-CoA dehydratase] (RASTannot_6738).

able storage compound but also would relieve the symbiont of superfluous reducing equivalents.

Intriguingly, one of the closest free-living relatives of the γ1-symbiont, *Allochromatium vinosum*, whose genome was sequenced recently, does not possess the genes needed for the 3-HPB or its modified version (http://genome.jgi-psf.org/allvi/allvi.home.html). The absence of these genes suggests that the genes for the 3-HPB pathway were gained through lateral transfer. Certainly, there is a strong selective advantage for this pathway in the γ1-symbionts. The γ1-symbionts are present in almost all gutless oligochaete species and therefore are assumed to be the ancient primary symbionts that first established a mutualistic relationship with the oligochaetes (5). The ability to recycle organic host waste would have been a considerable advantage during the early stages of the symbiosis, before the establishment of associations with other bacteria such as the heterotrophic sulfate-reducing symbionts.

Uptake and recycling of nitrogenous compounds. Because sources of nitrogen are extremely limited in the habitat of *O. algarvensis* (38), efficient strategies for dealing with nitrogen limitation have a selective advantage. Our metaproteomic and metabolomic analyses of the *O. algarvensis* association indicate two major strategies for dealing with nitrogen limitation: (*i*) the use of high-affinity systems for the uptake of nitrogenous compounds from the environment, and (*ii*) conservation of nitrogen within the symbiosis through recycling.

Environmental nitrogen is most likely assimilated by the symbionts using glutamine synthetases as well as high-affinity uptake transporters. The γ1-, γ3-, and δ1-symbionts abundantly expressed glutamine synthetases (Dataset S2). This enzyme assimilates ammonia into glutamine with high affinity at very low ammonia concentrations and is expressed in cultured organisms only under low-nitrogen conditions (39, 40). Uptake of organic compounds from the environment presumably is a further source of nitrogen, given the abundant expression of high-affinity amino acid- and peptide-uptake transporters in the δ1-symbiont that enable it to acquire nitrogen-containing substrates at extremely low concentrations.

The second proposed strategy of the *O. algarvensis* association for dealing with low nitrogen availability is the internal recycling of nitrogenous host osmolytes and waste products by the symbionts. In many invertebrates, these compounds are removed through excretory organs called "nephridia." Gutless oligochaetes are the only known annelid worms without nephridia, and their absence suggests that their symbionts have taken over the role of waste and osmolyte management. Our metabolomic analyses revealed high concentrations of two nitrogenous osmolyte and waste compounds in *O. algarvensis*, glycine betaine and urea (*SI Appendix*, Table S2), with glycine betaine being the most abundant metabolite detected in NMR measurements (~60 mM) (*SI Appendix*, Fig. S7). Glycine betaine is a well-known osmolyte in all kingdoms of life (41) and most likely also serves this function in *O. algarvensis*. The relatively high amounts of urea in *O. algarvensis* are unusual, because this nitrogenous waste compound and osmolyte is not commonly found in aquatic animals (41). The *O. algarvensis* symbionts abundantly expressed proteins for glycine betaine and urea uptake and for the pathways required to use them as carbon and nitrogen sources (Fig. 2 and *SI Appendix*, *SI Text*).

Energy Conservation with Proton-Translocating Pyrophosphatases. We propose several pathways for energy conservation in the *O. algarvensis* symbiosis. Both the γ-symbionts and the δ1-symbiont expressed pyrophosphate-dependent enzymes that could conserve energy in as yet undescribed modifications of classical metabolic pathways. Our analyses of published genomes indicate that these pathways may be common in sulfate reducers and chemoautotrophic bacteria.

The key enzyme for the proposed energy conservation pathways is a membrane-bound proton-translocating pyrophosphatase (H^+-PPase), which is abundantly expressed in both the γ- and the δ1-symbionts (*SI Appendix*, *SI Text*). H^+-PPases are widespread in all three domains of life. Despite their pervasiveness, remarkably little is known about the metabolic pathways in which they are used (42). H^+-PPases are proton pumps that use the hydrolysis of inorganic pyrophosphate (PPi) instead of ATP to generate a proton-motive force through the translocation of protons across biological membranes (Fig. 4). They also can work reversibly as proton-translocating pyrophosphate synthases (H^+-PPi synthase) and produce PPi using a proton-motive force (42).

H^+-PPase energy conservation in sulfate reducers. Sulfate-reducing bacteria produce large amounts of PPi as a by-product of the first step of sulfate reduction (Fig. 4). This PPi must be removed immediately to pull the reaction in the direction of sulfate reduction (43). For most sulfate reducers the mechanism of PPi removal is unknown. In some, it occurs through a wasteful hydrolysis of PPi by a soluble inorganic pyrophosphatase (44). In others, the energy from PPi hydrolysis may be conserved with an H^+-PPase (45), but to date this process has not been proven. Our metaproteomic analyses support the conclusion that the sulfate-reducing δ1-symbiont uses the H^+-PPase to conserve energy from PPi, based on the abundant expression of a H^+-PPase and the absence of a soluble pyrophosphatase. The stoichiometry of the H^+-PPase yields one ATP molecule per hydrolysis of three PPi molecules (46), providing the δ1-symbiont with a considerable energy gain of one additional ATP per three molecules of sulfate reduced.

Other sources of PPi besides sulfate reduction also appear to play an important role in the metabolism of the δ1-symbiont. In addition to expressing PPi-producing enzymes found in all organisms such as aminoacyl-tRNA synthetases and RNA and DNA polymerases, the δ1-symbiont abundantly expressed at

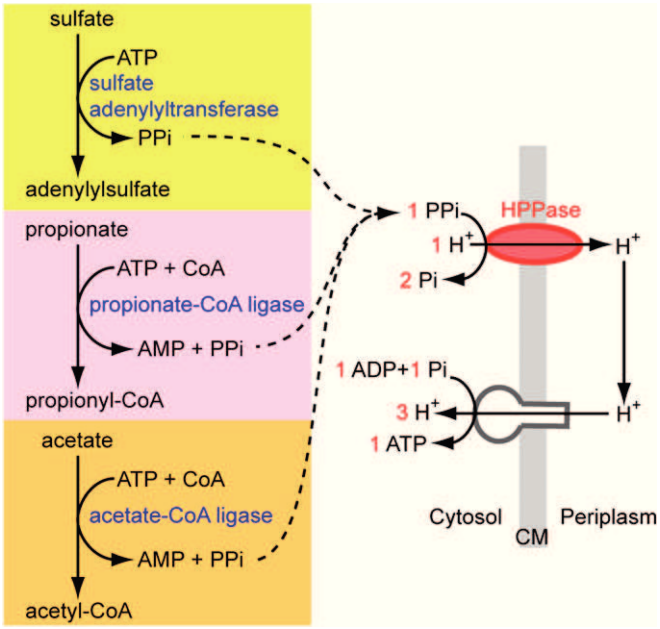

Fig. 4. Suggested role of H^+-PPase in the δ1-symbiont. Energy is conserved through the use of a membrane-bound proton-translocating pyrophosphatase instead of a cytosolic pyrophosphatase. PPi is produced by abundantly expressed enzymes, which catalyze the initial steps of sulfate reduction, propionate oxidation, and acetate oxidation. Red numbers show the stoichiometry.

least two other PPi-producing enzymes: the acetate-CoA ligase (2004210485) and the propionate-CoA ligase (2004210481). Therefore, based on the abundant expression of numerous PPi-producing enzymes in the δ1-symbiont, we postulate that H^+-PPase plays a key role in energy conservation in its metabolism (Fig. 4 and *SI Appendix*, Fig. S3*A*).

To examine how widespread H^+-PPases are in sulfate reducers, we analyzed the genomes of sulfate reducers available in the databases. These analyses revealed H^+-PPases in several sulfate reducers from two bacterial divisions, *Desulfatibacillum alkenivorans* AK-01 and *Desulfococcus oleovorans* Hxd3 from the Deltaproteobacteria, and *Candidatus Desulforudis audaxviator* MP104C and *Desulfotomaculum reducens* MI-1 from the division Clostridia. This finding suggests that the use of H^+-PPases for energy conservation may be widely distributed among phylogenetically diverse sulfate-reducing bacteria.

Energy-efficient PPi-dependent pathways in sulfur oxidizers. We propose that the γ-symbionts use novel energy-saving modifications of the Calvin cycle, glycolysis, and gluconeogenesis pathways. The key enzymes for the proposed modifications are the H^+-PPase and a closely coupled PPi-dependent 6-phosphofructokinase (PPi-PFK). We show that these enzymes could save as much as 30% of the energy used by the ATP-dependent pathways and that this energy-saving pathway may be widespread in chemoautotrophic bacteria.

Metagenomic analyses of the *O. algarvensis* consortium showed that the γ1-symbiont lacks two key enzymes of the classical Calvin cycle, fructose-1,6-bisphosphatase and sedoheptulose-1,7-bisphosphatase (the γ3-symbiont lacks only the latter) (Fig. 5*C*). Interestingly, the chemoautotrophic symbionts of the hydrothermal vent tubeworm *Riftia pachyptila* and the vesicomyid clams *Calyptogena magnifica* and *Calyptogena okutanii* also lack the genes for these two enzymes, even though all of them fix CO_2 via the Calvin cycle (47–49). Newton et al. (48) hypothesized that a PPi-PFK might replace fructose-1,6-bisphosphatase for the *C. magnifica* symbiont, but no enzyme was found that could replace sedoheptulose-1,7-bisphosphatase. Therefore it remained unclear how the Calvin cycle could function in these chemoautotrophic symbionts.

We found that both γ-symbionts of *O. algarvensis* possess a gene for a PPi-PFK that is highly similar to that of the methaneoxidizer *Methylococcus capsulatus*; amino acid identities were 71% for γ1 and 69% for γ3. The *M. capsulatus* PPi-PFK catalyzes three reactions: (*i*) the reversible, phosphate-dependent transformation of fructose-1,6-bisphosphate to fructose-6-phosphate and PPi; (*ii*) the reversible, phosphate-dependent transformation of sedoheptulose-1,7-bisphosphate to seduheptulose-7-phosphate and PPi; and (*iii*) the PPi-dependent phosphorylation of ribulose-5-phosphate to ribulose-1,5-bisphosphate (50). Thus, PPi-PFK can replace the enzymes involved in these three reactions (fructose-1,6-bisphosphatase, sedoheptulose-1,7-bisphosphatase, and phosphoribulokinase) (Fig. 5 *B* and *C* and *SI Appendix*, *SI Text*). The PPi-PFK was abundantly expressed in the γ1-symbiont (the low coverage of the γ3-symbiont proteome might explain why it was not detected in this symbiont). We propose that in the *O. algarvensis* γ-symbionts, and possibly in other chemoautotrophs (see below), the PPi-PFK has multiple functions in the Calvin Cycle, glycolysis and gluconeogenesis, and that this leads to considerable energy savings as described below (Fig. 5 *A* and *B*).

In the classical Calvin cycle, the reactions catalyzed by fructose-1,6-bisphosphatase and sedoheptulose-1,7-bisphosphatase produce phosphate ions that cannot be used for energy gain. In contrast, if PPi-PFK replaces these enzymes, both reactions produce energy-rich pyrophosphates. Interestingly, in the genomes of both γ-symbionts, the genes for PPi-PFK are located in the immediate neighborhood of H^+-PPases, indicating a close metabolic relationship between these two enzymes and their cotranscription (Fig. 5*D*), as shown for *M. capsulatus,* in which these genes also cooccur (Fig. 5*D*) (50). We propose that the pyrophosphate produced by the PPi-PFK in the Calvin cycle is used to conserve energy via the proton-motive force generated by the H^+-PPase (Fig. 5*B*). This metabolic coupling between the PPi-PFK and H^+-PPase would lead to energy savings of at least 9.25% ($1^2/_3$ fewer molecules of ATP per six molecules of fixed CO_2 in comparison with the classical Calvin cycle, in which 18 molecules of ATP are used for the fixation of six molecules of CO_2). An even higher energy gain (31.5%) is possible if PPi-PFK also replaces ATP-dependent phosphoribulokinase in the last step of the Calvin cycle: The conversion of ribulose-5-phosphate to ribulose-1,5-bisphosphate could be energized with PPi from the two other Calvin-cycle reactions and/or the H^+-PPase working in PPi synthesis direction, so that a total of $5^2/_3$ molecules of ATP (31.5%) would be saved per six molecules of CO_2 fixed.

In addition to their proposed role in the Calvin cycle, we hypothesize that the PPi-PFK and H^+-PPase also provide considerable energy savings in glycolysis and gluconeogenesis through several additional enzymes (*SI Appendix*, *SI Text*). Thus we conclude that PPi-PFK and H^+-PPase might play a key role in energy conservation in the γ1-symbiont and most likely also in the γ3-symbiont.

Widespread occurrence of colocalized H^+-PPase/PPi-PFK genes in chemoautotrophic bacteria. To examine if other microorganisms also could use the PPi-PFK and H^+-PPase for the pathways we propose above, we analyzed all bacterial (1,354) and archaeal (58) genomes available in the National Center for Biotechnology Information genomic database on January 29, 2009 (http://www.ncbi.nlm.nih.gov/sutils/genom_table.cgi). We discovered colocalized H^+-PPase/PPi-PFK genes, indicating close metabolic coupling and cotranscription, in the chemoautotrophic sulfur-oxidizing symbionts of *C. magnifica* and *C. okutanii* as well as in eight free-living bacterial species (Gamma- and Betaproteobacteria and Thermotogae), all of which possess ribulose-1,5-bisphosphate carboxylase/oxygenase genes for autotrophic CO_2 fixation (Fig. 5*D*). This broad distribution of colocalized H^+-PPase/PPi-PFK genes in bacteria for which genomes are available suggests that H^+-PPase/PPi-PFK–dependent pathways for energy conservation are widespread in both symbiotic and free-living chemoautotrophic bacteria.

The discovery of these pathways in chemoautotrophic bacteria is particularly interesting in light of evidence that H^+-PPases may have an ancient origin (42). H^+-PPase is the simplest known primary proton pump. It is the only known alternative to ATP synthases for the production of energy-rich phosphoanhydride bonds and is the only primary pump that is preserved in all three domains of life (42, 51). Given mounting evidence that the earliest forms of life were chemoautotrophic (52), the apparent pervasiveness of energy-conserving H^+-PPase pathways in chemoautotrophs adds further weight to the hypothesis that PPi preceded ATP as the central energy carrier in the early evolution of life (51, 53, 54).

Conclusions

Our metaproteomic and metabolomic analyses of the *O. algarvensis* symbiosis provide strong indirect evidence for a number of unexpected and some as yet undescribed metabolic pathways and strategies that were not identified in the metagenomic analysis of the symbiotic consortium (9). We gained further functional insights by using proteomics-based binning. This method allowed us to include an additional 9 Mb of sequences in our analyses that could not be mined for genomic information by Woyke et al. (9) because their lengths were too short to enable a clear assignment to a specific symbiont.

One of the key questions in the metagenomic analyses of complex symbiotic consortia, including those of the human gut, is why there is so much functional redundancy (55, 56). The selective advantage for *O. algarvensis* of harboring two sulfur-oxi-

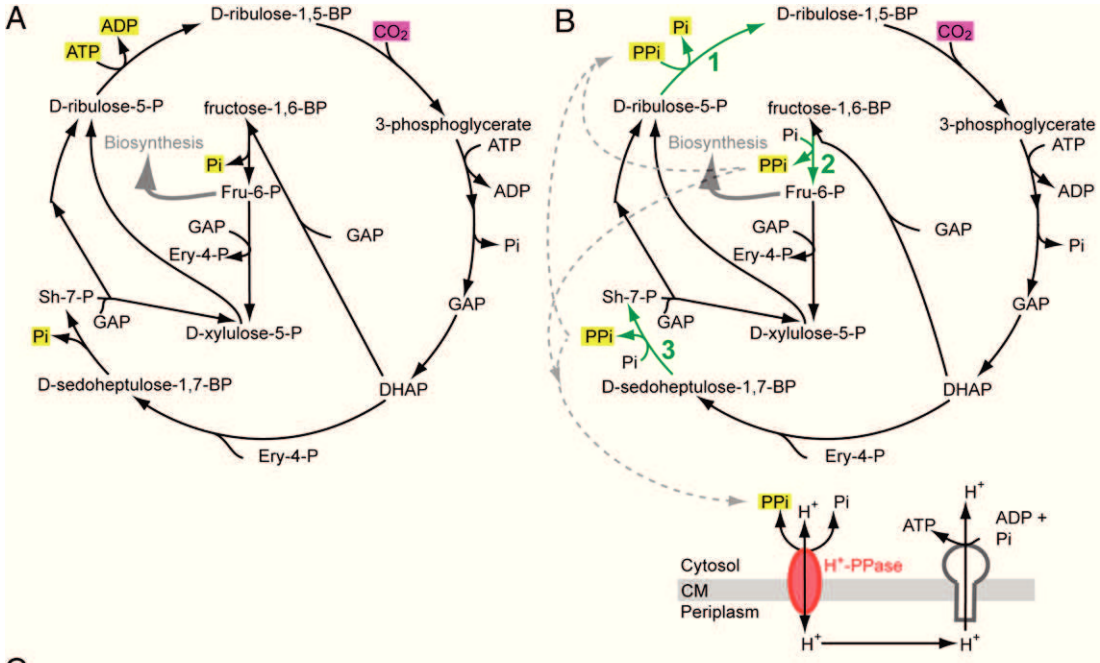

C

No. in (b)	Enzyme	Pathway	γ1-symbiont Gene	γ1-symbiont Proteome	γ3-symbiont Gene	γ3-symbiont Proteome	M. c.* Gene	E. p.* Gene	R. m.* Gene	V. o.* Gene
1, 2 and 3	PPi-PFK (PPi dependent phosphofructokinase)	Glycolysis / Calvin cycle / Gluconeogenesis	Yes	Yes	Yes	No	Yes	Yes	Yes	Yes
2	Fructose-1,6-bisphosphatase	Gluconeogenesis / Calvin cycle	No	No	Yes	No	No	No	No	No
3	Sedoheptulose-1,7-bisphosphatase	Calvin cycle	No	No	No	No	No	No	No	No
1	Phosphoribulokinase	Calvin cycle	No	Yes**	Yes	Yes	Yes	Yes	Yes	Yes
Not shown	ATP dependent phosphofructokinase	Glycolysis	No	No	No	No	No	No	No	No

* M. c. *Methylococcus capsulatus*, E. p. *Riftia pachyptila symbiont*, R. m. *Calyptogena magnifica* symbiont, V. o. C. okutanii symbiont

** Detected with gene of *Thiobacillus denitrificans*

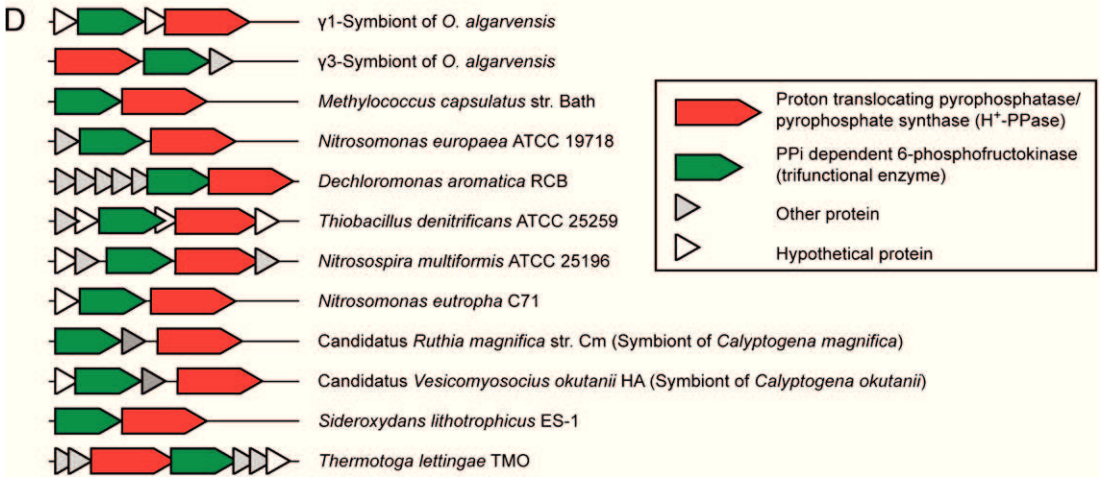

Fig. 5. Comparison of the classical Calvin cycle with a proposed version that is more energy efficient. (*A*) The text book version of the Calvin cycle. (*B*) The more energy-efficient version of the Calvin cycle in the γ-symbionts through the use of PPi-dependent trifunctional 6-phosphofructokinase/sedoheptulose-1,7-bisphosphatase/phosphoribulokinase (green) and a proton-translocating pyrophosphatase/proton-translocating pyrophosphate synthase (H^+-PPase/H^+-PPi synthase) (red). The main differences between the cycles are highlighted in yellow. CM, cell membrane; DHAP, dihydroxyacetone phosphate; GAP, D-glyceraldehyde-3-phosphate; PPi, inorganic pyrophosphate; Sh-7-P, D-sedoheptulose-7-phosphate. (*C*) Overview of genes that are replaced by the trifunctional PPi-dependent enzyme in different organisms. (*D*) Colocalized H^+-PPase/PPi-PFK genes in the γ-symbionts and other symbiotic and free-living bacteria.

dizing γ-symbionts with apparent functional redundancy was not clear. Our study shows that the only physiological traits shared by these two symbionts are their common use of reduced sulfur and carbon fixation via the Calvin cycle. Otherwise, they show very marked differences in their use of additional energy and carbon sources as well as electron acceptors. The γ3-symbionts may use CO and the host-derived osmolyte glycine betaine as additional energy and carbon sources, whereas the γ1-symbionts may use fermentative waste products from their hosts as additional carbon sources. Furthermore, the γ1-symbionts appear to rely heavily on storage compounds such as sulfur and polyhydroxyalkanoates, but storage compounds do not appear to play a dominant role in the metabolism of the γ3-symbionts. Resource partitioning also is visible in the differences in the electron acceptors used by the two symbionts. The γ1-symbionts may depend predominantly on oxygen for their respiration, but the γ3-symbionts apparently are not able to use this electron acceptor and instead use the energetically less favorable nitrate (*SI Appendix, SI Text*). Our metaproteomic analyses thus indicate functional differences in key metabolic pathways for chemosynthesis in the metabolism of these two symbionts, despite their genetic similarities. This theme appears to be a common one in microbial communities, because several recent proteomic and metaproteomic studies have shown that ecological differences between microorganisms with similar genomes are the result of major differences in their protein expression (57–59).

Although resource partitioning provides the association versatility and the ability to harvest a wide spectrum of energy and carbon sources, in one key aspect all four symbionts appear to share a remarkably similar metabolic strategy. They all express proteins involved in highly efficient pathways for the uptake, recycling, and conservation of energy and carbon sources. These pathways include (*i*) multiple strategies for the recycling of host waste products; (*ii*) the possible use of inorganic energy sources, such as hydrogen and CO, in addition to reduced sulfur compounds; (*iii*) the extremely abundant expression of high-affinity uptake transporters that would allow the uptake of a wide range of substrates at very low concentrations; and (*iv*) as yet undescribed energy-efficient steps in the pathways for sulfate reduction and CO_2 fixation. Given the oligotrophic, nutrient-poor nature of the worm's environment in which organic compounds were below detection limits and reduced sulfur compounds were barely detectable, the selective pressure for metabolic pathways that maximize energy and carbon acquisition and conservation appears to have been very strong in shaping these symbioses.

Materials and Methods

Sample Collection and Symbiont Enrichment. Worms were removed from the sediment via decantation and were frozen immediately, or symbionts were enriched via isopycnic centrifugation using a HistoDenz-based (Sigma) density gradient before freezing (*SI Appendix, SI Text*). Symbiont abundance and composition in density-gradient fractions were analyzed with catalyzed reporter deposition-FISH using symbiont-specific probes (*SI Appendix, SI Text*, Fig. S1, and Table S6). Density-gradient fractions in which specific symbionts were enriched were chosen for subsequent analyses.

Protein Identification and Proteome Analyses. 1D PAGE followed by liquid chromatography (1D-PAGE-LC) and 2D-LC were used for protein and peptide separation as described previously (60, 61), with slight modifications (*SI Appendix, SI Text*). MS spectra and MS/MS spectra were acquired with a hybrid linear ion trap-Orbitrap (Thermo Fischer Scientific) as described previously (60, 62), with minor modifications (*SI Appendix, SI Text*). All MS/MS spectra were searched against two protein sequence databases composed of the symbiont metagenomes and the genomes of related organisms using the SEQUEST algorithm (see *SI Appendix, SI Text* for details). For protein identification only peptides identified with high mass accuracy (maximum ± 10 ppm difference between calculated and observed mass) were considered, and at least two different peptides were required to identify a protein. False-discovery rates were estimated with searches against a target-decoy database, as described previously (63, 64), and were determined to be between 0–3.27% (*SI Appendix, SI Text* and Table S7). For relative quantitation of proteins, normalized spectral abundance factor values were calculated for each sample according to the method of Florens et al. (65). All identified proteins and their relative abundance in different samples are shown in Datasets S1 and S2. Protein databases, peptide and protein identifications, and all MS/MS spectra are available from http://compbio.ornl.gov/olavius_algarvensis_symbiont_metaproteome/.

Proteomics-Based Binning. Proteins encoded on metagenome fragments that were not assigned previously to a specific symbiont were assigned tentatively (binned) to a specific symbiont if they were detected repeatedly in higher abundances in enrichments of only one specific symbiont (*SI Appendix, SI Text* and Dataset S3). To validate this approach and to calculate a false-assignment rate, we also did proteomics binning with the proteins that already had been assigned to a specific symbiont in the metagenomic study (*SI Appendix, SI Text* and Table S3).

Enzyme Tests. Enzymatic activities were determined in cell extracts from whole worms or from enriched symbionts (*SI Appendix, SI Text* and Table S5). Detailed methods for all enzyme activity assays are provided in the *SI Appendix, SI Text*.

Measurement of Hydrogen and CO Concentrations in the *O. algarvensis* Habitat. Seawater and pore water samples from a sediment depth of 25 cm were collected by research divers using a stainless steel needle and capped syringes. A total of nine sites within an area of ~100 m^2 at the *O. algarvensis* collection site were sampled. Hydrogen and CO concentrations were measured the same day using an RGA3 reduction gas analyzer (Trace Analytical Inc.) (*SI Appendix, SI Text*).

Metabolite Identification and Quantification in Whole Worms and Pore Water. Whole worms were extracted using ice-cold ethanol-based solvent mixture and ultrasonication. Metabolites were measured with GC-MS, LC-MS, and ^{1}H-NMR as described previously (66), with minor modifications (*SI Appendix, SI Text*). Detected metabolites are shown in *SI Appendix*, Table S2. Relative quantification of metabolites was performed on the basis of complete spectrum/chromatogram intensities (*SI Appendix, SI Text*).

Pore water was sampled at different sediment depths in the *O. algarvensis* habitat by scuba divers with Rhizon MOM 10-cm soil water samplers (Rhizosphere Research Products, Wageningen, The Netherlands) and was measured using GC-MS as described in Liebeke et al. (66).

ACKNOWLEDGMENTS. We thank Tanja Woyke and Friedrich Widdel for stimulating scientific discussions, Thomas Holler and Harald Gruber-Vodicka for helpful comments on the manuscript, and many members of the working groups of Michael Hecker and Thomas Schweder for technical assistance. We also thank Daniel Kockelkorn for providing enzymes for 3-HPB–related enzyme assays, Bernd Giese for help with confocal laser-scanning microscopy, Ivaylo Kostadinov and Jost Waldmann for help with creating protein identification databases, Ann Hedley for providing the worm EST library sequences and support, and Martha Schattenhofer for assistance with automated cell counting. We thank the editor and reviewers of this paper, in particular Samantha B. Joye, for their insightful comments and feedback. M. Kleiner and C. Wentrup were supported by Studienstiftung des deutschen Volkes scholarships. Funding for this study was provided by the Max Planck Society; by the Laboratory Directed Research and Development support at the Oak Ridge National Laboratory, managed by UT-Battelle, LLC, for the US Department of Energy under Contract DE-AC05-00OR22725; and by Grant SCHW595/3-3 from the German Research Foundation (to T.S.).

1. Baumann P (2005) Biology bacteriocyte-associated endosymbionts of plant sap-sucking insects. *Annu Rev Microbiol* 59:155–189.
2. Felbeck H (1981) Chemoautotrophic Potential of the Hydrothermal Vent Tube Worm, *Riftia pachyptila* Jones (Vestimentifera). *Science* 213:336–338.
3. Cavanaugh CM, Gardiner SL, Jones ML, Jannasch HW, Waterbury JB (1981) Prokaryotic Cells in the Hydrothermal Vent Tube Worm *Riftia pachyptila* Jones: Possible Chemoautotrophic Symbionts. *Science* 213:340–342.
4. Dubilier N, Bergin C, Lott C (2008) Symbiotic diversity in marine animals: The art of harnessing chemosynthesis. *Nat Rev Microbiol* 6:725–740.
5. Dubilier N, Blazejak A, Rühland C (2006) *Molecular Basis of Symbiosis, Symbiosis between bacteria and gutless marine oligochaetes, Progress in Molecular and Subcellular Biology*, ed Overmann J (Springer, Berlin), Vol 41, pp 251–275.
6. Dubilier N, et al. (2001) Endosymbiotic sulphate-reducing and sulphide-oxidizing bacteria in an oligochaete worm. *Nature* 411:298–302.

7. Giere O, Erséus C (2002) Taxonomy and new bacterial symbioses of gutless marine Tubificidae (Annelida, Oligochaeta) from the Island of Elba (Italy). *Org Divers Evol* 2: 289–297.
8. Ruehland C, et al. (2008) Multiple bacterial symbionts in two species of co-occurring gutless oligochaete worms from Mediterranean sea grass sediments. *Environ Microbiol* 10:3404–3416.
9. Woyke T, et al. (2006) Symbiosis insights through metagenomic analysis of a microbial consortium. *Nature* 443:950–955.
10. Kleiner M, Woyke T, Ruehland C, Dubilier N (2011) The *Olavius algarvensis* metagenome revisited: Lessons learned from the analysis of the low diversity microbial consortium of a gutless marine worm. *Handbook of Molecular Microbial Ecology II: Metagenomics in Different Habitats*, ed Bruijn FJd (John Wiley & Sons, Inc., Hoboken, NJ), Vol 2, pp 321–334.
11. Warnecke F, Hugenholtz P (2007) Building on basic metagenomics with complementary technologies. *Genome Biol* 8:231.
12. King GM, Weber CF (2007) Distribution, diversity and ecology of aerobic CO-oxidizing bacteria. *Nat Rev Microbiol* 5:107–118.
13. Oelgeschläger E, Rother M (2008) Carbon monoxide-dependent energy metabolism in anaerobic bacteria and archaea. *Arch Microbiol* 190:257–269.
14. Conrad R, Meyer O, Seiler W (1981) Role of carboxydobacteria in consumption of atmospheric carbon monoxide by soil. *Appl Environ Microbiol* 42:211–215.
15. Moran MA, et al. (2004) Genome sequence of Silicibacter pomeroyi reveals adaptations to the marine environment. *Nature* 432:910–913.
16. King GM (2007) Microbial carbon monoxide consumption in salt marsh sediments. *FEMS Microbiol Ecol* 59:2–9.
17. Moran JJ, House CH, Vrentas JM, Freeman KH (2008) Methyl sulfide production by a novel carbon monoxide metabolism in *Methanosarcina acetivorans*. *Appl Environ Microbiol* 74:540–542.
18. Thauer RK, Stackebrandt E, Hamilton WA (2007) *Sulphate-Reducing Bacteria: Environmental and Engineered Systems, Energy Metabolism and Phylogenetic Diversity of Sulphate-Reducing Bacteria*, eds Barton LL, Hamilton WA (Cambridge Univ Press, New York), pp 1–37.
19. Mörsdorf G, Frunzke K, Gadkari D, Meyer O (1992) Microbial growth on carbon monoxide. *Biodegradation* 3:61–82.
20. Caffrey SM, et al. (2007) Function of periplasmic hydrogenases in the sulfate-reducing bacterium *Desulfovibrio vulgaris* Hildenborough. *J Bacteriol* 189:6159–6167.
21. Goodwin S, Conrad R, Zeikus JG (1988) Influence of pH on microbial hydrogen metabolism in diverse sedimentary ecosystems. *Appl Environ Microbiol* 54:590–593.
22. Novelli PC, et al. (1988) Hydrogen and acetate cycling in two sulfate-reducing sediments: Buzzards Bay and Town Cove, Mass. *Geochim Cosmochim Acta* 52: 2477–2486.
23. Karadagli F, Rittmann BE (2007) Thermodynamic and kinetic analysis of the H_2 threshold for *Methanobacterium bryantii* M.o.H. *Biodegradation* 18:439–452.
24. Petersen JM, et al. (2011) Hydrogen is an energy source for hydrothermal vent symbioses. *Nature* 476:176–180.
25. Sowell SM, et al. (2009) Transport functions dominate the SAR11 metaproteome at low-nutrient extremes in the Sargasso Sea. *ISME J* 3:93–105.
26. Rees DC, Johnson E, Lewinson O (2009) ABC transporters: The power to change. *Nat Rev Mol Cell Biol* 10:218–227.
27. Forward JA, Behrendt MC, Wyborn NR, Cross R, Kelly DJ (1997) TRAP transporters: A new family of periplasmic solute transport systems encoded by the dctPQM genes of *Rhodobacter capsulatus* and by homologs in diverse gram-negative bacteria. *J Bacteriol* 179:5482–5493.
28. Wick LM, Quadroni M, Egli T (2001) Short- and long-term changes in proteome composition and kinetic properties in a culture of *Escherichia coli* during transition from glucose-excess to glucose-limited growth conditions in continuous culture and *vice versa*. *Environ Microbiol* 3:588–599.
29. Mauchline TH, et al. (2006) Mapping the *Sinorhizobium meliloti* 1021 solute-binding protein-dependent transportome. *Proc Natl Acad Sci USA* 103:17933–17938.
30. Ferenci T (1999) Regulation by nutrient limitation. *Curr Opin Microbiol* 2:208–213.
31. Sowell SM, et al. (2011) Environmental proteomics of microbial plankton in a highly productive coastal upwelling system. *ISME J* 5:856–865.
32. Kelly DJ, Thomas GH (2001) The tripartite ATP-independent periplasmic (TRAP) transporters of bacteria and archaea. *FEMS Microbiol Rev* 25:405–424.
33. Ames GFL (1986) Bacterial periplasmic transport systems: Structure, mechanism, and evolution. *Annu Rev Biochem* 55:397–425.
34. Grieshaber MK, Hardewig I, Kreutzer U, Pörtner H-O (1994) Physiological and metabolic responses to hypoxia in invertebrates. *Rev Physiol Biochem Pharmacol* 125: 43–147.
35. van Hellemond JJ, van der Klei A, van Weelden SW, Tielens AG; Hellemond JJv (2003) Biochemical and evolutionary aspects of anaerobically functioning mitochondria. *Philos Trans R Soc Lond B Biol Sci* 358:205–213, discussion 213–215.
36. Zarzycki J, Brecht V, Müller M, Fuchs G (2009) Identifying the missing steps of the autotrophic 3-hydroxypropionate CO2 fixation cycle in *Chloroflexus aurantiacus*. *Proc Natl Acad Sci USA* 106:21317–21322.
37. Zarzycki J, Fuchs G (2011) Coassimilation of organic substrates via the autotrophic 3-hydroxypropionate bi-cycle in *Chloroflexus aurantiacus*. *Appl Environ Microbiol* 77: 6181–6188.
38. Nemecky SN-M (2008) Benthic degradation rates in shallow subtidal carbonate and silicate sands. PhD thesis (Univ of Bremen, Bremen, Germany).
39. Hua Q, Yang C, Oshima T, Mori H, Shimizu K (2004) Analysis of gene expression in *Escherichia coli* in response to changes of growth-limiting nutrient in chemostat cultures. *Appl Environ Microbiol* 70:2354–2366.
40. Voigt B, et al. (2007) The glucose and nitrogen starvation response of *Bacillus licheniformis*. *Proteomics* 7:413–423.
41. Yancey PH (2005) Organic osmolytes as compatible, metabolic and counteracting cytoprotectants in high osmolarity and other stresses. *J Exp Biol* 208:2819–2830.
42. Serrano A, Pérez-Castiñeira JR, Baltscheffsky M, Baltscheffsky H (2007) H^+-PPases: Yesterday, today and tomorrow. *IUBMB Life* 59:76–83.
43. Liu CL, Peck HD, Jr. (1981) Comparative bioenergetics of sulfate reduction in *Desulfovibrio* and *Desulfotomaculum* spp. *J Bacteriol* 145:966–973.
44. Liu M-Y, Le Gall J (1990) Purification and characterization of two proteins with inorganic pyrophosphatase activity from *Desulfovibrio vulgaris*: Rubrerythrin and a new, highly active, enzyme. *Biochem Biophys Res Commun* 171:313–318.
45. Thebrath B, Dilling W, Cypionka H (1989) Sulfate activation in *Desulfotomaculum*. *Arch Microbiol* 152:296–301.
46. Schöcke L, Schink B (1998) Membrane-bound proton-translocating pyrophosphatase of *Syntrophus gentianae*, a syntrophically benzoate-degrading fermenting bacterium. *Eur J Biochem* 256:589–594.
47. Robidart JC, et al. (2008) Metabolic versatility of the *Riftia pachyptila* endosymbiont revealed through metagenomics. *Environ Microbiol* 10:727–737.
48. Newton ILG, et al. (2007) The *Calyptogena magnifica* chemoautotrophic symbiont genome. *Science* 315:998–1000.
49. Kuwahara H, et al. (2007) Reduced genome of the thioautotrophic intracellular symbiont in a deep-sea clam, *Calyptogena okutanii*. *Curr Biol* 17:881–886.
50. Reshetnikov AS, et al. (2008) Characterization of the pyrophosphate-dependent 6-phosphofructokinase from *Methylococcus capsulatus* Bath. *FEMS Microbiol Lett* 288: 202–210.
51. Baltscheffsky H (1996) *Origin and Evolution of Biological Energy Conversion, Energy Conversion Leading to the Origin and Early Evolution of Life: Did Inorganic Pyrophosphate Precede Adenosine Triphosphate?* ed Baltscheffsky H (Wiley-VCH, New York), pp 1–9.
52. Say RF, Fuchs G (2010) Fructose 1,6-bisphosphate aldolase/phosphatase may be an ancestral gluconeogenic enzyme. *Nature* 464:1077–1081.
53. Baltscheffsky H (1967) Inorganic pyrophosphate and the evolution of biological energy transformation. *Acta Chem Scand* 21:1973–1974.
54. Miller SL, Parris M (1964) Synthesis of pyrophosphate under primitive earth conditions. *Nature* 204:1248–1250.
55. Turnbaugh PJ, et al. (2007) The human microbiome project. *Nature* 449:804–810.
56. Yin B, Crowley D, Sparovek G, De Melo WJ, Borneman J (2000) Bacterial functional redundancy along a soil reclamation gradient. *Appl Environ Microbiol* 66:4361–4365.
57. Denef VJ, et al. (2010) Proteogenomic basis for ecological divergence of closely related bacteria in natural acidophilic microbial communities. *Proc Natl Acad Sci USA* 107:2383–2390.
58. Wilmes P, et al. (2008) Community proteogenomics highlights microbial strain-variant protein expression within activated sludge performing enhanced biological phosphorus removal. *ISME J* 2:853–864.
59. Konstantinidis KT, et al. (2009) Comparative systems biology across an evolutionary gradient within the *Shewanella* genus. *Proc Natl Acad Sci USA* 106:15909–15914.
60. Otto A, et al. (2010) Systems-wide temporal proteomic profiling in glucose-starved *Bacillus subtilis*. *Nat Commun* 1:137.
61. Washburn MP, Wolters D, Yates JR, 3rd (2001) Large-scale analysis of the yeast proteome by multidimensional protein identification technology. *Nat Biotechnol* 19: 242–247.
62. Verberkmoes NC, et al. (2009) Shotgun metaproteomics of the human distal gut microbiota. *ISME J* 3:179–189.
63. Peng J, Elias JE, Thoreen CC, Licklider LJ, Gygi SP (2003) Evaluation of multidimensional chromatography coupled with tandem mass spectrometry (LC/LC-MS/MS) for large-scale protein analysis: The yeast proteome. *J Proteome Res* 2:43–50.
64. Elias JE, Gygi SP (2007) Target-decoy search strategy for increased confidence in large-scale protein identifications by mass spectrometry. *Nat Methods* 4:207–214.
65. Florens L, et al. (2006) Analyzing chromatin remodeling complexes using shotgun proteomics and normalized spectral abundance factors. *Methods* 40:303–311.
66. Liebeke M, et al. (2011) A metabolomics and proteomics study of the adaptation of *Staphylococcus aureus* to glucose starvation. *Mol Biosyst* 7:1241–1253.

Supporting Information

Kleiner et al.

SI Results and Discussion

Aerobic and anaerobic respiration and fermentation

In the host proteome we detected almost all enzymes used by invertebrates during anaerobic metabolism (1, 2), including enzymes for cytosolic glycolysis as well as the mitochondrial malate dismutation and acetate-propionate pathway (Fig. S6, Dataset S2). Furthermore, metabolomic analyses of whole worms revealed high concentrations of metabolites such as acetate, succinate and malate that are known to accumulate in aquatic invertebrates during environmental anaerobiosis (1, 3) (Fig. S6, Table S2). We also found host enzymes in the metaproteome that are used during aerobic metabolism such as cytochrome c oxidase and NADH-ubiquinone oxidoreductase (Dataset S2). The presence of host enzymes used for both aerobic and anaerobic metabolism provides strong support for our assumption that the worms migrate between the upper oxic and lower anoxic sediment layers (4).

Our metaproteomic analyses of respiration in the symbionts show that these make use of different terminal electron acceptors (TEAs) as the worms shuttle between the upper and lower sediment layers. The sulfate-reducing δ-symbionts abundantly expressed proteins for the dissimilatory reduction of sulfate as well as a number of proteins that enable them to deal with reactive oxygen species during periods when the worms inhabit the upper oxygenated layers of the sediment such as catalases/peroxidases, alkylhydroperoxidases and superoxide dismutases (Dataset S2, Fig. S3a).

The sulfur-oxidizing γ1-symbiont expressed a cytochrome c oxidase protein (2004222648) for the use of oxygen as TEA and a second TEA protein (2004222690) for an acceptor that could be nitrate, perchlorate or DMSO (Datasets S1 and S2).

One of the 10 most abundant proteins in the γ3-symbiont was the catalytic NapA subunit of the respiratory nitrate reductase (2004225019), which is encoded in the γ3-symbiont metagenome as a part of the *nap*-operon (*nap*DAGHBFC). This indicates that the γ3-symbiont predominantly uses nitrate as a TEA. Surprisingly, no proteins for the use of oxygen as a TEA were found in the γ3-symbiont despite the assumption by Woyke et al. (5) that oxygen can be respired by this symbiont. We therefore re-evaluated the metagenome and found that terminal oxidases for the use of oxygen as a TEA are not present (no cytochrome bo ubiquinol -, cytochrome c – or cytochrome bd quinol oxidase). The only cytochrome-c like terminal oxidase (2004227159) in the γ3-symbiont metagenome has its best BLASTp hit to a protein that is specifically characterized as lacking the necessary residues for oxygen reduction and proton pumping (*Magnetospirillum magnetotacticum*, Q9XDX1) (6, 7). While the incomplete nature of the γ3-symbiont metagenome (approx. 10% of genome lacking) precludes absolute certainty, the lack of terminal oxidases for oxygen in the metagenome and metaproteome indicate that the γ3-symbiont always respires nitrate even under oxygenated conditions. Such a constitutive nitrate respiration was shown for the thiotrophic symbiont of the clam *Lucinoma aequizonata* using calorimetry, and the authors concluded that the obligate use of nitrate by the symbionts prevents competition with the host for the limited amount of oxygen available in its environment (8). In *O. algarvensis*, the obligate use by the γ3-symbiont of nitrate for respiration would not only avoid competition for oxygen with the host, but also with the γ1-symbiont.

Autotrophic fixation of CO_2

One of the distinguishing characteristics of chemosynthetic associations is that the bacterial symbionts provide their hosts with carbon through the autotrophic fixation of CO_2. The metagenomic analysis of the *O. algarvensis* symbionts revealed that both sulfur-oxidizing γ-symbionts as well as both sulfate-reducing δ-symbionts have the potential for autotrophic CO_2 fixation (5). Our metaproteomic analysis confirmed that autotrophy plays an important role in the metabolism of the two γ-symbionts since both abundantly expressed enzymes of the Calvin-Benson-Bassham cycle (see 'Energy efficient PPi-dependent pathways in sulfur oxidizers'). For the δ-symbionts the case is not as clear. Both δ-symbionts abundantly expressed the enzymes of the Wood-Ljungdahl pathway (Datasets S1 and S2). However, it is not clear if they use this pathway for autotrophic or heterotrophic growth, since the Wood-Ljungdahl pathway is reversible and can operate both in the direction of acetyl-CoA production during autotrophy and acetyl-CoA oxidation during heterotrophy (9). Depending on the available substrates and energy sources, it is possible that the δ-symbionts use the Wood-Ljungdahl pathway in both directions: Acetate produced by the host might be a source for heterotrophic growth (see 'Recycling and waste management'), whereas the use of hydrogen or CO as an energy source would allow the δ-symbionts to grow autotrophically (see 'Energy sources for the symbiosis'). Woyke et al. (2006) (5) also proposed that the reverse tricarboxylic acid pathway might play a role in autotrophic CO_2 fixation by the δ-symbionts, however we did not find the characteristic enzymes for this pathway in the metaproteome.

Carbon monoxide dehydrogenases

Of the expressed CODHs for the anaerobic oxidation of CO in the two deltaproteobacterial symbionts, one in each symbiont clustered in their genomes with the CO-methylating acetyl-CoA synthase (δ1: 2004216583; δ4:

2004219036). This indicates that these CODHs take part in the Wood-Ljungdahl pathway (10) and not in energy gain through CO oxidation. The other three expressed δ-symbiont CODHs (δ1: 2004209677, 6frame_RASTannot_31067; δ4: 2004219762) are most likely used for energy production with CO under anaerobic conditions, as shown for different bacterial species including sulfate reducers (11-13).
The γ3-symbiont CODH for the aerobic use of CO as an energy source consists of three subunits, which are all encoded in the metagenome (*cox*MSL) including several additional *cox*-gene cluster proteins (*cox*GDEFI). Both the large and the medium CODH subunits were expressed in the γ3-symbionts (L: 2004227646, 2004227235, M: 2004227232) (Datasets S1 and S2). The remaining γ3-symbiont Cox-proteins were most likely not detected because of the low coverage of the γ3-symbiont proteome.

Use of fermentative host waste by the sulfate reducing δ-Symbionts

Both δ-symbionts abundantly expressed the complete Wood-Ljungdahl pathway, which can be used to oxidize host derived acetate (9, 14). The δ1-symbiont also abundantly expressed the enzymes for the methylmalonyl-CoA pathway for propionate oxidation (14-16) (Fig. S3a). An extremely abundant solute:sodium symporter (TC 2.A.21, 2004210484) in the δ1-symbiont also appears to be involved in the use of acetate and propionate. Its gene is located in the immediate vicinity of the highly expressed acetate-CoA ligase (EC 6.2.1.1, 2004210485) and propionate-CoA ligase (EC 6.2.1.17, 2004210481). These enzymes catalyze the initial steps of acetate and propionate oxidation, respectively. A similar operon-like structure of a nearly identical transporter and an acetate-CoA ligase is present in the δ4-symbiont genome (2004220449, 2004220450). These metagenomic and metaproteomic data provide strong support that these transporters are used for acetate and propionate uptake in the δ-symbionts. We therefore reclassified both transporters as putative acetate(propionate):sodium symporters.

Use and recycling of nitrogenous compounds

Both the γ3-symbiont and the δ1-symbiont abundantly expressed proteins for glycine betaine uptake (γ3:2004227807; δ1: 2004211353) and metabolism (γ3: 2004224976, 6frame_RASTannot_75195; δ1: 2004210590, 2004212610, 2004208989, 2004217075, 2004214110) (Datasets S2 and S3). In both symbionts, almost all enzymes for the degradation of glycine betaine to pyruvate and ammonia were expressed. This pathway would allow these symbionts to use this osmolyte as their sole source of carbon and nitrogen, as shown for example in the plant symbiont *Sinorhizobium meliloti* (17).
Our metaproteomic analyses indicate that the *O. algarvensis* γ3-symbiont degrades urea, based on the expression of the alpha subunit of urease (2004226389) (Dataset S2). The smaller urease subunits and the urea ABC-transporter are encoded in an operon with the alpha subunit in the γ3-symbiont metagenome. Their co-occurrence in the same operon makes it very likely that they were also expressed, but not detected because of the low coverage of the γ3-symbiont metaproteome. Urea, which is the major source of nitrogen for some bacteria (18), is degraded by urease to ammonia and CO_2 in an ATP-independent step. Given the expression of glutamine synthetase and the Calvin cycle in this symbiont, it is likely that both the ammonia and the CO_2 from urea degradation are re-assimilated by the γ3-symbiont. In an interesting parallel, the hydrothermal vent tubeworm *Riftia pachyptila* also produces large amounts of urea (19). However, the *Riftia* symbionts do not posses the ability to degrade urea (20).
Other nitrogenous waste compounds that might also be assimilated by the *O. algarvensis* symbionts are the sulfur-containing amino acid taurine and the polyamine putrescine. Although not found in the metabolome, the expression of proteins for the uptake (γ3 and δ1) and degradation (γ3) of putrescine and the uptake of taurine (γ3) indicate that the symbionts are involved in the recycling of these presumably host derived nitrogenous compounds.

Details on the proton translocating pyrophosphatases

The H^+-PPases of the γ1-symbiont (2004223049) and the δ1-symbiont (2004209116) were abundantly expressed, whereas the standard enzyme for pyrophosphate hydrolysis - the soluble inorganic pyrophosphatase - was neither found in the symbionts metagenomes nor their metaproteomes. We therefore conclude that the H^+-PPases in the γ1-symbionts and the δ1-symbionts conserve energy in novel metabolic pathways.

The PPi-dependent phosphofructokinase (PPi-PFK) in the γ-symbionts

We propose that in the *O. algarvensis* γ-symbionts fructose-1,6-bisphosphatase and sedoheptulose-1,7-bisphosphatase are replaced by a PPi-PFK based on its presence in the metagenomes of both γ-symbionts (γ1: 2004223047, γ3: 2004227099) and abundant expression in the γ1-symbiont (the low coverage of the γ3-symbiont proteome could explain why it was not detected in this symbiont). The γ-symbiont PPi-PFKs are highly similar to the PPi-PFK of *Methylococcus capsulatus* (γ1: 71% amino acid identity; γ3: 69% amino acid identity) which is not only able to catalyze the same reactions as fructose-1,6-bisphosphatase and sedoheptulose-1,7-bisphosphatase but also that of a third enzyme of the Calvin cycle, phosphoribulokinase (21). It is therefore possible that the γ-symbiont PPi-PFK also catalyzes this third reaction in the Calvin cycle. It should be noted, however, that an ATP-dependent phosphoribulokinase is present in both the γ-symbionts as well as *M. capsulatus* (Fig. 5c).
In glycolysis, PPi-PFK most likely replaces the ATP-dependent phosphofructokinase, which is neither present in the two *O. algarvensis* γ-symbiont metagenomes, nor in the genomes of *M. capsulatus* and the symbionts of *R. pachyptila*, *C. magnifica* and *C. okutanii* (Fig. 5c). The full reversibility of the PPi-PFK reaction as well as the H^+-PPase means that these enzymes could also replace the fructose-1,6-bisphosphatase reaction in gluconeogenesis. Depending on environmental conditions, either the

forward or the reverse reactions could be catalyzed. Under anoxic conditions, glycogen remobilization and glucose degradation via glycolysis would consume PPi produced by the H^+-PPi synthase activity, whereas under oxic conditions remobilization of stored PHA and subsequent generation of glucose/glycogen via gluconeogenesis would produce PPi consumed through H^+-PPase activity. As in the δ1-symbiont, several additional enzymes that produce PPi are also expressed in the γ1-symbiont such as propionate-CoA ligase, acetate-CoA ligase and pyruvate phosphate dikinase (the latter in high amounts) (Fig. S3b).

Although H^+-PPases are widespread in bacteria (22) their key role in energy conservation has rarely been recognized and is only described in one phototrophic and two heterotrophic species. In *Rhodospirillum rubrum* they play an important role in photosynthesis (22), in an anaerobic bacterium they are involved in benzoate degradation (23), and in a hydrogen-producing bacterium H^+-PPases conserve energy during glycolysis (24). To our knowledge, our study provides the first description of an extensive involvement of H^+-PPases in the Calvin cycle and the central carbon metabolism of a chemolithoautotrophic organism, and we propose that other chemoautotrophic organisms also use H^+-PPases to conserve energy in these pathways.

SI Materials and Methods

Sample collection

Gutless oligochaete worms were collected in October 2007, April 2008 and October 2008 at the same site where the samples for the metagenome analysis of *O. algarvensis* were taken in 2004 (5). The site is located in the bay of Sant'Andrea, Elba, Italy (42°48'26''N, 010°08'28''E). Worms were collected from silicate sediments near seagrass beds of *Posidonia oceanica*, in a water depth of 4 - 8 m, transported with the sediment to the laboratory in buckets, and removed from the sediment via decantation on the same day or the day after their collection. Worms were freed from adhering particles (mostly small pieces of sea grass) by letting them migrate into a thin layer of clean sediment, rinsed in seawater, and rinsed a second time in sterile-filtered PBS (phosphate buffered saline: 137 mM NaCl, 2.7 mM KCl, 10 mM Na_2HPO_4, 2 mM KH_2PO_4). Between 1000 and 2000 worms were collected per day and either immediately frozen in liquid nitrogen or used in the density gradient centrifugation procedure described below.

At the sampling site, two additional *Olavius* species – *O. ilvae* (25) and *O.* sp. – co-occur with *O. algarvensis*, but in much lower abundances. The ratio of *O. algarvensis* to *O. ilvae* at the sampling site has been estimated at 30:1 (25), for *O.* sp. the ratio is presumably even higher. These three species can only be distinguished under a microscope when sexually mature. The majority of the worms used in this study were not sexually mature and could therefore not be distinguished based on their morphological characteristics. Subsamples of sexually mature worms were checked whenever available, and the majority of these were *O. algarvensis*. For a more detailed molecular evaluation of the host species composition in our samples we analyzed these with symbiont specific probes (see below).

Symbiont enrichment via density gradient centrifugation

To separate the different symbionts from the worm tissue and from each other, an isopycnic density gradient centrifugation was applied to several samples. A discontinuous density gradient with large density steps (10% steps) in the high density range (1.159 – 1.372 g/ml) and small density steps (2% steps) in the low density range (1.052 – 1.159 g/ml) was assembled 10 minutes prior to centrifugation with HistoDenz™ (Sigma® Saint Louis, Missouri, USA) dissolved in PBS.

Between 1000 - 2000 worms were transferred with 1 – 2 ml PBS to a Duall® homogenizer (Tissue grind pestle and tube SZ22, Kontes Glass Company, Vineland, New Jersey) and homogenized with about 20 strokes. The resulting homogenate with a volume between 1 - 2.5 ml was immediately loaded onto the prepared density gradient by slowly pipetting onto the wall of the 15 ml tube containing the gradient.

The centrifugation was carried out at 5445 x g and 4°C for 1 hour using a Sigma® 3K15 centrifuge (Sigma Laborzentrifugen GmbH, Osterode am Harz, Germany) equipped with a Sigma® 11133 swing out rotor. After centrifugation, the density gradient was divided into equally-sized fractions and a small subsample was taken from every fraction for later analysis of sample composition (see below). The remaining larger part of the sample was washed two times with PBS to remove the gradient medium and the resulting pellets frozen in liquid nitrogen.

Assessing symbiont composition in density gradient fractions

Catalyzed reporter deposition-fluorescence *in situ* hybridization (CARD-FISH) (26) was used to determine the abundance and composition of the different symbiont species in the gradient fractions. Subsamples (20 µl) from the density gradient fractions (see above) were fixed over night at 4°C in 1 ml of 1% formaldehyde (Fluka, Taufkirchen, Germany) in PBS pH 7.6. The next morning, cells were washed three times in PBS and then stored at -20°C in 100 µl of a 50% PBS and 50% ethanol mix. In preparation for the CARD-FISH analysis, the cells were filtered onto GTTP polycarbonate filters with a pore size of 0.2 µm (Millipore, Billerica, MA). CARD-FISH was done as described previously (26) with the minor modification that endogenous peroxidases in the cells were inactivated by a 5 minute incubation of the filters at 22°C in 0.01 M HCl. For CARD-FISH, group specific and *O. algarvensis* symbiont specific oligonucleotide probes labeled at the 5' end with horseradish peroxidase (HRP) (biomers.net, Ulm, Germany) were used (Table S6). For CARD-FISH dual hybridizations with probes specific to the γ1-symbionts (see below), after the hybridization and amplification with the first probe the HRP was inactivated with methanol/0.5% hydrogen peroxide for 30 min before beginning the second hybridization and amplification steps.

The relative proportion of contamination with symbionts from *O. ilvae* and *O.* sp. was examined with CARD-FISH double hybridizations using probes specific to the γ1-symbionts in each host species. The previously described FISH-probes for the *O. ilvae* and *O. algarvensis* γ1-symbionts (27) were not sufficiently specific for symbionts immobilized on filters even when different helpers and competitors were added to the hybridization mix. Additionally, no probe for the γ1-symbiont of the third *Olavius* species existed. Therefore we designed two new FISH probes. One specifically targets the *O. algarvensis* γ1-symbiont, the other targets both the *O. ilvae* and the third *O.* sp. γ1-symbiont. For both probes additional unlabeled helper probes were designed to improve hybridization specificity (Table S6).
The fraction of cells with species specific CARD-FISH signal in at least 1000 DAPI-stained cells per filter section was quantified either by manual counting on a Zeiss Axioplan epifluorescence microscope or semi-automatically with a cell counting machine developed at the Max Planck Institute for Marine Microbiology (28). For all density gradients analyzed with CARD-FISH, several filter sections hybridized with the NON338 and the EUB338-probe respectively were subjected to semi-automated counting as a negative and positive control. Images for documentation of some filter sections were taken with a confocal laser scanning microscope (Zeiss LSM 510 Meta, Carl Zeiss Microimaging, Jena, Germany) (Fig. S1).
The abundance of non *O. algarvensis* γ1-symbionts was determined by manual counting as the percentage of *O. ilvae*/*O.* sp. γ1-symbionts out of the total γ1-symbionts. The average "contamination level" with non *O. algarvensis* γ1-symbionts in the samples was 17.6% (n=16), with a minimum of 3% in one sample and a maximum of 31% in another sample. We therefore conclude that in all samples, the majority of the proteins originated from *O. algarvensis* symbionts.

Proteomics

Two different methods were used for protein identification and quantification to obtain high proteome coverage: one dimensional polyacrylamide gel electrophoresis followed by liquid chromatography and tandem mass spectrometry (1D-PAGE-LC-MS/MS) and two dimensional liquid chromatography followed by tandem mass spectrometry (2D-LC-MS/MS).

Protein extraction for 1D-PAGE-LC-MS/MS

Frozen whole worms were suspended in 400 µl of lysis buffer (10 mM Tris-HCl, pH 8; 10 mM EDTA; 1.7 mM PMSF; 1x complete Protease Inhibitor Cocktail (Roche Applied Science, Mannheim, Germany)) and homogenized in a Duall® homogenizer. Alternatively, frozen bacterial pellets from several density gradient fractions were re-suspended and combined in 0.5 ml lysis buffer. The homogenate or the cell suspension was transferred into prelubricated 1.7 ml reaction tubes (Sorenson BioScience Inc., Salt Lake City, UT, USA). Cells were disrupted on ice with a sonication probe (Labsonic U, B. Braun, 3 x 30 seconds with one minute breaks with the following settings: a repeating duty cycle of 0.7, the 'low' setting and a power level of -0.65). Cell debris was removed by centrifugation. Protein was concentrated by lyophilisation.

1D-PAGE-LC-MS/MS

Between 50 and 150 µg of protein extract were lyophilized and the resulting pellet was dissolved in 20 µl of SDS sample buffer (65.5 mM Tris-HCl (pH 6.8); 2% SDS; 20% glycerin; 5% β-mercapto-ethanol; bromophenol blue). Proteins were separated according to their molecular weight by 1D-SDS-PAGE (29). After electrophoresis, gels were stained with Colloidal Coomassie (0.04% w/v Coomassie Brilliant Blue G250; 8% w/v ammonium sulfate; 0.8% phosphoric acid; 20% ethanol). Each gel lane was cut into 12 equal sized pieces. In-gel digestion of proteins and peptide elution was done as described previously (30).
Separation by liquid chromatography and mass spectrometry analysis of peptides obtained from in-gel digestion were conducted as described recently (31). Briefly, a nanoACQUITY UPLC™ System (Waters Corp., Milford, MA, USA) was used. For every run approximately 500 ng of the peptide mixture from one gel piece was loaded onto the trapping column (nanoAcquity™ UPLC™ Column, Symmetry® C_{18} 5 µm, 180 µm x 20 mm, Waters) and washed for 3 minutes with 99% buffer A (0.1% acetic acid) at a flow rate of 10 µl min^{-1}. Afterwards peptides were eluted and separated at a flow rate of 1 µl min^{-1} on an analytical column (nanoAcquity™ UPLC™ Column, BEH130 C_{18} 1.7 µm, 100 µm x 100 mm, Waters). A gradient going from buffer A to 60% buffer B (0.1% acetic acid in acetonitrile) in 90 min was applied. Eluting peptides were ionized with electrospray ionization (ESI) and analyzed in a LTQ Orbitrap™ hybrid mass spectrometer (Thermo Fisher Scientific, Waltham, MA, USA). Full scans were acquired at 30,000 resolution in the Orbitrap, MS/MS scans of the five most abundant precursor ions were acquired in the LTQ. Ions with no assigned charge state or with a charge state +1 were not analyzed in the LTQ. One or two microscans were taken for each scan type and dynamic exclusion was enabled (either 30 sec or 180 sec exclusion duration with one or two repeats).

2D-LC-MS/MS

The enriched microbial pellets or frozen whole worms were lysed via a single-tube small processing method (32). Briefly, cells were lysed and proteins were denatured and reduced overnight by suspending the microbial pellets or whole worms in 6 M guanidine/10 mM DTT in 50 mM Tris buffer (pH 7.6) with gently rocking at 37° C. Samples were then digested with sequencing-grade trypsin, desalted via solid phase extraction, filtered and aliquoted.
All samples were analyzed in duplicate via 24 hr multidimensional nano-2D-LC MS/MS system with a split-phase column (RP-SCX-RP) (33, 34) on a hybrid linear ion trap-Orbitrap (Thermo Fischer Scientific). Full scans were acquired at 30,000 resolution in the Orbitrap, MS/MS scans were acquired in the LTQ. Two microscans were taken for each scan type, dynamic exclusion was enabled as previously described (35).

Protein identification for 1D-PAGE-LC-MS/MS and 2D-LC-MS/MS

All MS/MS spectra from 1D-PAGE-LC-MS/MS and 2D-LC-MS/MS experiments were searched against two protein sequence databases (see below) using the SEQUEST algorithm (36) with the following parameters: Parent Mass Tolerance, 3.0; Fragment Ion Tolerance, 0.5; up to 4 missed cleavages allowed (internal lysine and arginine residues), fully tryptic peptides only, and filtered with DTASelect (37) at the peptide level (SEQUEST Xcorrs of at least 1.8 (+1), 2.5 (+2) 3.5 (+3), DeltCN>0.08). To further validate peptides monoisotopic theoretical masses for all peptides identified by SEQUEST were generated and compared to observed masses. Observed high-resolution masses were extracted from .RAW files from the full scan preceding best identified spectra; parts per million (ppm) calculations were made comparing each identified peptide's observed and theoretical mass. When quality MS/MS spectra did not have an observed mass (low intensity) a mass of 0 was reported and ppm was calculated as infinity. The final datasets for our biological analyses (Datasets S1 and S2) were generated by only considering peptides with <10 ppm and >-10 ppm differences between observed and calculated mass. Only proteins identified with at least two different peptides were included in the final datasets (identical peptides with different charge states were identified as different peptides).

The first sequence database - Oalgarvensis_Symbiont_Metagenome_JGI-IMGM – contained a total of 21,162 protein sequences from the published *O. algarvensis* symbiont metagenome (5) and common contaminants. The second database - Oalgarvensis_V7_SymbiontAndHostExtendedDB_fr - contained a total of 338,052 protein sequences, which included: the published symbiont metagenome (5), re-annotated symbiont metagenome seleno- and pyrroproteins (38), a six reading frame translation of symbiont metagenome fragments that could not be assigned to a specific symbiont (http://genome.jgi-psf.org/olaal/olaal.download.ftp.html), genomes of symbiont related bacteria (http://img.jgi.doe.gov/cgi-bin/m/main.cgi), common contaminants and genomes/EST libraries from the host related annelids *Helobdella robusta* (http://genome.jgi-psf.org/Helro1/Helro1.home.html), *Capitella teleta* (http://genome.jgi-psf.org/Capca1/Capca1.home.html) and *Lumbricus rubellus* (39) (http://www.ncbi.nlm.nih.gov/dbEST/). The six reading frame translation of symbiont sequences and the host sequences were, if possible, automatically annotated with RAST (40). Since large amounts of redundancies were introduced into the second database by the six reading frame translation and the use of several bacteria and annelid genomes, we used the CD-HIT software (41) to remove redundancies from the database. Additionally, we manually removed the largest part of the genomes from symbiont related bacteria and the *Helobdella robusta* genome from the database after running several test searches, which yielded no hits with these sequences.

To determine false discovery rates (FDR) of protein identification both protein sequence databases were reversed and appended to the original databases as decoy databases. FDRs were determined according to the method of Peng et al., 2003 and Elias and Gygi, 2007 (42, 43) using the above peptide filtering criteria. FDRs varied strongly between methods, search databases and samples (Table S7). For searches against the Oalgarvensis_V7_SymbiontAndHostExtendedDB_fr database, on which we focused our analysis, the FDRs were between 0-3.27% (Table S7).

For relative quantitation of proteins, normalized spectral abundance factor (NSAF) values were calculated for each sample according to the method of Florens et al. (44). NSAF values give the relative abundance of a protein in a sample as a fraction of 1. Since NSAF calculations considered hits with sequences of contaminants and with sequences in the decoy database the total NSAF for symbiont + host proteins is slightly smaller than 1.

All identified proteins and their relative abundance in different samples are shown in datasets S1 and S2. These tables also contain accession numbers for protein sequences that are available in public databases. Accession numbers in the article and tables refer to the accession numbers of proteins in the protein sequence databases, which are available from the following website: http://compbio.ornl.gov/olavius_algarvensis_symbiont_metaproteome/. The website also grants open access to all peptide and protein results as well as all MS/MS spectra (up to date java is needed to view spectra).

Proteomics-based binning

In the metagenomic study of the *O. algarvensis* symbionts, only genome fragments larger than 5 kb could be assigned (binned) to a specific symbiont based on their genomic signatures (5). We identified many proteins encoded on metagenome fragments that were not assigned to a specific symbiont because they were shorter than 5 kb. We tentatively assigned these proteins to a specific symbiont using proteomics-based binning. The prerequisite for the proteomics-based binning was the specific enrichment of symbiont species with density gradient centrifugation prior to proteome analysis and the detailed characterization of symbiont enrichments with CARD-FISH (see above) (Fig. S1).

Proteomics-based binning was done on all symbiont proteins identified with 1D-PAGE-LC-MS/MS and 2D-LC-MS/MS in at least two samples (Dataset S3). For each protein the NSAF values in a specific symbiont enrichment were averaged: for example, for protein x the average NSAF value for all δ1-symbiont enrichment samples was calculated. The averages from the different enrichment types were then compared and proteins with an average NSAF value that was larger in a given symbiont enrichment than in all other symbiont enrichments was putatively binned to the symbiont with the largest average NSAF value. For example, if protein x had an average NSAF value in the γ1-symbiont enrichment that was larger than its average NSAF values in the γ3-, δ1- and δ4-symbiont enrichments, it was putatively binned to the γ1-symbiont.

For the δ4-symbionts, only one enrichment sample was available, so that proteomics-based binning could not be performed for this symbiont. For the γ3-symbionts, only two enrichment samples were available; proteins were

therefore only binned to the γ3-symbionts if all above criteria were met by a protein and additionally the protein was detected in both γ3-symbionts samples.
As an internal control for the accuracy of our proteomics based-binning approach, we applied the proteomics-based binning not only to the previously unassigned proteins, but also to the proteins that were identified with metagenome fragments that were already assigned to a specific symbiont in the metagenomic study. Based on species assignments that conflicted between metagenomic and proteomic binning we calculated a false assignment rate of 9.3% for our proteomics-based binning approach (Table S3).

Metabolic reconstruction

The symbiont and host metabolisms were reconstructed using current literature and the MetaCyc database (45). For the metabolic reconstruction we focused primarily on the abundant proteins in the metaproteome and considered mainly the metabolism of the host, γ1- and δ1-symbiont (Fig. 2, S3 and S6).

Enzyme tests

Enzymatic activities were determined in cell extracts from either whole worms or enriched symbionts. In both cases the samples were stored for varying amounts of time at -80° C.

Preparation of cell extracts from whole worms

200 worms were homogenized in 350 µl of 200 mM MOPS-K^+ buffer (pH 7.8) with Complete Protease Inhibitor (Roche, Mannheim, Germany) (buffer A). After addition of 350 mg glass beads (0.1 - 0.25 mm) the homogenate was treated in a mixer mill (type MM2; Retsch, Haare, Germany) for 7.5 min at 30 Hz. The supernatant obtained after centrifugation (15 min, 16,000 × *g*, 4°C) was used for the enzyme assays. The protein content of the cell extract was determined with the Bradford method using BSA as a standard.
Alternatively, whole worms (400 specimens) were homogenized with a glass potter in 2 ml of buffer A. After addition of 0.1 mg DNase I the homogenate was passed three times through a chilled French pressure cell at 137 MPa. The lysate was centrifuged for 15 min at 16,000 × *g* at 4 °C and the supernatant was used for enzyme assays or stored at -20°C in the presence of 20% glycerol.

Preparation of cell extracts from enriched symbionts

Six or eight pellets of enriched γ1-symbionts were resuspended in 1 ml buffer A. After addition of 0.1 mg DNase I the cell suspension was passed twice through a chilled French pressure cell at 137 MPa. The cell lysate was centrifuged for 15 min at 16,000 × *g* at 4 °C and the supernatant was used for enzyme assays or stored at -20°C in the presence of 20% glycerol.

Syntheses

(i) **Propionyl-CoA** was synthesized from its anhydride by a modified method of Stadtman (46). (ii) **β-Methylmalyl-CoA** was synthesized enzymatically as described previously (47). (iii) **3-Hydroxypropionate** was synthesized chemically from β-propiolactone. A solution (6 ml) of 5 M NaOH in water was stirred at room temperature and 1.25 ml β-propiolactone was added drop-wise (0.025 mol). The solution was lyophilized and the dry powder was stored at room temperature. (iv) **Mesaconyl-CoA** was synthesized with recombinant enzymes of *Chloroflexus aurantiacus* as described previously (47).

Enzyme Assays

The habitat temperature of *O. algarvensis* fluctuates between 15 and 25°C. All enzyme assays were performed at 30°C to slightly increase activities. One U corresponds to 1 µmol × min^{-1}.
(i) Malonyl-CoA reductase: Two different assays were used to measure malonyl-CoA reductase activity. First, the malonyl-CoA dependent oxidation of NADPH was monitored spectrophotometrically at 365 nm. The assay mixture (0.25 ml) contained 200 mM MOPS-K^+ buffer (pH 7.8), 0.3 mM NADPH, 1 mM malonyl-CoA, and *O. algarvensis* cell extract (0.3 mg protein). The reaction was started by addition of malonyl-CoA.
Second, the cell extracts were tested for malonyl-CoA reductase activity in thin layer chromatography experiments. The assay mixture (0.2 ml) contained 200 mM MOPS-K^+ buffer (pH 7.8) with Complete Protease Inhibitor (Roche, Mannheim, Germany), 10 mM $MgCl_2$, 5 mM DTE, 2 mM NADPH, 0.8 mM malonyl-CoA, 37 kBq [2-^{14}C]malonyl-CoA, and enriched γ1-symbiont cell extract (0.4 mg protein). After 1, 3, and 6 h samples of 50 µl were withdrawn, transferred to ice and stopped by addition of 5 µl of ≥ 99% formic acid. In a control experiment NADPH was omitted and the reaction was stopped after 6 h. Precipitated protein was removed by centrifugation and 10 µl of the respective supernatants were analyzed by thin layer chromatography. The same assays were performed with *C. aurantiacus* cell extract (250 µg protein) at 55 °C, with malonyl-CoA reductase (0.5 U) from *Metallosphaera sedula* at 40 °C, and with malonyl-CoA reductase combined with malonic semialdehyde reductase (0.5 U) also from *M. sedula* at 40°C. Both *M. sedula* enzymes were kindly provided by Dr. Daniel Kockelkorn (48, 49).
TLC was performed using silica gel 60 F_{254} plates (20 x 20 cm, Merck, Darmstadt, Germany) and butanol-acetic acid-water (12:3:5) as solvent. The plates were dried for 20 min at room temperature; then radioactivity was detected by phosphoimaging using FUJI-BAS100X phosphoimager plates (Fuji, Japan).
In the following assays, the samples were transferred to ice and the reaction was stopped by addition of 10 µl of 99% formic acid. Precipitated protein was removed by centrifugation. The supernatants were analyzed by HPLC (system 1 or system 2 in case of (vi)).
(ii) Propionyl-CoA synthase: The formation of propionyl-CoA was monitored in an HPLC-based assay. The reaction mixture (200 µl) contained 200 mM MOPS-K^+ (pH 7.8), 5 mM $MgCl_2$, 10 mM KCl, 2 mM 3-hydroxypropionate, 3 mM ATP, 1.5 mM CoA, 3 mM NADPH, and *O. algarvensis* whole worm or γ1-symbiont cell extract (0.1 mg protein). ATP was omitted in a

control. Samples of 80 µl were taken after 1 and 3 hours of incubation.

(iii) Mesaconyl-C1-CoA hyadratase: The dehydration of β-methylmalyl-CoA to mesaconyl-CoA in *Olavius algarvensis* cell extract was followed in a spectrophotometric assay at 30°C. An estimated absorption coefficient at 290 nm of 3400 M^{-1} cm^{-1} for the formation of mesaconyl-CoA was used. The assay mixture (120 µl) contained 200 mM MOPS-K^+ (pH 7.8), 0.25 mM β-methylmalyl-CoA, and cell extract (0.1 mg protein). The reaction was started with either substrate or cell extract. After 20 and 60 min of incubation samples of 50 µl were withdrawn.

(iv) β-methylmalyl-CoA lyase: The condensation of propionyl-CoA and glyoxylate to β-methylmalyl-CoA was monitored in an HPLC-based assay. The reaction mixture (200 µl) contained 200 mM MOPS-K^+ (pH 7.8), 5 mM $MgCl_2$, 1.25 mM propionyl-CoA, 7.5 mM glyoxylate, and *O. algarvensis* cell extract (0.1 mg protein). Glyoxylate was omitted in a control. Samples of 80 µl were taken after 1 and 3 hours of incubation. The samples were transferred on ice and the reaction was stopped by addition of 10 µl of ≥ 99% formic acid. Precipitated protein was removed by centrifugation and the supernatants were analyzed by HPLC (system 1).

(v) Mesaconyl-CoA C1:C4 CoA transferase: The conversion of mesaconyl-C1-CoA to mesaconyl-C4-CoA in cell extract of enriched γ1-symbionts was followed in an HPLC-based assay. The reaction mixture (200 µl) contained buffer A, 1 mM mesaconyl-C1-CoA, and extracts of enriched γ1-symbionts (40 µg protein). After 1 and 3 h of incubation samples of 100 µl were withdrawn. The same assay conditions were used with *Olavius* extracts (0.2 mg protein) in a reaction volume of 300 µl. In control experiments the extracts were omitted.

(vi) Mesaconyl-C4-CoA hydratase and (*S*)-citramalyl-CoA lyase: The hydration of mesaconyl-C4-CoA to (*S*)-citramalyl-CoA and its subsequent cleavage into pyruvate and acetyl-CoA by (*S*)-malyl-CoA/β-methylmalyl-CoA/(*S*)-citramalyl-CoA lyase was monitored in an HPLC-based assay. The reaction mixture (300 µl) contained buffer A, 5 mM $MgCl_2$, 1 mM mesaconyl-C4-CoA, and *O. algarvensis* cell extract (0.2 mg protein). Samples of 60 µl were taken after 3, 10, 60, and 180 min of incubation.

(vii) Acetyl-CoA carboxylase and propionyl-CoA carboxylase: Extract of enriched γ1-symbionts was tested for activities of acetyl-CoA carboxylase and propionyl-CoA carboxylase. The assay mixture (1 ml) contained buffer A, 5 mM $MgCl_2$, 5 mM DTE, 10 mM $NaHCO_3$, 200 kBq [^{14}C]Na_2CO_3, 2 mM ATP, 0.4 mM acetyl-CoA or propionyl-CoA (respectively), and γ1 extract (0.1 mg protein). Samples of 100 µl were withdrawn after 5, 10, 30, 60, 180 min, and a sample of 500 µl was taken after over night incubation. The samples were stopped in a 2 fold volume of 2% trichloroacetic acid and then incubated at room temperature while shaking for 12 hours to remove all non incorporated radioactive CO_2. In respective control experiments acetyl-CoA or propionyl-CoA was omitted. The remaining radioactivity in the samples was measured by liquid scintillation counting.

Analytical high performance liquid chromatography (HPLC)

Two different HPLC separation systems were used. Reaction products and standard compounds were detected by UV absorbance at 260 nm with a photodiode array detector (Waters, Eschborn, Germany). **System 1:** A reversed phase C_{18} column (LiChrospher 100, end-capped, 5 µm, 125 × 4 mm; Merck, Darmstadt, Germany) was used. The column was developed at a flow rate of 1 ml min^{-1} for 7 min under isocratic conditions with 100 mM NaH_2PO_4 (pH 4.0) in 7.5% methanol (v/v), followed by a linear 10 min gradient from 0% to 60% of 100 mM sodium acetate (pH 4.2) in 90% methanol (v/v). **System 2:** A reversed phase C_{18} column (NUCLEODUR C18 Gravity, 5 µm, 250 × 4 mm; Macherey-Nagel, Düren, Germany) was used. A gradient of 30 min from 2 to 20 % acetonitrile in 40 mM K_2HPO_4/HCOOH buffer (pH 4.2), with a flow rate of 0.6 ml min^{-1}, was applied.

Measurement of hydrogen and CO concentrations in the O. algarvensis habitat

Sediment pore waters and seawater above the sediment were sampled by research divers in the *O. algarvensis* habitat at multiple sites using a 1 m long stainless steel needle coupled to 12 ml syringes. The syringes were prefilled with 0.5 ml of a 50% $ZnCl_2$ solution to kill all biological activity upon sampling. For pore water extraction, the needle was inserted to a depth of 25 cm into the sediment. Seawater samples were collected ~5 cm above the sediment surface using the same methods and equipment as for pore water collection. The needle was pre-flushed by drawing 10 ml of the respective sample with a second syringe before taking the actual sample. Syringes were capped under water immediately after sampling and brought ashore. On shore samples were carefully transferred into 12 ml Exetainer vials (Labco Limited, Buckinghamshire, UK), which were then closed immediately with caps containing pierceable rubber septa. Samples were brought back to the lab and analyzed the same day.

A 1 ml headspace was created in the Exetainers by injecting 1 ml of ultra pure nitrogen gas (purity level 5.0; SOL s.p.a., Monza, Italy) through the septum, while enabling pressure compensation by outflow of water using a second needle. Samples were then vigorously shaken and left standing for 1 hour to allow for degassing of hydrogen and CO into the headspace.

Hydrogen and CO concentrations in the headspace were measured using a RGA3 reduction gas analyzer (Trace Analytical Inc., Menlo Park, CA, USA). Hydrogen- and CO-free nitrogen gas (purity level 5.0) was used as carrier gas. Hydrogen and CO standards were produced from pure hydrogen (purity level 5.0; Air Liquide, Düsseldorf, Germany) and CO (purity level 3.7; Messer, Bad Soden, Germany) gas in ultra pure nitrogen gas. Data recording and peak area integration were performed using the ECW 2000 software (Knauer, Berlin, Germany).

Blanks were used to determine potential contamination with CO and hydrogen introduced during sample processing e.g. through contact with atmosphere, sampling vials, nitrogen gas and reagents during sample

processing. Blanks were created by processing de-ionized water in parallel to the samples ($ZnCl_2$ addition, transfer to Exetainers, headspace generation with nitrogen gas). Eight blanks were measured. CO concentrations in blanks were 2.1 to 3.9 nM and hydrogen concentrations in blanks were 10.7 to 29.2 nM. Pore water and seawater concentrations were blank-corrected with average CO (3.1 nM) and hydrogen (21.5 nM) blank concentrations. Concentrations reported in Figures S4 and S5 and article are blank-corrected values.

Metabolomics

Whole worms

A defined number of frozen whole worms were resuspended on ice with 500 µl extraction solution consisting of ethanol/water (60/40 vol./vol.) for extraction of metabolites covering a broad spectrum of compounds. Cells were lysed using ultrasonication (Labsonic U, B.Braun®; 3x30 sec; repeating duty cycle 0.7, 'low' setting, power level of -0.65 with one minute breaks, samples were cooled on ice throughout the procedure). Cell debris was removed from the cell extract by centrifugation (5 min x 12000 rpm, -4°C). The supernatant was lyophilized with a Christ®beta 1–8 lyophilizer at −52°C and 0.25 mbar. Lyophilized extracts were measured with GC-MS and LC-MS in parallel for comprehensive metabolome coverage. Subsamples for GC-MS measurements were derivatized using a common protocol with methoxyamine and MSTFA as described earlier (50). To achieve higher coverage of metabolites, samples were measured in splitless mode (Agilent® split/splitless liner, taper, glasswool, deactivated; splitvent at 1.5 min 25 ml/min, gas saver at 2.0 min with 20 ml/min). Metabolite identification in GC-MS spectra was performed by deconvolution of peaks with AMDIS® and mass spectral comparison with NIST-library and an in-house database of mass spectra from pure standard compounds. For LC-MS measurements lyophilized extracts were redissolved in 100 µl LC-MS water (Sigma-Aldrich), samples were centrifuged (5 min x 12000 rpm, -4°C) and the supernatant transferred into LC-MS vials. After injection of 50 µl sample, measurement was performed with an ion-pairing method on a waters® RP Symmetry shield column. This method described in Liebeke et al. (51) allows the separation of a wide range of polar compounds. Compounds were identified by comparing their high resolution mass spectra and retention time against an in-house database of pure compounds and searching against mass spectra in common databases such as metlin, human metabolome data base (HMBD) and massbank.jp. For GC-MS and LC-MS data evaluation, prominent peaks with unknown identity were named with the following code: GC-MS peaks (OA_ion_ion_retention time in minutes) and LC-MS peaks (OA_$[M-H]^-$ion_retention time in min).

For ^{1}H-NMR analysis, extraction with ultrasonication of whole frozen worms was performed with 500 µl pure water. By avoiding the use of organic solvents we were able to measure the obtained solution directly without drying. This prevented the evaporation of slightly volatile compounds such as formic, acetic and propionic acid. Cell debris was removed by centrifugation after ultrasonication and a phosphate buffer in H_2O/D_2O was added to the supernatants. Samples were measured with the technical set up described earlier (52). In total 1024 scans with the NOESY-Presat pulse sequence were collected for 1D ^{1}H-NMR spectra. For 2D COSY measurements 8 scans were performed for spectra acquisition. Referencing and quantification was done to the internal standard (1mM sodium 3-trimethylsilyl-[2,2,3,3-D_4]-1-propionic acid) in added phosphate buffer. Compound identification was done by matching the obtained spectra with a ^{1}H-NMR spectra databank using AMIX®Viewer Version 3.8.2 (Bruker Biospin) and comparing with spectra of standard compounds.

Detected metabolites are shown in Table S2 and Fig. S7. Relative quantification of metabolites was performed on the basis of complete spectrum/chromatogram intensities. A signal intensity cut-off was set for each method applied, approximately the intensities were portioned in three similar parts and metabolites were assigned to less (+), middle (++) and high (+++) abundant. The three methods used here have a very different array of detectable metabolites, thus the measured abundances should be interpreted cautiously. In contrast to proteomics signal, intensity depends strongly on the chemical and physical properties of a compound and thus the abundance of a given metabolite can not be easily standardized. However, a metabolite found to be highly abundant in one of the three methods can be considered to be very abundant in the worm sample.

Porewater

Pore water was sampled in situ by scuba divers with RHIZON ® MOM 10 cm soil water samplers (F. Meijboom, Wageningen, NL), basically a porous hydrophilic polymer tube with 0.1 µm pore size attached to plastic syringes of 10 ml. The RHIZON samplers were placed horizontally at 2 cm increments in the sediment to about 25 cm depth below the sediment surface and the syringes filled with pore water. At the end of the dive, the water samples were immediately transferred from the syringes to 2 ml Eppendorf tubes, stored on ice and frozen upon arrival in the laboratory (within 1 h), or immediately frozen on dry ice. The frozen samples were stored at –20°C until analysis. A total of 6 samples from depths between 8 and 16 cm sediment depth from 3 different profiles and 8 samples from the water column as controls were chosen for analysis.

Pore water samples were thawed and spiked with 100 µl internal standards (ribitol/norvaline, 1µmol*l^{-1}) and 500 µl of this solution lyophilized as described above. Dry samples were derivatized with a high excess of methoxyamine (200µL) and MSTFA (400µL). Samples were centrifuged and the supernatant was concentrated by slight heating. After transferring the obtained solution into GC-MS vials, samples were measured with splitless mode as described above.

SI References

1. Grieshaber MK, Hardewig I, Kreutzer U, Pörtner H-O (1994) Physiological and metabolic responses to hypoxia in invertebrates. *Rev Physiol Biochem Pharmacol* 125:43-147.
2. Hellemond JJv, Klei Avd, Weelden SHv, Tielens AGM (2003) Biochemical and evolutionary aspects of anaerobically functioning mitochondria. *Philos Trans R Soc Lond B Biol Sci* 358:205-215.
3. Schöttler U, Bennet EM (1991) in *Metazoan Life without Oxygen,* Annelids, ed Bryant C (Chapman and Hall, London, UK), pp 165-185.
4. Dubilier N, Blazejak A, Rühland C (2006) in *Molecular Basis of Symbiosis,* Symbiosis between bacteria and gutless marine oligochaetes, Progress in Molecular and Subcellular Biology, ed Overmann J (Springer, Berlin Heidelberg), Vol 41, pp 251-275.
5. Woyke T, et al. (2006) Symbiosis insights through metagenomic analysis of a microbial consortium. *Nature* 443:950-955.
6. Tanimura Y-s, Fukumori Y (2000) Heme-copper oxidase family structure of *Magnetospirillum magnetotacticum* 'cytochrome a1'-like hemoprotein without cytochrome c oxidase activity. *J Inorg Biochem* 82:73-78.
7. Tamegai H, Yamanaka T, Fukumori Y (1993) Purification and properties of a `cytochrome a1'-like hemoprotein from a magnetotactic bacterium, *Aquaspirillum magnetotacticum*. *Biochim Biophys Acta - General Subjects* 1158:237-243.
8. Hentschel U, Hand S, Felbeck H (1996) The contribution of nitrate respiration to the energy budget of the symbiont-containing clam *Lucinoma aequizonata*: a calorimetric study. *J Exp Biol* 199:427-433.
9. Schauder R, Eikmanns B, Thauer RK, Widdel F, Fuchs G (1986) Acetate oxidation to CO_2 in anaerobic bacteria via a novel pathway not involving reactions of the citric acid cycle. *Arch Microbiol* 145:162-172.
10. Ragsdale SW, Pierce E (2008) Acetogenesis and the Wood-Ljungdahl pathway of CO2 fixation. *Biochim Biophys Acta - Proteins & Proteomics* 1784:1873-1898.
11. Mörsdorf G, Frunzke K, Gadkari D, Meyer O (1992) Microbial growth on carbon monoxide. *Biodegradation* 3:61-82.
12. Techtmann SM, Colman AS, Robb FT (2009) 'That which does not kill us only makes us stronger': the role of carbon monoxide in thermophilic microbial consortia. *Environ Microbiol* 11:1027-1037.
13. Oelgeschläger E, Rother M (2008) Carbon monoxide-dependent energy metabolism in anaerobic bacteria and archaea. *Arch Microbiol* 190:257-269.
14. Thauer RK, Stackebrandt E, Hamilton WA (2007) in *Sulphate-reducing Bacteria: Environmental and Engineered Systems,* Energy metabolism and phylogenetic diversity of sulphate-reducing bacteria, eds Barton LL,Hamilton WA (Cambridge University Press, New York), pp 1-37.
15. Kremer DR, Hansen TA (1988) Pathway of propionate degradation in *Desulfobulbus propionicus*. *FEMS Microbiol Lett* 49:273-277.
16. Houwen FP, Plokker J, Stams AJM, Zehnder AJB (1990) Enzymatic evidence for involvement of the methylmalonyl-CoA pathway in propionate oxidation by *Syntrophobacter wolinii*. *Arch Microbiol* 155:52-55.
17. Smith LT, Pocard JA, Bernard T, Le Rudulier D (1988) Osmotic control of glycine betaine biosynthesis and degradation in *Rhizobium meliloti*. *J Bacteriol* 170:3142-3149.
18. Mobley HL, Hausinger RP (1989) Microbial ureases: significance, regulation, and molecular characterization. *Microbiol Mol Biol Rev* 53:85-108.
19. De Cian M, Regnault M, Lallier FH (2000) Nitrogen metabolites and related enzymatic activities in the body fluids and tissues of the hydrothermal vent tubeworm *Riftia pachyptila*. *J Exp Biol* 203:2907-2920.
20. Robidart JC, et al. (2008) Metabolic versatility of the *Riftia pachyptila* endosymbiont revealed through metagenomics. *Environ Microbiol* 10:727-737.
21. Reshetnikov AS, et al. (2008) Characterization of the pyrophosphate-dependent 6-phosphofructokinase from *Methylococcus capsulatus* Bath. *FEMS Microbiol Lett* 288:202-210.
22. Serrano A, Pérez-Castiñeira JR, Baltscheffsky M, Baltscheffsky H (2007) H^+-PPases: yesterday, today and tomorrow. *IUBMB Life* 59:76-83.
23. Schöcke L, Schink B (1998) Membrane-bound proton-translocating pyrophosphatase of *Syntrophus gentianae*, a syntrophically benzoate-degrading fermenting bacterium. *Eur J Biochem* 256:589-594.
24. Bielen AAM, et al. (2010) Pyrophosphate as a central energy carrier in the hydrogen-producing extremely thermophilic *Caldicellulosiruptor saccharolyticus*. *FEMS Microbiol Lett* 307:48-54.
25. Giere O, Erséus C (2002) Taxonomy and new bacterial symbioses of gutless marine Tubificidae (Annelida, Oligochaeta) from the Island of Elba (Italy). *Org Divers Evol* 2:289-297.
26. Pernthaler A, Pernthaler J, Amann R (2002) Fluorescence *In Situ* Hybridization and Catalyzed Reporter Deposition for the Identification of Marine Bacteria. *Appl Environ Microbiol* 68:3094-3101.
27. Ruehland C, et al. (2008) Multiple bacterial symbionts in two species of co-occurring gutless oligochaete worms from Mediterranean sea grass sediments. *Environ Microbiol* 10:3404-3416.
28. Pernthaler J, Pernthaler A, Amann R (2003) Automated Enumeration of Groups of Marine Picoplankton after Fluorescence *In Situ* Hybridization. *Appl Environ Microbiol* 69:2631-2637.
29. Laemmli UK (1970) Cleavage of Structural Proteins during the Assembly of the Head of Bacteriophage T4. *Nature* 227:680-685.
30. Eymann C, et al. (2004) A comprehensive proteome map of growing *Bacillus subtilis* cells. *Proteomics* 4:2849-2876.
31. Otto A, et al. (2010) Systems-wide temporal proteomic profiling in glucose-starved *Bacillus subtilis*. *Nat Commun.* 1(137):137. 10.1038/ncomms1137.
32. Thompson MR, et al. (2008) Experimental Approach for Deep Proteome Measurements from Small-Scale Microbial Biomass Samples. *Anal Chem* 80:9517-9525.
33. Washburn MP, Wolters D, Yates JR (2001) Large-scale analysis of the yeast proteome by multidimensional protein identification technology. *Nat Biotech* 19:242-247.
34. McDonald WH, Ohi R, Miyamoto DT, Mitchison TJ, Yates JR (2002) Comparison of three directly coupled HPLC MS/MS strategies for identification of proteins from complex mixtures: single-dimension LC-MS/MS, 2-phase MudPIT, and 3-phase MudPIT. *Int J Mass Spectrom* 219:245-251.
35. Verberkmoes NC, et al. (2009) Shotgun metaproteomics of the human distal gut microbiota. *ISME J* 3:179-189.
36. Eng JK, McCormack AL, Yates JR (1994) An approach to correlate tandem mass spectral data of peptides with amino acid sequences in a protein database. *J Am Soc Mass Spectr* 5:976-989.
37. Tabb DL, McDonald WH, Yates JR (2002) DTASelect and Contrast: Tools for Assembling and Comparing Protein Identifications from Shotgun Proteomics. *J Proteome Res.* 1(1):21-26. 10.1021/pr015504q.
38. Zhang Y, Gladyshev VN (2007) High content of proteins containing 21st and 22nd amino acids, selenocysteine and pyrrolysine, in a symbiotic deltaproteobacterium of gutless worm *Olavius algarvensis*. *Nucleic Acids Res* 35:4952-4963.
39. Stürzenbaum SR, et al. (2003) The earthworm Expressed Sequence Tag project. *Pedobiologia* 47:447-451.
40. Aziz R, et al. (2008) The RAST Server: Rapid Annotations using Subsystems Technology. *BMC Genomics.* 9(1):75. 10.1186/1471-2164-9-75.
41. Li W, Godzik A (2006) Cd-hit: a fast program for clustering and comparing large sets of protein or nucleotide sequences. *Bioinformatics* 22:1658-1659.
42. Peng J, Elias JE, Thoreen CC, Licklider LJ, Gygi SP (2002) Evaluation of Multidimensional Chromatography Coupled with Tandem Mass Spectrometry (LC/LC-MS/MS) for Large-Scale Protein Analysis: The Yeast Proteome. *J Proteome Res.* 2(1):43-50. 10.1021/pr025556v.
43. Elias JE, Gygi SP (2007) Target-decoy search strategy for increased confidence in large-scale protein identifications by mass spectrometry. *Nat Meth* 4:207-214.
44. Florens L, et al. (2006) Analyzing chromatin remodeling complexes using shotgun proteomics and normalized spectral abundance factors. *Methods* 40:303-311.
45. Caspi R, et al. (2008) The MetaCyc Database of metabolic pathways and enzymes and the BioCyc collection of Pathway/Genome Databases. *Nucl. Acids Res.* 36:D623-631.
46. Stadtman ER (1957) in *Methods Enzymol,* Preparation and assay of acyl coenzyme A and other thiol esters; use of hydroxylamine, (Academic Press), Vol 3, pp 931-941.
47. Zarzycki J, Brecht V, Müller M, Fuchs G (2009) Identifying the missing steps of the autotrophic 3-hydroxypropionate CO2 fixation cycle in *Chloroflexus aurantiacus*. *Proc Natl Acad Sci USA* 106:21317-21322.
48. Alber BE, et al. (2006) Malonyl-Coenzyme A reductase in the modified 3-hydroxypropionate cycle for autotrophic carbon fixation in archaeal *Metallosphaera* and *Sulfolobus* spp. *J Bacteriol* 188:8551-8559.
49. Kockelkorn D, Fuchs G (2009) Malonic Semialdehyde Reductase, Succinic Semialdehyde Reductase, and Succinyl-Coenzyme A Reductase from *Metallosphaera sedula*: Enzymes of the Autotrophic 3-Hydroxypropionate/4-Hydroxybutyrate Cycle in *Sulfolobales*. *J Bacteriol* 191:6352-6362.
50. Liebeke M, et al. (2008) Depletion of thiol-containing proteins in response to quinones in *Bacillus subtilis*. *Mol Microbiol* 69:1513-1529.

51. Liebeke M, Meyer H, Donat S, Ohlsen K, Lalk M (2010) A Metabolomic View of *Staphylococcus aureus* and Its Ser/Thr Kinase and Phosphatase Deletion Mutants: Involvement in Cell Wall Biosynthesis. *Chemistry & Biology* 17:820-830.
52. Liebeke M, Brözel V, Hecker M, Lalk M (2009) Chemical characterization of soil extract as growth media for the ecophysiological study of bacteria. *Appl Microbiol Biotechnol* 83:161-173.
53. Sowell SM, et al. (2009) Transport functions dominate the SAR11 metaproteome at low-nutrient extremes in the Sargasso Sea. *ISME J* 3:93-105.
54. VerBerkmoes NC, et al. (2006) Determination and Comparison of the Baseline Proteomes of the Versatile Microbe *Rhodopseudomonas palustris* under Its Major Metabolic States. *J Proteome Res* 5:287-298.
55. Wallner G, Amann R, Beisker W (1993) Optimizing fluorescent in situ hybridization with rRNA-targeted oligonucleotide probes for flow cytometric identification of microorganisms. *Cytometry* 14:136-143.
56. Amann RI, et al. (1990) Combination of 16S rRNA-targeted oligonucleotide probes with flow cytometry for analyzing mixed microbial populations. *Appl Environ Microbiol* 56:1919-1925.
57. Manz W, Amann R, Ludwig W, Wagner M, Schleifer KH (1992) Phylogenetic oligodeoxynucleotide probes for the major subclasses of proteobacteria: problems and solutions. *Syst Appl Microbiol* 15:593-600.
58. Dubilier N, et al. (2001) Endosymbiotic sulphate-reducing and sulphide-oxidizing bacteria in an oligochaete worm. *Nature* 411:298-302.
59. Eisen JA, et al. (2002) The complete genome sequence of *Chlorobium tepidum* TLS, a photosynthetic, anaerobic, green-sulfur bacterium. *Proc Natl Acad Sci USA* 99:9509-9514.
60. Frigaard N-U, Dahl C (2008) Sulfur Metabolism in Phototrophic Sulfur Bacteria. *Adv Microb Physiol* 54:103-200.

SI Tables

Table S1: Number of proteins from specific symbionts identified by 2D-LC-MS/MS (gelfree) or 1D-PAGE-LC-MS/MS (gelbased) for each sample

2D-LC-MS/MS

Organism*	Delta1 Run2	Delta1 Run3	Gamma1 Run1	Gamma1 Run2	Whole Worm Run1	Whole Worm Run2	Whole Worm2 Run3	Whole Worm4 Run4
γ1-symbiont	175	168	871	771	255	325	227	316
γ3-symbiont	36	36	44	45	36	47	33	37
δ1-symbiont	586	601	34	32	39	41	33	41
δ4-symbiont	71	73	9	9	10	14	15	17
Unassigned Symbiont	35	40	134	68	20	29	20	27
Host	194	191	168	183	209	239	204	205
Total	**1097**	**1109**	**1260**	**1108**	**569**	**695**	**532**	**643**

1D-LC-MS/MS

Organism*	Delta1 Run1 Exp009	Delta4 Run1 Exp009	Gamma1 Run1 Exp009	Gamma3 Run1 Exp009	Gamma3 Run2 Exp009	Delta1 Run1 Exp020	Delta1 Run2 Exp020	Gamma1 Run1 Exp020	Whole Worm Run1 Exp021	**Total both methods**
γ1-symbiont	63	67	240	30	48	17	24	229	165	**945**
γ3-symbiont	12	32	14	31	58	10	10	11	20	**141**
δ1-symbiont	373	193	24	13	35	271	234	6	15	**783**
δ4-symbiont	27	32	4	9	15	14	14	1	7	**93**
Unassigned Symbiont	21	28	8	3	16	7	7	6	11	**327**
Host	79	93	59	85	140	52	45	44	147	**530**
Total	**575**	**445**	**349**	**171**	**312**	**371**	**334**	**297**	**365**	**2819**

* For species assignment both the metagenomic binning information and the proteomics binning information were used. In case of conflict, metagenomic binning information was given priority over proteomics binning information.

Table S2: All metabolites detected with NMR, LC-MS and GC-MS in extracts from whole worms

For GC-MS and LC-MS data evaluation, prominent peaks with unknown identity were named with the following code: GC-MS peaks (OA_ion_ion_retention time in minutes) and LC-MS peaks (OA_[M-H]-ion_retention time in min)

Metabolite	**KEGG entry**	**NMR**		**GC-MS**			**LC-MS**		
		rel. abund.	Chemical shift [ppm] (multiplicity)	rel. abund.	m/z*	ret. time [min]	rel. abund.	m/z	ret. time [min]
(Deoxy?) ribose-5-P	-			+	315, 299	33.13			
2-dCMP	C00239						+	306.04	20.1
2-hydroxyglutaric acid	C02630	+	2.45 (t)	+	247, 129	22.19			
3-phosphoglyceric acid	C00197			+	299, 315	27.31			
4-aminobutyric acid	C00334			+	216, 174	21.03			
acetic acid	C00033	+	1.92 (s)						
adenosine	C00212						+	268.08	15.8
adenylsuccinate	C03794						+	462.06	34
ADP	C00008						+	426.02	30
ADP-glc	C00498						+	588.08	27
ADP-ribose	C00301						++	558.06	28
alanine	C01401	+	1.48 (d)	+	190, 116	9.7			
AMP	C00020						+++	346.05	23.9
APS	C00224						+	426.01	24.1

Metabolite	KEGG entry	NMR		GC-MS			LC-MS		
		rel. abund.	Chemical shift [ppm] (multiplicity)	rel. abund.	m/z*	ret. time [min]	rel. abund.	m/z	ret. time [min]
arginine	C00062	+++	3.24 (t)						
aspartate	C00049			+	100, 232	20.8			
ATP	C00002						+	505.98	37
CDP	C00112						+	402.01	28.3
citramalyl-CoA (no reference substance measured)	C00904						+	896.119	41.1
citric acid	C00158			+	363, 273	27.53			
citrulline	C00327			+	75, 171	19.99			
CMP	C00055						+	322.04	18
coenzyme A	C00010						+	766.09	39.8
CTP	C00063						+	481.97	35
Cystathionine, di-TMS	C00542			+	120, 174	21.4			
cysteine	C00097			+	218, 220	21.6			
dAMP	C00360						+	330.05	26
D-erythro-2-Pentulose	C00309			+	357, 299	33.2			
disaccharide	-			+	217, 361	30.3			
disaccharide	-	+	5.40 (d)						
disaccharide-P	-						+	421.07	16.5
dTMP	C00364						+	321.04	23.8
erythrose-4-P	C00279						+	198.99	15.6
ethanol	C00469	++	1.18 (t)						
formic acid	C00058	+	8.45 (s)						
fructose	C10906			+	217, 306	27.21			
fructose-1-6-bP	C05378						+	338.98	30.1
fructose-6-P	C05345						+	259.01	16
fumaric acid	C00122	+	6.52 (s)	+	147, 245	16.61			
GDP	C00035						+	442.01	29
glucose	C00267	+++	5.25 (d)	+++	191, 204	28.4			
glucose-6-P	C01172						+	259.01	16
glucose-P	-			+	387, 299	37.95			
glutamic acid	C00025	++	2.35 (m)	+++	128, 246	23.27			
glutathione	C00051						+	306.07	20.1
glutathione disulfide	C00127						++	611.14	23.2
glycerol	C00116	++	3.54 (dd)	+	218, 205	14.51			
glycerol 1-phosphate	C00623			++	357, 299	26.36			
glycine	C00037	+	3.56 (s)	+	248, 174	15.31			
glycine betaine	C00719	+++	3.90, 3.26 (s)						
glycogen	C00089	++	5.41 (d)						
GMP	C00144						++	362.04	21.3
guanosine	C00387						+	282.08	15.5
IDP	C00104	++	6.16 (d)				+++	426.99	29
IMP	C00130						+++	347.03	21.4
inosine	C00294						+	267.07	14.7
inositol	C00137			++	305, 318	31.61			
inositol-bP	-						+	338.98	31.9
inositol-bP	-						+	338.98	32.7
ITP	C00081						+	506.98	34.8
lactic acid	C00256	++	1.33 (d)	+++	117, 191	8.81			
lauric acid	C02679			+	257, 117	24.01			
leucine	C00123	+	0.96 (t)	+	218, 158	15.01			
lysine	C00047	+	3.03 (t)	+	156, 174	29.72			
malic acid	C00149	++	2.67 (m), 4.30 (m)	+++	190, 233	20.33			
methionine	C00073	+	2.14 (m), 2.64 (t)	+	128, 176	20.77			
myo-inositol-P	C01177			+	387, 299	36.89			
N,N-dimethylglycine	C01026	++	2.93 (s)						
N-acetylglucoseamine	C00140			+	272, 200	29.87			

Metabolite	KEGG entry	NMR		GC-MS			LC-MS		
		rel. abund.	Chemical shift [ppm] (multiplicity)	rel. abund.	m/z*	ret. time [min]	rel. abund.	m/z	ret. time [min]
ornithine	C00077			+	200, 174	26.03			
palmitic acid	C00249			+	117, 313	32.2			
phenylalanine	C00079	+	7.33 (d)	+	192, 218	23.24			
phosphate	C13558			+++	314, 299	13.81			
proline	C00148	++	4.15 (m)	+	258, 156	20.87			
pyroglutamic acid	C01879			++	156, 230	20.84			
pyruvic acid	C00022	+	2.39 (s)	+	174, 89	8.51			
ribonic acid	C01685			+	292, 217	26.72			
ribose-1,5-bP	C01151						+	308.07	30
sedoheptulose-7-P	C05382						+	289.03	17.1
serine	C00065	+	3.97 (m)						
serine (2TMS)	C00065			+	218, 204	16.83			
stearic acid	C01530			+	117, 341	35.52			
succinic acid	C00042	++	2.41 (s)	+++	147, 247	15.72			
sucrose (saccharose)	C00089			+++	217, 361	41.8			
thiourea	C14415			+	205, 171	20.4			
threonine	C00188	+	1.33 (d), 4.25 (m)						
threonine (3TMS)	C00188			+	291, 218	17.48			
thymine	C00178			+	243, 147	18.72			
tryptophane	C00078	+	7.74 (d)	+	159, 130	34.6			
tyrosine	C00082	+	6.90 (d)	+	280, 218	29.98			
UDP	C00015						+	402.99	33
UDP-glc	C00029						++	565.04	24
UDP-GlcA/glucuronic/galact-uronic	-						++	579.02	30.1
UDP-GlcNAc	C00043						+	606.07	24.5
UDP-ManNAcA	C06240						+	620.05	33
UDP-MurNAc	C05887						++	678.09	34.1
UDP-xylose/arabinose	-						+	535.03	24.5
UMP	C00105						+	323.02	21.1
urea	C00086			++	130, 189	13.2			
uridine	C00299			+		40.78			
valine	C00183	+	1.04 (d), 0.99 (d)	+	144, 218	9.44			
OA_203.07_21.0	-						+	203.07	21
OA_205_319_29.5 (monosaccharid)	-			+++	205, 319	29.55			
OA_274.08_20.2	-						+	274.08	20.2
OA_319_205 _30.87 (monosaccharid)	-			+	319, 205	30.87			
OA_319_217_28.1	-			+	319, 217	28.1			
OA_329.02_33.2	-						+	329.02	33.2
OA_361_204 _42.3 (disaccharid)	-			++	361, 204	42.3			
OA_372.06_28.3	-						+	372.06	28.3
OA_386.03_25.1	-						+	386.03	25.1
OA_399.04_23.4	-						+	399.04	23.4
OA_444.02_24.3	-						+	444.02	24.3
OA_447.17_21.5	-						+	447.17	21.5
OA_448.96_30.0	-						+	448.96	30
OA_477.17_18.5	-						+	477.17	18.5
OA_485.19_45.2	-						++	485.19	45.2
OA_486.29_28.9	-						+	486.29	28.9
OA_489.10_36.1	-						+	489.1	36.1
OA_492.17_27.5	-						+	492.17	27.5
OA_501.26_28.1	-						+	501.26	28.1
OA_502.05_24.2	-						+	502.05	24.2

Metabolite	KEGG entry	NMR		GC-MS			LC-MS		
		rel. abund.	Chemical shift [ppm] (multiplicity)	rel. abund.	m/z*	ret. time [min]	rel. abund.	m/z	ret. time [min]
OA_503.13_33.4	-						+	503.13	33.4
OA_508.10_22.1	-						+	508.1	22.1
OA_524.10_21.2	-						++	524.1	21.2
OA_541.98_24.6	-						+	541.98	24.6
OA_549.05_26.7	-						+	549.05	26.7
OA_554.11_23.6	-						+	554.11	23.6
OA_568.07_33.0	-						+	568.07	33
OA_576.06_25.5	-						+	576.06	25.5
OA_588.65_36.1	-						+	588.65	36.1
OA_590.08_28.1	-						+	590.08	28.1
OA_595.09_28.5	-						+	595.09	28.5
OA_597.16_35.7	-						+	597.16	35.7
OA_599.18_34.0	-						+	599.18	34
OA_618.08_27.3	-						+	618.08	27.3
OA_619.25_21.3	-						+	619.25	21.3
OA_634.10_29.8	-						+	634.1	29.8
OA_635.09_29.4	-						+	635.09	29.4
OA_638.02_36.3	-						++	638.02	36.3
OA_643.11_26.0	-						+	643.11	26
OA_654.86_41.5	-						+	654.86	41.5
OA_698.17_27.0	-						+	698.17	27
OA_720.11_26.9	-						+	720.11	26.9
OA_744.37_34.1	-						+	744.37	34.1
OA_784.14_37.0	-						+	784.14	37

* Fragment ions, first is identification ion, second is quantification ion

Table S3: Statistics of proteomics based binning

	No. of proteins that had the same assignment in the metagenome (correctly binned)	No. of proteins with contradicting assignment in the metagenome (incorrectly binned)	No. of proteins with no previous assignment (newly binned)	Total
No. of proteins binned to δ1-symbiont based on proteomics	466	60[a]	78	604
No. of proteins binned to γ1-symbiont based on proteomics	332	22	462	816
No. of proteins binned to γ3-symbiont based on proteomics	20	2	4	26
Total	**818**	**84**	**544**	**1446**
% of proteins that had a previous assignment based on the metagenome	**90.68**	**9.31**		

[a] γ3: 10 proteins; γ1: 6 proteins; δ4: 44 proteins

Table S4: Transporter protein abundances in symbionts and comparable studies

Dataset or type of study	Organism	Proportion (%) of transporter related proteins of all identified proteins [a]	Proportion (%) of transporter related spectra of all identified spectra [a]
This study			
2D-LC-MS/MS and 1D-PAGE-LC-MS/MS average	δ1-symbiont enrichment	28.6 ± 10	38 ± 8 [b], n=5
2D-LC-MS/MS and 1D-PAGE-LC-MS/MS average	γ1-symbiont enrichment	3 ± 1	0.75 ± 0.25 [b], n=4
Comparable studies			
Sargasso Sea Metaproteomics (53)	SAR11	17.37	67.14
Sargasso Sea Metaproteomics (53)	*Synechococcus* sp. CC9605	2.97	24.96
Proteomics of cultured bacterium (54)	*Rhodopseudomonas palustris* (aerob, chemoorganoheterotroph)	7.54	8.96
Proteomics of cultured bacterium (54)	*Rhodopseudomonas palustris* (anaerob, photoautotroph)	7.53	16.14
Proteomics of cultured bacterium Adkins et al. (2006)*	*Salmonella typhimurium*	9.63	7.06
Proteomics of cultured bacterium Elias et al. (2008)*	*Shewanella oneidensis*	5.12	3.94

* Values taken from Sowell et al. (53)
[a] Values were calculated from database searches against the published metagenome; proportions are calculated for all transport related proteins and spectra that were identified in a sample with sequences of the specified organism; proton and electron transporting proteins were not considered to be transporters (Dataset S4).
[b] NSAF values were used for calculation

Table S5: Enzyme activities of the 3-hydroxypropionate bicycle

Enzyme	Reaction	Spec. activity [nmol min^{-1} $mg^{-1}_{protein}$]	
		extracts of whole worms	extracts of enriched γ1-symbionts
(*S*)-Malyl-CoA/ β-methylmalyl-CoA/	propionyl-CoA + glyoxylate → β-methylmalyl-CoA	4	n.d.
(*S*)-citramalyl-CoA lyase	(*S*)-citramalyl-CoA → acetyl-CoA + pyruvate	6	n.d.
Mesaconyl-C1-CoA hydratase	β-methylmalyl-CoA → mesaconyl-C1-CoA + H_2O	15	n.d.
Mesaconyl-CoA C1-C4 CoA transferase	mesaconyl-C1-CoA → mesaconyl-C4-CoA	n.a.	40
Mesaconyl-C4-CoA hydratase	mesaconyl-C4-CoA → (*S*)-citramalyl-CoA	260	25
Malonyl-CoA reductase	malonyl-CoA + 2 NADPH + 2 H^+ → 3-OH-propionate + CoA	n.a.	n.a.
Propionyl-CoA synthase	3-OH-propionate + CoA + NADPH + H^+ + ATP → propionyl-CoA + AMP + PP_i + H_2O	n.a.	n.a.
Acetyl-CoA carboxylase	acetyl-CoA + HCO_3^- + ATP → malonyl-CoA + ADP + P_i	n.d.	≤ 0.01
Propionyl-CoA carboxylase	propionyl-CoA + HCO_3^- + ATP → (*S*)-methylmalonyl-CoA + ADP + P_i	n.d.	≤ 0.025
RubisCO	ribulose 1,5-bisphosphate + CO_2 → 2 3-phosphoglycerate	n.d.	≥ 0.65

n.d.: not determined, n.a.: no activity detectable

Table S6: Oligonucleotide probes used for CARD-FISH in this study.

Probe	Target organisms	Probe sequence (5'-3')	Position[a]	FA [%][b]	NaCl [mM][c]	Literature reference
NON338	Negative control, nonsense probe, complementary to EUB338	ACTCCTACGGGAGGCAGC	338-355	0	900	(55)
EUB338	Bacteria	GCTGCCTCCCGTAGGAG	338-355	0	900	(56)
Gam42a	Gammaproteobacteria	GCCTTCCCACATCGTTT	1027-1043[d]	35	70	(57)
OalgGAM1-445	*O. algarvensis* / ***O. ilvae*** Gamma 1 symbiont	CTCGAGATCTTTCTTCCC	445-462	10	450	(58)
Oilv/OcraGAM1	***O. algarvensis*** / *O. ilvae* / *O. crassitunicatus* Gamma 1 symbiont	CATACTCTAGCCGAACAG	643-660	10	450	(27)
Oalg/OilvGAM3	*O. algarvensis* / *O. ilvae* Gamma 3 symbiont	CCGGAATTCCACTTGCCT	665-682	30	102	(27)
OalgDEL1	*O. algarvensis* Delta 1 symbiont	GTTATCCCCGACTCGGGG	136-153	10	450	(58)
OalgDEL4	*O. algarvensis* Delta 4 symbiont	GCCCAACAACTTCCGGTA	1427-1444	30	102	(27)
SPIRO	*O. algarvensis* / *O. crassitunicatus* / *O. loisae* spirochete symbionts	GCTATCCCCAACCAAAAG	136-153	10	450	(27)
OalgGAM1-643	*O. algarvensis* Gamma 1 symbiont	TACCACACTCTAGCCGGACA	643-663	35	70	This study
Oilv/Elba3GAM1-464	*O. ilvae* / *Olavius* sp. (Elba 3) Gamma 1 symbiont	TCAAGGCCCTGGGGTATT	464-482	35	70	This study
Oilv/Elba3GAM1-464 Helper1		AACCCAAGGCATTTCTTCCCG	444-463	35	70	This study
Oilv/Elba3GAM1-464 Helper2		GTGCTTCTTCTGTCGGTAACG	483-503	35	70	This study

a. Position in the 16S rRNA of E. coli.
b. Formamide concentrations used in the CARD-FISH hybridization buffer, percentage (v/v).
c. NaCl concentration in the washing buffer
d. Position in the 23S rRNA of E. coli.

Table S7: Peptide identification false discovery rates in %, determined with reverse database searches according to the method of Elias and Gygi 2007(43)

Sample	O. algarvensis symbiont metagenome	Oalgarvensis_V7 Symbiont and host extended database
Delta1_Run2_gelfree	1.28	0.95
Delta1_Run3_gelfree	1.19	0.96
Gamma1_Run1_gelfree	3.99	1.48
Gamma1_Run2_gelfree	4.5	1.26
WholeWorm_Run1_gelfree	6.25	2.28
WholeWorm_Run2_gelfree	7.33	2.66
WholeWorm2_Run3_gelfree	13.05	3.27
WholeWorm4_Run4_gelfree	5.49	2.24
Delta1_Run1_gelbased_Exp009	0.15	0.24
Delta4_Run1_gelbased_Exp009	0	0.20
Gamma1_Run1_gelbased_Exp009	0.78	0.42
Gamma3_Run1_gelbased_Exp009	0	0.54
Gamma3_Run2_gelbased_Exp009	0	0.29
Delta1_Run1_gelbased_Exp020	0	0.00
Delta1_Run2_gelbased_Exp020	0	0.25
Gamma1_Run1_gelbased_Exp020	0.47	0.24
WholeWhiteWorm_Run1_gelbased_Exp021	1.29	0.26

Fig. S1: Distribution of *O. algarvensis* symbionts in density gradient fractions
(a) Three gradients were analyzed with CARD-FISH and cells counted semi-automatically. Relative abundances correspond to: cells with probe signals per total number of cells with DAPI signals. The error bars indicate standard deviations. If only one sample was analyzed in a given fraction, plain symbols without error bars are shown.
(b – i) Combined epifluorescence micrographs. CARD-FISH was applied with species-specific probes on filter sections with cells from density gradient fractions. Specific CARD-FISH signals are visible in green, DAPI-stained cells in blue. Scale bar 5 µm. (b) δ1-symbiont at density 1.147 g ml^{-1}; (c) γ3-symbiont at density 1.105 g ml^{-1}; (d) δ4-symbiont at density 1.105 g ml^{-1}; (e) γ1-symbiont at density 1.212 g ml^{-1} (the large blue ellipsoids are host nuclei); (f) spirochete at density 1.126 g ml^{-1}; (g) negative control NON338 probe against DAPI at density 1.136 g ml^{-1}; (h) same as (g), but only probe signal shown without DAPI; (i) same filter section as (g) but with positive control probe EUB338.

SI Figures

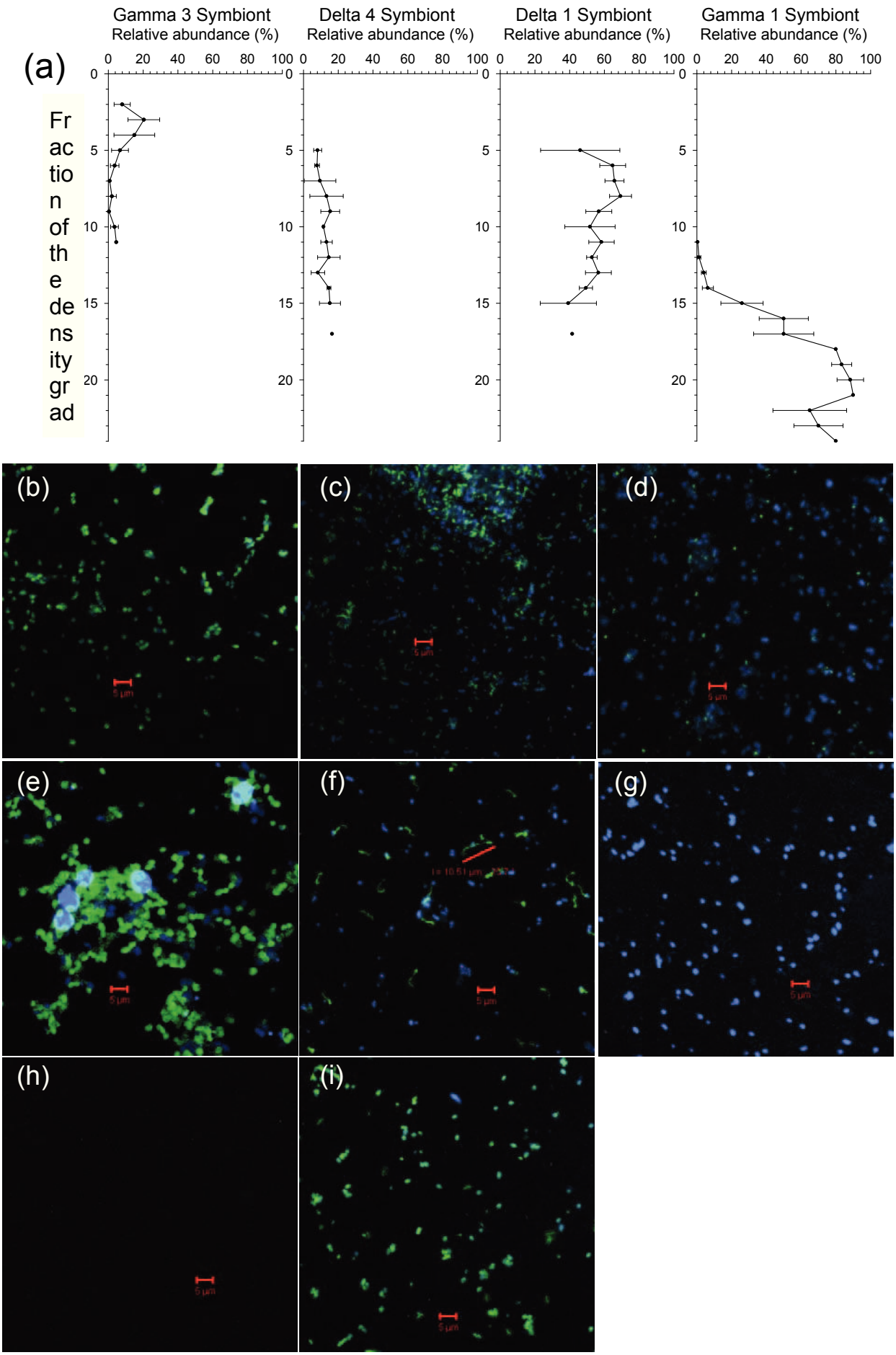
(a)
Gamma 3 Symbiont
Delta 4 Symbiont
Delta 1 Symbiont
Gamma 1 Symbiont
Relative abundance (%)
Fraction of the density grad
(b)
(c)
(d)
(e)
(f)
(g)
(h)
(i)

Fig. S2: Sulfur oxidation pathways in the γ-symbionts
(adapted from (59) and (60))

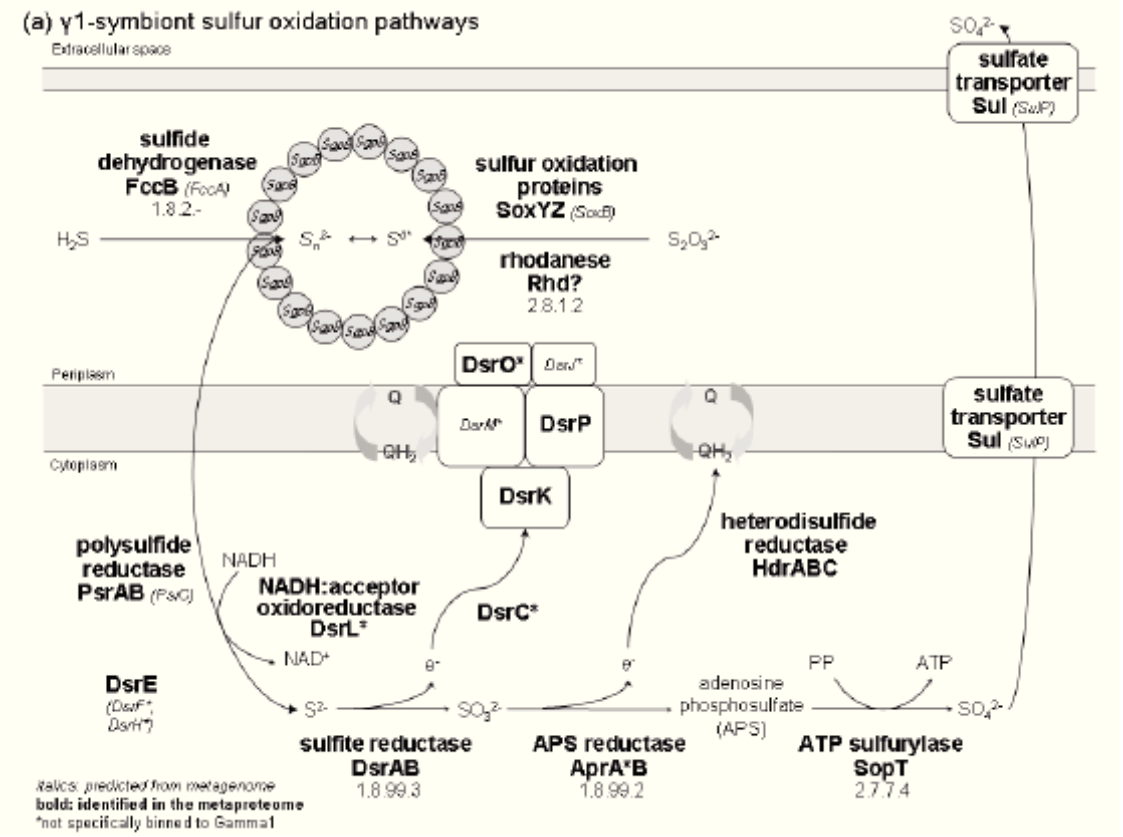

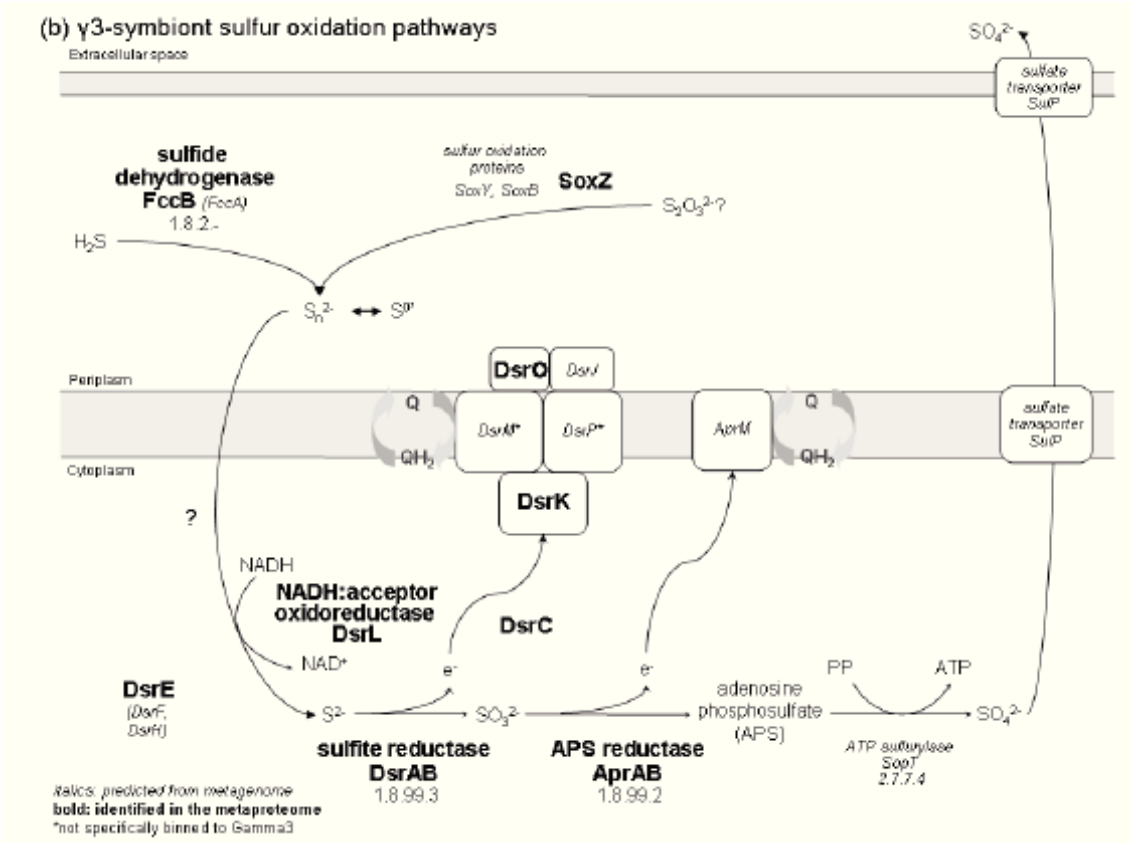
(b) γ3-symbiont sulfur oxidation pathways
Extracellular space
SO_4^{2-}
sulfate transporter SulP
sulfide dehydrogenase FccB (FccA) 1.8.2.-
H_2S
sulfur oxidation proteins SoxY, SoxB
SoxZ
$S_2O_3^{2-}$?
S_n^{2-} ↔ S^0
Periplasm
DsrO
DsrJ
Q
QH_2
DsrM*
DsrP*
AprM
Q
QH_2
sulfate transporter SulP
Cytoplasm
DsrK
?
NADH
NADH:acceptor oxidoreductase DsrL
DsrC
NAD^+
e⁻
e⁻
PP
ATP
DsrE (DsrF, DsrH)
S^{2-}
SO_3^{2-}
adenosine phosphosulfate (APS)
SO_4^{2-}
sulfite reductase DsrAB 1.8.99.3
APS reductase AprAB 1.8.99.2
ATP sulfurylase SopT 2.7.7.4
italics: predicted from metagenome
bold: identified in the metaproteome
*not specifically binned to Gamma3

Fig. S3: Reconstruction of symbiont metabolisms according to the metaproteome. Reconstruction of metabolism of δ1-symbiont (a) and γ1-symbiont (b).

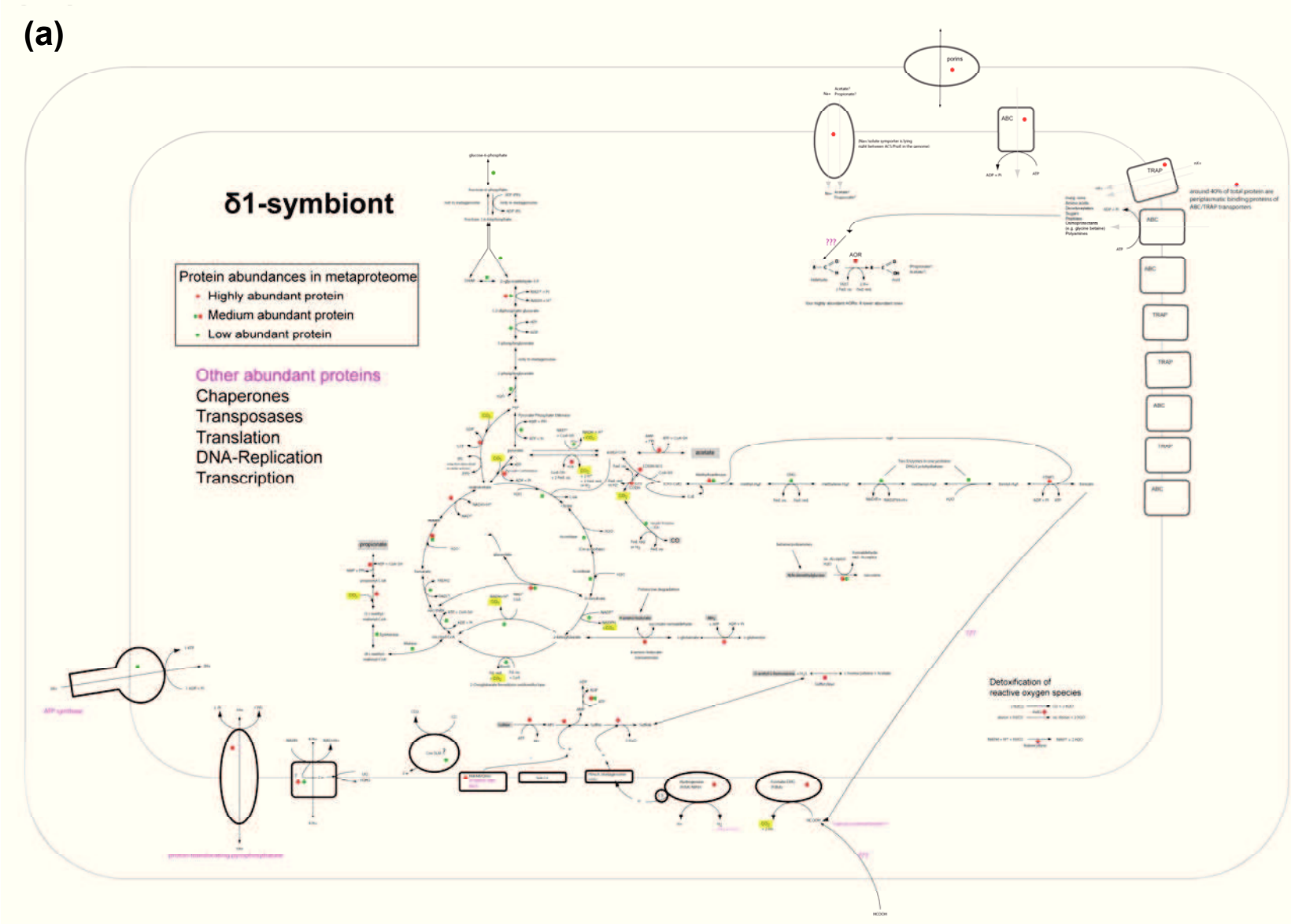

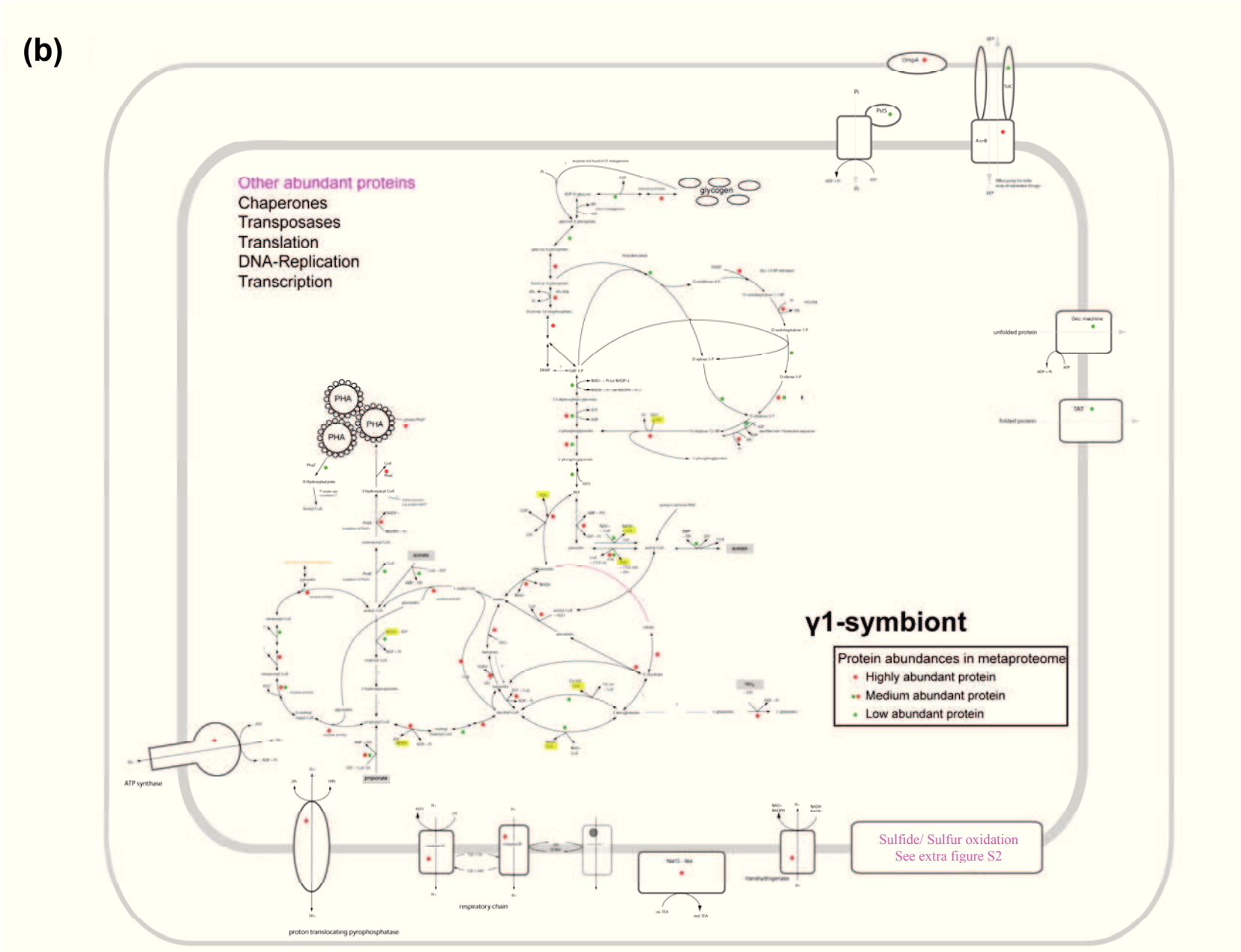
(b)
Other abundant proteins
Chaperones
Transposases
Translation
DNA-Replication
Transcription
glycogen
PHA
PHA
PHA
γ1-symbiont
Protein abundances in metaproteome
Highly abundant protein
Medium abundant protein
Low abundant protein
Sulfide/ Sulfur oxidation
See extra figure S2
ATP synthase
proton translocating pyrophosphatase
respiratory chain
unfolded protein
folded protein
TAT

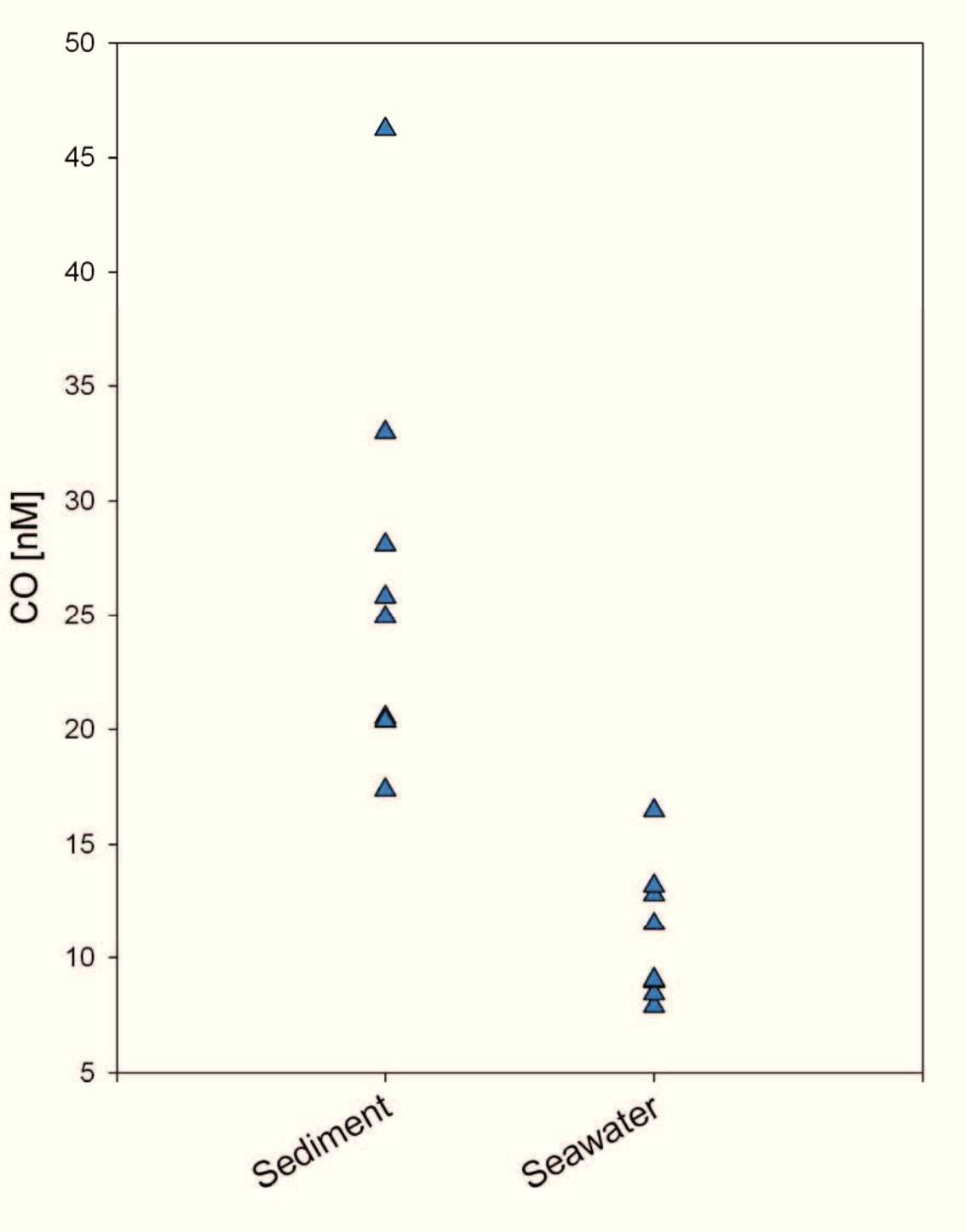

Fig. S4: Carbon monoxide concentrations in the *O. algarvensis* habitat
CO concentrations were measured in pore water samples taken from 25 cm sediment depth and in the seawater about 5 cm above the sediment (n=9). The concentrations shown here were blank corrected (see SI Materials and Methods).

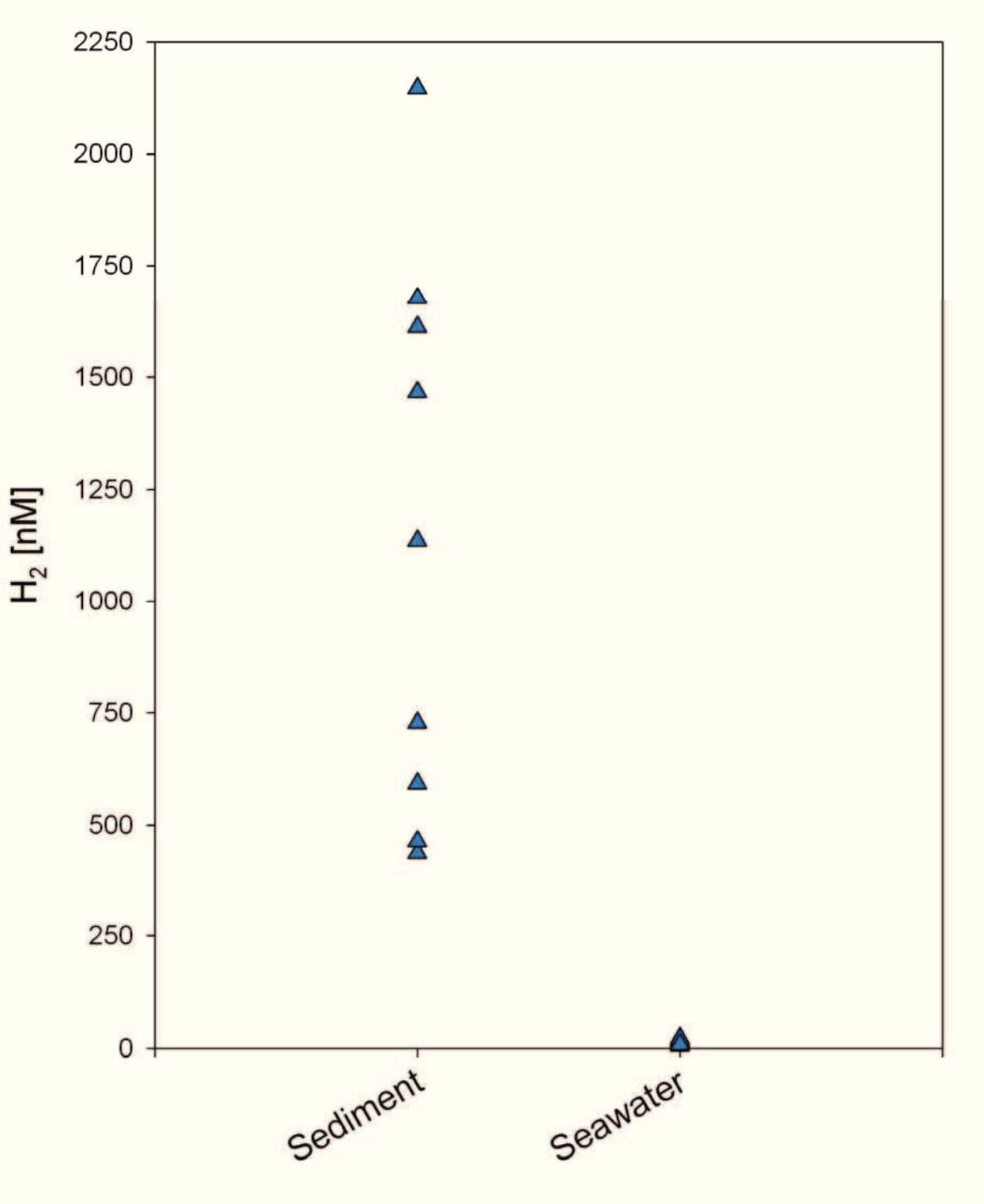

Fig. S5: Hydrogen concentrations in the *O. algarvensis* habitat
Hydrogen concentrations were measured in pore water samples taken from 25 cm sediment depth and in the seawater about 5 cm above the sediment (n=9). The concentrations shown here were blank corrected (see SI Materials and Methods).

Fig. S6: Expressed fermentation pathway used by the host under anoxic conditions

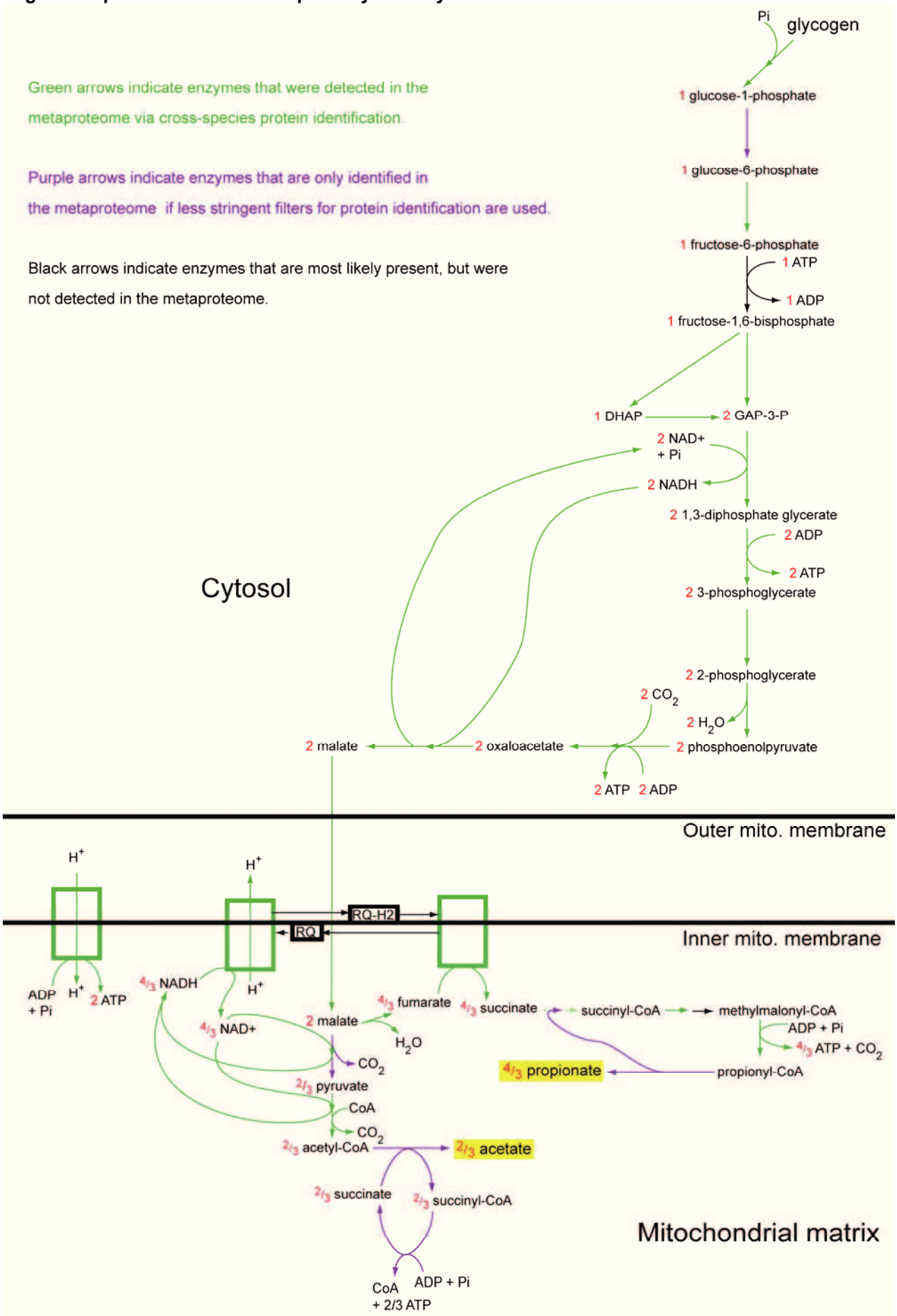

Fig. S6: Expressed fermentation pathway used by the host under anoxic conditions (see left side)
Anaerobic fermentation allows the host to gain more ATP under anoxic conditions than, for example, through simple lactic acid fermentation. The major end products of the pathway - acetate and propionate - are highlighted in yellow. These end products and some of the major intermediates (e.g. malate and succinate) can be used as substrates by the symbionts.

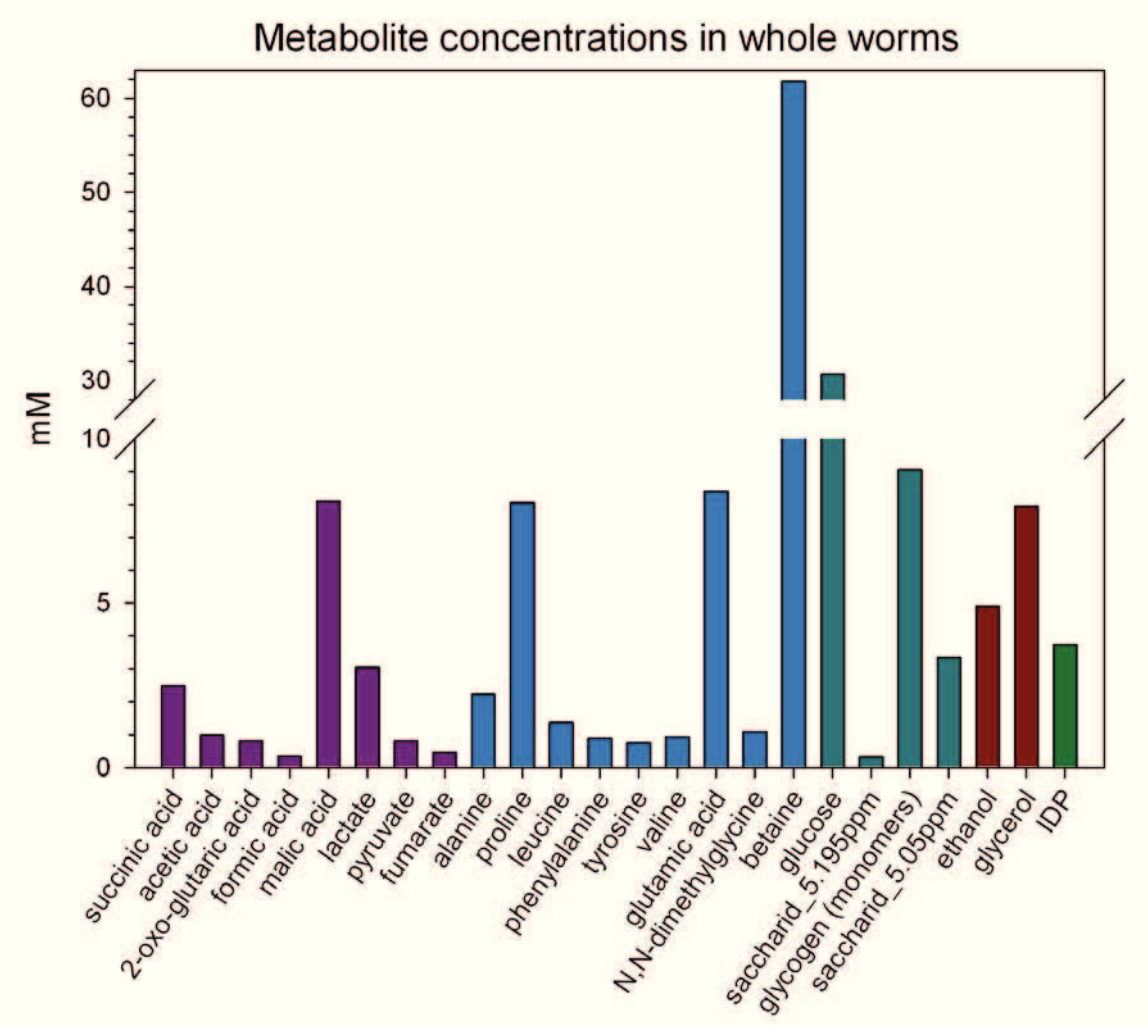

Fig. S7: Metabolite concentrations in whole worms
Concentrations were estimated based on ^{1}H-NMR data and normalized to the number of worms used for metabolite extraction. The worm volume of 1 µl was used for calculations, which is in our experience the average volume of *O. algarvensis* worms. Glycogen concentration is given as the number of glucose units that it contains.

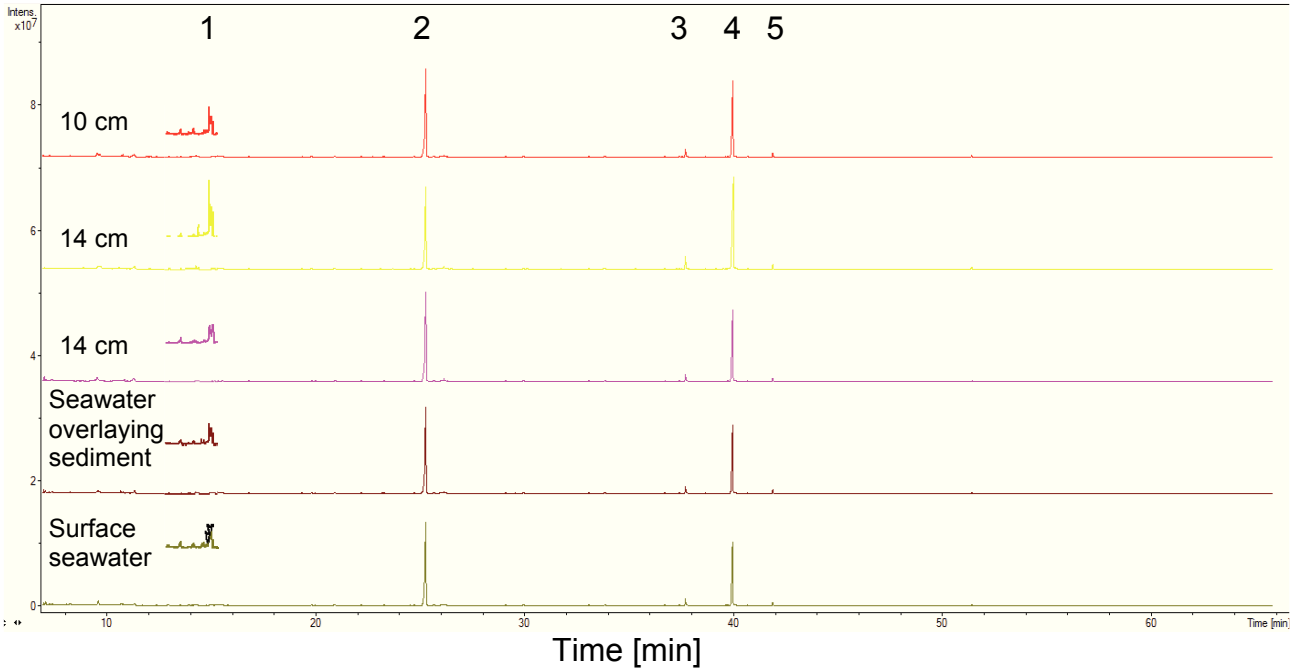

Fig. S8: Readily available organic substrates in pore water measured with GC-MS
Overlay of GC-MS chromatograms generated from pore water samples taken from different sediment depth in the *O. algarvensis* habitat. The method detects di- and tricarboxylates, amino acids and sugars down to ~10 nM concentrations. None of these metabolites were detected. The only peak present in the pore water samples, but not in the control, was derived from the softener of the reaction tubes in which the pore water was stored. Peak 1 at 14 minutes is phosphate, Peak 2 at 25 minutes is ribitol (internal standard, 0.66 nmol per sample), Peak 3 at 38 minutes softener from reaction tubes in which the samples were stored, Peak 4 at 40 minutes softener from derivatization reagent, Peak 5 at 42 minutes impurity of the derivatizing agent. Insert displays magnification of 14 min region for phosphate peak.

Other Supporting Information Files

(can be downloaded from: http://www.pnas.org/content/109/19/E1173/suppl/DCSupplemental)

Dataset S1 (XLS): All symbiont proteins identified with 2D-LC-MS/MS (gel-free) or 1D-PAGE-LC-MS/MS (gel-based) and the published symbiont metagenome

Dataset S2 (XLS): All symbiont and host proteins identified with 2D-LC-MS/MS (gel-free) or 1D-PAGE-LC-MS/MS (gel-based) and the comprehensive OlaviusV7 database

Dataset S3 (XLS): All symbiont proteins subjected to putative species assignment by proteomics binning

Dataset S4 (XLS): All transporter proteins and their putative substrates, identified with the published symbiont metagenome

Chapter 5: Carbon monoxide and hydrogen serve as alternative energy sources for a gutless worm symbiosis

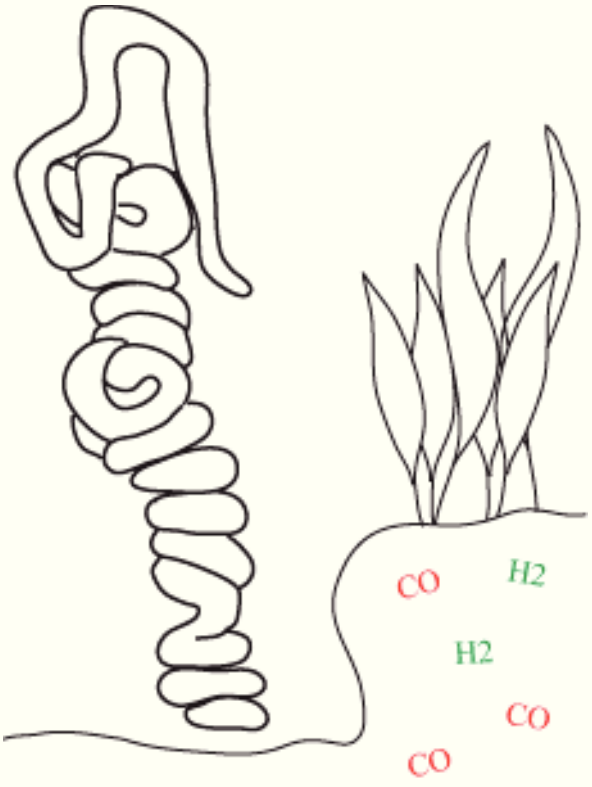

(modified after Dubilier *et al.* 2008)

Title: Carbon monoxide and hydrogen serve as alternative energy sources for a gutless worm symbiosis

Cecilia Wentrup[1#*], Manuel Kleiner[1#*], Thomas Holler[1], Gaute Lavik[1], Jens Harder[1], Christian Lott[1, 2], and Nicole Dubilier[1]

[1]Max Planck Institute for Marine Microbiology, Celsiusstrasse 1, 28359 Bremen, Germany

[2]Hydra Institute Centro Marino Elba, Via del Forno 80, 57034 Campo nel Elba (LI), Italy

[#]contributed equally

[*]corresponding authors

Email address: cwentrup@mpi-bremen.de, mkleiner@mpi-bremen.de

Key words: Carbon fixation, Gutless oligochaete, *Olavius algarvensis*,

Abstract

In chemosynthetic symbioses the symbionts supply their hosts with organic substances they have synthesized using the energy released during oxidation of reduced inorganic compounds. To date, reduced sulfur compounds and hydrogen (H_2) have been shown to be used by chemolithoautotrophic symbionts as energy sources to fix CO_2. In this study we show that in the energy poor marine sediments off Elba the symbiosis of the gutless worm *O. algarvensis* can also use H_2 and carbon monoxide (CO) as energy sources. To our knowledge this is the first study to show that CO can be used as an energy source by a chemosynthetic symbiosis to fix CO_2 and the first to show that a shallow water symbiosis consumes H_2. We measured elevated concentrations of both CO and hydrogen in the pore waters of the sediment and could clearly demonstrate that dead seagrass rhizomes are a major CO source. Relying on different energy sources for carbon fixation might be an adaptation to enhance the survival of chemosynthetic symbioses in environments that have patchy (spatial or temporarily changing) distributions of energy sources. Furthermore, CO is well recognized as an energy source for microorganisms in the water column, but it has not been previously assumed to play a role in the primary production of marine sediments. Based on our results and the large number of carbon monoxide dehydrogenases (the enzyme required for the oxidation of CO) that are present in published metagenomic and metaproteomic analyses of marine sediments, we hypothesize that CO may be an important energy source in marine sediments, particularly those with seagrass.

Introduction

Chemosynthetic symbioses have developed multiple times between a diversity of marine invertebrates and a variety of symbiotic bacterial species (Cavanaugh *et al.*, 2006; Dubilier *et al.*, 2008; Gruber-Vodicka *et al.*, 2011). The symbionts in these associations provide nutrition to the animal hosts by fixing carbon into biomass using the energy released during the oxidation of reduced inorganic compounds. Until last year reduced sulfur compounds such as sulfide and thiosulfate were the only known energy sources for CO_2 fixation by chemolithoautotrophic symbionts (Cavanaugh *et al.*, 1981; Felbeck, 1981). It was then discovered that hydrogen (H_2) could also serve as an energy source for chemolithoautotrophic symbionts (Petersen *et al.*, 2011).

Chemosynthetic symbioses occur in many different habitats from deep sea hydrothermal vents to shallow water sediments (Dubilier *et al.*, 2008). These habitats usually provide high amounts of reduced sulfur compounds that sustain chemosynthetic symbioses. In contrast, the habitat of the marine symbiotic worm *Olavius algarvensis* which inhabits the shallow water sediments of Elba (Italy) is characterized as nutrient poor and very low in sulfide concentrations (in the nM range) (Dubilier *et al.*, 2001; Kleiner *et al.*, 2012). The extraordinary feature of gutless oligochaetes like *O. algarvensis* is that they have no digestive or excretory system and instead rely on different symbionts. *O. algarvensis* relies on five different symbionts for nutritional supply and waste product recycling (Dubilier *et al.*, 2001; Giere and Erseus, 2002; Kleiner *et al.*, 2012; Ruehland *et al.*, 2008; Woyke *et al.*, 2006). It harbors two chemosynthetic sulfur-oxidizing gammaproteobacterial symbionts (γ1 and γ3), two sulfate-reducing deltaproteobacterial symbionts (δ1 and δ4) and a spirochete between its cuticle and epidermis cells (Giere and Erseus, 2002; Ruehland *et al.*, 2008). In the sulfide poor habitat of *O. algarvensis* the deltaproteobacterial symbionts are thought to provide the reduced sulfur compounds for the chemosynthetic sulfur-oxidizing symbionts (Dubilier *et al.*,

2001; Kleiner *et al.*, 2012). However, the main external energy sources for this symbiotic association have remained enigmatic until recently (Kleiner *et al.*, 2012).

In a metaproteomic study we found initial evidence that the symbionts of *O. algarvensis* might not only use reduced sulfur compounds as energy source, but also hydrogen and carbon monoxide (CO) (Kleiner *et al.*, 2012). Both the sulfur-oxidizing γ3-symbiont and the two sulfate-reducing symbionts abundantly expressed carbon monoxide dehydrogenases (CODHs) for the use of carbon monoxide as energy source. Additionally, the sulfate-reducing symbionts abundantly expressed hydrogenases for hydrogen use as an energy source. These findings were unexpected, because hydrogen concentrations that had been measured in marine sediments so far were very low (in the low nM range) (Hoehler *et al.*, 2002; Michener *et al.*, 1988; Novelli *et al.*, 1988) and CO had rarely been suggested and to our knowledge never been shown to play a role as an energy source in marine shallow water sediments (King, 2007; Martin-Cuadrado *et al.*, 2009). Preliminary measurements in the sediments inhabited by *O. algarvensis* showed elevated concentrations of H_2 and CO (Kleiner *et al.*, 2012) making it feasible that the use of both electron donors might be adaptations to life in the nutrient- and sulfide-depleted sediments of Elba and indeed fuel the *O. algarvensis* symbiosis. However, it was not shown whether the symbionts of *O. algarvensis* actually oxidize H_2 and CO and if they do, what the energy would be used for. Additionally, the distribution and source of hydrogen and CO in the sediment remained enigmatic.

In the study presented here we therefore examined if CO and H_2 are consumed by the *O. algarvensis* symbiosis and if the energy from CO and H_2 is used for autotrophic CO_2 fixation by the symbionts. Given that CO and H_2 are not known to occur in shallow water sediments in appreciable amounts our second aim was to study the distribution of CO and H_2 in the habitat of *O. algarvensis* and to find the sources of these compounds.

Material and Methods

Specimen collection and preparation for incubation

Worms were collected by SCUBA divers in October 2011 at the same site where the samples for the metagenome and metaproteome analysis of *O. algarvensis* were taken in 2004 (Woyke *et al.*, 2006) and 2007 (Kleiner *et al.*, 2012). Worms were collected from shallow water sediments (6-8 m water depth) surrounding seagrass beds of *Posidonia oceanica* in the bay off Capo di Sant' Andrea (Elba, Italy) and immediately shipped to Bremen. Gutless oligochaetes were removed from the sediment by carefully dispersing the sediment. Worms were checked under a dissecting scope and only specimens that were whole and behaved like freshly-collected worms were kept for incubation experiments. Sexually mature worms that were visibly *O. ilvae* specimens, a co-occurring less abundant gutless oligochaete species, were sorted out and not used in the experiments (Giere and Erseus, 2002).

When *O. algarvensis* is recovered from the environment its γ1-symbiont possesses lots of stored energy in form of sulfur granules (Giere and Erseus, 2002). This energy is used by the γ1-symbionts to fix massive amounts of CO_2 when exposed to oxic conditions (Bergin, 2009). To avoid that this massive CO_2 fixation with stored sulfur masks differences in CO_2 fixation between treatments in this study, we depleted the γ1-symbionts of their stored sulfur by pre-incubating all worms for a week in large glass bowls containing sterile filtered oxic sea water and a thin (0.1 mm) layer of glass beads. The water in the glass bowls was regularly mixed to ensure maximum oxygen supply for the worms and their symbionts. After this pre-incubation the symbionts had lost most of their stored sulfur as determined by the change of worm color from bright white to transparent and decreased CO_2 fixation rates in whole worms (Figure S1).

Preparation of serum bottles with artificial seawater

Suboxic artificial seawater (ASW) was prepared as follows in Widdel flasks. All chemicals were purchased from Sigma-Aldrich, Munich, Germany (final concentrations are given): 0.76 mM KBr, 8.05 mM KCl, 10 mM $CaCl_2*2H_2O$, 39.59 mM $MgCl_2*6H_2O$, 27.6 mM $MgSO_4*7H_2O$, 451.23 mM NaCl, 1mM $NaNO_3^-$, 0.467 mM NH_4Cl, 0.147 mM KH_2PO_4, 5.88 mM ^{13}C-labeled $NaHCO_3^-$, 0.024 µM $Na_2WO_4*2H_2O$, 0.023 µM $Na_2SeO_3*5H_2O$ and trace elements (for more information see Widdel and Bak, 1992).

To detect CO_2 fixation in the symbionts under our incubations we used ^{13}C-labeled bicarbonate. The pH of the ASW was adjusted to 7.5 and the salinity to 39 ‰ to match the conditions in the *O. algarvensis* habitat. Since some of the symbionts may be sensitive to high oxygen concentrations we prepared the ASW to be suboxic. For this we prepared the ASW anoxically in a Widdel flask and flushed the serum bottles with N_2 gas to remove oxygen before filling them. Oxygen concentrations were measured in the controls without worms after the incubation with an oxygen microsensor (made in the Microsensor group of the MPI for Marine Microbiology in Bremen, Germany) and found to be around 180 µM. This corresponds to 70% air saturation.

20 ml of ASW were filled into sterile 59 ml serum bottles containing a layer of a glass bead mix (2:1 (v/v); 0.75 – 1 mm (ROTH): 0.4 – 0.6 mm (B. Braun Biotech International)) to accommodate the worms. The remaining headspace was 35.5 ml. Serum bottles were closed with a gas-tight butyl rubber stopper.

CO and hydrogen consumption incubations

35 living worms were transferred into serum bottles with featherweight forceps and blotted beforehand on autoclaved blotting paper to reduce the transfer of water in which the worms were washed. Control bottles contained 35 dead worms, 5 µl of wash water (see below) or just ASW. Dead worms were killed with 4% (v/v) paraformaldehyde for 15 min at 4°C, washed

three times in ASW for 5 min and then used for incubations. Wash water was obtained from washing live worms in sterile ASW prior to the incubation experiment and was used as a control for potential free-living microorganisms detached from the worm surface or sediment particles during the washing process.

To start the incubation either 80 µl CO (purity level 3.7; Air Liquide, Düsseldorf, Germany), 80 µl hydrogen (purity level 5.0; Air Liquide, Düsseldorf, Germany) or no additional electron donor were injected into the headspace of the serum bottles. All incubation conditions were run in triplicates. Incubations took place in the shadow at 22°C for 6 days. Serum bottles were gently tilted back and forth (18x per min) on a shaker during the entire incubation to allow mixing of the gas phase with the medium and to avoid diffusion limitation. At given time points subsamples from the headspace were taken with gas-tight syringes to determine carbon monoxide and hydrogen concentrations. CO and hydrogen concentrations were measured using a gas chromatograph (Shimadzu GC-8A & 900 Series Interface PE Nelson) equipped with a molecular sieve 5A, a 80-100 Mesh-column and a mercury reduction detector (RGD2, Trace analytical) as previously described (Voordouw, 2002). Data recording and peak area integration were performed using the TotalChrom software from PerkinElmer, Inc., USA. Hydrogen and CO standards were produced from pure hydrogen (purity level 5.0; Air Liquide, Düsseldorf, Germany) and CO gas (purity level 3.7; Air Liquide, Düsseldorf, Germany) in pure nitrogen gas (purity level 5.0; Air Liquide, Düsseldorf, Germany).

Since hydrogen was consumed unexpectedly fast after a long lag time, we injected additional 80 µl hydrogen after 95.5 hours into the serum bottles containing live worms to get a better time resolution of hydrogen consumption by the *O. algarvensis* symbiosis (Figure 2). We did not inject additional hydrogen into the respective controls, because no hydrogen had been consumed in them.

CO and hydrogen consumption rates were calculated based on the whole incubation time (141 hours) for the CO incubation and for the last 17.5 hours of the hydrogen incubation. Rates

were normalized to gram wet weight of worms (the average wet weight of one worm is 0.5 mg). The molar volume of an ideal gas at 22°C (24.54 l mol^{-1}) was used to convert the partial pressure of CO and hydrogen (ppm) to the amount of the gas (in moles) in the headspace.

Incubations to investigate if CO is oxidized to CO_2 or assimilated

To investigate if CO consumption was caused by oxidation to CO_2 or by CO assimilation, we did a parallel experiment, in which unlabeled ^{12}C bicarbonate (Sigma-Aldrich) was used instead of ^{13}C-labeled bicarbonate and ^{13}CO (Sigma-Aldrich) instead of ^{12}CO. We ran four independent parallel incubations for each time point. Incubations took place in 12 ml exetainers without headspace. Each exetainer contained four worms and the incubation was started with the injection of 7 µM CO. At given time points samples were killed by addition of zinc chloride. Medium was then transferred to 6 ml exetainers (Labco, High Wycombe, UK), which were filled completely. Headspaces in the 6 ml exetainers were created by replacing 2 ml of medium with pure helium gas (purity level 5.0; Air Liquide, Düsseldorf, Germany). For outgassing of CO_2 into the headspace 0.2 ml of 85% phosphoric acid were injected into the exetainers. Samples were shaken thoroughly and stored up-side down for outgassing over night. 250 µl of the headspace were withdrawn for analysis using a gas-tight syringe, while allowing pressure compensation through the inflow of the same volume of ddH_2O from a second syringe. Samples were analyzed with a gas chromatography – isotope ratio mass spectrometer (VG Optima, Manchester, UK). Pure CO_2 (purity 4.5; Air Liquide, Düsseldorf, Germany) was used as a standard.

Bulk analysis of ^{13}C-incorporation in the incubated worms

To determine incorporation of ^{13}C-labeled bicarbonate into whole worms, 8 worms from every replicate were killed at the end of the incubation by putting them into exetainers containing 3 ml ASW and 100 µl of a 50% zinc chloride solution. Worms were washed three

times in ASW, dipped into a 0.1% HCl-solution to remove any unfixed labeled bicarbonate and washed again in ASW. Worms were filled into tin cups and their wet weight was recorded. Worms of the dead worm controls were treated the same way. Tin cups with worms were let dry over night at 70°C. Carbon isotope composition of the worms was then analyzed using an automated elemental analyzer coupled to a Delta Plus Advantage mass spectrometer as previously described (Ploug *et al.*, 2010). Caffeine was used as a standard for calibration. ^{13}C-enrichment in the worms was calculated in atom percent (AT% = (^{13}C/(^{12}C+^{13}C)*100).

Nanoscale secondary ion mass spectrometry (nanoSIMS) analysis of ^{13}C-incorporation into single symbiont cells

To determine how much ^{13}C was assimilated by each symbiont under the different conditions we analyzed the carbon isotope composition of single symbiont cells using nanoSIMS imaging (Musat *et al.*, 2012). Three worms from each treatment were homogenated after the incubation and fixed in 2% paraformaldehyde for 2 hours at 4°C. Cells were mounted onto gold-palladium coated filters with a pore size of 0.2 μm as described previously (Musat *et al.*, 2008). To identify the different symbionts we did catalyzed reporter deposition fluorescence *in situ* hybridizations (CARD-FISH) (Pernthaler *et al.*, 2002) using the general bacterial probe EUB338 (Daims *et al.*, 1999), the general gammaproteobacterial probe GAM42a (Manz *et al.*, 1996) and the γ3-symbiont specific probe (Ruehland *et al.*, 2008). Epi-fluorescent images of the hybridized symbionts on the filters were taken before nanoSIMS analysis and spots of interest were marked using a laser micro-dissecting microscope (LMD, Leica, Germany) to facilitate their localization during nanoSIMS analysis (Polerecky *et al.*, 2012). Fluorescent signals of the symbiont cells were processed by blind deconvolution in AutoQuant (Media Cybernetics, Bethesda, USA). Symbionts were distinguished based on probe signal and their known size and morphology (Giere and Erseus, 2002; Ruehland *et al.*, 2008).

For the nanoSIMS analysis, filters containing the fluorescently labeled cells were cut with a round stencil (Ø5 mm) and mounted onto a sample holder. The analysis was performed using a nanoSIMS 50 L manufactured by Cameca (Gennevilliers, France). We recorded secondary ion images of ^{12}C, ^{13}C, $^{12}C^{14}N$, ^{31}P, and ^{32}S using five electron multipliers in parallel. For each treatment we analyzed symbiont cells from three worms and recorded images from at least 30 single cells per symbiont and treatment (Table 1). An exception were the γ3-symbionts from the H_2 incubation out of which we analyzed 19 cells of two worms (Table 1).

Image and data processing were performed using the Look@NanoSIMS software (Polerecky *et al.*, 2012). ^{13}C-enrichment of single symbiont cells was calculated as atom percent (AT% = (^{13}C/(^{12}C+^{13}C)*100). For comparison of ^{13}C-enrichment in specific symbiont species between different treatments homogeneity of variance was tested using the Levene's test. Depending on the outcome of the Levene's test, significant differences between means were tested using either the ANOVA test or the Kruskal-Wallis test implemented in Look@NanoSIMS (Polerecky *et al.*, 2012).

Measurement of CO and H_2 concentrations in the worms' habitat

Sediment pore waters and seawater above the sediment were collected at the worm collection site (see above) by research divers and measured as previously described (Kleiner *et al.*, 2012). Pore water was extracted with porous hydrophilic polymer tubes with 0.1 μm pore size (RHIZON ® MOM 10 cm soil water samplers, F. Meijboom, Wageningen, NL) attached to plastic syringes of 10 ml from 15 and 25 cm sediment depth as well as to the deeper lying sediment layers containing dead seagrass rhizomes. 9 profiles within an area of approx. 100 m^2 were sampled. Seawater samples were collected ~5 cm above the sediment surface.

Blanks with ddH_2O were created accordingly to determine potential contamination with CO and hydrogen introduced during sample processing (e.g. through contact with atmosphere, sampling vials, nitrogen gas and reagents during sample processing). Eight blanks were

measured. CO concentrations in blanks were 2.1 to 3.9 nM and hydrogen concentrations in blanks were 10.7 to 29.2 nM. Pore water and seawater concentrations were blank-corrected with average CO (3.1 nM) and hydrogen (21.5 nM) blank concentrations. Concentrations reported throughout this article are blank-corrected.

Measuring CO and H_2 production in the *O. algarvenis* habitat

The shallow water habitat of *O. algarvensis* is characterized by sandy silicate sediment surrounding small patches of seagrass beds of *P. oceanica* (Figure 1). Seagrass is known to form rhizomes, horizontal stems that anchor the plant to the sediment and store carbohydrates (Alcoverro *et al.*, 2001).

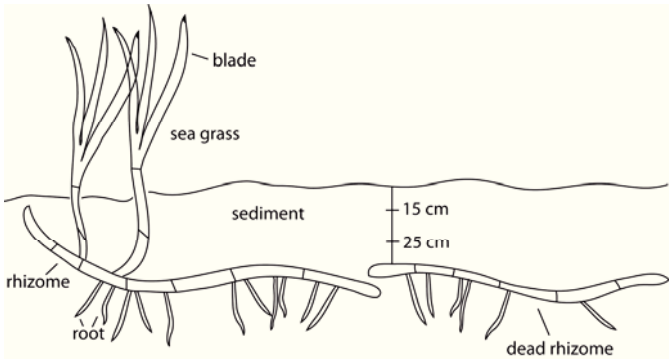

Figure 1: Layout of *P. oceanica* seagrass in sediment with rhizome anchoring the plant to the sediment and dead rhizome buried in the sediment. Depth profile of 15 and 25 cm are not to scale.

These rhizomes form a dense and robust mesh in the sediment and they are left behind in the sediment after the seagrass dies off. Because rhizomes are hard to degrade they are still found in the sediment years after the seagrass dies off. In the bay off Capo di Sant' Andrea dead seagrass rhizomes can be found in the entire bay buried underneath the sandy sediment.

To find the source of carbon monoxide and hydrogen in the Elba sediments we incubated different components from the *O. algarvenis* habitat. We collected dead rhizome, sediment and seawater from six different spots within the worm collection site (see above). From each spot 70 to 100 g wet rhizome, 250 ml sediment or unfiltered seawater were incubated in duplicates in 500 ml Schott bottles closed with caps containing pierceable rubber septa. Bottles with ddH_2O were used as controls. Rhizomes and sediment were covered with sterile filtered seawater (add 500 ml). To distinguish biotic from abiotic CO and H_2 production, samples were either incubated in their native state or alternatively killed with zinc chloride

($ZnCl_2$). The pH was adjusted to the pH of the native seawater (pH 7.7-7.8) in zinc chloride killed samples. A headspace was created by removing 20 ml seawater with one syringe and simultaneously allowing pressure compensation by inflow of air through a second needle. Bottles were incubated in a water bath set to 23°C for several hours in the dark to avoid photochemical CO production (King and Weber, 2007). To check whether killing of the samples with $ZnCl_2$ influenced CO and H_2 production we did a parallel experiment in which samples were killed by boiling them for 30 minutes instead of adding $ZnCl_2$.

Ten minutes before measuring hydrogen and CO concentrations in the headspace, bottles were shaken thoroughly to allow produced hydrogen and CO gas to accumulate in the headspace. Hydrogen and CO concentrations were measured using the RGA3 reduction gas analyzer as described previously (Kleiner *et al.*, 2012). Rhizome samples and sediment samples were washed and dried after the incubation to determine their dry weight.

Results

The *O. algarvensis* symbiosis consumes CO and H_2

CO consumption in living worms began almost immediately and CO concentrations in the headspace decreased linearly ($R^2 = 0.9675$) from 3038 ppm to 789 ppm during the 141 hours of incubation (Figure 2a). The mean CO consumption rate of *O. algarvensis* was 1.3 μmol h^{-1} g^{-1} (Figure 2a). In our parallel incubation experiment ^{13}C-labled CO was almost completely oxidized to CO_2 within 62 hours (Figure 3).

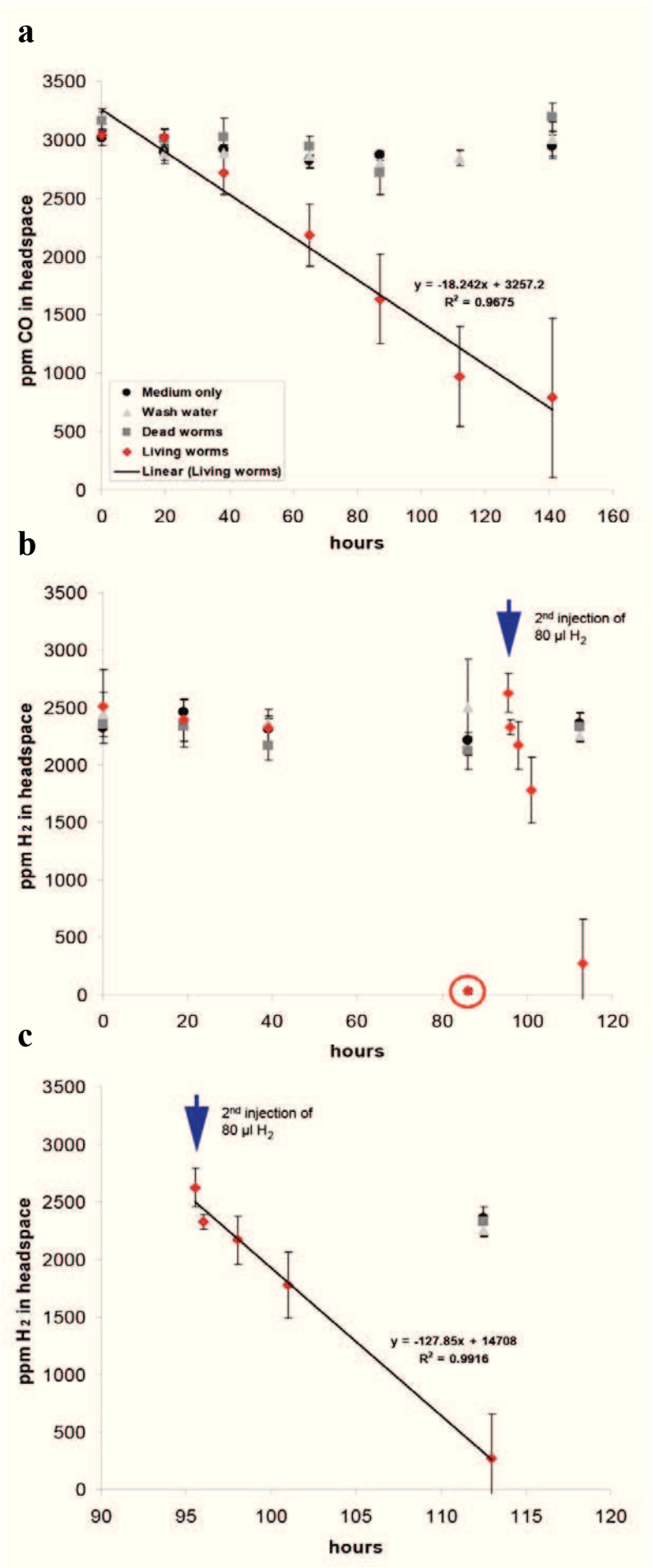

Figure 2: Carbon monoxide and hydrogen consumption by the *O. algarvensis* symbiosis over time. Mean values and standard deviations of three independent incubation bottles are plotted for each control and treatment. a) CO consumption by living *O. algarvensis* was linear over time. b) Hydrogen consumption of living worms started with a delay of at least 40 hours and H_2 was completely consumed after 86 hours (encircled in red) in all three replicates (the minimal standard deviation at this time point is not visible in this figure). A second injection of 80 µl H_2 to the incubation bottles with the living worms was monitored in shorter intervals and revealed a linear consumption of hydrogen. c) Close up of b) after second hydrogen injection.

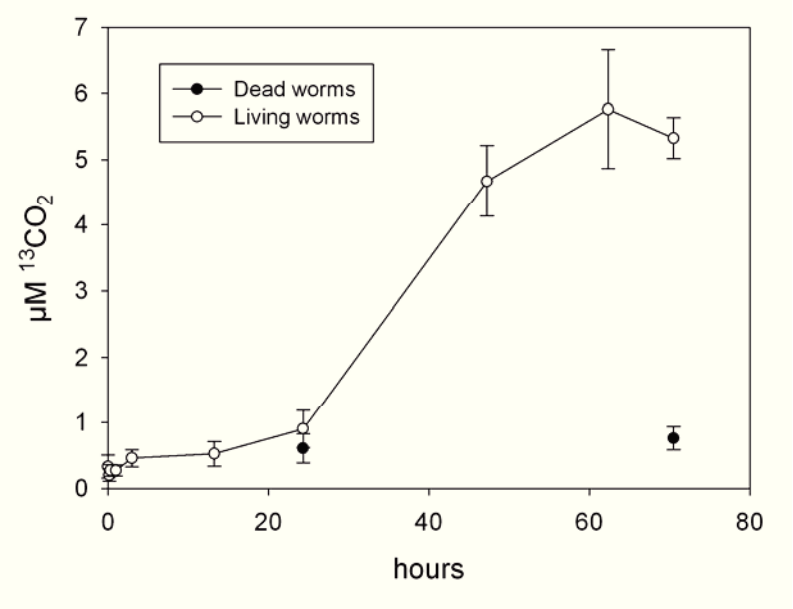

Figure 3: Conversion of ^{13}CO to $^{13}CO_2$. Mean values and standard deviations of four independent incubation bottles are plotted for the treatment and control. ^{13}C-labeled CO was oxidized to ^{13}C-labeled CO_2 over time.

In contrast, strong hydrogen consumption in the headspace of living worm incubations only started after at least 40 hours (Figure 2b). However, after this long lag phase hydrogen consumption set in with a high rate and hydrogen was completely consumed after 86 hours (decrease from 2509 ppm to 33 ppm; Figure 2b). Therefore we injected additional hydrogen into the running incubation (t = 95.5 hours) to follow hydrogen consumption over time. Hydrogen decreased from 2626 ppm to 271 ppm within 17.5 hours in a linear fashion (R^2 = 0.9916; Figure 2c). The mean hydrogen consumption rate of the *O. algarvensis* symbiosis was 10.97 µmol h^{-1} g^{-1}. In all controls there was no notable consumption of CO or hydrogen over time (Figure 2).

CO_2 incorporation in whole worms did not differ from controls

Combustion of whole worms after the incubation with ^{13}C-labeled bicarbonate and CO, hydrogen, and no added energy source revealed that live worms had incorporated ^{13}C in contrast to the dead worm controls, which only contained natural abundances of ^{13}C (Table 1). However, no significant difference in the ^{13}C-content of the living worms was found between the three treatments (^{13}C-labeled bicarbonate and CO, hydrogen, and no added energy source) (Table 1).

The γ3-symbiont fixes significantly more CO_2 when CO is present

Since our analyses of whole worms did not reveal differences in ^{13}C-incorporation between the three treatments, we analyzed the symbionts at the single cell level using the nanoSIMS. This was done to detect potentially increased CO_2 fixation into specific symbionts, which could have been masked by overall CO_2 fixation in the whole worm analyses. We found that all *O. algarvensis* symbionts except the δ4-symbiont had incorporated ^{13}C under all incubation conditions (Table 1). The δ4-symbiont only showed ^{13}C-incorporation in the incubations without any added e^--donor.

Table 1: ^{13}C-enrichment of entire worms and single symbiont cells. Mean ^{13}C-content of samples are given in AT%. For whole worms the minimum and maximum values are given in parentheses. For the single cells the means for the three independent replicate worms are given in parentheses.

	$^{13}CO_2$ + CO	**$^{13}CO_2$ + H_2**	**$^{13}CO_2$ w/o e^--donor**
Bulk whole worms (alive)	1.28 (1.27 – 1.30) n=3	1.29 (1.26 – 1.33) n=3	1.3 (1.26 – 1.36) n=3
Bulk whole worms (dead)	1.072 (1.067 – 1.073) n=9		
^{13}C in γ1-symbiont	1.168 (1.26, 1.192, 1.065) n=30	1.107 (1.077, 1.13, 1.098) n=39	1.161 (1.222, 1.181, 1.08) n=39
^{13}C in γ3-symbiont	1.982 (1.399, 1.915, 2.589)* n=31	1.234 (0.992, 1.918)[a] n=19	1.179 (1.207, 1.355, 1.056) n=44
^{13}C in δ1-symbiont	1.405 (1.437, 1.476, 1.343) n=75	1.34 (1.193, 1.49, 1.2) n=45	1.377 (1.376, 1.32, 1.516) n=35
^{13}C in δ4-symbiont	1.028 (1.041, 1.008, 1.044)* n=78	1.073 (1.112, 1.054, 1.049)* n=40	1.342 (1.389, 1.436, 1.127) n=28

AT%: atom percent ($^{13}C/(^{12}C+^{13}C)*100$)
w/o e^--donor: without electron donor in the medium
n: total number of bulk worm samples (8worms each) or single symbiont cells analyzed
*: statistically significant values
a: γ3-symbiont cells only analyzed in two worms

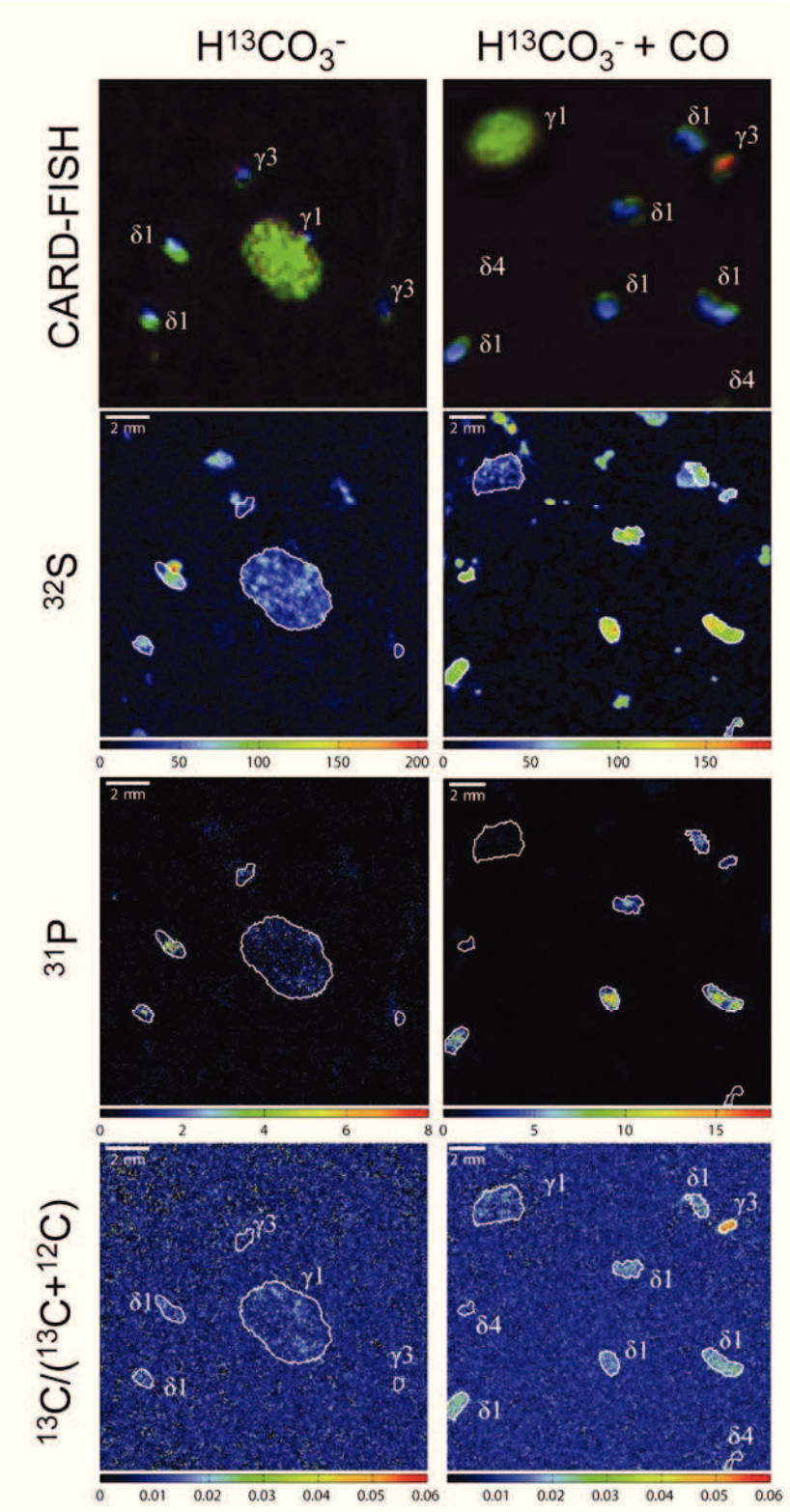

Figure 4: Increased ^{13}C-inorganic carbon uptake by the γ3-symbiont of *O. algarvensis* in the presence of CO. The left and right image columns show an epifluorescence micrographs of *O. algarvensis* symbionts on a filter in the top image, and then the three corresponding nanoSIMS images for elemental sulfur (^{32}S) and phosphorus (^{31}P) as well as the ratio of ^{13}C to ^{12}C (^{13}C/(^{13}C+^{12}C)). In the epifluorescence images symbiont cells hybridized with the general eubacterial probe (EUB338I-III) are green. The sulfur-oxidizing symbionts targeted by the gammaproteo-bacterial probe (Gam42a) are red. The strong green fluorescence signal of the EUBI-III probe masks the red fluorescence signal of the Gam42a probe in the γ1-symbiont. DAPI stain shows all cells in blue.

Statistical analyses revealed significant differences in ^{13}C-incorporation: (1) The γ3-symbiont incorporated significantly more ^{13}C-labeled bicarbonate in the presence of CO as an electron donor than without (Kruskal-Wallis, p = 7.69e-08). (2) The δ4-symbiont incorporated significantly less ^{13}C-labeled bicarbonate in the presence of CO compared to the incubation without an added e^--donor (Kruskal-Wallis, p = 4.20e-08). (3) The δ4-symbiont incorporated significantly less ^{13}C-labeled bicarbonate in the presence of H_2 compared to the incubation without an added e^--donor (Kruskal-Wallis, p = 1.76e-04). We did not find significant differences in the ^{13}C-enrichment of the γ1- and δ1-symbionts between treatments. We were unable to measure sufficient numbers of the spirochetal symbiont for statistical analyses. This symbiont is only 100-200 nm thick and it is therefore almost impossible to acquire enough image data with the nanoSIMS before the cell is completely sputtered away by the primary ion beam.

Elevated CO and H_2 concentrations in the marine sediments inhabited by *O. algarvensis*

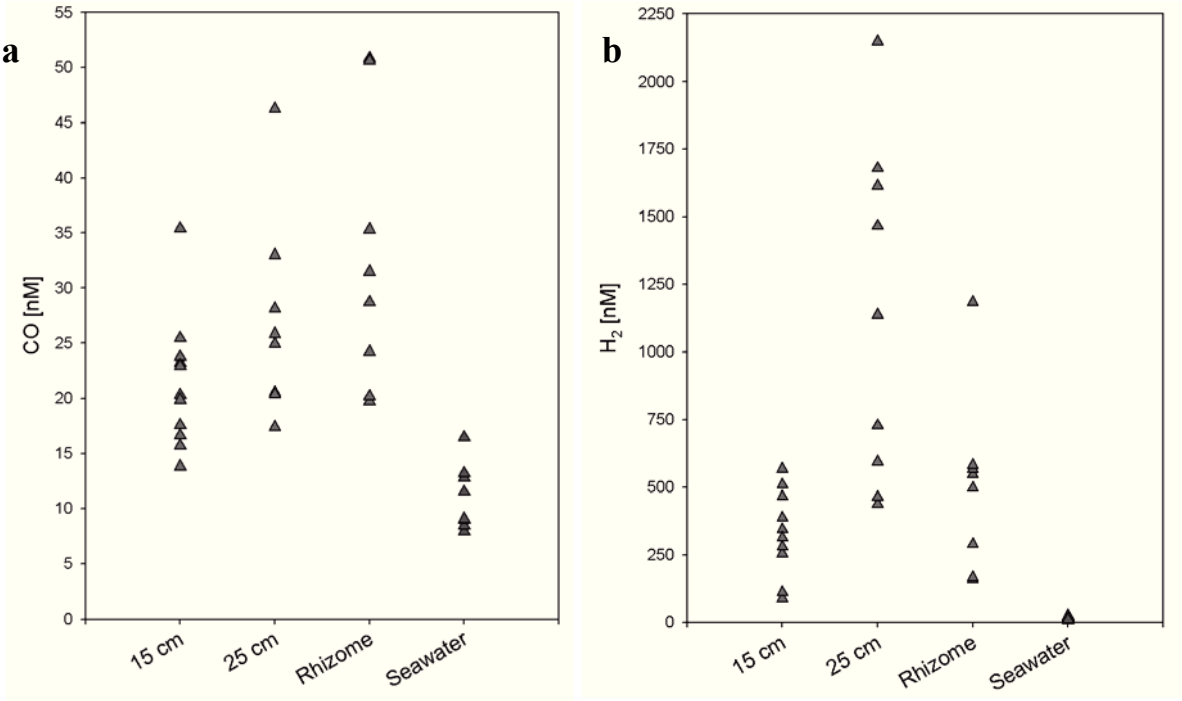

Figure 5: Blank corrected (a) CO and (b) H_2 concentrations in the marine sediment inhabited by *O. algarvensis*. Concentrations were determined at 15 and 25 cm sediment depth, in the dead rhizome material underneath the sandy sediment, and in the seawater right above the sediment. For each sediment depth or control we measured CO and H_2 concentrations in at least 8 independent samples.

CO and H_2 concentrations in the sediment pore water were much higher than in the seawater above the sediment (Figure 5). The CO concentration in the sediment (17-51 nM) was approximately double the seawater concentration (8-16 nM), with the highest CO concentrations detected in the dead rhizome material underneath the sandy sediment (Figure 5). The H_2 concentration in the sediment (89-2147 nM) was at least one hundred fold higher than the seawater concentration, which was close to zero. In contrast to CO the highest H_2 concentrations were measured at 25 cm sediment depth.

Table 2: Carbon monoxide release by different sediment components and ddH_2O controls in $nmol*day^{-1}*kg^{-1}$ (or l^{-1})

	Living material	**Killed with $ZnCl_2$**
Rhizome (dry weight)	333 – 17,460	3,640 – 55,596*
Seawater (liters)	1 – 40	9 – 11
Sediment (dry weight)	0.1 – 3.3	0.6 – 2.2
ddH_2O (liters)	11 – 18	14 – 18

$n \geq 3$

*We obtained similar values for incubations with rhizome that had been boiled for 30 min to kill all biological activity (data not shown).

Dead seagrass rhizomes are a major source of CO

The dead rhizome material from the *O. algarvensis* habitat released large amounts of CO, whereas both seawater and the sandy sediment only produced minor amounts (Table 2). The seawater and sediment values were comparable to the amount of CO released in the ddH_2O controls (Table 2). We recorded the highest CO release for dead rhizome material when the biological activity in the incubation was killed by addition of $ZnCl_2$ or by boiling (Table 2). Under these conditions one kg of rhizome produced between 3,640 – 55,596 nmol CO per day. We did not measure increased hydrogen production by any of the sediment compounds.

Discussion

CO as alternative energy source for the *O. algarvensis* symbiosis

The CO oxidation rate determined for the *O. algarvensis* symbiosis (1.3 μmol h^{-1} g^{-1} (wet weight of worm)) was in the same range as those measured in cultivated CO oxidizers. CO consumption rates of CO-oxidizing isolates from coastal seawater range between 0.015 and 0.46 μmol h^{-1} g^{-1} (cell weight) at a cell weight of 1 pg (Tolli *et al.*, 2006). In known carboxydotrophic microorganisms that can grow at elevated CO concentrations (> 10%) CO consumption rates are higher and between 0.8 μmol and 18 mmol h^{-1} g^{-1} (cell weight) (Cypionka *et al.*, 1980; Diekert and Thauer, 1978; Tolli *et al.*, 2006). The *O. algarvensis* symbiosis consumed CO faster than free-living microorganisms from coastal seawater, but slower than most carboxydotrophic organisms. However, since the CO-oxidizing symbionts make up only a small proportion of the *O. algarvensis* symbiosis and because we do not know exactly how much which symbiont (γ3-, δ1- and δ4-symbiont, see below) consumed, it is difficult to compare the consumption rates per weight of cultivated microorganisms with the one of *O. algarvensis* encompassing five symbionts and one animal host on an absolute level. Our data further showed that CO was consumed by the worm symbiosis down to very low concentrations (down to 16 ppm in one replicate). Since the consumption rate of CO was linear until the end of the incubation (Figure 2a) it is likely that the *O. algarvensis* symbiosis would have consumed CO even further. Concentrations of 10-100 ppm have been used successfully to incubate and isolate environmental CO oxidizers from soils and seawater (Hardy and King, 2001; Hendrickson and Kubiseski, 1991; King, 2007; Weber and King, 2010). In these studies the organisms were hypothesized to have a high-affinity CO-uptake system in contrast to carboxydotrophic microorganisms that tolerate and use much higher CO concentrations (up to 100%). The symbiosis of *O. algarvensis* therefore appears to have at least one symbiont with a high affinity CO-uptake system.

Use of CO by the γ3- and deltaproteobacterial symbionts of *O. algarvensis*

In the metaproteomic study of the *O. algarvensis* symbionts, three of the symbionts expressed CODHs necessary for CO oxidation (Kleiner *et al.*, 2012). The γ3-symbiont expressed an aerobic CODH that can be used with O_2 or nitrate as an electron acceptor to oxidize CO. Aerobic CO-oxidizers can use CO as an energy source to fix CO_2 into biomass typically by using the Calvin-Benson-Bassham (CBB) cycle (reviewed in King and Weber, 2007). Alternatively, they can use CO as a supplementary energy source for maintenance and survival that does not contribute directly to biomass (King and Weber, 2007). The deltaproteobacterial symbionts (δ1 and δ4), on the other hand, expressed anaerobic CO dehydrogenases (Kleiner *et al.*, 2012). In sulfate-reducing bacteria the oxidation of CO can be coupled to the reduction of sulfate to sulfide as well as the formation of acetate or molecular hydrogen (King and Weber, 2007; Oelgeschlager and Rother, 2008; Rabus *et al.*, 2006). Hydrogen can then be used for sulfate reduction (Rabus *et al.*, 2006). Since one of the major functions of the symbionts of *O. algarvensis* is to provide the host with nutrition we focused on the possible CO_2 fixation with CO as the energy source in the γ3- and deltaproteobacterial symbionts.

We could clearly demonstrate that the γ3-symbionts incorporated significantly more labeled CO_2 with CO as external energy source than without (Table 1). This strongly indicates that the γ3-symbionts used their CODH to oxidize CO to CO_2 and that they used at least some of the yielded energy to fix CO_2 via their CBB cycle.

The δ1-symbionts, on the other hand, did not incorporate significantly higher amounts of the labeled bicarbonate with CO as an external energy source than without. This indicates that CO was not used as an energy source to increase autotrophic CO_2 fixation in the δ1-symbionts under the incubation conditions used in this study. The δ4-symbionts incorporated even significantly less of the labeled bicarbonate with CO as electron donor than without. This could have had different reasons. Firstly, the isotopic composition of the CO that we used was

lighter (1.055 Atom%-^{13}C) in comparison to natural abundance (1.109 Atom%-^{13}C) (personal communication with Air Liquide). If CO was directly incorporated into the biomass of the δ4-symbionts via the acetyl-CoA pathway, this could have led to the observed increase in lighter cell carbon in the δ4-symbionts. Secondly, the δ4-symbionts could have used metabolic pathways that favor isotopic fractionation of carbon as has been shown for lithotrophic and heterotrophic growth in other sulfate-reducing bacteria (Goevert and Conrad, 2008; Londry and Marais, 2003). A third explanation that the δ4-symbionts were inhibited directly by the CO concentrations used in this study or indirectly by metabolic interactions with the other co-occurring symbionts is unlikely, because this would not explain why their cell carbon (on average 1.028 AT%, Table 1) was isotopically lighter in comparison to the natural ^{13}C abundance in dead worms (on average 1.072 AT%, Table 1).

H_2 as alternative energy source for the *O. algarvensis* symbiosis

Similar to CO we could also clearly demonstrate that hydrogen was consumed by the *O. algarvensis* symbiosis. However, in contrast to CO, this consumption did not occur until after a lag phase of almost two days (Figure 2b-c). The expression of hydrogenase is generally only induced in the presence of hydrogen in hydrogen-oxidizing microorganisms and negatively regulated by molecular oxygen (reviewed in Vignais and Billoud, 2007). Since we pre-incubated the worms under oxic conditions without hydrogen for several days it is likely that the symbionts did not have substantial amounts of hydrogenase at the beginning of the incubation. Furthermore, the elevated oxygen concentration at the beginning of the incubation might have initially repressed hydrogenase expression despite the fact that H_2 was present. Oxygen consumption by the worm and the sulfur-oxidizing symbionts would have led to lower oxygen concentrations in the medium in the course of the incubation. By the end of the incubation, oxygen concentrations had indeed dropped to 57% atmospheric saturation. The

decrease in oxygen could therefore have allowed for the induction of hydrogenase expression in the deltaproteobacterial symbionts.

In recent incubation experiments with chemosynthetic symbionts of the deep-sea hydrothermal vent mussel *Bathymodiolus*, the hydrogen consumption rate of gill tissue containing symbionts was determined to be ~ 3 μmol h^{-1} g^{-1} (wet weight of gill tissue) when using a similar initial H_2 concentration (1800 ppm) (Petersen *et al.*, 2011) as in this study. The consumption rate obtained for the gutless worm symbiosis (10.97 μmol h^{-1} g^{-1} (wet weight of worm)) in this study was higher than the one for the chemosynthetic symbionts of *Bathymodiolus* (Petersen *et al.*, 2011). However, the rates of the *Bathymodiolus* symbionts are likely to have been underestimated, because (1) in the Petersen et al. study the symbionts were incubated on board under normal pressure at sea level in contrast to the much higher pressures they usually experience in their habitat at 3000 m water depth and because (2) they were incubated with H_2 concentrations up to 30 times lower than the H_2 concentrations available in their environment. Since H_2 uptake was shown to be stimulated by increasing hydrogen concentrations in the sulfur-oxidizing symbionts of *Bathymodiolus* (Petersen *et al.*, 2011), higher hydrogen concentrations in the medium would likely have led to even higher consumption rates in these symbionts. On the other hand, the number of symbionts per gram weight is higher in the gill tissue of *Bathymodiolus* than it is in *O. algarvensis* (personal observation). The H_2 consumption rates of both the gutless oligochaete symbiosis and the *Bathymodiolus* symbiosis might thus be comparable.

Similar to carbon monoxide, H_2 was also consumed down to very low concentrations (9 ppm which roughly corresponds to 7.5 nM in solution, Figure 2b), indicating that the *O. algarvensis* symbionts can also use very low H_2 concentrations. This is in agreement with our previous metaproteome study in which we showed that the expressed uptake hydrogenases of the deltaproteobacterial symbionts are high-affinity hydrogenases (Kleiner *et al.*, 2012). The sulfate-reducing symbionts are the only symbionts in *O. algarvensis* known to have

hydrogenases based on the metagenomic (Woyke *et al.*, 2006) and metaproteomic study (Kleiner *et al.*, 2012). In sulfate reducers H_2 can be used to reduce sulfate, to gain energy through hydrogenases and to fix CO_2 heterotrophically with acetate or autotrophically via the acetyl-CoA-pathway (reviewed in Rabus *et al.*, 2006). As for CO we were again mainly interested in the possible CO_2 fixation, because the main function of the symbionts is to feed their host.

The sulfate-reducing symbiont of *O. algarvensis* did not show an increased incorporation of labeled bicarbonate in incubations with H_2 compared to ones without hydrogen (Table 1). This indicates that hydrogen was not used as an energy source to increase autotrophic CO_2 fixation in the deltaproteobacterial symbionts under the incubation conditions used here. Alternatively, hydrogen consumption could have fueled the symbiosis of *O. algarvensis* indirectly. Hydrogen could have been oxidized and coupled to the reduction of sulfate to sulfide, which could have been used by the sulfide-oxidizing symbionts of *O. algarvensis* to fix CO_2 chemoautotrophically (Bergin, 2009) or to store elemental sulfur intracellulary, which is known to occur in the environment (Giere and Erseus, 2002). We did not find sound evidence for either hypothesis: the sulfide-oxidizing symbionts did not incorporated more ^{13}C with hydrogen than without (Table 1) and we did not observe an increase of sulfur globules in the γ1-symbionts (data not shown). A third hypothesis is that hydrogen was not used by the deltaproteobacterial symbionts at all, but by one of the other symbionts. However, this would still not answer the question what hydrogen was used for as we did not observe additional CO_2 incorporation in any symbiont incubated with hydrogen in comparison to symbionts incubated without hydrogen. In summary we could show that hydrogen was consumed by the symbiosis of *O. algarvensis*, but it remains elusive for what it was used for.

CO and H_2 as energy sources in marine sediments

We found elevated concentrations of CO and H_2 (Figure 5) in the pore waters of the habitat of *O. algarvensis*, which would be high enough to sustain free-living marine CO-oxidizers (Conrad *et al.*, 1981; King and Weber, 2007; Moran *et al.*, 2004) as well as free-living and symbiotic H_2-oxidizers (Karadagli and Rittmann, 2007; Petersen *et al.*, 2011). We found a major source of CO in the sediments of Elba by incubating different sediment components under biotic and abiotic conditions. Dead seagrass rhizome produced large amounts of CO. Comparison of CO production of living material with killed material indicated that CO production occurred abiotically, as it was much higher in killed samples. This is in agreement with a previous study that showed that CO was formed abiotically from decaying organic plant matter in soils (Conrad and Seiler, 1985). In this study the authors hypothesized that CO might be formed via a radical reaction with oxygen, because CO production rates were 10 times higher when incubated with oxygen than with nitrogen. The same might have happened in our incubations. However, under natural conditions in the sediments of Elba CO formation would have to occur under anaerobic conditions, because oxygen is consumed completely within the top few mm of the sediment (C. Lott, unpublished data). Polystyrene is known to produce CO under such conditions and thus polystyrene-like compounds of seagrass could produce CO in the anaerobic sediment layers of Elba (personal communication Prof. R. Thauer). Further studies are needed to verify this hypothesis.

The high CO production of dead seagrass rhizome (up to 55,596 nmol CO per kg and day, Table 2) would enable a significant amount of primary production. To give some rough numbers: estimating that 10 kg (dry weight) of rhizome underlie 1 m² of sediment in the bay of Sant' Andrea about 560 µmol CO would be produced per day. If this amount of CO is oxidized with nitrate (ΔG = -86.1 kJ mol^{-1}) (Frunzke and Meyer, 1990) and the yielded energy used for CO_2 fixation without any energy loss (ΔG = 49.6 kJ mol^{-1}; http://www.atpsynthase.info/FAQ.html#Sec6), the CO production by dead rhizome would

enable the synthesis of 3.9 mg of biomass (dry weight) per day and m². It could be used to form even 3.5 times more biomass, if it was oxidized with oxygen instead of nitrate. Based on these numbers the energy from CO would be sufficient for 15 worms with an average dry weight of 0.25 mg per m² and day with nitrate as an electron acceptor. Given that dead rhizome is buried in the sandy sediment of the entire bay of Sant' Andrea and many other coastal areas all over the world accounting for 0.1-0.2 % of the global ocean (Duarte, 2002; Orth *et al.*, 2006), this indicates that the release of CO by dead sea grass rhizomes might be a major energy source in many coastal ecosystem for CO-oxidizing microorganisms in general.

In our current study we were unable to determine the source of H_2 in the sediment, as none of the investigated components released H_2. A potential source of H_2 could be the biological activity of anaerobic CO-oxidizers (reviewed in King and Weber, 2007). This would also be thermodynamically consistent with the elevated CO concentrations measured at the same collection site, as low CO concentrations can lead to high H_2 concentrations (personal communication Prof. F. Widdel).

Ecological importance of CO as an energy source for marine free-living and symbiotic microorganisms

To see how widespread the potential to oxidize CO is in marine microorganisms we screened available genomic, transcriptomic and proteomic data of marine symbiotic and free-living microorganisms. We found that at least one of the alphaproteobacterial symbionts of another gutless worm, called *Inanidrilus leukodermatus* from Bermuda, also possesses a CODH (Bergin, 2009). We do not know if the symbiosis of *I. leukodermatus* consumes CO actively. However, the finding of this gene indicates that CO could also play a role as an additional energy source in the symbiosis of that gutless worm. There is also recent evidence that symbionts of corals (Pollack *et al.*, 2009) and sponges (Radax *et al.*, 2012; Thomas *et al.*, 2010) express CO dehydrogenases under natural conditions. Since CO can arise from

photolytic or biologic reactions in the water column (King and Weber, 2007) or flow into the water column from the sediment, it is feasible that these symbionts might also use CO as an energy source.

Besides the symbiotic microorganisms in marine invertebrates, free-living microorganisms can also benefit from CO and H_2 as energy sources. Several studies have recently shown a high genetic potential of microorganisms to oxidize CO in marine sediments (Andreote *et al.*, 2012; Martin-Cuadrado *et al.*, 2009) and planktonic organisms (Cunliffe, 2011; Quaiser *et al.*, 2011; Smedile *et al.*, 2012). While CO is well recognized as an energy source for microorganisms in the water column (e. g. reviewed in King and Weber, 2007), it has not been previously assumed to play a role in the primary production of marine sediments. Based on our finding that dead seagrass rhizomes produce large amounts of CO, we hypothesize that CO may be an important energy source in marine sediments, particularly those with seagrass, and may play an important role in the global energy and carbon cycling. Investigating the formation and consumption of CO in these habitats will be crucial to understanding the full energy and carbon cycling in these ecosystems. It will furthermore also give information about potential CO release to the atmosphere. Since CO is known to be a potent green house gas any information about the amount of CO loss to the atmosphere from coastal regions will become valuable for climate change predictions.

Acknowledgments

We thank the team of the Hydra Institute on Elba for the extensive support with sample collection and on site experiments, Silke Wetzel, Agnes Zimmer, Nadine Lehnen for excellent technical assistance as well as all the people at the Max Planck Institute for Marine Microbiology who helped with and discussed the research for this manuscript. CW and MK were supported by Studienstiftung des deutschen Volkes scholarships. Funding for this study was provided by the Max Planck Society.

Supplemental figures

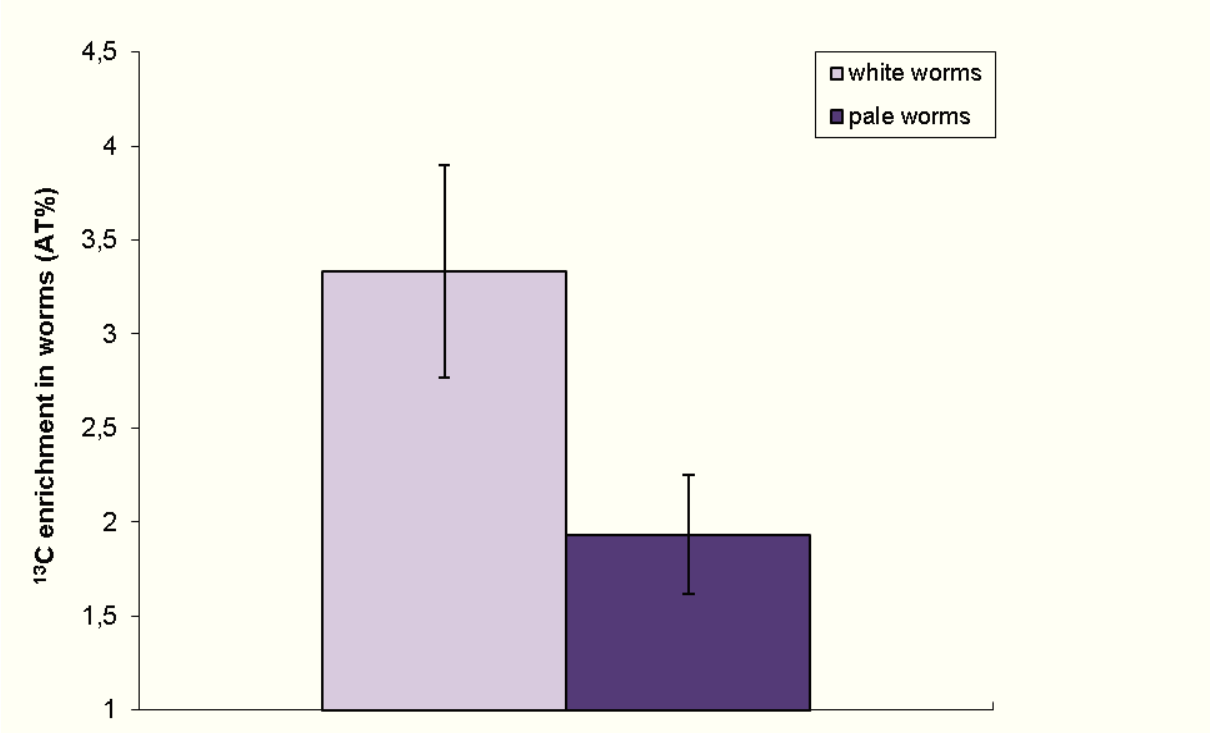

Figure S1: ^{13}C-bulk measurements of entire worms after a 36 hours incubation without an additional electron donor, but with nitrate, oxygen and ^{13}C-labeled bicarbonate. ^{13}C-enrichment values in atomic percentage (AT%= (^{13}C/(^{12}C+^{13}C)*100). The γ1-symbionts in white worms contained large amounts of stored elemental sulfur, which they can use for CO_2 fixation under oxic conditions (Bergin, 2009; Giere, 2006), whereas sulfur storage was reduced or depleted in pale worms by an oxic pre-incubation.

References

Alcoverro T, Manzanera M, Romero J (2001) Annual metabolic carbon balance of the seagrass Posidonia oceanica: the importance of carbohydrate reserves. *Mar Ecol Prog Ser* **211:** 105-116.

Andreote FD, Jimenez DJ, Chaves D, Dias ACF, Luvizotto DM, Dini-Andreote F *et al.* (2012) The Microbiome of Brazilian Mangrove Sediments as Revealed by Metagenomics. *Plos One* **7**.

Bergin C (2009) Phylogenetic diversity and metabolic versatility of the bacterial endosymbionts in marine gutless oligochaete worms. *Symbiosis Group* **PhD:** Max Planck Institute for Marine Microbiology, Germany.

Cavanaugh CM, Gardiner SL, Jones ML, Jannasch HW, Waterbury JB (1981) Prokaryotic cells in the hydrothermal vent tube worm *Riftia pachyptila* Jones: possible chemoautotrophic symbionts. *Science* **213:** 340-342.

Cavanaugh CM, McKiness ZP, Newton ILG, Stewart FJ (2006). Marine chemosynthetic symbioses. In: Dworkin M, Falkow SI, Rosenberg E, Schleifer K-H, Stackebrandt E (eds). *The Prokaryotes*. Springer: New York. pp 475-507.

Conrad R, Meyer O, Seiler W (1981) Role of Carboxydobacteria in Consumption of Atmospheric Carbon-Monoxide by Soil. *Appl Environ Microbiol* **42:** 211-215.

Conrad R, Seiler W (1985) Characteristics of abiological carbon monoxide formation from soil organic matter, humic acids, and phenolic compounds. *Environ Sci Technol* **19:** 1165-1169.

Cunliffe M (2011) Correlating carbon monoxide oxidation with cox genes in the abundant Marine Roseobacter Clade. *ISME J* **5:** 685-691.

Cypionka H, Meyer O, Schlegel HG (1980) Physiological-characteristics of various species of strains of carboxydobacteria. *Arch Microbiol* **127:** 301-307.

Daims H, Bruhl A, Amann R, Schleifer KH, Wagner M (1999) The domain-specific probe EUB338 is insufficient for the detection of all Bacteria: Development and evaluation of a more comprehensive probe set. *Syst Appl Microbiol* **22:** 434-444.

Diekert GB, Thauer RK (1978) Carbon monoxide oxidation by *Clostridium thermoaceticum* and *Clostridium formicoaceticum*. *J Bacteriol* **136:** 597-606.

Duarte CM (2002) The future of seagrass meadows. *Environ Conserv* **29:** 192-206.

Dubilier N, Mulders C, Ferdelman T, de Beer D, Pernthaler A, Klein M *et al.* (2001) Endosymbiotic sulphate-reducing and sulphide-oxidizing bacteria in an oligochaete worm. *Nature* **411:** 298-302.

Dubilier N, Bergin C, Lott C (2008) Symbiotic diversity in marine animals: the art of harnessing chemosynthesis. *Nat Rev Microbiol* **6:** 725-740.

Felbeck H (1981) Chemoautotrophic potential of the hydrothermal vent tube worm *Riftia pachyptila* Jones (Vestimentifera). *Science* **213:** 336-338.

Frunzke K, Meyer O (1990) Nitrate respiration, denitrification, and utilization of nitrogen-sources by aerobic carbon monoxide-oxidizing bacteria. *Arch Microbiol* **154:** 168-174.

Giere O, Erseus C (2002) Taxonomy and new bacterial symbioses of gutless marine Tubificidae (Annelida, Oligochaeta) from the Island of Elba (Italy). *Org Divers Evol* **2:** 289–297.

Giere O (2006) Ecology and biology of marine oligochaeta - an inventory rather than another review. *Hydrobiologia* **564:** 103-116.

Goevert D, Conrad R (2008) Carbon isotope fractionation by sulfate-reducing bacteria using different pathways for the oxidation of acetate. *Environ Sci Technol* **42:** 7813-7817.

Gruber-Vodicka HR, Dirks U, Leisch N, Baranyi C, Stoecker K, Bulgheresi S *et al.* (2011) *Paracatenula*, an ancient symbiosis between thiotrophic Alphaproteobacteria and catenulid flatworms. *Proc Natl Acad Sci U S A* **108:** 12078-12083.

Hardy KR, King GM (2001) Enrichment of high-affinity CO oxidizers in Maine forest soil. *Appl Environ Microbiol* **67:** 3671-3676.

Hendrickson OQ, Kubiseski T (1991) Soil microbial activity at high-levels of carbon-monoxide. *J Environ Qual* **20:** 675-678.

Hoehler TM, Albert DB, Alperin MJ, Bebout BM, Martens CS, Des Marais DJ (2002) Comparative ecology of H_2 cycling in sedimentary and phototrophic ecosystems. *Antonie Leeuwenhoek* **81:** 575-585.

Karadagli F, Rittmann BE (2007) Thermodynamic and kinetic analysis of the H_2 threshold for *Methanobacterium bryantii* M.o.H. *Biodegradation* **18:** 439-452.

King GM (2007) Microbial carbon monoxide consumption in salt marsh sediments. *FEMS Microbiol Ecol* **59:** 2-9.

King GM, Weber CF (2007) Distribution, diversity and ecology of aerobic CO-oxidizing bacteria. *Nat Rev Microbiol* **5:** 107-118.

Kleiner M, Wentrup C, Lott C, Teeling H, Wetzel S, Young J *et al.* (2012) Metaproteomics of a gutless marine worm and its symbiotic microbial community reveal unusual pathways for carbon and energy use. *Proc Natl Acad Sci U S A* **109:** E1173-1182.

Londry KL, Marais DJD (2003) Stable carbon isotope fractionation by sulfate-reducing bacteria. *Appl Environ Microbiol* **69:** 2942-2949.

Manz W, Amann R, Ludwig W, Vancanneyt M, Schleifer KH (1996) Application of a suite of 16S rRNA-specific oligonucleotide probes designed to investigate bacteria of the phylum cytophaga-flavobacter-bacteroides in the natural environment. *Microbiology-Uk* **142:** 1097-1106.

Martin-Cuadrado AB, Ghai R, Gonzaga A, Rodriguez-Valera F (2009) CO Dehydrogenase Genes Found in Metagenomic Fosmid Clones from the Deep Mediterranean Sea. *Appl Environ Microbiol* **75:** 7436-7444.

Michener RH, Scranton MI, Novelli P (1988) Hydrogen (H_2) Distributions in the Carmans River Estuary. *Estuar Coast Shelf Sci* **27:** 223-235.

Moran MA, Buchan A, Gonzalez JM, Heidelberg JF, Whitman WB, Kiene RP *et al.* (2004) Genome sequence of *Silicibacter pomeroyi* reveals adaptations to the marine environment. *Nature* **432:** 910-913.

Musat N, Halm H, Winterholler B, Hoppe P, Peduzzi S, Hillion F *et al.* (2008) A single-cell view on the ecophysiology of anaerobic phototrophic bacteria. *Proc Natl Acad Sci U S A* **105:** 17861-17866.

Musat N, Foster R, Vagner T, Adam B, Kuypers MM (2012) Detecting metabolic activities in single cells, with emphasis on nanoSIMS. *FEMS Microbiol Rev* **36:** 486-511.

Novelli PC, Michelson AR, Scranton MI, Banta GT, Hobbie JE, Howarth RW (1988) Hydrogen and acetate cycling in 2 sulfate-reducing sediments - Buzzards Bay and Town Cove, Mass. *Geochim Cosmochim Acta* **52:** 2477-2486.

Oelgeschlager E, Rother M (2008) Carbon monoxide-dependent energy metabolism in anaerobic bacteria and archaea. *Arch Microbiol* **190:** 257-269.

Orth RJ, Carruthers TJB, Dennison WC, Duarte CM, Fourqurean JW, Heck KL *et al.* (2006) A global crisis for seagrass ecosystems. *Bioscience* **56:** 987-996.

Pernthaler A, Pernthaler J, Amann R (2002) Fluorescence in situ hybridization and catalyzed reporter deposition for the identification of marine bacteria. *Appl Environ Microbiol* **68:** 3094-3101.

Petersen JM, Zielinski FU, Pape T, Seifert R, Moraru C, Amann R *et al.* (2011) Hydrogen is an energy source for hydrothermal vent symbioses. *Nature* **476:** 176-180.

Ploug H, Musat N, Adam B, Moraru CL, Lavik G, Vagner T *et al.* (2010) Carbon and nitrogen fluxes associated with the cyanobacterium Aphanizomenon sp. in the Baltic Sea. *ISME J* **4:** 1215-1223.

Polerecky L, Adam B, Milucka J, Musat N, Vagner T, Kuypers MM (2012) Look@NanoSIMS-a tool for the analysis of nanoSIMS data in environmental microbiology. *Environ Microbiol* **14:** 1009-1023.

Pollack K, Balazs K, Ogunseitan O (2009) Proteomic assessment of caffeine effects on coral symbionts. *Environ Sci Technol* **43:** 2085-2091.

Quaiser A, Zivanovic Y, Moreira D, Lopez-Garcia P (2011) Comparative metagenomics of bathypelagic plankton and bottom sediment from the Sea of Marmara. *ISME J* **5:** 285-304.

Rabus R, Hansen TA, Widdel F (2006). Dissimilatory sulfate- and sulfur-reducing prokaryotes. In: Dworkin M, Falkow SI, Rosenberg E, Schleifer K-H, Stackebrandt E (eds). *The Prokaryotes*. Springer: New York. pp 659-768.

Radax R, Rattei T, Lanzen A, Bayer C, Rapp HT, Urich T *et al.* (2012) Metatranscriptomics of the marine sponge *Geodia barretti*: tackling phylogeny and function of its microbial community. *Environ Microbiol* **14:** 1308-1324.

Ruehland C, Blazejak A, Lott C, Loy A, Erseus C, Dubilier N (2008) Multiple bacterial symbionts in two species of co-occurring gutless oligochaete worms from Mediterranean sea grass sediments. *Environ Microbiol* **10:** 3404-3416.

Smedile F, Messina E, La Cono V, Tsoy O, Monticelli LS, Borghini M *et al.* (2012) Metagenomic analysis of hadopelagic microbial assemblages thriving at the deepest part of Mediterranean Sea, Matapan-Vavilov Deep. *Environ Microbiol*.

Thomas T, Rusch D, DeMaere MZ, Yung PY, Lewis M, Halpern A *et al.* (2010) Functional genomic signatures of sponge bacteria reveal unique and shared features of symbiosis. *ISME J* **4:** 1557-1567.

Tolli JD, Sievert SM, Taylor CD (2006) Unexpected diversity of bacteria capable of carbon monoxide oxidation in a coastal marine environment, and contribution of the Roseobacter-associated clade to total CO oxidation. *Appl Environ Microbiol* **72:** 1966-1973.

Vignais PM, Billoud B (2007) Occurrence, classification, and biological function of hydrogenases: an overview. *Chem Rev* **107:** 4206-4272.

Voordouw G (2002) Carbon monoxide cycling by *Desulfovibrio vulgaris* Hildenborough. *J Bacteriol* **184:** 5903-5911.

Weber CF, King GM (2010) Distribution and diversity of carbon monoxide-oxidizing bacteria and bulk bacterial communities across a succession gradient on a Hawaiian volcanic deposit. *Environ Microbiol* **12:** 1855-1867.

Widdel F, Bak F (1992). Gram-negative mesophilic sulfate-reducing bacteria. In: A. Balows HGT, M. Dworkin, W. Harder, K-H. Schleifer (ed). *The Prokaryotes*, 2nd ed. edn. Springer, New York. pp 3352-3378.

Woyke T, Teeling H, Ivanova NN, Huntemann M, Richter M, Gloeckner FO *et al.* (2006) Symbiosis insights through metagenomic analysis of a microbial consortium. *Nature* **443:** 950-955.

Chapter 6: Concluding summary and perspectives

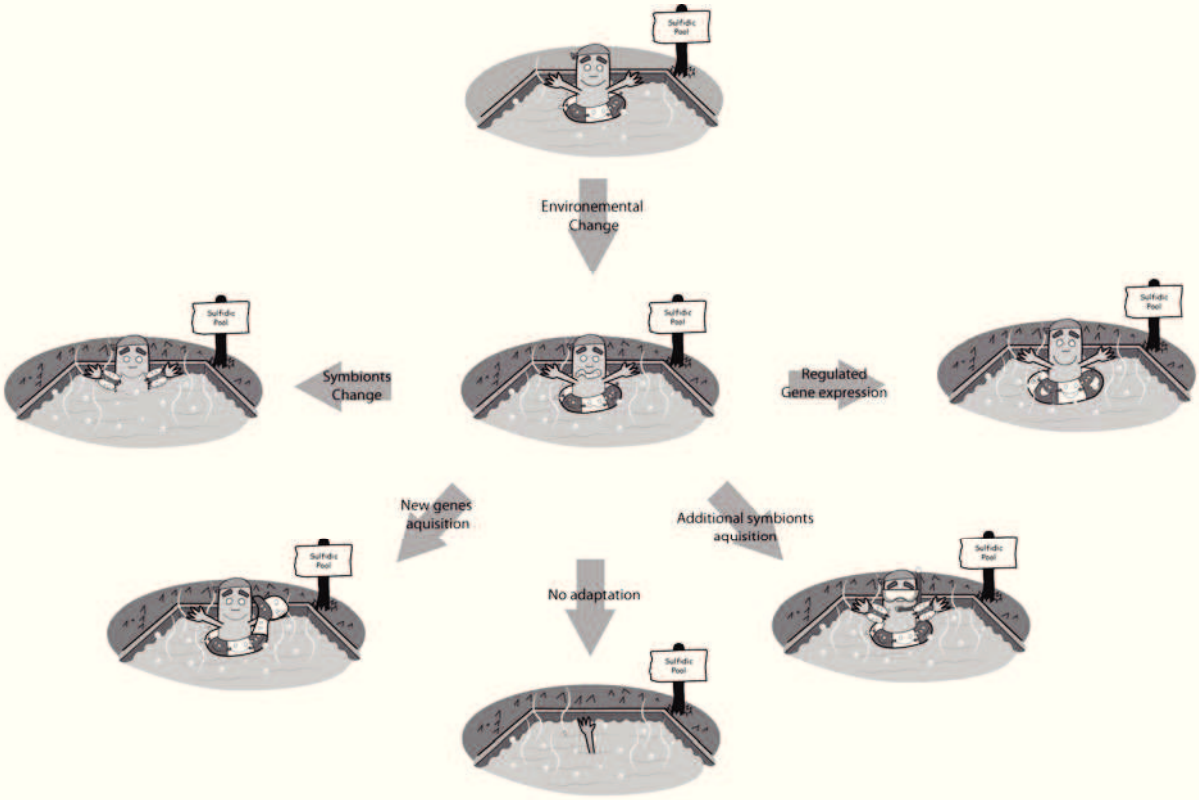

"Time of changes"

Concluding summary and perspectives

Chemosynthetic hosts usually harbor at least one sulfur-oxidizing symbiont that uses reduced sulfur compounds as energy source to fix CO_2 into biomass to feed the host (exceptions are some *Bathymodiolus* mussels which harbor only methane-oxidizing symbionts) (reviewed in Cavanaugh *et al.*, 2006; Dubilier *et al.*, 2008). This gives the hosts a physiological advantage to colonize and thrive in nutrient poor habitats. Most sulfur-oxidizing symbionts oxidize the reduced sulfur compounds using oxygen as electron acceptor, but some symbionts can also use nitrate (Cavanaugh *et al.*, 2006; Kleiner *et al.*, 2012, Chapter 4). Despite the fact that all symbiotic sulfur oxidizers share this similar chemolithoautotrophic lifestyle, they diverge in many other metabolic capabilities and functions (reviewed e.g. Kleiner *et al.*, submitted). For example, sulfur-oxidizing symbionts can possess more than one pathway for the fixation of CO_2. Others have metabolic pathways for the use of additional inorganic and organic energy sources as well as organic carbon sources. It has been proposed that these metabolic variations could reflect adaptations to different hosts and environmental conditions (Cavanaugh *et al.*, 2006; Childress & Girguis, 2011; Kleiner *et al.*, submitted; Stewart *et al.*, 2005). Another adaptation of chemosynthetic hosts to environmental conditions is the acquisition of additional symbionts that can use other energy sources to complement and increase the total energy yield of the symbiosis (for more information see Chapter 1: State of the Art).

Habitats at which chemosynthetic symbioses occur include ephemeral ones like deep-sea hydrothermal vents and cold seeps, whale carcasses and wood-falls that are all islands high in inorganic and organic energy sources in the otherwise desert-like deep-sea. Other more persistent environments are shallow water sediments with varying concentrations of energy sources that form large, continuous habitats along continental coasts. Animals inhabiting ephemeral environments must generally be fast growing species that reproduce early and disperse effectively into new habitats before their local habitat is extinguished,

although some vents and particularly seeps can exist for long time periods and correspondingly are colonized by more slow-growing species such as seep vestimentiferan tubeworms (Vrijenhoek, 2010). The habitat thus has a significant impact on shaping the persistence and stability of symbioses as well as the metabolism of the symbionts and the enzymes they use (e.g. Cavanaugh *et al.*, 2006; Kleiner *et al.*, submitted).

I investigated the symbiont colonization of host tissue in deep-sea bivalves (Chapter 2-3) as well as the metabolic capabilities of symbionts of the gutless worm *Olavius algarvensis* (Chapter 4-5). The results of this PhD thesis add to our understanding of when and how hosts acquire their symbionts and what additional energy sources chemosynthetic symbionts can use.

6.1 Symbiont colonization of host tissue

Hosts of chemosynthetic symbionts do not necessarily harbor symbionts when they are juveniles, but they always do in their adulthood. Their dependence on the symbionts is often also reflected in anatomical and morphological adaptations. As most hosts cannot survive and grow without their chemosynthetic symbionts, they acquire their symbionts at an early developmental stage (Bright & Bulgheresi, 2010). They either inherit the symbionts from their parents or they acquire the symbionts from the environment or they use a mix of both (for more information see Chapter 1: State of the Art). However, it remains elusive for most symbioses how newly formed host cells of symbiont-containing organs are colonized in later developmental stages. The best described colonization process is the one of the chemosynthetic symbiont *Candidatus* Endoriftia persephone into the trophosome, the symbiont hosting organ of *Riftia pachyptila* (Nussbaumer *et al.*, 2006). In this symbiosis, free living symbionts (Harmer *et al.*, 2008) colonize their host once at an early developmental stage and are later transferred directly to newly formed host cells of the trophosome during cell division of bacteriocytes (Pflugfelder *et al.*, 2009). In contrast, the flatworm *Paracatenula*

galateia transmits its intracellular chemosynthetic symbionts directly to the progeny via asexual fragmentation (Dirks *et al.*, 2012). However, the bacteriocytes of this flatworm are still formed aposymbiotically and colonized by the symbionts at a later stage.

During my PhD study I contributed additional information about symbiont colonization patterns in chemosynthetic symbioses. In deep-sea *Bathymodiolus* mussels, I observed an ontogenetic shift in symbiont colonization from indiscriminate infection of almost all epithelia in early life stages to spatially restricted colonization of gills in later developmental stages (Chapter 2). Gill tissues were always colonized by the chemosynthetic bacteria in all differently sized *Bathymodiolus* mussels (5-100 mm) investigated in this study. Only the budding zones at the posterior most gill tips that continuously produce new gill filaments, the youngest gill filaments and the ventral edges of the gills, where the gill enlarges ventrally by linear growth of the filaments, were devoid of symbionts (Chapter 3). As these three gill areas are known to be major growth zones of gill filaments, the absence of symbionts in these growth zones indicates that symbiont colonization of newly formed *Bathymodiolus* gill tissue happens at a later stage of host cell differentiation. It further indicates that symbionts inoculate newly formed gill cells continuously *de novo* throughout the mussel's life time, as the gills grow throughout the mussel's life. I made the same observation in gills of "*Calyptogena*" *ponderosa*, where symbionts colonized new gill filaments as they grow as well (Chapter 3). The trait of having to acquire symbionts *de novo* into newly formed bacteriocytes of the continuously growing gills could therefore be a trait common to all bivalves with chemosynthetic symbionts regardless of whether the symbionts are acquired from the parents (as in "*C.*" *ponderosa*) or the environment (as in *Bathymodiolus*). However, the mechanisms of how the symbionts get into newly formed gill tissues might differ. While *Bathymodiolus* gill cells are likely to be colonized by the symbionts through endocytosis, the symbionts of "*C.*" *ponderosa* might colonize new gill cells by infecting neighboring host cells through direct cell-to-cell infection (Chapter 3).

The gill structure of bivalves and the progressive colonization of the symbionts into newly formed gill tissues are an ideal model to monitor progressive changes involved in the establishment of a symbiosis at the cellular level. Comparison of the transcriptome and proteome of both host and symbionts in gill filaments from a) the budding zone that is free of symbionts, b) the transition zone in which young filaments harbor only a few symbionts, and c) the fully differentiated zone beginning at the ~10^{th} filament which is completely colonized by symbionts could provide valuable information about the cellular responses of the host to the invasion of symbionts and vice versa. In addition, comparison of the transcriptome and proteome of the 10 youngest gill filaments of one bivalve with inherited chemosynthetic symbionts to the ones of another bivalve harboring chemosynthetic symbionts acquired from the environment might provide insights into how the hosts have adapted to the different symbiont populations. These analyses will provide a better understanding of how bacterial colonization patterns are established, maintained, and regulated in animal symbioses.

6.2 Metabolic traits of chemosynthetic symbionts

Habitats of chemosynthetic symbioses usually provide considerable amounts of reduced sulfur compounds to fuel the chemosynthetic life style of the symbionts (reviewed in Cavanaugh *et al.*, 2006; Childress & Girguis, 2011; Dubilier *et al.*, 2008; Stewart *et al.*, 2005). Some habitats supply additional energy sources such as hydrogen and methane. In these habitats chemosynthetic symbioses can also live of H_2 (Petersen *et al.*, 2011) and methane (Childress *et al.*, 1986). Thus, depending on the energy sources offered in the environment, chemosynthetic symbioses can thrive on different or multiple energy sources (for more information see Chapter 1: State of the Art).

A metaproteomic approach and incubation experiments conducted during this PhD study (Chapter 4-5) demonstrated that hydrogen as well as carbon monoxide could be used by the

chemosynthetic symbionts of the gutless worm *Olavius algarvensis* as alternative energy sources. The oxidation of CO also led to an increase of CO_2 fixation in one of the sulfur-oxidizing symbionts of *O. algarvensis* under the incubation conditions used. Hence, four inorganic energy sources (reduced sulfur compounds, methane, hydrogen, and carbon monoxide) have now been shown to fuel chemosynthetic symbioses and more are likely to be shown. Iron (Fe^{2+}) for example has been proposed to be another electron donor for chemosynthetic symbioses (Cavanaugh *et al.*, 2006) and genomic indications suggest that the ectosymbionts of *Rimicaris exoculata*, a shrimp from hydrothermal vents, might actually use this electron donor (Jan *et al.*, in preparation). Our metaproteomic study of the *O. algarvensis* symbionts further showed that all symbionts expressed proteins involved in highly efficient pathways and high-affinity uptake transporters for the recycling and conservation of energy, nitrogen, and carbon sources in worms collected from the environment. These pathways included a pathway for symbiont assimilation of the host waste products acetate, propionate, succinate, and malate and as yet undescribed energy-efficient steps in CO_2 fixation and sulfate reduction (Kleiner *et al.*, 2012, Chapter 4). The high expression of proteins involved in pathways for energy and carbon uptake and conservation in the *O. algarvensis* symbiosis shows how a chemosynthetic symbiosis can adapt to a nutrient poor habitat with low concentrations of reduced sulfur compounds (Dubilier *et al.*, 2001; Kleiner *et al.*, 2012; Woyke *et al.*, 2006, Chapter 4).

Analyzing symbiotic consortia of the same host species from different habitats or different host species from the same habitat using traditional molecular methods such as the full cycle 16S rRNA analysis and also at the genomic, transcriptomic, and proteomic level might give new insights into how environmental conditions shape symbioses. The gutless worm symbioses are an ideal system to study this, because they are readily accessible in shallow water sediments with very different environmental parameters and because different species can share the same habitat just as one species can colonize and thrive in different habitats

(Dubilier *et al.*, 2008; Dubilier *et al.*, 2006). Such analyses will give information about the adaptations of both partners to their respective habitat. Possible adaptations might include: **1**) symbiont switches, **2**) affiliation of additional symbionts better adapted to the respective environmental conditions, **3**) rearrangements in the symbiont genomes or the acquisition of new genes (homologous recombination was shown for vesicomyid symbionts (Stewart *et al.*, 2009)), **4**) changed regulation of gene expression (recently shown for *Candidatus* Endoriftia persephone (Robidart *et al.*, 2011)), or **5**) a combination of these.

Ultimately the future research aim should be to cultivate the *O. algarvensis* symbiosis in the lab to specifically manipulate environmental parameters and to observe how the symbiosis adapts to these changes. So far, only long-term maintenance is possible for both the host *O. algarvensis* and its main sulfur-oxidizing symbiont allowing experimental manipulation, but no controlled experimental evolution set-ups. Cultivation of chemosynthetic symbioses is challenging and it has not been achieved for many symbiotic associations so far. To a certain degree it has been realized for the lucinid clams (Gros *et al.*, 1998b), the ciliate *Zoothamium* (Rinke *et al.*, 2007) and the flat worm *Paracatenula* (Dirks *et al.*, 2012). In the two latter the host can reproduce asexually. This provides numerous generations of the chemosynthetic symbiosis in a short period of time and promises to become great model systems to apply experimental evolution.

List of publications and manuscripts with author's contribution

1. **Wentrup, C.**, Wendeberg A., Huang J. Y., Borowski C., Dubilier, N. (under revision at the ISME-Journal). Shift from widespread symbiont infection of host tissues to specific colonization of gills in juvenile deep-sea mussels.

   Author's contribution: concept C.W., A.W., and N.D., FISH analyses C.W., J.Y.H., and A.W., figures and tables C.W., writing of manuscript C.W. and N.D., all authors read and commented the manuscript.

2. **Wentrup, C.**, Borowski C., Wendeberg A., Schimak M., Dubilier, N. (manuscript in preparation). Symbiont colonization in chemosynthetic deep-sea bivalves is a continuous process.

   Author's contribution: concept C.W., A.W., and N.D., FISH analyses C.W. and A.W., TEM analyses M.S., figures and tables C.W., writing of manuscript C.W. and C.B., manuscript revision N.D.

3. Kleiner, M., **Wentrup, C.**, Lott, C., Teeling, H., Wetzel, S., Young, J., Chang, Y. J., Shah, M., VerBerkmoes, N. C., Zarzycki, J., Fuchs, G., Markert, S., Hempel, K., Voigt, B., Becher, D., Liebeke, M., Lalk, M., Albrecht, D., Hecker, M., Schweder, T., Dubilier, N. (2012). Metaproteomics of a gutless marine worm and its symbiotic microbial community reveal unusual pathways for carbon and energy use. *Proc Natl Acad Sci U S A, 109*(19), E1173-1182

   Author contributions: M.K., G.F., B.V., D.B., M. Liebeke, M. Lalk, M.H., and T.S. designed research; M.K., C.W., C.L., H.T., S.W., J.Y., Y.-J.C., N.C.V., J.Z., K.H., M. Liebeke, and D.A. performed research; N.C.V., G.F., M. Lalk, M.H., T.S., and N.D. contributed new reagents/analytic tools; M.K., C.W., J.Y., M.S., N.C.V., J.Z., S.M., B.V., D.B., M. Liebeke, and N.D. analyzed data; and M.K. and N.D. wrote the paper.

4. **Wentrup, C.**, Kleiner M., Holler T., Lavik G., Harder J., Lott C., Dubilier N. (manuscript in preparation). Carbon monoxide and hydrogen serve as alternative energy sources for a gutless worm symbiosis.

   Author's contribution: C.W. and M.K. contributed equally to this manuscript. Concept C.W. and M.K., practical work C.W and M.K., data analyses C.W., M.K., T.H., G.L. and J.H., figures and tables C.W. and M.K., writing of manuscript C.W., manuscript revision M.K. and N.D.

5. Petersen J.M., **Wentrup C.**, Verna C., Knittel K., Dubilier N. (2012). Origins and evolutionary flexibility of chemosynthetic symbionts from deep-sea animals. *Biol Bull*, 223, 123-137

   Author's contribution: concept J.M.P., FISH and phylogenetic analyses J.M.P and C.V., figures C.W., tables J.M.P., writing of manuscript J.M.P., manuscript revision C.W. and N.D.

Not presented in this thesis

6. **Wentrup, C**., Giere O., Lott C., Noriega B., Erseus C., Wetzel S., Dubilier N. (manuscript in preparation). Taxonomic description of two gutless marine Tubificidae (Annelida, Oligochaeta) from the Mediterranean Sea and characterization of their bacterial symbionts.

   Author's contribution: concept C.W. and O.G., FISH and phylogenetic analyses C.W., B.N. and S.W., taxonomic description O.G., C.L. and C.E., figures C.W., tables C.W., writing of manuscript C.W. and O.G.

Acknowledgments

Thanks to ...

Prof. Dr. Nicole Dubilier for giving me the opportunity to do my PhD thesis in her lab, for valuable discussions, as well as for the advice and support she gave me when needed.

Prof. Dr. Monica Bright for your willingness to review this thesis.

Prof. Dr. Ulrich Fischer, **Jillian M. Petersen**, **Juliane Wippler** and **Miriam Sadowski** the members of my thesis committee

The Mollies and symbionts (former and present members ;-)) for support, advice, all scientific and every-day discussions, and the great amicable atmosphere. I very much enjoyed working with you.

Special thanks goes to **Manuel**, my 'work husband' without whom the gutless oligochaete part of this thesis would not have been as successful and fun as it was!

Special thanks goes also to my office and Mensa mates **Sara**, **Jill**, **Dennis**, **Chia-I**, **Karina**, **Silke**, **Caroline**, **Kyoko**, and **Andreas** for their support and friendship through the last past years!

Nicole, **Christian, Jill, Harald**, **Dirk** and **Claudia** are especially acknowledged for prove-reading some of the manuscripts and parts of this thesis!

Marc, who encouraged and supported me to come to the MPI.

Adrian for drawing the sketches of chapter 1 and 6.

Thomas, **Gaute**, **Jens**, **Richard**, **Tim**, **Christina**, and **Ramona** for patiently introducing me to methods and techniques of microbiologists and geochemists.

The Hydra-Team on Elba for encouraging and supporting crazy ideas and collecting thousands of worms.

The Studienstiftung des deutschen Volkes that provided my salary for three years.

Bernd Stickfort for always finding the required papers.

I also want to thank my **parents**, **siblings**, **parents-in-law**, **brother-in-law**, and **grandma-in-law** for their encouragement, love and support as well as **Petra**, **Petra**, **Michi**, **Sandra**, **Tine**, **the Pelzkragener-Haufen** and my **Wiener-Mädels**, who make life worth living with tons of fun. Thank you so much for being there!

Last but not least and because there are no words to describe my infinitive gratitude I want to thank my ‘life’ husband **Dirk** for being there in good times and in worse.

References

Amann, R. I., Ludwig, W., & Schleifer, K. H. (1995). Phylogenetic identification and in-situ detection of individual microbial-cells without cultivation. *Microbiol. Rev., 59*(1), 143-169.

Anderson, A. E., Childress, J. J., & Favuyyi, J. A. (1987). Net uptake of CO_2 driven by sulfide and thiosulfate oxidation in the bacterial symbiont-containing clam *Solemya reidi*. *J. Exp. Biol., 133*, 1-31.

Baker, B. J., Tyson, G. W., Webb, R. I., Flanagan, J., Hugenholtz, P., Allen, E. E., et al. (2006). Lineages of acidophilic archaea revealed by community genomic analysis. *Science, 314*(5807), 1933-1935.

Behrens, S., Losekann, T., Pett-Ridge, J., Weber, P. K., Ng, W. O., Stevenson, B. S., et al. (2008). Linking microbial phylogeny to metabolic activity at the single-cell level by using enhanced element labeling-catalyzed reporter deposition fluorescence in situ hybridization (EL-FISH) and NanoSIMS. *Appl. Environ. Microbiol., 74*(10), 3143-3150.

Bergin, C. (2009). Phylogenetic diversity and metabolic versatility of the bacterial endosymbionts in marine gutless oligochaete worms. *Symbiosis Group, PhD*, University of Bremen, Germany.

Bettencourt, R., Pinheiro, M., Egas, C., Gomes, P., Afonso, M., Shank, T., et al. (2010). High-throughput sequencing and analysis of the gill tissue transcriptome from the deep-sea hydrothermal vent mussel *Bathymodiolus azoricus*. *BMC Genomics, 11*.

Blazejak, A., Erseus, C., Amann, R., & Dubilier, N. (2005). Coexistence of bacterial sulfide oxidizers, sulfate reducers, and spirochetes in a gutless worm (Oligochaeta) from the Peru margin. *Appl. Environ. Microbiol., 71*(3), 1553-1561.

Blazejak, A., Kuever, J., Erseus, C., Amann, R., & Dubilier, N. (2006). Phylogeny of 16S rRNA, ribulose 1,5-bisphosphate carboxylase/oxygenase, and adenosine 5'-phosphosulfate reductase genes from gamma- and alphaproteobacterial symbionts in gutless marine worms (oligochaeta) from Bermuda and the Bahamas. *Appl. Environ. Microbiol., 72*(8), 5527-5536.

Boetius, A., Ravenschlag, K., Schubert, C. J., Rickert, D., Widdel, F., Gieseke, A., et al. (2000). A marine microbial consortium apparently mediating anaerobic oxidation of methane. *Nature, 407*(6804), 623-626.

Bordenstein, S. R., & Reznikoff, W. S. (2005). Mobile DNA in obligate intracellular bacteria. *Nat. Rev. Microbiol., 3*(9), 688-699.

Boss, K. J., & Turner, R. D. (1980). The giant white clam from the Galapagos Rift, *Calyptogena magnifica* species novum. *Malacologia, 20*, 161-194.

Bright, M., & Bulgheresi, S. (2010). A complex journey: transmission of microbial symbionts. *Nat. Rev. Microbiol., 8*(3), 218-230.

Bright, M., & Giere, O. (2005). Microbial symbiosis in Annelida. *Symbiosis, 38*(1), 1-45.

Bright, M., Keckeis, H., & Fisher, C. R. (2000). An autoradiographic examination of carbon fixation, transfer and utilization in the *Riftia pachyptila* symbiosis. *Mar. Biol., 136*(4), 621-632.

Cary, C. S., Fisher, C. R., & Felbeck, H. (1988). Mussel growth supported by methane as sole carbon and energy source. *Science, 240*, 78-80.

Cary, S. C. (1994). Vertical transmission of a chemoautotrophic symbiont in the protobranch bivalve, *Solemya reidi*. *Mol. Mar. Biol. Biotechnol., 3*(3), 121-130.

Cary, S. C., & Giovannoni, S. J. (1993). Transovarial inheritance of endosymbiotic bacteria in clams inhabiting deep-sea hydrothermal vents and cold seeps. *Proc. Natl. Acad. Sci. U. S. A., 90*(12), 5695-5699.

Cavanaugh, C. M. (1983). Symbiotic chemoautotrophic bacteria in marine invertebrates from sulfide-rich habitats. *Nature, 302*(5903), 58-61.

Cavanaugh, C. M., Gardiner, S. L., Jones, M. L., Jannasch, H. W., & Waterbury, J. B. (1981). Prokaryotic cells in the hydrothermal vent tube worm *Riftia pachyptila* Jones - possible chemoautotrophic symbionts. *Science, 213*(4505), 340-342.

Cavanaugh, C. M., McKiness, Z. P., Newton, I. L. G., & Stewart, F. J. (2006). Marine chemosynthetic symbioses. In M. Dworkin, S. I. Falkow, E. Rosenberg, K.-H. Schleifer & E. Stackebrandt (Eds.), *The Prokaryotes* (Vol. 1, pp. 475-507). New York: Springer.

Childress, J. J., Fisher, C. R., Brooks, J. M., Kennicutt, M. C., 2nd, Bidigare, R., & Anderson, A. E. (1986). A methanotrophic marine molluscan (bivalvia, mytilidae) symbiosis: mussels fueled by gas. *Science, 233*(4770), 1306-1308.

Childress, J. J., Fisher, C. R., Favuzzi, J. A., Kochevar, R. E., Sanders, N. K., & Alayse, A. M. (1991). Sulfide-driven autotrophic balance in the bacterial symbiont-containing hydrothermal vent tubeworm, *Riftia pachyptila* Jones. *Biol. Bull., 180*, 135-153.

Childress, J. J., & Girguis, P. R. (2011). The metabolic demands of endosymbiotic chemoautotrophic metabolism on host physiological capacities. *J. Exp. Biol., 214*(Pt 2), 312-325.

Dale, C., & Moran, N. A. (2006). Molecular interactions between bacterial symbionts and their hosts. *Cell, 126*(3), 453-465.

Dale, C., Wang, B., Moran, N., & Ochman, H. (2003). Loss of DNA recombinational repair enzymes in the initial stages of genome degeneration. *Mol. Biol. Evol., 20*(8), 1188-1194.

de Bary, A. (1879). *Die Erscheinung der Symbiose*. Strassburg (Strasbourg): Verlag von Karl J. Trubner.

DeChaine, E. G., Bates, A. E., Shank, T. M., & Cavanaugh, C. M. (2006). Off-axis symbiosis found: characterization and biogeography of bacterial symbionts of *Bathymodiolus* mussels from Lost City hydrothermal vents. *Environ. Microbiol., 8*(11), 1902-1912.

DeChaine, E. G., & Cavanaugh, C. M. (2006). Symbioses of methanotrophs and deep-sea mussels (Mytilidae: Bathymodiolinae). *Prog. Mol. Subcell. Biol., 41*, 227-249.

Dirks, U., Gruber-Vodicka, H. R., Leisch, N., Bulgheresi, S., Egger, B., Ladurner, P., et al. (2012). Bacterial symbiosis maintenance in the asexually reproducing and regenerating flatworm *Paracatenula galateia*. *Plos One, 7*(4).

Distel, D. L. (1998). Evolution of chemoautotrophic endosymbioses in bivalves - Bivalve-bacteria chemosymbioses are phylogenetically diverse but morphologically similar. *Bioscience, 48*(4), 277-286.

Distel, D. L., & Cavanaugh, C. M. (1994). Independent phylogenetic origins of methanotrophic and chemoautotrophic bacterial endosymbioses in marine bivalves. *J. Bacteriol., 176*, 1932-1938.

Distel, D. L., Lane, D. J., Olsen, G. J., Giovannoni, S. J., Pace, B., Pace, N. R., et al. (1988). Sulfur-oxidizing bacterial endosymbionts: analysis of phylogeny and specificity by 16S rRNA sequences. *J. Bacteriol., 170*(6), 2506-2510.

Distel, D. L., Lee, H. K.-W., & Cavanaugh, C. M. (1995). Intracellular coexistence of methano- and thioautotrophic bacteria in a hydrothermal vent mussel. *Proc. Natl. Acad. Sci. U. S. A., 92*, 9598-9602.

Dobrindt, U., Hochhut, B., Hentschel, U., & Hacker, J. (2004). Genomic islands in pathogenic and environmental microorganisms. *Nat. Rev. Microbiol., 2*(5), 414-424.

Dubilier, N., Amann, R., Erséus, C., Muyzer, G., Park, S., Giere, O., et al. (1999). Phylogenetic diversity of bacterial endosymbionts in the gutless marine oligochaete *Olavius loisae* (Annelida). *Mar. Ecol. Prog. Ser., 178*, 271-280.

Dubilier, N., Bergin, C., & Lott, C. (2008). Symbiotic diversity in marine animals: the art of harnessing chemosynthesis. *Nat. Rev. Microbiol., 6*(10), 725-740.

Dubilier, N., Blazejak, A., & Ruehland, C. (2006). Symbioses between bacteria and gutless marine oligochaetes. In *Prog. Mol. Subcell. Biol.* (pp. 251-275): Springer-Verlag Berlin.

Dubilier, N., Giere, O., Distel, D. L., & Cavanaugh, C. M. (1995). Characterization of chemoautotrophic bacterial symbionts in a gutless marine worm Oligochaeta, Annelida) by phylogenetic 16S rRNA sequence analysis and in situ hybridization. *Appl. Environ. Microbiol., 61*(6), 2346-2350.

Dubilier, N., Mulders, C., Ferdelman, T., de Beer, D., Pernthaler, A., Klein, M., et al. (2001). Endosymbiotic sulphate-reducing and sulphide-oxidizing bacteria in an oligochaete worm. *Nature, 411*(6835), 298-302.

Dufour, S. C. (2005). Gill anatomy and the evolution of symbiosis in the bivalve family Thyasiridae. *Biol. Bull., 208*(3), 200-212.

Duperron, S. (2010). The Diversity of Deep-Sea Mussels and Their Bacterial Symbioses. In S. Kiel (Ed.), *Vent and Seep Biota: Aspects from Microbes to Ecosystems* (Vol. 33, pp. 137-167): Springer Netherlands.

Duperron, S., Bergin, C., Zielinski, F., Blazejak, A., Pernthaler, A., McKiness, Z. P., et al. (2006). A dual symbiosis shared by two mussel species, *Bathymodiolus azoricus* and *Bathymodiolus puteoserpentis* (Bivalvia: Mytilidae), from hydrothermal vents along the northern Mid-Atlantic Ridge. *Environ. Microbiol., 8*(8), 1441-1447.

Duperron, S., Halary, S., Lorion, J., Sibuet, M., & Gaill, F. (2008). Unexpected co-occurrence of six bacterial symbionts in the gills of the cold seep mussel *Idas* sp. (Bivalvia : Mytilidae). *Environ. Microbiol., 10*(2), 433-445.

Duperron, S., Sibuet, M., MacGregor, B. J., Kuypers, M. M. M., Fisher, C. R., & Dubilier, N. (2007). Diversity, relative abundance and metabolic potential of bacterial endosymbionts in three *Bathymodiolus* mussel species from cold seeps in the Gulf of Mexico. *Environ. Microbiol., 9*(6), 1423-1438.

Elisabeth, N. H., Gustave, S. D., & Gros, O. (2012). Cell proliferation and apoptosis in gill filaments of the lucinid *Codakia orbiculata* (Montagu, 1808) (Mollusca: Bivalvia) during bacterial decolonization and recolonization. *Microsc. Res. Tech.*

Elsaied, H. E., Kaneko, R., & Naganuma, T. (2006). Molecular characterization of a deep-sea methanotrophic mussel symbiont that carries a RuBisCO gene. *Mar. Biotechnol., 8*(5), 511-520.

Endow, K., & Ohta, S. (1990). Occurence of bacteria in the primary oocytes of vesicomyid clam *Calyptogena soyae*. *Mar. Ecol. Prog. Ser., 64*(3), 309-311.

Erseus, C. (1984). Taxonomy and Phylogeny of the Gutless Phallodrilinae (Oligochaeta, Tubificidae), with Descriptions of One New Genus and 22 New Species. *Zool. Scr., 13*(4), 239-272.

Erseus, C. (1992). A generic revision of the Phallodrilinae (Oligochaeta, Tubificiade). *Zool. Scr., 21*(1), 5-48.

Erséus, C. (1979). Taxonomic revision of the marine genus *Phallodrilus* Pierantoni (Oligochaeta, Tubificidae), with descriptions of thirteen new species. *Zool. Scr., 8*, 187-208.

Erseus, C., & Bergfeldt, U. (2007). Six new species of the gutless genus *Olavius* (Annelida: Clitellata: Tubificidae) from New Caledonia. *Zootaxa, 1400*, 45-58.

Erseus, C., Dubilier, N., & Giere, O. (2004). Gutless marine oligochaetes and their bacterial symbionts. *Cladistics, 20*(6), 593-593.

Erseus, C., Kallersjo, M., Ekman, M., & Hovmoller, R. (2002). 18S rDNA phylogeny of the Tubificidae (Clitellata) and its constituent taxa: dismissal of the Naididae. *Mol. Phylogenet. Evol., 22*(3), 414-422.

Felbeck, H. (1981). Chemoautotrophic potential of the hydrothermal vent tube worm *Riftia pachyptila* Jones (Vestimentifera). *Science, 213*, 336-338.

Felbeck, H. (1983). Sulfilde oxidation and carbon fixation by the gutless clam *Solemya reidi*, an animal-bacterial symbiosis. *J. Comp. Physiol., 152*(1), 3-11.

ffrench-Constant, R., Daborn, P., & Feyereisen, R. (2006). Resistance and the jumping gene. *BioEssays, 28*(1), 6-8.

Fiala-Médioni, A., & Le Pennec, M. (1987). Trophic structural adaptations in relation to the bacterial association of bivalve mollusks from hydrothermal vents and subduction zones. *Symbiosis, 4*(1-3), 63-74.

Fiala-Médioni, A., McKiness, Z. P., Dando, P., Boulegue, J., Mariotti, A., Alayse-Danet, A. M., et al. (2002). Ultrastructural, biochemical, and immunological characterization of two populations of the mytilid mussel *Bathymodiolus azoricus* from the Mid-Atlantic ridge: evidence for a dual symbiosis. *Mar. Biol., 141*, 1035-1043.

Fiala-Médioni, A., & Metivier, C. (1986). Ultrastructure of the gill of the hydrothermal vent bivalve *Calyptogena magnifica*, with a discussion of its nutrition. *Mar. Biol., 90*(2), 215-222.

Fiala-Médioni, A., Metivier, C., Herry, A., & Lepennec, M. (1986). Ultrastructure of the gill of the hydrothermal-vent mytilid *Bathymodiolus* sp. *Mar. Biol., 92*(1), 65-72.

Fisher, C. R. (1996). Ecophysiology of primary production at deep-sea vents and seeps. In *Biosystematics and Ecology Series; Deep-sea and extreme shallow-water habitats: Affinities and adaptations* (pp. 313-336).

Fisher, C. R., Brooks, J. M., Vodenichar, J. S., Zande, J. M., Childress, J. J., & Burke, R. A. J. (1993). The co-occurrence of methanotrophic and chemoautotrophic sulfur-oxidizing bacterial symbionts in a deep-sea mussel. *Marine Ecology Pubblicazioni Della Stazione Zoologica Di Napoli I, 14*, 277-289.

Fisher, C. R., & Childress, J. J. (1986). Translocation of fixed carbon from symbiotic bacteria to host tissues in the gutless bivalve *Solemya reidi*. *Mar. Biol., 93*(1), 59-68.

Fisher, C. R., & Childress, J. J. (1992). Organic-carbon transfer from methanotrophic symbionts to the host hydrocarbon-seep mussel. *Symbiosis, 12*(3), 221-235.

Fisher, C. R., Childress, J. J., Arp, A. J., Brooks, J. M., Distel, D. L., Dugan, J. A., et al. (1988). Variation in the hydrothermal vent clam, *Calyptogena magnifica*, at the Rose Garden vent on the Galapagos Spreading-Center. *Deep Sea Res. Part 1 Oceanogr. Res. Pap., 35*(10-11), 1811-1831.

Fisher, C. R., Childress, J. J., Oremland, R. S., & Bidigare, R. R. (1987). The importance of methane and thiosulfate in the metabolism of the bacterial symbionts of 2 deep-sea mussels. *Mar. Biol., 96*(1), 59-71.

Foster, R. A., Kuypers, M. M., Vagner, T., Paerl, R. W., Musat, N., & Zehr, J. P. (2011). Nitrogen fixation and transfer in open ocean diatom-cyanobacterial symbioses. *ISME J, 5*(9), 1484-1493.

Frank, A. B. (1877). Über die biologischen Verhältnisse des Thallus einiger Krustenflechten. *Beiträge zur Biologie der Pflanzen, 2*, 123-200.

Fraune, S., & Bosch, T. C. G. (2010). Why bacteria matter in animal development and evolution. *BioEssays, 32*(7), 571-580.

Fujiwara, Y., Kawato, M., Noda, C., Kinoshita, G., Yamanaka, T., Fujita, Y., et al. (2010). Extracellular and mixotrophic symbiosis in the whale-fall mussel *Adipicola pacifica*: A trend in evolution from extra- to intracellular symbiosis. *Plos One, 5*(7).

Gardebrecht, A., Markert, S., Sievert, S. M., Felbeck, H., Thurmer, A., Albrecht, D., et al. (2011). Physiological homogeneity among the endosymbionts of *Riftia pachyptila* and *Tevnia jerichonana* revealed by proteogenomics. *ISME J, 6*(4), 766-776.

German, C. R., & Lin, J. (2004). The thermal structure of oceanic crust, ridge-spreading and hydrothermal circulation: how well do we understand their interconnections. In C. R. German, J. Lin & L. M. Parson (Eds.), *Mid-ocean ridges: hydrothermal interactions between the lithosphere and oceans* (Vol. 148, pp. 1-18): American Geophysical Union.

Giere, O. (1979). Studies on marine Oligochaeta from Bermuda, with emphasis on new *Phallodrillus* species (Tubificidae). *Cah. Biol. Mar., 20*(3), 310-314.

Giere, O. (1981). The gutless marine oligochaete *Phallodrilus leukodermatus* - structural studies on an aberrant tubificid associated with bacteria. *Mar. Ecol. Prog. Ser., 5*(3), 353-357.

Giere, O. (1985). The gutless marine tubificid *Phallodrilus planus*, a flattened oligochaete with symbiotic bacteria. Results from morphological and ecological studies. *Zool. Scr., 14*(4), 279-286.

Giere, O. (2006). Ecology and biology of marine oligochaeta - an inventory rather than another review. *Hydrobiologia, 564*, 103-116.

Giere, O., Conway, N. M., Gastrock, G., & Schmidt, C. (1991). Regulation of gutless annelid ecology by endosymbiotic bacteria. *Mar. Ecol. Prog. Ser., 68*(3), 287-299.

Giere, O., & Erseus, C. (2002). Taxonomy and new bacterial symbioses of gutless marine Tubificidae (Annelida, Oligochaeta) from the Island of Elba (Italy). *Org. Divers. Evol., 2*, 289–297.

Giere, O., Erseus, C., & Stuhlmacher, F. (1998). A new species of *Olavius* (Tubificidae) from the Algarve coast in Portugal, the first East Atlantic gutless oligochaete with symbiotic bacteria. *Zool. Anz., 237*(2-3), 209-214.

Giere, O., & Krieger, J. (2001). A triple bacterial endosymbiosis in a gutless oligochaete (Annelida): ultrastructural and immunocytochemical evidence. *Invertebr. Biol., 120*(1), 41-49.

Giere, O., & Langheld, C. (1987). Structural organization, transfer and biological fate of endosymbiotic bacteria in gutless oligochaetes. *Mar. Biol., 93*(4), 641-650.

Giere, O., Nieser, C., Windoffer, R., & Erseus, C. (1995). A comparative structural study on bacterial symbioses of Caribbean gutless Tubificidae (Annelida, Oligochaeta). *Acta Zool. (Stockh.), 76*(4), 281-290.

Giere, O., Wirsen, C. O., Schmidt, C., & Jannasch, H. W. (1988). Contrasting effects of sulfide and thiosulfate on symbiotic CO_2-assimilation of *Phallodrilus leukodermatus* (Annelida). *Mar. Biol., 97*(3), 413-419.

Glover, E. A., & Taylor, J. D. (2007). Diversity of chemosymbiotic bivalves on coral reefs: Lucinidae (Mollusca, Bivalvia) of New Caledonia and Lifou. *Zoosystema, 29*(1), 109-181.

Glover, E. A., Taylor, J. D., & Williams, S. T. (2008). Mangrove-associated lucinid bivalves of the Central Indo-West Pacific: Review of the "Austriella" group with a new genus and species (Mollusca: Bivalvia: Lucinidae). *Raffles Bull. Zool.*, 25-40.

Grieshaber, M. K., Hardewig, I., Kreutzer, U., & Portner, H. O. (1994). Physiological and metabolic responses to hypoxia in invertebrates. *Rev. Physiol. Biochem. Pharmacol., 125*, 43-147.

Gros, O., Darrasse, A., Durand, P., Frenkiel, L., & Moueza, M. (1996). Environmental transmission of a sulfur-oxidizing bacterial gill endosymbiont in the tropical lucinid bivalve *Codakia orbicularis*. *Appl. Environ. Microbiol., 62*(7), 2324-2330.

Gros, O., De Wulf-Durand, P., Frenkiel, L., & Moueza, M. (1998a). Putative environmental transmission of sulfur-oxidizing bacterial symbionts in tropical lucinid bivalves inhabiting various environments. *FEMS Microbiol. Lett., 160*(2), 257-262.

Gros, O., Duplessis, M. R., & Felbeck, H. (1999). Embryonic development and endosymbiont transmission mode in the symbiotic clam *Lucinoma aequizonata* (Bivalvia : Lucinidae). *Invertebr. Reprod. Dev., 36*(1-3), 93-103.

Gros, O., Elisabeth, N. H., Gustave, S. D., Caro, A., & Dubilier, N. (2012). Plasticity of symbiont acquisition throughout the life cycle of the shallow-water tropical lucinid *Codakia orbiculata* (Mollusca: Bivalvia). *Environ. Microbiol., 14*(6), 1584-1595.

Gros, O., Frenkiel, L., & Moueza, M. (1998b). Gill filament differentiation and experimental colonization by symbiotic bacteria in aposymbiotic juveniles of *Codakia orbicularis* (Bivalvia : Lucinidae). *Invertebr. Reprod. Dev., 34*(2-3), 219-231.

Gros, O., Liberge, M., & Felbeck, H. (2003). Interspecific infection of aposymbiotic juveniles of *Codakia orbicularis* by various tropical lucinid gill-endosymbionts. *Mar. Biol., 142*(1), 57-66.

Gruber-Vodicka, H. R., Dirks, U., Leisch, N., Baranyi, C., Stoecker, K., Bulgheresi, S., et al. (2011). *Paracatenula*, an ancient symbiosis between thiotrophic Alphaproteobacteria and catenulid flatworms. *Proc. Natl. Acad. Sci. U. S. A., 108*(29), 12078-12083.

Grzymski, J. J., Murray, A. E., Campbell, B. J., Kaplarevic, M., Gao, G. R., Lee, C., et al. (2008). Metagenome analysis of an extreme microbial symbiosis reveals eurythermal

adaptation and metabolic flexibility. *Proc. Natl. Acad. Sci. U. S. A., 105*(45), 17516-17521.

Gustafson, R. G., & Reid, R. G. B. (1988). Association of bacteria with larvae of the gutless protobranch bivalve *Solemya reidi* (Cryptodonta, Solemyidae). *Mar. Biol., 97*(3), 389-401.

Haeder, S., Wirth, R., Herz, H., & Spiteller, D. (2009). Candicidin-producing *Streptomyces* support leaf-cutting ants to protect their fungus garden against the pathogenic fungus *Escovopsis*. *Proc. Natl. Acad. Sci. U. S. A., 106*(12), 4742-4746.

Harmer, T. L., Rotjan, R. D., Nussbaumer, A. D., Bright, M., Ng, A. W., DeChaine, E. G., et al. (2008). Free-living tube worm endosymbionts found at deep-sea vents. *Appl. Environ. Microbiol., 74*(12), 3895-3898.

Heindl, N. R., Gruber-Vodicka, H. R., Bayer, C., Luecker, S., Ott, J. A., & Bulgheresi, S. (2011). First detection of thiotrophic symbiont phylotypes in the pelagic marine environment. *FEMS Microbiol. Ecol., 77*(1), 223-227.

Hentschel, U., Steinert, M., & Hacker, J. (2000). Common molecular mechanisms of symbiosis and pathogenesis. *Trends Microbiol., 8*(5), 226-231.

Hettich, R. L., Sharma, R., Chourey, K., & Giannone, R. J. (2012). Microbial metaproteomics: identifying the repertoire of proteins that microorganisms use to compete and cooperate in complex environmental communities. *Curr. Opin. Microbiol., 15*, 1-8.

Hu, B., Du, J., Zou, R. Y., & Yuan, Y. J. (2010). An environment-sensitive synthetic microbial ecosystem. *Plos One, 5*(5).

Hurtado, L. A., Mateos, M., Lutz, R. A., & Vrijenhoek, R. C. (2003). Coupling of bacterial endosymbiont and host mitochondrial genomes in the hydrothermal vent clam *Calyptogena magnifica*. *Appl. Environ. Microbiol., 69*(4), 2058-2064.

Jan, C., Petersen, J. M., Werner, J., Huang, S., Teeling, H., Glockner, F. O., et al. (in preparation). The gill chamber epibiosis of deep-sea *Rimicaris exoculata* shrimp revisited by metagenomics and discovery of zetaproteobacterial epibionts.

Jannasch, H. W., & Wirsen, C. O. (1979). Chemosynthetic primary production at East Pacific sea-floor spreading centers. *Bioscience, 29*(10), 592-598.

Kadar, E., Bettencourt, R., Costa, V., Santos, R. S., Lobo-Da-Cunha, A., & Dando, P. (2005). Experimentally induced endosymbiont loss and re-acquirement in the hydrothermal vent bivalve *Bathymodiolus azoricus*. *J. Exp. Mar. Biol. Ecol., 318*(1), 99-110.

Kaiser, D. (2006). Cell-cell interactions. In M. Dworkin, S. I. Falkow, E. Rosenberg, K.-H. Schleifer & E. Stackebrandt (Eds.), *The Prokaryotes* (Vol. 1, pp. 221-245). New York: Springer.

Kaltenpoth, M., Gottler, W., Herzner, G., & Strohm, E. (2005). Symbiotic bacteria protect wasp larvae from fungal infestation (vol 15, pg 475, 2005). *Curr. Biol., 15*(9), 882-882.

Kenk, V. C., & B.R., W. (1985). A new mussel (Bivalvia, Mytilidae) from hydrothermal vents in the Galapagos Rift zone. *Malacologia, 26*, 253-271.

Kimbell, J. R., & McFall-Ngai, M. J. (2004). Symbiont-induced changes in host actin during the onset of a beneficial animal-bacterial association. *Appl. Environ. Microbiol., 70*(3), 1434-1441.

Kleiner, M., Petersen, J. M., & Dubilier, N. (submitted). Convergent and divergent evolution of metabolism in sulfur-oxidizing symbionts and the role of horizontal gene transfer. *Curr. Opin. Microbiol.*

Kleiner, M., Wentrup, C., Lott, C., Teeling, H., Wetzel, S., Young, J., et al. (2012). Metaproteomics of a gutless marine worm and its symbiotic microbial community reveal unusual pathways for carbon and energy use. *Proc. Natl. Acad. Sci. U. S. A., 109*(19), E1173-1182.

Kleiner, M., Woyke, T., Ruehland, C., & Dubilier, N. (2011). The *Olavius algarvensis* metagenome revisited: lessons learned from the analysis of the low-diversity microbial consortium of a gutless marine worm. In F. J. de Brujin (Ed.), *Handbook of Molecular Microbial Ecology II: Metagenomics in Different Habitats*. New York: Wilez/Blackwell.

Kochevar, R. E., Childress, J. J., Fisher, C. R., & Minnich, E. (1992). The methane mussel: roles of symbiont and host in the metabolic utilization of methane. *Mar. Biol., 112*, 389-401.

Kouris, A., Juniper, S. K., Frebourg, G., & Gaill, F. (2007). Protozoan-bacterial symbiosis in a deep-sea hydrothermal vent folliculinid ciliate (*Folliculinopsis* sp.) from the Juan de Fuca Ridge. *Mar. Ecol. Evol. Pers., 28*(1), 63-71.

Krieger, J. (2000). Funktion und Übertragung endosymbiotischer Bakterien bei bakteriensymbiontischen, darmlosen marinen Oligochaeten. (Function and transmission of endosymbiotic bacteria in gutless marine oligochaetes.). *Dept. of Biology, PhD*, University of Hamburg, Germany.

Krieger, J., Giere, O., & Dubilier, N. (2000). Localization of RubisCO and sulfur in endosymbiotic bacteria of the gutless marine oligochaete *Inandrilus leukodermatus* (Annelida). *Mar. Biol., 137*(2), 239-244.

Krueger, D. M., Gustafson, R. G., & Cavanaugh, C. M. (1996). Vertical transmission of chemoautotrophic symbionts in the bivalve *Solemya velum* (Bivalvia: Protobranchia). *Biol. Bull., 190*(2), 195-202.

Krylova, E. M., Sahling, H., & Janssen, R. (2010). Abyssogena: a new genus of the family Vesicomyidae (Bivalvia) from deep-water vents and seeps. *J. Molluscan Stud., 76*, 107-132.

Kuwahara, H., Takaki, Y., Yoshida, T., Shimamura, S., Takishita, K., Reimer, J. D., et al. (2008). Reductive genome evolution in chemoautotrophic intracellular symbionts of deep-sea *Calyptogena* clams. *Extremophiles, 12*(3), 365-374.

Kuwahara, H., Yoshida, T., Takaki, Y., Shimamura, S., Nishi, S., Harada, M., et al. (2007). Reduced genome of the thioautotrophic intracellular symbiont in a deep-sea clam, *Calyptogena okutanii*. *Curr. Biol., 17*(10), 881-886.

Kuypers, M. M. (2007). Microbiology. Sizing up the uncultivated majority. *Science, 317*(5844), 1510-1511.

Kuypers, M. M. M., & Jorgensen, B. B. (2007). The future of single-cell environmental microbiology. *Environ. Microbiol., 9*(1), 6-7.

Lechene, C., Hillion, F., McMahon, G., Benson, D., Kleinfeld, A. M., Kampf, J. P., et al. (2006). High-resolution quantitative imaging of mammalian and bacterial cells using stable isotope mass spectrometry. *J. Biol., 5*(6), 20.

Lechene, C. P., Luyten, Y., McMahon, G., & Distel, D. L. (2007). Quantitative imaging of nitrogen fixation by individual bacteria within animal cells. *Science, 317*(5844), 1563-1566.

Li, T., Wu, T. D., Mazeas, L., Toffin, L., Guerquin-Kern, J. L., Leblon, G., et al. (2008). Simultaneous analysis of microbial identity and function using NanoSIMS. *Environ. Microbiol., 10*(3), 580-588.

Margulis, L. (1970). *Origin of eukaryotic cells; evidence and research implications for a theory of the origin and evolution of microbial, plant, and animal cells on the Precambrian earth*: New Haven, Yale University Press.

Margulis, L. (1993). *Symbiosis in cell evolution*. New York: W. H. Freeman.

Margulis, L., & Fester, R. (1991). Bellagio conference and book. Symbiosis as source of evolutionary innovation: speciation and morphogenesis. Conference-June 25-30, 1989, Bellagio Conference Center, Italy. *Symbiosis, 11*, 93-101.

Markert, S., Arndt, C., Felbeck, H., Becher, D., Sievert, S. M., Hugler, M., et al. (2007). Physiological proteomics of the uncultured endosymbiont of *Riftia pachyptila*. *Science, 315*(5809), 247-250.

McCutcheon, J. P., & Moran, N. A. (2007). Parallel genomic evolution and metabolic interdependence in an ancient symbiosis. *Proc. Natl. Acad. Sci. U. S. A., 104*(49), 19392-19397.

McFall-Ngai, M. J. (2001). Identifying 'prime suspects': symbioses and the evolution of multicellularity. *Comp. Biochem. Physiol. B Biochem. Mol. Biol., 129*(4), 711-723.

McFall-Ngai, M. J. (2002). Unseen forces: the influence of bacteria on animal development. *Dev. Biol., 242*(1), 1-14.

Moran, N. A. (2003). Tracing the evolution of gene loss in obligate bacterial symbionts. *Curr. Opin. Microbiol., 6*(5), 512-518.

Moran, N. A. (2007). Symbiosis as an adaptive process and source of phenotypic complexity. *Proc. Natl. Acad. Sci. U. S. A.*, 0611659104.

Moran, N. A., McCutcheon, J. P., & Nakabachi, A. (2008). Genomics and evolution of heritable bacterial symbionts. *Annu. Rev. Genet., 42*, 165-190.

Moran, N. A., McLaughlin, H. J., & Sorek, R. (2009). The dynamics and time scale of ongoing genomic erosion in symbiotic bacteria. *Science, 323*(5912), 379-382.

Moran, N. A., & Plague, G. R. (2004). Genomic changes following host restriction in bacteria. *Curr. Opin. Genet. Dev., 14*(6), 627-633.

Moya, A., Pereto, J., Gil, R., & Latorre, A. (2008). Learning how to live together: genomic insights into prokaryote-animal symbioses. *Nat. Rev. Genet., 9*(3), 218-229.

Musat, N., Foster, R., Vagner, T., Adam, B., & Kuypers, M. M. (2012). Detecting metabolic activities in single cells, with emphasis on nanoSIMS. *FEMS Microbiol. Rev., 36*(2), 486-511.

Musat, N., Halm, H., Winterholler, B., Hoppe, P., Peduzzi, S., Hillion, F., et al. (2008). A single-cell view on the ecophysiology of anaerobic phototrophic bacteria. *Proc. Natl. Acad. Sci. U. S. A., 105*(46), 17861-17866.

Nelson, D. C., & Fisher, C. R. (1995). Chemoautotrophic and methanotrophic endosymbiotic bacteria at deep-sea vents and seeps. In D. M. Karl (Ed.), *The Microbiology of Deep-Sea Hydrothermal Vents* (pp. 125-167). Boca Raton: CRC Press.

Newton, I. L. G., Woyke, T., Auchtung, T. A., Dilly, G. F., Dutton, R. J., Fisher, M. C., et al. (2007). The *Calyptogena magnifica* chemoautotrophic symbiont genome. *Science, 315*(5814), 998-1000.

Noriega, B. E. (2011). Symbiont transmission in *Olavius algarvensis*. *Symbiosis Group, Bachelor thesis*, Max Planck Institute for Marine Microbiology, Germany.

Nussbaumer, A. D., Fisher, C. R., & Bright, M. (2006). Horizontal endosymbiont transmission in hydrothermal vent tubeworms. *Nature, 441*(7091), 345-348.

Nylander, J. A. A., Erseus, C., & Kallersjo, M. (1999). A test of monophyly of the gutless Phallodrilinae (Oligochaeta, Tubificidae) and the use of a 573-bp region of the mitochondrial cytochrome oxidase I gene in analysis of annelid phylogeny. *Zool. Scr., 28*(3-4), 305-313.

Ochman, H., & Moran, N. A. (2001). Genes lost and genes found: evolution of bacterial pathogenesis and symbiosis. *Science, 292*(5519), 1096-1099.

Oliver, K. M., Degnan, P. H., Burke, G. R., & Moran, N. A. (2010). Facultative symbionts in aphids and the horizontal transfer of ecologically important traits. *Annu. Rev. Entomol., 55*, 247-266.

Page, H. M., Fisher, C. R., & Childress, J. J. (1990). Role of filter-feeding in the nutritional biology of a deep-sea mussel with methanotrophic symbionts. *Mar. Biol., 104*(2), 251-257.

Paracer, S., & Ahmadjian, V. (2000). *Symbiosis. An Introduction to Biological Associations*. New York: Oxford University Press.

Parkhill, J., Sebaihia, M., Preston, A., Murphy, L. D., Thomson, N., Harris, D. E., et al. (2003). Comparative analysis of the genome sequences of *Bordetella pertussis*, *Bordetella parapertussis* and *Bordetella bronchiseptica*. *Nat. Genet., 35*(1), 32-40.

Paulsen, I. T., Seshadri, R., Nelson, K. E., Eisen, J. A., Heidelberg, J. F., Read, T. D., et al. (2002). The *Brucella suis* genome reveals fundamental similarities between animal and plant pathogens and symbionts. *Proc. Natl. Acad. Sci. U. S. A., 99*(20), 13148-13153.

Peek, A. S., Feldman, R. A., Lutz, R. A., & Vrijenhoek, R. C. (1998). Cospeciation of chemoautotrophic bacteria and deep sea clams. *Proc. Natl. Acad. Sci. U. S. A., 95*(17), 9962-9966.

Pernice, M., Meibom, A., Van Den Heuvel, A., Kopp, C., Domart-Coulon, I., Hoegh-Guldberg, O., et al. (2012). A single-cell view of ammonium assimilation in coral-dinoflagellate symbiosis. *ISME J, 6*(7), 1314-1324.

Pernthaler, A., Pernthaler, J., & Amann, R. (2002). Fluorescence in situ hybridization and catalyzed reporter deposition for the identification of marine bacteria. *Appl. Environ. Microbiol., 68*(6), 3094-3101.

Petersen, J. M., & Dubilier, N. (2009). Methanotrophic symbioses in marine invertebrates. *Environ. Microbiol. Rep., 1*(5), 319-335.

Petersen, J. M., Ramette, A., Lott, C., Cambon-Bonavita, M. A., Zbinden, M., & Dubilier, N. (2010). Dual symbiosis of the vent shrimp *Rimicaris exoculata* with filamentous

gamma- and epsilonproteobacteria at four Mid-Atlantic Ridge hydrothermal vent fields. *Environ. Microbiol., 12*(8), 2204-2218.

Petersen, J. M., Wentrup, C., Verna, C., Knittel, K., & Dubilier, N. (2012). Origins and evolutionary flexibility of chemosynthetic symbionts from deep-sea animals. *Biol. Bull., 223*, 123-137.

Petersen, J. M., Zielinski, F. U., Pape, T., Seifert, R., Moraru, C., Amann, R., et al. (2011). Hydrogen is an energy source for hydrothermal vent symbioses. *Nature, 476*(7359), 176-180.

Pflugfelder, B., Cary, S. C., & Bright, M. (2009). Dynamics of cell proliferation and apoptosis reflect different life strategies in hydrothermal vent and cold seep vestimentiferan tubeworms. *Cell Tissue Res., 337*(1), 149-165.

Polerecky, L., Adam, B., Milucka, J., Musat, N., Vagner, T., & Kuypers, M. M. (2012). Look@NanoSIMS-a tool for the analysis of nanoSIMS data in environmental microbiology. *Environ. Microbiol., 14*(4), 1009-1023.

Purnick, P. E. M., & Weiss, R. (2009). The second wave of synthetic biology: from modules to systems. *Nat. Rev. Mol. Cell Biol., 10*(6), 410-422.

Raggi, L. (2010). Bacterial-invertebrate symbioses: from an asphalt cold seep to shallow waters. *Symbiosis Group, PhD*, University of Bremen, Germany.

Rau, G. H. (1981). Hydrothermal vent clam and tube worm $^{13}C/^{12}C$: further evidence of nonphotosynthetic food sources. *Science, 213*(4505), 338-340.

Reid, R. G. B. (1980). Aspects of the biology of a gutless species of *Solemya* (Bivalvia: Protobranchia). *Can. J. Zool., 58*, 386-393.

Rinke, C., Lee, R., Katz, S., & Bright, M. (2007). The effects of sulphide on growth and behaviour of the thiotrophic *Zoothamnium niveum* symbiosis. *Proc. R. Soc. B Biol. Sci., 274*(1623), 2259-2269.

Robidart, J. C., Bench, S. R., Feldman, R. A., Novoradovsky, A., Podell, S. B., Gaasterland, T., et al. (2008). Metabolic versatility of the *Riftia pachyptila* endosymbiont revealed through metagenomics. *Environ. Microbiol., 10*(3), 727-737.

Robidart, J. C., Roque, A., Song, P., & Girguis, P. R. (2011). Linking hydrothermal geochemistry to organismal physiology: physiological versatility in *Riftia pachyptila* from sedimented and basalt-hosted vents. *PLoS One, 6*(7), e21692.

Ruby, E. G., Wirsen, C. O., & Jannasch, H. W. (1981). Chemolithotrophic sulfur-oxidizing bacteria from the Galapagos Rift hydrothermal vents. *Appl. Environ. Microbiol., 42*(2), 317-324.

Ruehland, C., Blazejak, A., Lott, C., Loy, A., Erseus, C., & Dubilier, N. (2008). Multiple bacterial symbionts in two species of co-occurring gutless oligochaete worms from Mediterranean sea grass sediments. *Environ. Microbiol., 10*(12), 3404-3416.

Ruehland, C., & Dubilier, N. (2010). Gamma- and epsilonproteobacterial ectosymbionts of a shallow-water marine worm are related to deep-sea hydrothermal vent ectosymbionts. *Environ. Microbiol., 12*(8), 2312-2326.

Sachs, J. L., & Wilcox, T. P. (2006). A shift to parasitism in the jellyfish symbiont *Symbiodinium microadriaticum*. *Proc. Biol. Sci., 273*(1585), 425-429.

Salerno, J. L., Macko, S. A., Hallam, S. J., Bright, M., Won, Y. J., McKiness, Z., et al. (2005). Characterization of symbiont populations in life-history stages of mussels from chemosynthetic environments. *Biol. Bull., 208*(2), 145-155.

Sapp, J. (1994). *Evolution by Association. A History of Symbiosis*. New York: Oxford University Press.

Schink, B., & Stams, A. J. M. (2006). Syntrophism among prokaryotes. In M. Dworkin, S. I. Falkow, E. Rosenberg, K.-H. Schleifer & E. Stackebrandt (Eds.), *The Prokaryotes* (Vol. 2, pp. 309-335). New York: Springer.

Schmidt, C., Vuillemin, R., Le Gall, C., Gaill, F., & Le Bris, N. (2008). Geochemical energy sources for microbial primary production in the environment of hydrothermal vent shrimps. *Mar. Chem., 108*(1-2), 18-31.

Schoell, M. (1988). Multiple origins of methane in the earth. *Chem. Geol., 71*(1-3), 1-10.

Schweder, T., Markert, S., & Hecker, M. (2008). Proteomics of marine bacteria. *Electrophoresis, 29*(12), 2603-2616.

Siegl, A., Kamke, J., Hochmuth, T., Piel, J., Richter, M., Liang, C., et al. (2010). Single-cell genomics reveals the lifestyle of Poribacteria, a candidate phylum symbiotically associated with marine sponges. *ISME J, 5*(1), 61-70.

Siguier, P., Filee, J., & Chandler, M. (2006). Insertion sequences in prokaryotic genomes. *Curr. Opin. Microbiol., 9*(5), 526-531.

Sjolin, E., Erseus, C., & Kallersjo, M. (2005). Phylogeny of Tubificidae (Annelida, Clitellata) based on mitochondrial and nuclear sequence data. *Mol. Phylogenet. Evol., 35*(2), 431-441.

Southward, E. C. (2008). The morphology of bacterial symbioses in the gills of mussels of the genera *Adipicola* and *Idas* (Bivalvia : Mytilidae). *J. Shellfish Res., 27*(1), 139-146.

Stahl, D. A., Hullar, M., & Davidson, S. (2006). The structure and function of microbial communities. In M. Dworkin, S. I. Falkow, E. Rosenberg, K.-H. Schleifer & E. Stackebrandt (Eds.), *The Prokaryotes* (Vol. 1, pp. 299-327). New York: Springer.

Starr, M. P. (1975). A generalized scheme for classifying organismic associations in symbiosis. *Symp. Soc. Exp. Biol., 29*, 1-20.

Stein, C. A., & Stein, S. (1994). Constraints on hydrothermal heat flux through the oceanic lithosphere from global heat flow. *J. Geophys. Res., 99*, 3081-3096.

Steward, G. F., & Rappe, M. S. (2007). What's the 'meta' with metagenomics? *ISME J, 1*(2), 100-102.

Stewart, F. J., & Cavanaugh, C. M. (2006). Bacterial endosymbioses in *Solemya* (Mollusca : Bivalvia) - Model systems for studies of symbiont-host adaptation. *Antonie Leeuwenhoek, 90*(4), 343-360.

Stewart, F. J., & Cavanaugh, C. M. (2009). Pyrosequencing analysis of endosymbiont population structure: co-occurrence of divergent symbiont lineages in a single vesicomyid host clam. *Environ. Microbiol., 11*(8), 2136-2147.

Stewart, F. J., Dmytrenko, O., Delong, E. F., & Cavanaugh, C. M. (2011). Metatranscriptomic analysis of sulfur oxidation genes in the endosymbiont of *Solemya velum*. *Front Microbiol., 2*, 134.

Stewart, F. J., Newton, I. L., & Cavanaugh, C. M. (2005). Chemosynthetic endosymbioses: adaptations to oxic-anoxic interfaces. *Trends Microbiol., 13*(9), 439-448.

Stewart, F. J., Young, C. R., & Cavanaugh, C. M. (2008). Lateral symbiont acquisition in a maternally transmitted chemosynthetic clam endosymbiosis. *Mol. Biol. Evol., 25*(4), 673-687.

Stewart, F. J., Young, C. R., & Cavanaugh, C. M. (2009). Evidence for homologous recombination in intracellular chemosynthetic clam symbionts. *Mol. Biol. Evol., 26*(6), 1391-1404.

Suen, G., Scott, J. J., Aylward, F. O., Adams, S. M., Tringe, S. G., Pinto-Tomas, A. A., et al. (2010). An insect herbivore microbiome with high plant biomass-degrading capacity. *Plos Genetics, 6*(9).

Szathmary, E., & Smith, J. M. (1995). The major evolutionary transitions. *Nature, 374*(6519), 227-232.

Taylor, J. D., & Glover, E. A. (2006). Lucinidae (Bivalvia) - the most diverse group of chemosymbiotic molluscs. *Zool. J. Linn. Soc., 148*(3), 421-438.

Taylor, J. D., Glover, E. A., & Kiel, S. (2010). Chemosymbiotic bivalves. In S. Kiel (Ed.), *Vent and Seep Biota: Aspects from Microbes to Ecosystems* (Vol. 33, pp. 107-135): Springer Netherlands.

van Dover, C. L. (2000). *The ecology of deep-sea hydrothermal vents*. Princeton, New Jersey: Princeton University Press.

van Hellemond, J. J., van der Klei, A., van Weelden, S. W. H., & Tielens, A. G. M. (2003). Biochemical and evolutionary aspects of anaerobically functioning mitochondria. *Philosophical Transactions of the Royal Society of London Series B-Biological Sciences, 358*(1429), 205-213.

Verna, C., Ramette, A., Wiklund, H., Dahlgren, T. G., Glover, A. G., Gaill, F., et al. (2010). High symbiont diversity in the bone-eating worm *Osedax mucofloris* from shallow whale-falls in the North Atlantic. *Environ. Microbiol., 12*(8), 2355-2370.

von Cosel, R. (2002). A new species of bathymodioline mussel (Mollusca, Bivalvia, Mytilidae) from Mauritania (West Africa), with comments on the genus *Bathymodiolus* Kenk & Wilson, 1985. *Zoosystema, 24*(2), 259-271.

Vrijenhoek, R. C. (2010). Genetics and evolution of deep-sea chemosynthetic bacteria and their invertebrate hosts. In S. Kiel (Ed.), *Vent and Seep Biota: Aspects from Microbes to Ecosystems* (Vol. 33, pp. 15-49): Springer Netherlands.

Walker, A., & Crossman, L. C. (2007). This place is big enough for both of us. *Nat. Rev. Microbiol., 5*(2), 90-92.

Warnecke, F., & Hugenholtz, P. (2007). Building on basic metagenomics with complementary technologies. *Genome Biol., 8*(12), 231.

Watsuji, T. O., Nakagawa, S., Tsuchida, S., Toki, T., Hirota, A., Tsunogai, U., et al. (2010). Diversity and function of epibiotic microbial communities on the galatheid crab, *Shinkaia crosnieri*. *Microbes Environ., 25*(4), 288-294.

Wendeberg, A., Zielinski, F. U., Borowski, C., & Dubilier, N. (2012). Expression patterns of mRNAs for methanotrophy and thiotrophy in symbionts of the hydrothermal vent mussel *Bathymodiolus puteoserpentis*. *ISME J., 6*(1), 104-112.

Wernegreen, J. J. (2005). For better or worse: genomic consequences of intracellular mutualism and parasitism. *Curr. Opin. Genet. Dev., 15*(6), 572-583.

Won, Y. J., Hallam, S. J., O'Mullan, G. D., Pan, I. L., Buck, K. R., & Vrijenhoek, R. C. (2003). Environmental acquisition of thiotrophic endosymbionts by deep-sea mussels of the genus *Bathymodiolus*. *Appl. Environ. Microbiol., 69*, 6785-6792.

Won, Y. J., Jones, W. J., & Vrijenhoek, R. C. (2008). Absence of cospeciation between deep-sea Mytilids and their thiotrophic endosymbionts. *J. Shellfish Res., 27*(1), 129-138.

Woyke, T., Teeling, H., Ivanova, N. N., Huntemann, M., Richter, M., Gloeckner, F. O., et al. (2006). Symbiosis insights through metagenomic analysis of a microbial consortium. *Nature, 443*(7114), 950-955.

Zhang, J.-Z., & Millero, F. j. (1993). The products from the oxidation of H_2S in seawater. *Geochim. Cosmochim. Acta., 57*(8), 1705/1718.

Appendix-A

Reference: *Biol. Bull.* **223:** 123–137. (August 2012)

Origins and Evolutionary Flexibility of Chemosynthetic Symbionts From Deep-Sea Animals

JILLIAN M. PETERSEN*, CECILIA WENTRUP, CAROLINE VERNA, KATRIN KNITTEL, AND NICOLE DUBILIER

Max Planck Institute for Marine Microbiology, Celsiusstrasse 1, 28359 Bremen, Germany

Abstract. Bathymodiolin mussels dominate hydrothermal vent and cold seep communities worldwide. Symbiotic associations with chemosynthetic sulfur- and methane-oxidizing bacteria that provide for their nutrition are the key to their ecological and evolutionary success. The current paradigm is that these symbioses evolved from two free-living ancestors, one methane-oxidizing and one sulfur-oxidizing bacterium. In contrast to previous studies, our phylogenetic analyses of the bathymodiolin symbionts show that both the sulfur and the methane oxidizers fall into multiple clades interspersed with free-living bacteria, many of which were discovered recently in metagenomes from marine oxygen minimum zones. We therefore hypothesize that symbioses between bathymodiolin mussels and free-living sulfur- and methane-oxidizing bacteria evolved multiple times in convergent evolution. Furthermore, by 16S rRNA sequencing and fluorescence *in situ* hybridization, we show that close relatives of the bathymodiolin symbionts occur on hosts belonging to different animal phyla: *Raricirrus beryli*, a terebellid polychaete from a whale-fall, and a poecilosclerid sponge from a cold seep. The host range within the bathymodiolin symbionts is therefore greater than previously recognized, confirming the remarkable flexibility of these symbiotic associations.

Introduction

Intimate associations between chemosynthetic bacteria and marine invertebrates are widespread in the world's oceans. They are prominent in a range of habitats including deep-sea hydrothermal vents and cold seeps, and shallow-water sea grass and coral reef sediments (for example, Cavanaugh *et al.*, 2006; Dubilier *et al.*, 2008). These habitats all provide the energy sources needed by the bacteria—reduced compounds such as hydrogen and hydrogen sulfide (used by the sulfur-oxidizing symbionts), methane (used by the methane-oxidizing symbionts), and oxidized compounds such as oxygen and nitrate (Cavanaugh *et al.*, 1981; Childress *et al.*, 1986; Hentschel and Felbeck, 1993; Petersen *et al.*, 2011). Chemosynthetic bacteria use the energy released during oxidation of these reduced compounds to fix carbon dioxide or methane carbon into organic matter, thus providing their animal hosts with a source of nutrition (Stewart *et al.*, 2005; DeChaine and Cavanaugh, 2006; Petersen and Dubilier, 2009, 2010). The establishment of symbioses with chemosynthetic bacteria is the evolutionary innovation that allowed invertebrate animals to thrive in novel and in some cases extreme habitats such as deep-sea hydrothermal vents and cold seeps where the input of organic matter from photosynthesis is extremely low (Van Dover, 2000). However, how these associations are established remains poorly understood.

The first molecular studies showed that the diversity of chemosynthetic symbionts is limited. For example, in 1994, Distel and Cavanaugh showed that all sulfur-oxidizing symbionts from diverse host animals form a distinct monophyletic clade (Appendix Fig. A1) (Distel and Cavanaugh, 1994). However, as more sequences from symbiotic and free-living bacteria have become available, a different picture is beginning to emerge, and recent analyses have uncovered the remarkable phylogenetic diversity of bacterial groups that have established chemosynthetic symbioses. For example, within the Gammaproteobacteria, Dubilier *et al.* (2008) identified at least nine distinct lineages of chemosynthetic symbionts that are interspersed with free-living

Received 30 March 2012; accepted 12 July 2012.

* To whom correspondence should be addressed. E-mail: jmpeters@mpi-bremen.de

Abbreviations: CARD-FISH, catalyzed reporter deposition–fluorescence *in situ* hybridization; MOX, methane-oxidizing; OMZ, oxygen minimum zone; SOX, sulfur-oxidizing.

bacteria, indicating that chemosynthetic symbioses with marine invertebrates have evolved in at least nine bacterial groups. Furthermore, chemosynthetic symbionts are not limited to the Gammaproteobacteria, as sulfur-oxidizing bacteria from the Alpha- and Epsilonproteobacteria have also formed associations with numerous marine invertebrates (for example, Polz and Cavanaugh, 1995; Suzuki *et al.*, 2005; Goffredi *et al.*, 2008; Gruber-Vodicka *et al.*, 2011). The evolutionary diversity of other symbioses besides chemosynthetic associations is also beginning to be recognized: as Sachs *et al.* (2011) show in their recent analysis of the evolutionary history of bacterial symbiosis at broad phylogenetic scales, associations between eukaryotes and bacteria have evolved at least 42 times.

Bathymodiolin mussels within the family Mytilidae are prominent members of deep-sea chemosynthetic communities in habitats such as hydrothermal vents and cold seeps and on sunken organic debris such as wood- and whale-falls worldwide. All bathymodiolin mussels investigated to date live in obligate symbiosis with chemosynthetic bacteria (reviewed by DeChaine and Cavanaugh, 2006; Petersen and Dubilier, 2009; Duperron, 2010). A number of bathymodiolin genera have been described on the basis of morphology, including *Bathymodiolus, Gigantidas, Benthomodiolis, Adipicola,* and *Idas*, but molecular studies suggest that they may be even more diverse (Duperron, 2010). Some bathymodiolins host only sulfur-oxidizing (SOX) symbionts and some host only methane-oxidizing (MOX) symbionts. Some species host both SOX and MOX bacteria in a dual symbiosis.

Although it is widely accepted that chemosynthetic symbioses evolved multiple times from different bacterial lineages, the symbionts of closely related host animals in many cases form monophyletic clades that exclude the symbionts of other animals and all free-living bacteria. For example, in all analyses to date, 16S rRNA gene sequences from the methane-oxidizing symbionts of bathymodiolin mussels form a monophyletic clade that is a sister-group to the free-living cultivated aerobic methanotrophs of the genera *Methylobacter*, *Methylosarcina*, and *Methylomicrobium* (reviewed by Cavanaugh *et al.*, 2006; DeChaine and Cavanaugh, 2006; Dubilier *et al.*, 2008; Petersen and Dubilier, 2009, 2010; Duperron, 2010). Similarly, previous analyses showed that the SOX symbionts of bathymodiolin mussels grouped with each other in a single clade, with the symbionts of vesicoymid clams as their closest relatives (Distel, 1998). These bathymodiolin symbiont clades contained very few sequences from free-living bacteria, usually clone sequences from samples taken directly in mussel habitats. As the bathymodiolin SOX and MOX symbionts are thought to be horizontally transmitted and acquired by each host generation from the environment, these few environmental sequences could represent either free-living stages of the symbiotic bacteria or symbionts released by the mussels (Won *et al.*, 2003, 2008; Kadar *et al.*, 2005; DeChaine *et al.*, 2006). The monophyly of bathymodiolin SOX and MOX bacteria identified in previous studies indicated that these symbioses evolved only twice in bathymodiolin mussels, once with sulfur-oxidizing bacteria and once with methane-oxidizing bacteria.

Recently, large-scale metagenomic and 16S rRNA gene diversity studies discovered close free-living relatives of the bathymodiolin SOX and MOX symbionts that are abundant in marine oxygen minimum zones and in cold seep sediments worldwide (Walsh *et al.*, 2009; Canfield *et al.*, 2010; Zaikova *et al.*, 2010). However, the phylogenetic relationships between these widespread free-living bacteria and the bathymodiolin symbionts are unclear, because no study has analyzed a large number of sequences from both groups. Furthermore, sequence data are continually becoming available due to ongoing sampling and sequencing efforts, and tools for analyzing these data have been developed. Such tools include ARB-Silva, a curated database of full-length high-quality 16S rRNA gene sequences including those from genome and metagenome studies (Pruesse *et al.*, 2007). Finally, relatives of the bathymodiolin SOX symbionts were recently identified in clone libraries from cold seep and hydrothermal vent sponges, indicating that the host range of these symbionts may be wider than previously assumed (Nishijima *et al.*, 2010). Here we show by 16S rRNA sequencing and CARD-FISH (catalyzed reporter deposition–fluorescence *in situ* hybridization) that close relatives of the bathymodiolin SOX and MOX symbionts associate with two other marine invertebrates—*Raricirrus beryli*, a polychaete worm found on whale-falls, and a poecilosclerid sponge from a cold seep. In addition, we analyzed the phylogeny of 16S rRNA genes from the bathymodiolin symbionts and their animal-associated and free-living close relatives to better understand their origins and evolutionary history.

Materials and Methods

Sampling and storage

Specimens of the polychaete *Raricirrus beryli* were collected from a 5.3-m-long minke whale-fall, sunk in the Kosterfjord, Sweden (58°53.1′N; 11°06.4′E) at 125-m depth in October 2003 (Dahlgren *et al.*, 2006). Using a Phantom XL remotely operated vehicle (ROV), we recovered whale bones in 2004, 2006, 2007, and 2008. The recovered bones were placed in seawater and transferred to aquaria in the laboratory with flow-through seawater at 8.0 °C, where they were kept for hours to months. *R. beryli* individuals were mostly sampled from the bottom of the aquaria where the whale bones were kept. They were identified as *R. beryli* on the basis of their morphology (Gordon Paterson, Natural History Museum, London, pers. comm.). One individual collected in 2007 was fixed in 96% ethanol.

Table 1

Summary of 16S rRNA clone library analysis of Raricirrus beryli

Individual*	Fixed†	Sampling name	Year sampled	Clone library‡	Clone group	Number of clones#	Description/Best BLAST hits (% identity)¶
1 (A)	EtOH	Rber031	2007	A (86)	1	18 (4)	Bathymodiolin sulfur-oxidizing symbionts (94%–99%)
					2	13	Uncultured Oceanospirallales (93%–95%)
					3	16	Group JTB23, marine invertebrate associates and free-living bacteria from chemosynthetic environments (89%–95%)
					4	2	*Cytophaga fermentans* (89%)
					5	5	Uncultured flexibacteria from chemosynthetic environments (92%–96%)
					6	2	Uncultured *Filifactor* (80%–83%)
					7	11	Uncultured Mollicutes, invertebrate gut associates (84%–89%)
					8	19	Others
2 (A)	PFA	Rber2	2008	A (89)	1	1 (1)	Bathymodiolin sulfur-oxidizing symbionts (94%–99%)
					2	11	*Colwellia psychrerythraea* (95%)
					3	5	*Osedax* endosymbionts (92%–97%)
					4	14	Uncultured *Acidithiobacillus* from chemosynthetic environments (90%)
					5	1	Uncultured *Filifactor* (80%–83%)
					6	57	Others
				B (7)	1	6	Bathymodiolin sulfur-oxidizing symbionts (94%–99%)
					2	1	Others
3 (B)	PFA	Rber5		A (90)	1	24 (4)	Bathymodiolin sulfur-oxidizing symbionts (94%–99%)
					2	30	Uncultured *Acidithiobacillus* from chemosynthetic environments (90%)
					3	5	*Cytophaga fermentans* (89%)
					4	16	Uncultured *Filifactor* (80%–83%)
					5	4	Uncultured Mollicutes, invertebrate gut associates (84%–89%)
					6	11	Others
4 (B)	PFA	Rber3	2008	B (8)	1	6	Bathymodiolin sulfur-oxidizing symbionts (94%–99%)
					2	2	Others
5 (B)	PFA	Rber6	2008	B (6)	1	6	Bathymodiolin sulfur-oxidizing symbionts (94%–99%)
6 (B)	PFA	Rber7	2009	B (15)	1	1	Bathymodiolin sulfur-oxidizing symbionts (94%–99%)
					2	14	Others
7 (B)	PFA	Rber8	2009	B (8)	1	8	Bathymodiolin sulfur-oxidizing symbionts (94%–99%)
8 (B)	PFA	Rber10	2009	B (15)	1	1	Bathymodiolin sulfur-oxidizing symbionts (94%–99%)
					2	14	Others
9 (?)	PFA	Rber1	2008				

* Letters in parentheses refer to the COI haplotype, A or B. A question mark indicates that this individual was embedded whole for CARD-FISH and therefore no COI sequence was available.

† Fixation method: EtOH = ethanol; PFA = paraformaldehyde.

‡ A = clone library constructed with primers GM3 and GM4; B = clone library constructed with primers BMARt193 and GM4. Numbers in parentheses indicate total number of clones screened by partial sequencing.

In parentheses, number of clones fully sequenced.

¶ Others includes clone groups found in only one individual that contained less than four clones.

All other *R. beryli* individuals were washed in sterile seawater and fixed in 1× phosphate-buffered saline (PBS) with 4% formaldehyde for 30 min to 24 h at 4 °C. The samples were washed three times in 1× PBS and stored in 1× PBS/50% ethanol at –20 °C. Details are shown in Table 1.

Unidentified sponges (Antje Boetius, Max Planck Institute for Marine Microbiology, and Alfred Wegener Institute, pers. comm.) attached to pieces of asphalt were collected from the Chapopote asphalt seep in the southern Gulf of Mexico (station 10621-3, dive 83, 21°53.98′N; 93°26.12′W, 2923-m water depth). Samples were collected using the ROV *Quest* (Marum, Bremen) operated from the research vessel *Meteor* during the M67/2 cruise in April 2005. Sponge-asphalt samples were immediately frozen on

board and stored at –20 °C until further processing for DNA extraction or fixed in absolute ethanol for fluorescence *in situ* hybridization (FISH).

DNA extraction and PCR amplification

DNA was extracted from one ethanol-fixed and seven paraformaldehyde-fixed *R. beryli* individuals with a DNeasy Blood and Tissue kit (Qiagen, Hilden, Germany) (Table 1). Cytochrome oxidase I (COI) genes were amplified and sequenced from 8 *R. beryli* individuals to confirm the identity of the hosts. The primers LCO1490 and LCO2198 were used with the following PCR cycling conditions: initial denaturation at 94 °C for 5 min; followed by 35 cycles at 94 °C for 1 min, 42 °C for 1 min, and 72 °C for 1 min; followed by a final elongation step at 72 °C for 10 min (Folmer *et al.*, 1994). Either three or four reactions were pooled to minimize PCR bias. PCR products were directly sequenced in both directions. Two haplotypes were found, which differed at two nucleotide positions (Table 1). BLASTn of these COI sequences showed that the polychaetes were related to members of the family Ctenodrilidae. Three *R. beryli* individuals, one ethanol-fixed and two paraformaldehyde-fixed, were used for 16S rRNA gene sequence analysis (Table 1) using the general bacterial primers GM3F and GM4R (Muyzer *et al.*, 1995) and the following PCR cycling conditions: initial denaturation at 94 °C for 5 min; followed by 20–25 cycles at 94 °C for 1 min, 43 °C for 1 min 30 s, and 72 °C for 2 min; followed by a final elongation step at 72 °C for 10 min. To test how widespread the association of *R. beryli* with bacteria related to the *Bathymodiolus* SOX symbionts is, five additional individuals were used for 16S rRNA gene sequence analysis with the primers BMARt193 forward, designed as a specific probe for the *Bathymodiolus* SOX symbionts (Duperron *et al.*, 2006), and GM4R. The PCR cycling conditions were as follows: initial denaturation at 94 °C for 5 min; followed by 45 cycles at 94 °C for 1 min, 50 °C for 1 min 30 s, and 72 °C for 2 min; followed by a final elongation step at 72 °C for 10 min. The Takara ex Taq polymerase (Takara Bio Inc., Shiga, Japan) was used. At least five PCR products from each host individual were pooled, purified with the QIAquick PCR Purification kit (Qiagen), and run on 1% agarose gels. A band of the correct size was extracted from the gels using a QIAquick Gel Purification kit (Qiagen). For cloning, PCR products were ligated into the PCR4 TOPO vector (Invitrogen, Carlsbad, CA) or into the vector pGEM-T Easy (Promega, Madison, WI) and transformed into *Escherichia coli* TOP10 cells (Invitrogen). Clones were checked for the correct insert size by PCR with vector primers M13F and M13R (Invitrogen). Clones were screened by sequencing primer 907R (Lane *et al.*, 1985). Sequences with lengths between 500 and 900 nt were aligned in ARB (Ludwig *et al.*, 2004) using the Silva database (Pruesse *et al.*, 2007). Representative clones from the *Bathymodiolus* symbiont-related group were chosen for plasmid preparation using the QIAprep Spin Miniprep kit (Qiagen). The plasmid inserts were fully sequenced (both strands) using the following primers: M13F (Invitrogen), M13R (Invitrogen), and 1114F (Lane, 1991). Full sequences were assembled with DNA Baser Sequence Assembler ver. 2.x (2009) (Heracles BioSoft S.R.L., 2012).

Total community DNA was extracted from 40 mg of sponge-asphalt material as described by Zhou *et al.* (1996). This material was used to construct a clone library with general bacterial primers. PCR amplification of 16S rRNA genes, purification, cloning (pGEM-T-Easy vector used), and sequencing were done as described above, with the only exceptions that 30 cycles were used for amplification and GM1F, which binds at *E. coli* positions 518–534 (Muyzer *et al.*, 1993), was used for partial sequencing instead of 907R. A COI gene clone library was constructed with this material using the primers LCO1490 and HCO2198 (Folmer *et al.*, 1994; 38 PCR cycles, conditions as described above for 16S rRNA sponge clone library). BLASTn of the COI sequence showed that the sponge is related to members of the Poecilosclerida. The DNeasy blood and tissue kit (Qiagen, Hilden, Germany) was used to extract DNA from a piece of a second sponge. The COI gene of this individual was amplified and sequenced as described above for *R. beryli*. The resulting sequence had one base difference from the COI sequence of the first sponge individual (A→C at position 56).

Phylogenetic analysis

Full-length (>1400 nt) 16S rRNA gene sequences were imported into the most recent ARB Silva database (release Ref108, 09.09.2011), and aligned with the SINA aligner (Pruesse *et al.*, 2007, 2012). Alignments were manually corrected. Phylogenetic trees were calculated in ARB with maximum likelihood (PhyML and RaXML), parsimony, and neighbor-joining methods. Because the PhyML and RaXML phylogenies had identical branching patterns, we used only PhyML phylogenies in further analyses. In all cases, a positional variability filter for Bacteria excluding the most variable positions was used (Peplies *et al.*, 2008). Maximum likelihood bootstrap values were calculated with 100 resamplings.

Probe design and fluorescence in situ *hybridization*

One *R. beryli* individual (specimen 9, Table 1) was dehydrated in an ethanol series and embedded in paraffin (melting temperature 58–60 °C). This individual was sectioned (sections 3–8 ìm) and mounted on SuperFrost plus slides (Menzel-Gläser, Braunschweig, Germany). Before dewaxing, the slides were incubated for 2 h at paraffin melting temperature. Paraffin was removed in three to four Roti-Histol (Carl Roth, Karlsruhe, Germany) baths, each 10

min, and the sections were rehydrated in an ethanol series. Each section was encircled with a liquid-repellent marker pen (Super Pap Pen, Kisker Biotechnology, Steinfurt, Germany). CARD FISH was done on one *R. beryli* individual with horseradish peroxidase (HRP)-labeled probes (Biomers, Ulm, Germany). The hybridization time was 4–5 h, and CARD was done at room temberature for 1.5 h. Buffer composition was as described in Pernthaler *et al*. (2002). Probe BMARt193 perfectly matched our *R. beryli* bathymodiolin SOX symbiont-related sequences, so we used this probe in CARD-FISH hybridizations with 30% formamide as described in Duperron *et al.* (2006). Probe Non338 (Wallner *et al.*, 1993) was used as a control for background autofluorescence. Sections were additionally stained with 4′,6-diamidino-2-phenylindole (DAPI) 1 μg/ml for 10–20 min at 37 °C.

The probe BMARt193 (Duperron *et al.*, 2006) had a single mismatch to the sequences from the Chapopote asphalt-seep sponge that were related to the bathymodiolin SOX symbionts. We modified this probe to match the sponge-associated bacteria. The sequence of the new probe called BMARt193modSponge was 5′-CGAAGATCCTCCACTTTA-3′. We used the PROBE_MATCH function in ARB to test the coverage of this new probe. Only SOX symbionts of bathymodiolin mussels had perfect matches to this probe. To test the specificity of the probe, we used sections of *Bathymodiolus puteoserpentis*, whose SOX symbiont 16S rRNA sequence has one mismatch to the BMARt193modSponge probe. At 30% formamide concentration, the probe bound the symbionts of the Chapopote sponge, but not those in sections of *B. puteoserpentis* (Appendix Fig. A2). Details of the sampling, fixation, embedding, and sectioning of *B. puteoserpentis* (specimen 281ROV/3) can be found in Petersen *et al*. (2011). All CARD-FISH experiments using this probe were therefore done using 30% formamide. A new probe was designed with the PROBE_DESIGN tool in ARB to target sequences from the Chapopote sponge that were related to the bathymodiolin MOX symbionts. The new probe, called CspongeMeth208, had the sequence 5′-CGCAAGGCTCTATCCGAA-3′. The PROBE_MATCH function in ARB identified no non-target perfect matches in the ARB Silva Ref108 database, and the closest non-target hits had at least three mismatches. We also used this probe on sections of *B. puteoserpentis*, whose methanotrophic symbiont had five mismatches to the probe sequence, as a negative control. This probe bound the symbionts of the Chapopote sponge at 30% formamide, but not the *B. puteoserpentis* MOX symbionts (Appendix Fig. A2). Chapopote sponge pieces were embedded in Steedman's wax and sectioned as previously described (Petersen *et al.*, 2010). Slides were dewaxed in three baths of 96% ethanol each for 10 min. Slides were hybridized for 1.5 h, and CARD was done for 10 min (CspongeMeth208) or 40 min (BMARt193modSponge) at room temperature. Buffer composition was as described in Pernthaler *et al*. (2002). Sections were stained with DAPI as described above. All photomicrographs were taken on a Zeiss Axioplan 2 fitted with an AxioCam camera and the AxioVision software, ver. 4.7 (Carl Zeiss AG, Jena, Germany). Images were processed by blind deconvolution in AutoQuant (Media Cybernetics, Bethesda, MD).

All sequences from this study have been submitted to the EMBL database and can be found under the following accession numbers: *R. beryli* COI (two haplotypes, HE863972 & HE863973), *R. beryli*-associated 16S rRNA genes (HE814584–HE814592), Chapopote sponge COI (HE814566), sponge-associated 16S rRNA genes (HE814567–HE814583).

Results and Discussion

Relationship of bathymodiolin sulfur-oxidizing (SOX) and methane-oxidizing (MOX) bacteria to other Gammaproteobacteria

Consistent with previous analyses, the MOX symbionts of bathymodiolin mussels grouped together with cultured Gammaproteobacterial methanotrophs of the genera *Methylomicrobium*, *Methylosarcina,* and *Methylobacter* (Fig. 1). However, the placement of the SOX symbionts in relation to cultivated bacteria contradicted earlier analyses. The chemolithoautotrophic sulfur-oxidizer *Thiomicrospira crunogena* is widely considered to be the closest cultured relative to the bathymodiolin and vesicomyid SOX symbionts (for example, Stewart *et al.*, 2005; Cavanaugh *et al.*, 2006; Dubilier *et al.*, 2008) (Appendix Fig. A1). We could not confirm this in our phylogenetic analyses. Cultured marine heterotrophic Gammaproteobacteria of the genus *Reinekea* grouped together with the bathymodiolin SOX symbionts (Fig. 1). Although this grouping had a low bootstrap value, it was present in all three tree-construction methods (Fig. 1). *Thiomicrospira* strains always grouped together with *Hydrogenovibrio* spp. and *Thioalkalimicrobium* spp., and this grouping had >90% bootstrap support (Fig. 1).

Phylogenies of the bathymodiolin sulfur- and methane-oxidizing symbionts and their free-living close relatives.

In contrast to previous phylogenetic studies of the bathymodiolin SOX and MOX symbionts, our analysis shows that neither of these symbiont groups form a monophyletic clade that excludes all free-living bacteria. Both the SOX and MOX symbionts fell into multiple clades that were interspersed with free-living bacteria (Figs. 2, 3). Some of these free-living bacteria were from reducing habitats where chemosynthetic symbioses occur, such as hydrothermal vents and cold seeps. We therefore cannot rule out the possibility that these sequences are from symbiotic bacteria that were released by host animals that we have not yet

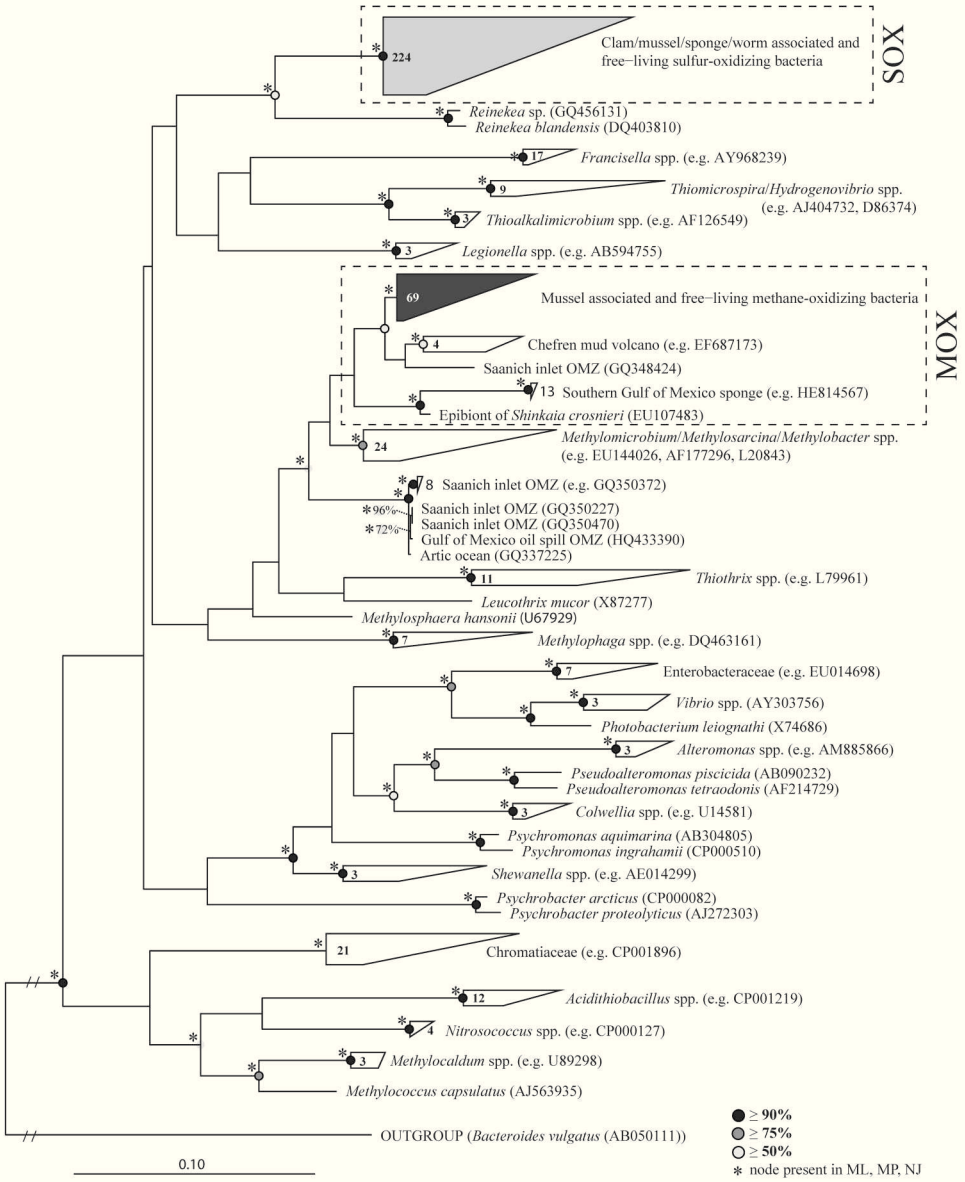

Figure 1. Overview maximum likelihood 16S rRNA phylogeny of Gammaproteobacteria. For a detailed view of the sulfur-oxidizing (SOX) and methane-oxidizing (MOX) clades, see Figures 2 and 3. Black, gray, and white circles at nodes indicate maximum likelihood bootstrap values (100 resamplings), and asterisks show nodes that were also present in neighbor-joining and maximum parsimony phylogenies. Scale bar represents 10% sequence divergence.

sampled and sequenced. Intriguingly however, a large number of the free-living sulfur-oxidizers that fell within the SOX clade were from two groups of marine Gammaproteobacteria called "SUP05" and "GSO" (Fuchs *et al.*, 2005; Lavik *et al.*, 2009; Schmidtova *et al.*, 2009; Walsh *et al.*, 2009; Canfield *et al.*, 2010; Zaikova *et al.*, 2010). These bacteria are abundant in marine oxygen minimum zones (OMZs), oxygen-starved regions that occur from Canadian fjords, to the Pacific open ocean, the Namibian and Chilean upwelling regions, and the Arabian Sea. SUP05 and GSO bacteria have been sampled from the water column in locations far from any hydrothermal vent or cold seep where bathymodiolin mussels and other animals that host chemosynthetic symbionts are found. These bacteria are therefore unlikely to be symbionts of yet-unsampled host species. Like the SOX symbionts, SOX-related bacteria from OMZs are chemolithoautotrophic sulfur oxidizers. However, unlike the symbionts, they seem to be strict anaerobes that use nitrate only as a terminal electron acceptor (Walsh *et al.*, 2009; Canfield *et al.*, 2010). Our results show that the

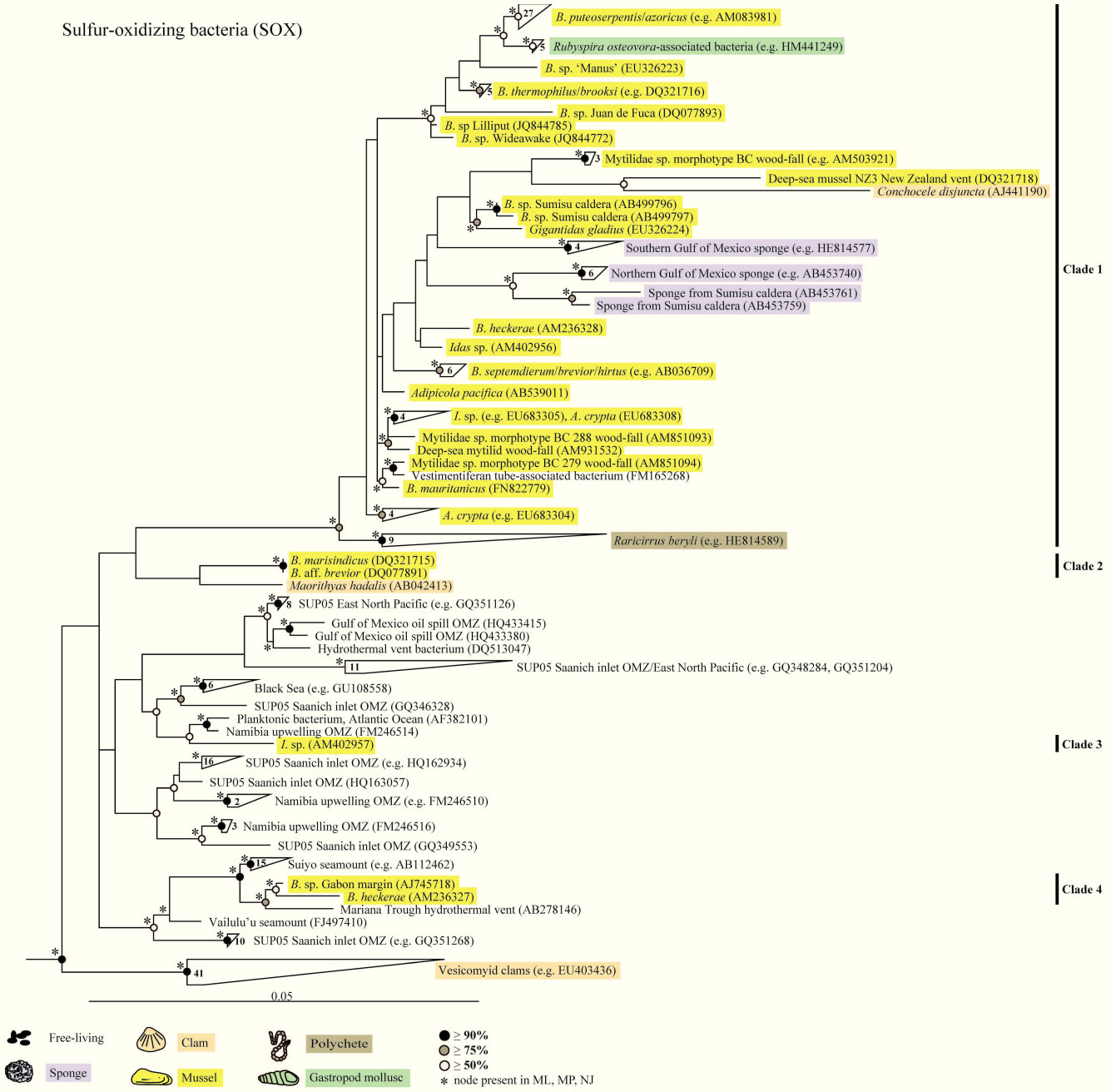

Figure 2. Maximum likelihood phylogeny of 16S rRNA genes from the bathymodiolin sulfur-oxidizing symbionts and their free-living and symbiotic close relatives. For symbiotic bacteria, species names of the hosts are shown. Symbiont sequences are highlighted according to their host animal group. Symbionts of bathymodiolin mussels (highlighted in yellow) fall into four different clades, shown on the right. Black, gray, and white circles indicate maximum likelihood bootstrap values (100 resamplings). Branches also present in maximum parsimony and neighbor-joining phylogenies are indicated with asterisks. Scale bar represents 5% sequence divergence.

SOX-related 16S rRNA sequences from OMZs did not form an exclusive group, but instead formed a number of distinct well-supported clusters, some of which contained symbiont sequences and sequences from hydrothermal vents (Fig. 2).

Multiple origins of bathymodiolin symbioses?

For the bathymodiolin mussels, we asked the question, did only two bacterial lineages give rise to symbioses, one

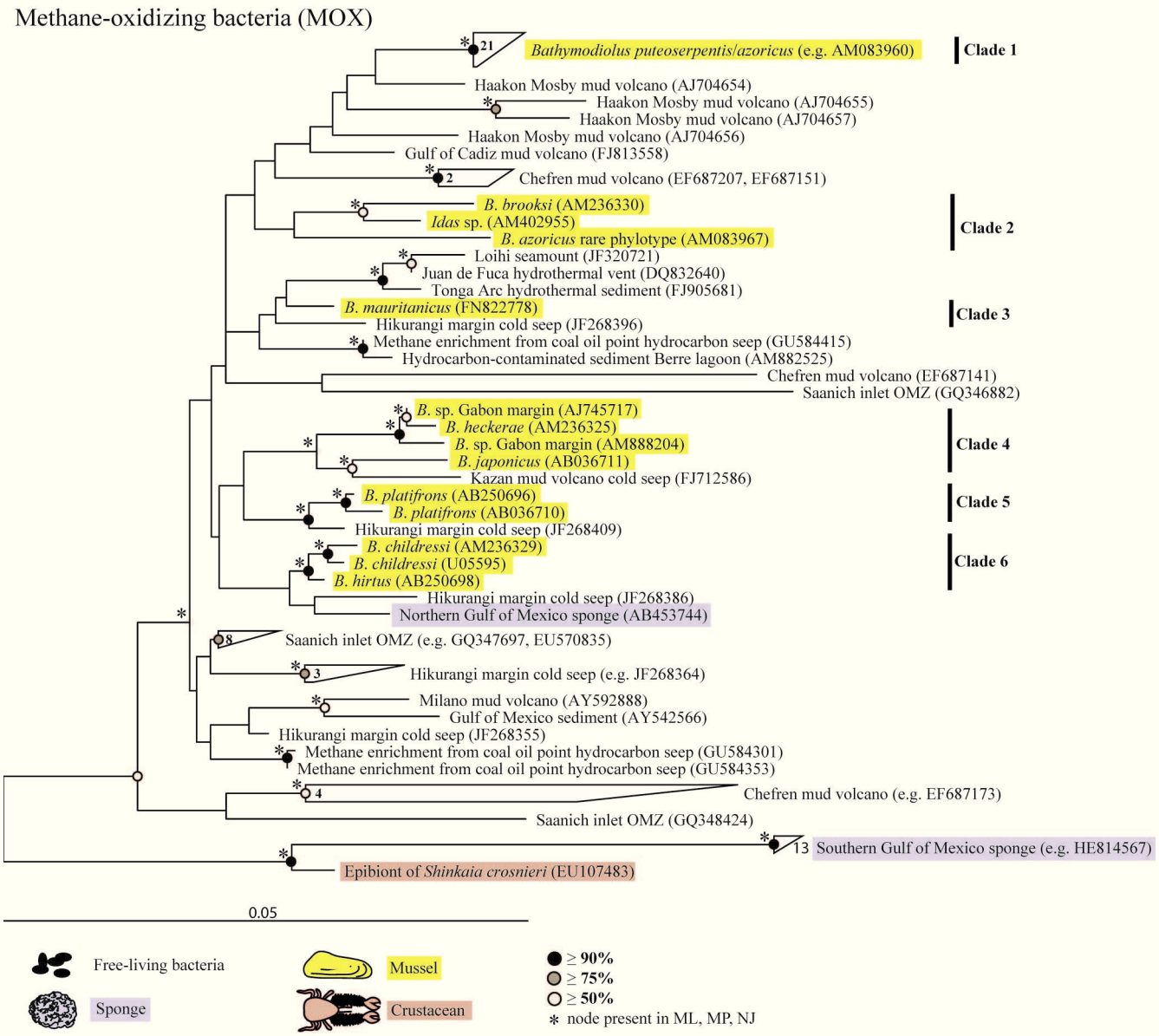

Figure 3. Maximum likelihood phylogeny of 16S rRNA genes from the bathymodiolin methane-oxidizing symbionts and their free-living and symbiotic close relatives. For symbiotic bacteria, species names of the hosts are shown. Symbiont sequences are highlighted according to their host animal group. Symbionts of bathymodiolin mussels (highlighted in yellow) fall into six different clades, shown on the right. Black, gray, and white circles indicate maximum likelihood bootstrap values (100 resamplings). Branches also present in maximum parsimony and neighbor-joining phylogenies are indicated with asterisks. Scale bar represents 5% sequence divergence.

SOX lineage and one MOX lineage, with subsequent diversification of hosts and symbionts as previously assumed? Or did multiple closely related free-living strains of sulfur oxidizers and methane oxidizers colonize different species of bathymodiolin mussels independently? Put simply, how many times during evolution were bathymodiolin mussels colonized by free-living bacteria? We would expect a symbiont lineage that originated from a single free-living ancestor to form an exclusive clade containing only its symbiotic descendents. For example, the SOX symbionts of the bathymodiolin mussels in Clade 1 are monophyletic and contain exclusively symbiotic bacteria (Fig. 2). This lineage therefore appears to have a single common ancestor, and one explanation is that this lineage originated from a single free-living sulfur oxidizer. If bathymodiolin mussels were colonized multiple times independently by different lin-

eages of free-living bacteria, we would expect to see symbiont sequences falling into separate groups. This is what we saw when we compared all known SOX and MOX symbionts of bathymodiolin mussels with their free-living relatives. The SOX sequences fell into four clades, the MOX into six, and these clades were interspersed with sequences from free-living bacteria (Figs. 2, 3). All clades were supported by the three methods of tree construction used, but due to limitations in the resolution of the 16S rRNA gene, the relationships between the groups were unclear. Clade 4 of the SOX symbionts provides the clearest example for an independent lineage, separate from the major group of bathymodiolin symbionts (Clade 1). It groups together with free-living bacteria, which fall basal to the symbiont sequences, providing further support for the hypothesis that free-living ancestors of this clade established symbioses with bathymodiolin mussels independently of Clades 1–3. We therefore hypothesize that symbioses with bathymodiolin mussels were established more than once by free-living sulfur-oxidizing bacteria. The same may be true for the methane-oxidizing symbionts, but more marker gene sequences would be needed to confirm this. This observation is consistent with the recent awareness that chemosynthetic symbioses were formed in a multitude of bacterial lineages (Dubilier *et al.*, 2008; Gruber-Vodicka *et al.*, 2011). It shows how often these associations can evolve, reflecting the strong selective advantage of forming such symbioses.

An alternative hypothesis that would explain why symbiont sequences were interspersed with those from free-living bacteria is that facultative symbiotic bacteria occasionally switch back to an obligate free-living lifestyle (Sachs *et al.*, 2011). Since horizontal transmission, which has been proposed for the bathymodiolin symbionts, implies a free-living environmental stage, this would also seem to be a reasonable interpretation of the phylogeny of the bathymodiolin SOX symbionts and their free-living relatives. Such "abandonment events," in which symbionts switch back to an exclusively free-living lifestyle, have been hypothesized for the nitrogen-fixing rhizobial symbionts of legumes. Phylogenetic reconstructions for these symbionts showed similar phylogenetic patterns to ours, in which symbiont sequences are interspersed with those from free-living bacteria (Sachs *et al.*, 2009, 2010). In some cases, the rhizobial symbiont sequences could be identified as basal to their free-living relatives, which supports this interpretation. However, we do not think that abandonment of the symbiotic lifestyle is the most reasonable explanation for our results for a number of reasons. Firstly, symbiont sequences never fell basal to free-living sequences. In the one case where such relationships could be determined, sequences from free-living bacteria were basal to the symbiont sequences (Clade 4, Fig. 2). In this case, we would have to assume (1) gain of symbiotic function at the node common to the vesicomyid and bathymodiolin symbionts, (2) subsequent loss of symbiotic function (abandonment) to explain the presence of free-living bacteria in this clade, and (3) re-gain of symbiotic function by the symbionts of *B.* sp. Gabon Margin and *B. heckerae* (Clade 4, Fig. 2). Secondly, experimental evidence has recently shown that adaptation to a host-associated lifestyle carries fitness trade-offs in the free-living state. In competition assays, the *Vibrio fisheri* strains that were the most successful colonizers of their *Euprymna scolopes* squid hosts were also the least fit when grown in seawater (Wollenberg and Ruby, 2012). For these reasons, and considering that beneficial animal-microbe associations have clearly been established multiple times during evolution from multiple lineages of free-living bacteria (Dubilier *et al.*, 2008; Sachs *et al.*, 2011), we consider multiple origins to be the most parsimonious explanation for the observed phylogeny of bathymodiolin SOX symbionts and their free-living relatives.

Evolutionary flexibility: Close relatives of the bathymodiolin sulfur- and methane-oxidizing symbionts associate with phylogenetically distant host animals

In this study, we found close relatives of the bathymodiolin SOX symbionts in 16S rRNA clone libraries from eight individuals of the terebellid polychaete *R. beryli* from a whale-fall in Sweden (Table 1). CARD-FISH with a probe designed specifically for bathymodiolin SOX symbionts, which perfectly matched our *R. beryli*-associated sequences, showed that the SOX-related bacteria were epibionts in a mucous layer outside of the worm (Fig. 4). Phylogenetic analysis showed that the SOX-related sequences from *R. beryli* formed a well-supported clade within the bathymodiolin sulfur-oxidizing symbiont group (Fig. 2). Although the role of the SOX-related epibionts of *R. beryli* is unclear, the association appears to be specific. Firstly, no bathymodiolin mussels are known to occur at the whale-fall where we sampled *R. beryli*, indicating that these epibionts are not contaminants from co-occurring mussels. Secondly, the SOX-related epibionts were consistently found in clone libraries from all individuals investigated, even those sampled in different years (Table 1). Finally, SOX-related sequences were never found in a previous study in which extensive clone library and FISH analyses were done on co-occurring *Osedax* worms from the same whale-fall (Verna *et al.*, 2010).

In a 16S rRNA gene clone library from a poecilosclerid sponge from the southern Gulf of Mexico, we identified two groups closely related to bathymodiolin symbionts. One was related to the sulfur-oxidizing (4 clones) and one to the methane-oxidizing symbionts of bathymodiolin mussels (43 clones out of 85). In phylogenetic analyses, these groups formed two distinct clades that grouped together with the bathymodiolin symbionts but were distinct from them (Figs.

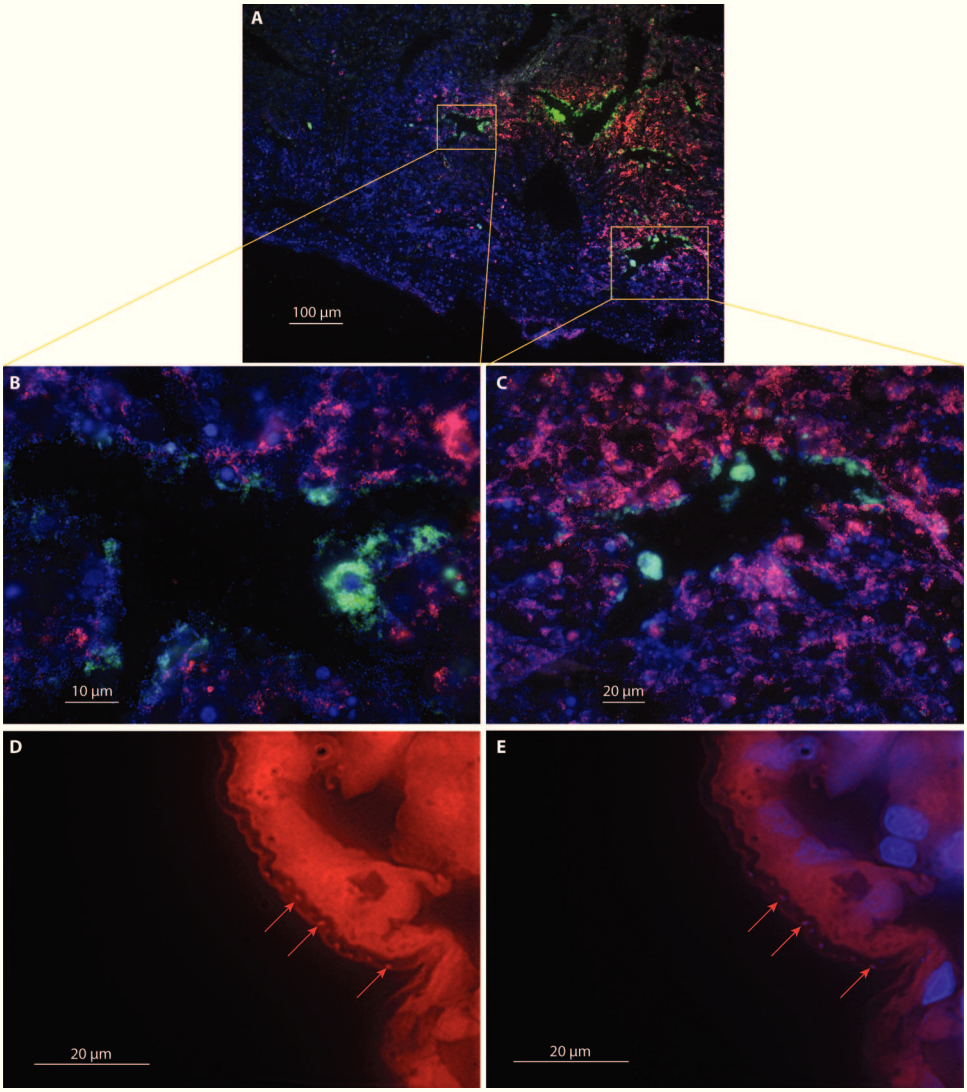

Figure 4. CARD-FISH images of sections of the poecilosclerid sponge (A–C) and *Raricirrus beryli* (D, E). A–C show double CARD-FISH with the specific probe for the sponge sulfur-oxidizing (SOX)-related symbionts in green, and the specific probe for the sponge methane-oxidizing (MOX)-related symbionts in red. The DAPI stain is shown in blue. B and C are closer views of the regions in A outlined with yellow boxes. D and E show CARD-FISH of the SOX-related epibiont of *R. beryli* using the probe BMARt193 from Duperron *et al*. (2006). D shows only the CARD-FISH probe signals in red; E shows the overlap of these signals with DAPI (shown in blue). The red arrows indicate the probe signals.

2, 3). To investigate the abundance and location of the SOX- and MOX-related phylotypes in sponge tissues, we designed specific oligonucleotide probes for both groups. CARD-FISH with these probes showed that both groups were abundant within the sponge tissue (Fig. 4). MOX relatives were more abundant than SOX relatives, reflecting their relative abundance in the clone library. Like the epibionts of *R. beryli*, the beneficial role of the sponge-associated SOX- and MOX-related bacteria remains unclear. Nishijima *et al.* (2010) also found bathymodiolin SOX- and MOX-related bacteria in an unidentified poecilosclerid sponge from the northern Gulf of Mexico. These authors concluded that the SOX-related bacteria from the sponge were likely to be specific to their hosts. This was based on two observations: Firstly, the sponge-associated bacteria were distinct from the symbionts of the co-occurring bathymodiolin mussels at this site, indicating that they were not symbionts released by the mussels and taken up by the sponge through filter-feeding. Secondly, if the SOX-related bacteria were contaminants from the environment, then co-occurring sponges that filter-feed would be expected to have the same SOX-related bacteria. This was not the case. An astrophorid sponge from the same site in the northern Gulf of Mexico had SOX-related bacteria that were distinct

from those associated with the co-occurring poecilosclerid sponge. The SOX- and MOX-related bacteria in the sponges we investigated are also distinct from the SOX and MOX symbionts of the *Bathymodiolus* mussels they co-occur with at Chapopote (Figs. 2, 3; L. Raggi, F. Schubotz, K.-U. Hinrichs, N. Dubilier, J. Petersen, unpubl. results). Furthermore, they were present in both sponge individuals that were available for this study, and were not yet found in environmental clone libraries from Chapopote (K. K. *et al*., unpubl. results). These preliminary observations indicate that the Chapopote sponge association with SOX- and MOX-related bacteria may be specific. Sampling and analysis of more individuals would be needed to confirm this.

Our clone library and CARD-FISH analyses of *R. beryli* and the poecilosclerid sponge show that close relatives of the bathymodiolin SOX and MOX symbionts also associate with these hosts. Furthermore, 16S rRNA sequences related to the bathymodiolin SOX symbionts were recently found in clone libraries from the whale-fall snail *Rubyspira osteovora* in the East Pacific (Johnson *et al.*, 2010). Our results, together with those from Johnson *et al.* (2010) and Nishijima *et al.* (2010), show that the bathymodiolin SOX symbionts and their close relatives can associate with three animal phyla, Mollusca, Annelida and Porifera, and four animal classes, Bivalvia, Gastropoda, Polychaeta, and Demospongiae. The host range of the bathymodiolin SOX group is therefore greater than previously recognized. This kind of evolutionary flexibility has not yet been shown for the bathymodiolin symbionts. The only other chemosynthetic symbiont lineage that is assumed to be so flexible in associating with diverse host animals is the sulfur-oxidizing symbionts of marine oligochaetes and nematodes, where symbiont transfer between hosts of the phyla Annelida and Nematoda may have occurred (Dubilier *et al.*, 2008; Heindl *et al.*, 2011).

Intriguingly, the bacteria associated with distantly related hosts are sometimes more closely related to each other than to the symbionts of closely related hosts or to free-living bacteria. For example, the closest relatives of the sulfur-oxidizing symbionts of *B. puteoserpentis* and *B. azoricus* from hydrothermal vents on the northern Mid-Atlantic Ridge are not the symbionts of *B*. sp., a closely-related species from the southern Mid-Atlantic Ridge, but bacteria associated with the snail *Rubyspira osteovora* from the Monterrey Canyon whale-fall (Fig. 2) (Johnson *et al.*, 2010; van der Heijden *et al.*, 2012). This indicates that these symbionts might have been transferred between distantly related hosts throughout their evolutionary history. It is currently unclear how such a transfer between bathymodiolin mussels from hydrothermal vents in the Atlantic and *R. osteovora* from a Monterrey Canyon whale-fall could have happened. Since these host animals are not known to co-occur, the transfer presumably happened by the uptake of free-living symbionts and not by direct contact between hosts. The distribution of the free-living symbionts must therefore be immense in order to explain the presence of such closely related symbionts at sites in different ocean basins, separated by an entire continent.

Conclusions and Outlook

We identified close relatives of the bathymodiolin sulfur- and methane-oxidizing symbionts that associate with hosts from different animal phyla, indicating that the host range of these symbiont lineages is greater than previously assumed. The diversity of their hosts underscores the remarkable evolutionary flexibility of these bacteria to form associations with animals. It reflects the strong selective pressure in these bacterial lineages to hitch a ride with an animal host. Future studies should address the following questions:

(1) How are symbionts transferred between phylogenetically and geographically distant hosts?
(2) Is there a free-living form of these symbionts? They are widely assumed to exist, but so far have not yet been identified. If there are free-living forms, what is their geographic distribution?
(3) Which genomic changes allow symbionts to colonize novel hosts?

A recent study by Mandel *et al.* (2009) showed that horizontally transmitted luminescent *Vibrio fisheri* symbionts can colonize novel hosts by acquiring a single regulatory gene, which demonstrates that simple genetic changes might be sufficient for such host-swapping to occur. Our 16S rRNA gene phylogenies, including sequences from metagenome studies, identified many free-living bacteria from open-ocean environments that fell within the sulfur- and methane-oxidizing symbiont clades, in contrast to previous studies that identified only a few free-living bacteria in each clade. Intriguingly, close relatives of the sulfur-oxidizing symbionts are highly abundant members of the bacterioplankton in marine oxygen minimum zones worldwide, which attests to the unparalleled success of this group in distant and disparate habitats, and with contrasting lifestyles. Genomes or metagenomes are available for symbiotic and free-living members of this group (Kuwahara *et al.*, 2007; Newton *et al.*, 2007; Walsh *et al.*, 2009; Petersen *et al.*, 2011), and comparative genome studies, which are underway in our laboratory, might identify common attributes that allowed these bacteria to become so successful.

Acknowledgments

We thank Antje Boetius and Elva Escobar for providing sponge samples, and the captain and crew of the RV *Meteor* and ROV *Quest* (expedition M67/2) for support with work at sea. Thanks to Thomas Dahlgren for helping to sample *Raricirrus beryli*, to Gordon Paterson for help in identification, and to Helena Wiklund for providing some of the

samples. We also thank Silke Wetzel, Lisa Drews, Kay Simmack, Viola Beier, and Nicole Roediger for excellent technical assistance. We very much appreciate the insightful comments of two reviewers, which helped us to improve this manuscript. This work was supported by the Max Planck Society, the Studienstiftung des deutschen Volkes (CW), and an EU Early Stage Training fellowship, MarMicEST (CV).

Literature Cited

Canfield, D. E., F. J. Stewart, B. Thamdrup, L. De Brabandere, T. Dalsgaard, E. F. Delong, N. P. Revsbech, and O. Ulloa. 2010. A cryptic sulfur cycle in oxygen-minimum-zone waters off the Chilean coast. *Science* **330:** 1375–1378.

Cavanaugh, C. M., S. L. Gardiner, M. L. Jones, H. W. Jannasch, and J. B. Waterbury. 1981. Prokaryotic cells in the hydrothermal vent tube worm *Riftia pachyptila* Jones: possible chemoautotrophic symbionts. *Science* **213:** 340–342.

Cavanaugh, C. M., Z. P. McKiness, I. L. G. Newton, and F. J. Stewart. 2006. Marine chemosynthetic symbioses. Pp. 475–507 in *The Prokaryotes: An Evolving Electronic Resource for the Microbial Community*, M. Dworkin, S. I. Falkow, E. Rosenberg, K.-H. Schleifer, and E. Stackebrandt, eds. Springer, New York.

Childress, J. J., C. R. Fisher, J. M. Brooks, M. C. Kennicutt II, R. Bidigare, and A. E. Anderson. 1986. A methanotrophic marine molluscan (Bivalvia, Mytilidae) symbiosis: mussels fueled by gas. *Science* **233:** 1306–1308.

Dahlgren, T. G., H. Wiklund, B. Källström, T. Lundälv, C. R. Smith, and A. G. Glover. 2006. A shallow-water whale-fall experiment in the north Atlantic. *Cah. Biol. Mar.* **47:** 385–389.

DeChaine, E. G., and C. M. Cavanaugh. 2006. Symbioses of methanotrophs and deep-sea mussels (Mytilidae: Bathymodiolinae). Pp. 227–249 in *Molecular Basis of Symbiosis*, J. Overmann, ed. Springer-Verlag, Berlin.

DeChaine, E. G., A. E. Bates, T. M. Shank, and C. M. Cavanaugh. 2006. Off-axis symbiosis found: characterization and biogeography of bacterial symbionts of *Bathymodiolus* mussels from Lost City hydrothermal vents. *Environ. Microbiol.* **8:** 1902–1912.

Distel, D. L. 1998. Evolution of chemoautotrophic endosymbioses in bivalves–bivalve-bacteria chemosymbioses are phylogenetically diverse but morphologically similar. *Bioscience* **48:** 277–286.

Distel, D. L., and C. M. Cavanaugh. 1994. Independent phylogenetic origins of methanotrophic and chemoautotrophic bacterial endosymbioses in marine bivalves. *J. Bacteriol.* **176:** 1932–1938.

Dubilier, N., C. Bergin, and C. Lott. 2008. Symbiotic diversity in marine animals: the art of harnessing chemosynthesis. *Nat. Rev. Microbiol.* **6:** 725–739.

Duperron, S. 2010. The diversity of deep-sea mussels and their bacterial symbioses. Pp. 137–167 in *The Vent and Seep Biota*, S. Kiel, ed. Springer, Dordrecht.

Duperron, S., C. Bergin, F. Zielinski, A. Blazejak, A. Pernthaler, Z. P. McKiness, E. DeChaine, C. M. Cavanaugh, and N. Dubilier. 2006. A dual symbiosis shared by two mussel species, *Bathymodiolus azoricus* and *Bathymodiolus puteoserpentis* (Bivalvia : Mytilidae), from hydrothermal vents along the northern Mid-Atlantic Ridge. *Environ. Microbiol.* **8:** 1441–1447.

Folmer, O., M. B. Black, W. R. Hoeh, R. A. Lutz, and R. C. Vrijenhoek. 1994. DNA primers for amplification of mitochondrial cytochrome C oxidase subunit I from metazoan invertebrates. *Mol. Mar. Biol. Biotechnol.* **3:** 294–299.

Fuchs, B., D. Woebken, M. V. Zubkov, P. Burkhill, and R. Amann. 2005. Molecular identification of picoplankton populations in contrasting waters of the Arabian Sea. *Aquat. Microb. Ecol.* **39:** 145–157.

Goffredi, S. K., W. J. Jones, H. Erhlich, A. Springer, and R. C. Vrijenhoek. 2008. Epibiotic bacteria associated with the recently discovered Yeti crab, *Kiwa hirsuta*. *Environ. Microbiol.* **10:** 2623–2634.

Gruber-Vodicka, H. R., U. Dirks, N. Leisch, C. Baranyi, K. Stoecker, S. Bulgheresi, N. R. Heindl, M. Horn, C. Lott, A. Loy, M. Wagner, and J. Ott. 2011. *Paracatenula*, an ancient symbiosis between thiotrophic Alphaproteobacteria and catenulid flatworms. *Proc. Natl. Acad. Sci. USA* **108:** 12078–12083.

Heindl, N. R., H. R. Gruber-Vodicka, C. Bayer, S. Lücker, J. A. Ott, and S. Bulgheresi. 2011. First detection of thiotrophic symbiont phylotypes in the pelagic marine environment. *FEMS Microbiol. Ecol.* **77:** 223–227.

Hentschel, U., and H. Felbeck. 1993. Nitrate respiration in the hydrothermal vent tubeworm *Riftia pachyptila*. *Nature* **366:** 338–340.

Heracles BioSoft S.R.L. 2012. DNA Baser. [Online] Available: http://www.dnabaser.com/index.html [2012, August 6].

Johnson, S. B., A. Waren, R. W. Lee, Y. Kano, A. Kaim, A. Davis, E. E. Strong, and R. C. Vrijenhoek. 2010. *Rubyspira*, new genus and two new species of bone-eating deep-sea snails with ancient habits. *Biol. Bull.* **219:** 166–177.

Kadar, E., R. Bettencourt, V. Costa, R. S. Santos, A. Lobo-Da-Cunha, and P. Dando. 2005. Experimentally induced endosymbiont loss and re-acquirement in the hydrothermal vent bivalve *Bathymodiolus azoricus*. *J. Exp. Mar. Biol. Ecol.* **318:** 99–110.

Kuwahara, H., T. Yoshida, Y. Takaki, S. Shimamura, S. Nishi, M. Harada, K. Matsuyama, K. Takishita, M. Kawato, K. Uematsu *et al.* 2007. Reduced genome of the thioautotrophic intracellular symbiont in a deep-sea clam, *Calyptogena okutanii*. *Curr. Biol.* **17:** 881–886.

Lane, D. J. 1991. 16S/23S rRNA sequencing. Pp. 115–175 in *Nucleic Acid Techniques in Bacterial Systematics*, E. Stackebrandt and M. Goodfellow, eds. John Wiley, New York.

Lane, D. J., B. Pace, G. J. Olsen, D. A. Stahl, M. L. Sogin, and N. R. Pace. 1985. Rapid determination of 16S ribosomal RNA sequences for phylogenetic analyses. *Proc. Natl. Acad. Sci. USA* **82:** 6955–6959.

Lavik, G., T. Stuhrmann, V. Bruchert, A. Van der Plas, V. Mohrholz, P. Lam, M. Muszmann, B. M. Fuchs, R. Amann, U. Lass, and M. M. M. Kuypers. 2009. Detoxification of sulphidic African shelf waters by blooming chemolithotrophs. *Nature* **457:** 581–584.

Ludwig, W., O. Strunk, R. Westram, L. Richter, H. Meier, Yadhukumar, A. Buchner, T. Lai, S. Steppi, G. Jobb *et al.* 2004. ARB: a software environment for sequence data. *Nucleic Acids Res.* **32:** 1363–1371.

Mandel, M. J., M. S. Wollenberg, E. V. Stabb, K. L. Visick, and E. G. Ruby. 2009. A single regulatory gene is sufficient to alter bacterial host range. *Nature* **458:** 215–U217.

Muyzer, G., E. C. Dewaal, and A. G. Uitterlinden. 1993. Profiling of complex microbial populations by denaturing gradient gel electrophoresis analysis of polymerase chain reaction-amplified genes coding for 16S rRNA. *Appl. Environ. Microbiol.* **59:** 695–700.

Muyzer, G., A. Teske, C. O. Wirsen, and H. W. Jannasch. 1995. Phylogenetic relationships of *Thiomicrospira* species and their identification in deep-sea hydrothermal vent samples by denaturing gradient gel electrophoresis of 16S rDNA fragments. *Arch. Microbiol.* **164:** 165–172.

Newton, I. L. G., T. Woyke, T. A. Auchtung, G. F. Dilly, R. J. Dutton, M. C. Fisher, K. M. Fontanez, E. Lau, F. J. Stewart, P. M. Richardson *et al.* 2007. The *Calyptogena magnifica* chemoautotrophic symbiont genome. *Science* **315:** 998–1000.

Nishijima, M., D. Lindsay, J. Hata, A. Nakamura, H. Kasai, Y. Ise, C. Fisher, Y. Fujiwara, M. Kawato, and T. Maruyama. 2010. As-

sociation of thioautotrophic bacteria with deep-sea sponges. *Mar. Biotechnol.* **12:** 253–260.

Peplies, J., R. Kottmann, W. Ludwig, and F. O. Glöckner. 2008. A standard operating procedure for phylogenetic inference (SOPPI) using (rRNA) marker genes. *Syst. Appl. Microbiol.* **31:** 251–257.

Pernthaler, A., J. Pernthaler, and R. Amann. 2002. Fluorescence in situ hybridization and catalyzed reporter deposition for the identification of marine bacteria. *Appl. Environ. Microbiol.* **68:** 3094–3101.

Petersen, J. M., and N. Dubilier. 2009. Methanotrophic symbioses in marine invertebrates. *Environ. Microbiol. Rep.* **1:** 319–335.

Petersen, J. M., and N. Dubilier. 2010. Symbiotic methane oxidizers. Pp. 1977–1996 in *Handbook of Hydrocarbon and Lipid Microbiology*, K. Timmis, ed. Springer, Berlin.

Petersen, J. M., A. Ramette, C. Lott, M. A. Cambon-Bonavita, M. Zbinden, and N. Dubilier. 2010. Dual symbiosis of the vent shrimp *Rimicaris exoculata* with filamentous gamma- and epsilonproteobacteria at four Mid-Atlantic Ridge hydrothermal vent fields. *Environ. Microbiol.* **12:** 2204–2218.

Petersen, J. M., F. U. Zielinski, T. Pape, R. Seifert, C. Moraru, R. Amann, S. Hourdez, P. R. Girguis, S. D. Wankel, V. Barbe, E. Pelletier, D. Fink, C. Borowski, W. Bach, and N. Dubilier. 2011. Hydrogen is an energy source for hydrothermal vent symbioses. *Nature* **476:** 176–180.

Polz, M. F., and C. M. Cavanaugh. 1995. Dominance of one bacterial phylotype at a Mid-Atlantic Ridge hydrothermal vent site. *Proc. Natl. Acad. Sci. USA* **92:** 7232–7236.

Pruesse, E., C. Quast, K. Knittel, B. M. Fuchs, W. G. Ludwig, J. Peplies, and F. O. Glockner. 2007. SILVA: a comprehensive online resource for quality checked and aligned ribosomal RNA sequence data compatible with ARB. *Nucleic Acids Res.* **35:** 7188–7196.

Pruesse, E., J. Peplies, and F. O. Glöckner. 2012. SINA: accurate high throughput multiple sequence alignment of ribosomal RNA genes. *Bioinformatics* doi:10.1093/bioinformatics/bts252.

Sachs, J. L., S. W. Kembel, A. H. Lau, and E. L. Simms. 2009. In situ phylogenetic structure and diversity of wild *Bradyrhizobium* communities. *Appl. Environ. Microbiol.* **75:** 4727–4735.

Sachs, J. L., M. O. Ehinger, and E. L. Simms. 2010. Origins of cheating and loss of symbiosis in wild *Bradyrhizobium*. *J. Evol. Biol.* **23:** 1075–1089.

Sachs, J. L., R. G. Skophammer, and J. U. Regus. 2011. Evolutionary transitions in bacterial symbiosis. *Proc. Natl. Acad. Sci. USA* **108:** 10800–10807.

Schmidtova, J., S. J. Hallam, and S. A. Baldwin. 2009. Phylogenetic diversity of transition and anoxic zone bacterial communities within a near-shore anoxic basin: Nitinat Lake. *Environ. Microbiol.* **11:** 3233–3251.

Stewart, F. J., I. L. G. Newton, and C. M. Cavanaugh. 2005. Chemosynthetic endosymbioses: adaptations to oxic-anoxic interfaces. *Trends Microbiol.* **13:** 439–448.

Suzuki, Y., T. Sasaki, M. Suzuki, Y. Nogi, T. Miwa, K. Takai, K. H. Nealson, and K. Horikoshi. 2005. Novel chemoautotrophic endosymbiosis between a member of the Epsilonproteobacteria and the hydrothermal-vent gastropod *Alviniconcha* aff. *hessleri* (Gastropoda: Provannidae) from the Indian Ocean. *Appl. Environ. Microbiol.* **71:** 5440–5450.

van der Heijden, K., J. M. Petersen, N. Dubilier, and C. Borowski. 2012. Genetic connectivity between North and South Mid-Atlantic Ridge chemosynthetic bivalves and their symbionts. *PLoS One* **7(7):** e39994.

Van Dover, C. L. 2000. *The Ecology of Deep-Sea Hydrothermal Vents.* Princeton University Press, Princeton, NJ.

Verna, C., A. Ramette, H. Wiklund, T. G. Dahlgren, A. G. Glover, F. Gaill, and N. Dubilier. 2010. High symbiont diversity in the bone-eating worm *Osedax mucofloris* from shallow whale falls in the North Atlantic. *Environ. Microbiol.* **12:** 2355–2370.

Wallner, G., R. Amann, and W. Beisker. 1993. Optimizing fluorescent in situ hybridization with rRNA-targeted oligonucleotide probes for flow cytometric identification of microorganisms. *Cytometry* **14:** 136–143.

Walsh, D. A., E. Zaikova, C. G. Howes, Y. C. Song, J. J. Wright, S. G. Tringe, P. D. Tortell, and S. J. Hallam. 2009. Metagenome of a versatile chemolithoautotroph from expanding oceanic dead zones. *Science* **326:** 578–582.

Wollenberg, M. S., and E. G. Ruby. 2012. Phylogeny and fitness of *Vibrio fischeri* from the light organs of *Euprymna scolopes* in two Oahu, Hawaii populations. *ISME J.* **6:** 352–362.

Won, Y.-J., S. J. Hallam, G. D. O'Mullan, I. L. Pan, K. R. Buck, and R. C. Vrijenhoek. 2003. Environmental acquisition of thiotrophic endosymbionts by deep-sea mussels of the genus *Bathymodiolus*. *Appl. Environ. Microbiol.* **69:** 6785–6792.

Won, Y.-J., W. J. Jones, and R. C. Vrijenhoek. 2008. Absence of cospeciation between deep-sea mytilids and their thiotrophic endosymbiont. *J. Shellfish Res.* **27:** 129–138.

Zaikova, E., D. A. Walsh, C. P. Stilwell, W. W. Mohn, P. D. Tortell, and S. J. Hallam. 2010. Microbial community dynamics in a seasonally anoxic fjord: Saanich Inlet, British Columbia. *Environ. Microbiol.* **12:** 172–191.

Zhou, J., M. A. Bruns, and M. Tiedje. 1996. DNA recovery from soils of diverse composition. *Appl. Environ. Microbiol.* **62:** 316–322.

Appendix

Figure A1. Schematic representation of previous phylogenetic analyses of 16S rRNA genes from chemosynthetic symbionts. (A) In one of the pioneering molecular studies published in 1994, Distel and Cavanaugh showed that sulfide- and methane-oxidizing symbioses have independent evolutionary origins. Phylogeny modified from Distel and Cavanaugh (1994). (B) A recent analysis by Dubilier *et al.* (2008) showed that sulfur-oxidizing symbioses originated independently in at least nine bacterial groups. Sequences from sulfur-oxidizing symbionts are highlighted in gray boxes; those from methane-oxidizing symbionts in black boxes. Phylogeny modified from Dubilier *et al.* (2008).

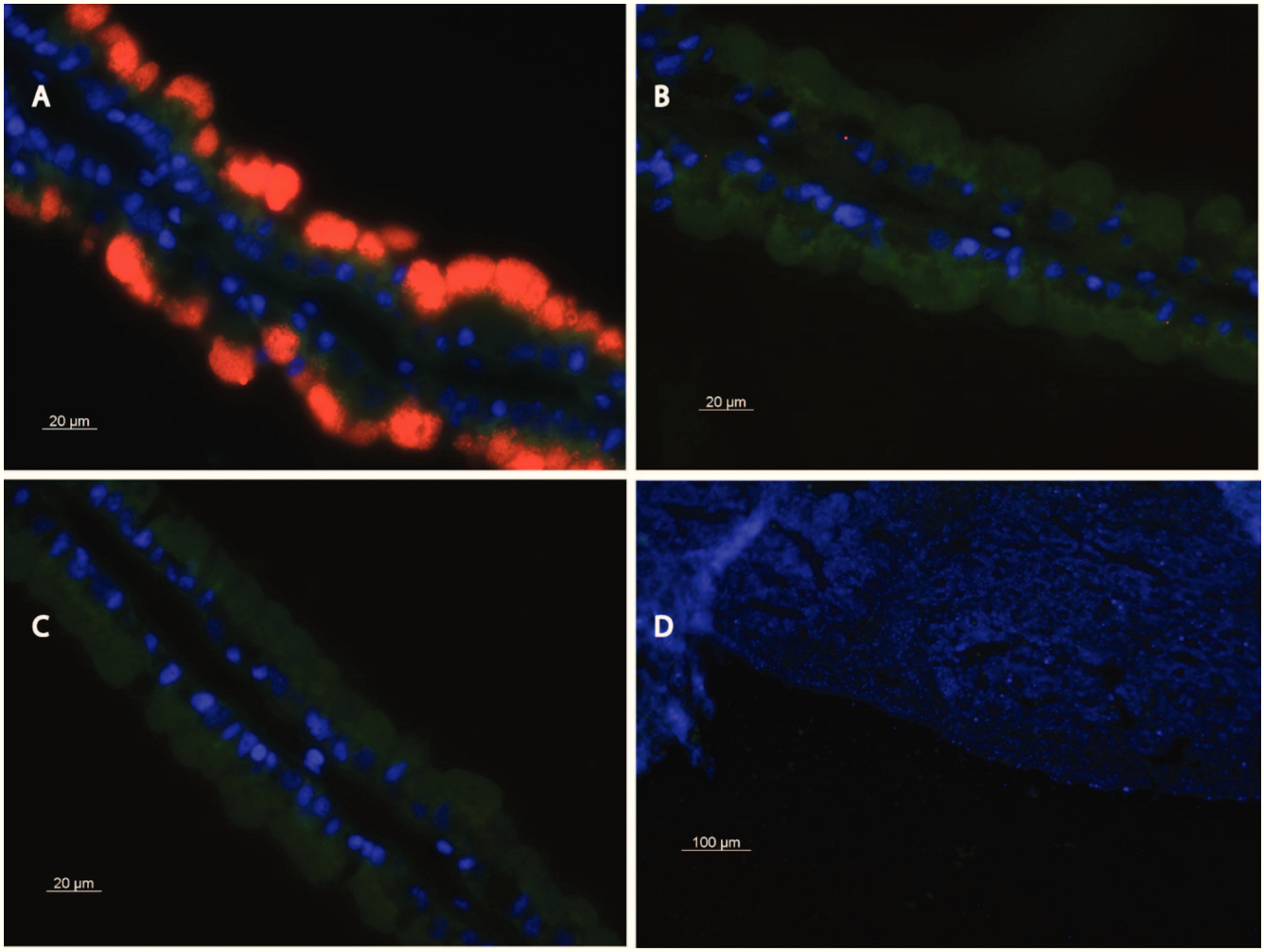

Figure A2. Negative controls for fluorescence *in situ* hybridation. (A) FISH of *Bathymodiolus puteoserpentis* with the probe EUB338 shown in red, DAPI in blue, and animal tissue autofluorescence in green. The methane-oxidizing and sulfur- oxidizing symbionts can be seen as "clouds"of bacteria in host bacteriocytes. (B) CARD-FISH of *B. puteoserpentis* with the BMARt193modSponge in red (no signal was seen with this probe). DAPI is shown in blue and animal tissue in green. (C) CARD-FISH of *B. puteoserpentis* with the probe CspongeMeth208 in red (no signal was seen with this probe). DAPI is shown in blue and animal tissue in green. (D) Hybridization with the NON338 probe of the Chapopote sponge. This is an overlayed image of DAPI in blue, and images from the red and green channels taken using the same camera and microscope settings as for Figure 4A.

Literature Cited

Distel, D. L., and C. M. Cavanaugh. 1994. Independent phylogenetic origins of methanotrophic and chemoautotrophic bacterial endosymbioses in marine bivalves. *J. Bacteriol.* **176:** 1932–1938.

Dubilier, N., C. Bergin, and C. Lott. 2008. Symbiotic diversity in marine animals: the art of harnessing chemosynthesis. *Nat. Rev. Microbiol.* **6:** 725–739.